

S.I.S.S.A.



I.S.A.S.

SCUOLA INTERNAZIONALE SUPERIORE DI STUDI AVANZATI

INTERNATIONAL SCHOOL FOR ADVANCED STUDIES

**Structural and functional insights
into the biological function
of mouse proNGF**

Thesis submitted for the degree of
“Doctor Philosophiæ”

Candidate

Francesca Paoletti

Supervisors

Prof. Antonino Cattaneo

Dr. Dorian Lamba

Trieste, April 4th 2006

*The history of NGF is more like a detective story
than a scientific enterprise,
which usually unfolds according to well-defined rules
along a route paved by previous findings*

Rita Levi-Montalcini

INDEX

INTRODUCTION – The molecular scenario	1
1. <u><i>The neurotrophin Nerve Growth Factor</i></u>	2
1.1 Discovery and characterization of NGF	2
1.2 Structure of NGF	4
1.3 Biological function of NGF	6
2. <u><i>The receptors of Nerve Growth Factor</i></u>	9
3. <u><i>The precursor protein of Nerve Growth Factor: pre-proNGF</i></u>	16
3.1 Identification and sequence	16
3.2 Biological activity of NGF precursor protein	21
3.3 The proNGF receptor	27
4. <u><i>NGF, proNGF and Alzheimer's Disease</i></u>	31
ABSTRACT OF THE THESIS	34
EXPERIMENTAL SECTION	37
1. Materials	37
2. Methods	45
RESULTS - PART 1: BIOCHEMICAL CHARACTERIZATION AND STRUCTURAL	
INSIGHTS OF M-PRONGF IN ITS DIFFERENT FORMS	73
1. <u><i>rm-proNGF expression in E.coli: a tool for high-scale</i></u>	
<u><i>production of m-NGF and rm-proNGF</i></u>	76
1.1 RT-PCR and cloning	76
1.2 Expression, refolding and purification of rm-proNGF	80
1.3 Characterization of rm-proNGF	84
1.4 Limited proteolysis of rm-proNGF to release	
mature NGF	91
1.5 Guanidinium-dependent denaturation of rm-proNGF	97
1.6 Looking for a functional mutation in rm-proNGF	98
1.7 Looking for the role of the pro-peptide of rm-proNGF	101
2. <u><i>m-pre-proNGF: a long-short equilibrium of different forms</i></u>	
<u><i>of the protein</i></u>	106
3. <u><i>effect of rm-proNGF on living cells</i></u>	110
3.1 Differentiation experiment on PC12 cells	110

3.2 TrkA – receptor activation assay on 3T3 and PC12 cells	122
4. <u>differential interaction of rm-proNGF and m-NGF with the receptors TrkA and p75NTR and with a panel of anti-NGF antibodies</u>	126
4.1 Kinetic analysis on the binding of m-NGF and rm-proNGF to their receptors p75NTR and TrkA	128
4.2 Interaction of of NGF and proNGF with a panel of anti-NGF antibodies	134
4.2.1 Analysis using ELISA assay	134
4.2.2 Surface Plasmon Resonance using BIAcore	139
5. <u>Structural characterization of rm-proNGF and of its complex with the anti-NGF antibody αD11</u>	157
5.1 Structural arrangement of rm-proNGF in solution using SAXS	161
5.2 Solution scattering experiment on h-NGF	165
5.3 Structural insights into the complex rm-proNGF/Fab α D11	166
RESULTS - PART 2: SELECTION, BIOCHEMICAL CHARACTERIZATION AND STRUCTURAL INSIGHTS INTO A NOVEL ANTI-PRONGF SCFV ANTIBODY	172
<u>Introduction</u>	173
1. <u>Selection and characterization of a novel anti-proNGF antibody in the scFv format</u>	177
1.1 Cloning of the constructs for the SPLINT selection	177
1.2 Selection of scFvs via SPLINT using the pro-10 bait	182
1.3 In vivo epitope mapping of the selected scFv	183
1.4 Sequencing of the selected scFv	184
1.5 Expression and purification of the scFv anti-proNGF in the periplasm of E.coli	185
1.6 Binding properties of the scFv – ELISA assay	187
1.7 Behaviour of the scFv anti-proNGF in vivo	190
2. <u>Cloning, expression, refolding and physico-chemical</u>	

<u>characterization of the selected scFv anti-proNGF</u> <u>in the cytoplasm of E.coli</u>	191
2.1 Expression of the scFv in <i>E.coli</i> cytoplasm	191
2.2 Establishing a refolding procedure of the scFv from the IB of <i>E.coli</i>	192
2.3 Physico-chemical characterization of the expressed scFv	198
3. <u>Binding properties of the selected scFv anti-proNGF</u>	202
3.1 ELISA assay for the binding properties of the scFv anti-proNGF	203
3.2 ELISA assay – concentration dependency of the scFv/proNGF binding	208
3.3 Binding properties – dependency from the aggregation state	209
3.4 Kinetic analysis of binding using BIAcore	211
3.5 Formation of the complex scFv anti-proNGF/proNGF	212
3.6 The use of the scFv anti-proNGF as a primary antibody	215
4. <u>Structural characterization of the scFv and of its complex with rm-proNGF</u>	217
4.1 Structural analysis of scFv anti-proNGF by SAXS data	218
4.2 Structural analysis of the complex between the scFv anti-proNGF and the rm-proNGF by SAXS data	221
DISCUSSION AND PERSPECTIVES	224
REFERENCES	238
APPENDIX 1: <u>Sequence alignments</u>	253
APPENDIX 2: <u>A novel experimental approach to the refolding of proteins on a western blotting nitrocellulose membrane</u>	257
APPENDIX 3: <u>Fluorescence cycloheximide as a tool for the visualization of protein synthesis in living cells</u>	266
ACKNOWLEDGEMENTS	269

INTRODUCTION

The molecular scenario

In the recent years one of the lines of investigation in the Neurobiology Laboratory at SISSA has been to study the molecular determinants of Alzheimer's Disease (AD), one of the most known and diffused neurodegenerative aging diseases. AD is characterized by lesions in the brain cortex, including the presence of β -amyloid plaques and neurofibrillary tangles containing phosphorylated tau protein.

In Alzheimer's disease neuronal degeneration is found in selected areas of the brain, in particular in cortical, hippocampal and basal forebrain cholinergic neurons (reviewed in Price *et al.*, Ann. Rev. Neurosci., 1986). The investigation on the involvement of the neurotrophin Nerve Growth Factor (NGF) in AD has been extensive, because it promotes the survival and regulates the function of cholinergic neurons of the basal forebrain. (reviewed in Counts *et al.*, J. Neuropath. Exp. Neuro., 2005).

NGF is translated as a pre-pro-protein, proNGF, the importance of which in the recent years has grown much, thanks to important findings on its biological functions, besides the one of promoting protein folding. Accordingly, the increasing number of involved new actors has complicated also the scenario of the investigations on the molecular determinants in AD.

1. The neurotrophin Nerve Growth Factor

1.1 Discovery and characterization of NGF

Nerve Growth Factor (NGF) is the most well known and the first to be identified of the neurotrophins protein family.

Its initial existence was proven thanks to the work of Levi-Montalcini and Hamburger in the early '50, in the frame of neuro-embryology studies (Levi-Montalcini, Science, 1987).

The history of the identification of NGF remains a fascinating scientific report, as it well emerges from the numerous publications, especially by Levi-Montalcini (Ann. Rev. Neurosci., 1982).

NGF was initially found to be an essential factor in the survival of sympathetic and embryonic sensory nerve cells, but its frame of activity was soon extended to many other functions. It is now very well established that NGF plays a central role in the development, survival and repair of peripheral and central nervous tissue, of both embryos and adults, (Angeletti *et al.*, J.Ultrastr. Res.,1971) as well as in cells of the immune and endocrine systems (Levi-Montalcini *et al.*, PNEI 1990).

NGF was initially found to be abundantly present in the venom of various species of snakes (Cohen, PNAS, 1956; Cohen, JBC, 1959), and subsequently the most rich source of the protein was found in submaxillary salivary glands of male mouse (Cohen, PNAS, 1960); NGF from both sources was identified as a protein of around 22 kDa and it was defined as heat labile, non dialyzable, acid labile, alkaline stable. The isolation of NGF from submaxillary glands was optimized by Angeletti, and was known as 2.5S NGF according to the sedimentation coefficient.

Lately, it has been proven that NGF is present in other tissues, although in much lesser amounts than in salivary glands, namely target tissues of sensory, sympathetic and central nervous system cholinergic neurons that are NGF responsive (reviewed in Shooter, Ann.Rev. Neurosci., 2001). The mode of action of NGF was deeply investigated and its effect on the biochemistry of the cells has been elucidated (Levi-Montalcini and Angeletti, Organogenesis, 1965).

Along with the investigation on the protein, new pieces were added to the forming puzzle. For example, a higher molecular weight form of NGF was isolated from mouse submandibular glands (Varon *et al.*, Biochem., 1967), as a form of around

140 kDa, defined as 7S according to its sedimentation coefficient. This high molecular weight NGF can be dissociated at acidic pH into three subunits, named α , β and γ (Varon *et al.*, Biochem., 1968). They have very similar sedimentation coefficient (2.6 S) but different isoelectric point, being the α an acidic protein, the γ a more neutral protein and the β a basic protein, respectively (reviewed in Shooter, Ann. Rev. Neuro., 2001). The survival biological activity of NGF resides in the β subunit, whereas the γ subunit functions as a protease and the α subunit remains still without a clear biological function (Shooter, Ann.Rev.Neuorosc., 2001). Seemingly, the 7S complex protects the β -NGF from proteolysis and release it by dissociation of the subunits when needed. It is worth noting that the 7S NGF is found only in the submaxillary gland, where its functions are unknown, but could be unrelated to the neurobiology of NGF (Shooter, Ann.Rev.Neurosc., 2001).

The NGF isolated with the procedure of Angeletti was subsequently sequenced; it resulted to be 118 amino acids long, with a molecular weight of 13.2 kDa and was found to be active as a homodimer. The subsequent sequencing of β -NGF demonstrated that the two forms are indeed the same protein, except that the 2.5S NGF lacks 8 amino acids at the N-terminus in comparison to the β form; it was found that kallikrein is the enzyme responsible for this proteolytic cleavage in submaxillary glands (reviewed in Shooter, Ann.Rev.Neurosc., 2001). However, the biological activity of the two forms, is the same (Shooter, Ann.Rev.Neurosc., 2001).

Human NGF was isolated later from other species, and its sequence demonstrated that it is highly homologous to that of mouse (Ullrich *et al.*, Nature, 1983).

Submandibular glands still remain the main source of mouse NGF for scientific and clinical purposes, according to the well established extraction protocol by Bocchini and Angeletti (PNAS, 1969).

On the contrary, no major source of the human protein has been identified yet, and the best way to obtain active human NGF (h-NGF) is the recombinant production of the protein, using different methods. h-NGF was expressed in inclusion bodies of *E. coli* and refolded, as described by Dicou (Neurochem. Int., 1992) or by Rattenholl and colleagues (Eur. J. Biochem., 2001), or in the periplasm of *E. coli* together with disulfide isomerases, as presented by Kurokawa and colleagues (JBC, 2001). More recently, a novel method has been proposed for the production of recombinant

human NGF, using a mammalian expression system. It allowed the production of a fully biologically protein, therefore increasing the range of possible applications of the method for large scale neurotrophin production for clinical purposes (Colangelo *et al.*, PNAS, 2005).

1.2 Structure of NGF

The existence of NGF as a dimer was confirmed by a thorough equilibrium denaturation study (Timm & Neet, Protein Science 1992), which also proved that the dimer is held together by non-covalent interchain interactions.

The active β -NGF contains three disulfide bridges, and its three-dimensional crystallographic structure has been determined at 2.3 Å resolution, revealing a compact β structure protein; in space, the three intra-chain disulfide bridges form the so-called “cystin knot motif”, defining a very complex interconnection of the disulfide bridges. The latter confers a compact structure to the protein (McDonald *et al.*, Nature 1991), as depicted in fig.1.2.1 (PDB entry: 1bet). The fold of each protomer is formed by three extended segments of twisted anti-parallel β -sheet linked by turns, so that the molecule is somewhat elongated. It is to be noted that the N-terminus (the first ten residues) of the protein was not resolved, as well as residues 112-118 at the C-terminus, suggesting a high flexibility for these terminal regions. The central core of the protein, formed by the facing β strands of the two monomers, gives rise to an extensive subunit interface with a largely hydrophobic character primarily because of aromatic residues (reviewed in McDonald and Chao, JBC, 1995). The three β -hairpin loops in the structure are composed by the most part of the variable residues in the different species, while the compact core represent a well conserved region (see also Bradshaw *et al.*, TIBS, 1993).

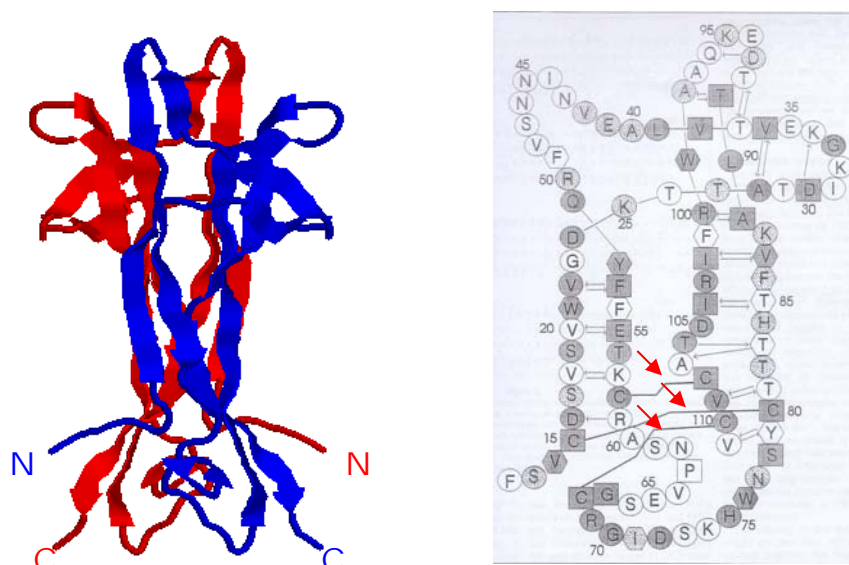


Figure 1.2.1 – Structure of mouse β -NGF. On the left side, a representation of the crystallographic three-dimensional structure of mouse β -NGF; the N- and C-termini of the two NGF monomers are indicated. The figure was generated with the program VMD (ref) from the PDB entry 1BET. On the right side, a representation of the primary structure of a single monomer. In particular the arrows indicate the position of the three intra-chain disulfide bridges forming the “cystine-knot” motif; the figure is taken from Bradshaw *et al.*, TiBS, 1993

Besides the structure of β -NGF, also the crystal structure of the whole 7S NGF complex has been determined (McDonald and Blundell, JMB, 1991; Bax *et al.*, Structure, 1997). The structure confirmed the stoichiometric composition of the 7S complex, built up by two α -subunits, two γ -subunits and one β -NGF dimer. It is interesting that two zinc ions were found to be integral part of its structure, and to inhibit the protease activity of the γ -subunit ; zinc ions were also found to stabilize the 7S complex: their removal caused its dissociation (reviewed in Shooter, Ann.Rev.Neurosc., 2001). The structure also revealed that the C-terminal residues of β -NGF were in this case well structured and were located at the active site of the γ -subunit. In the complex, the β -NGF dimer is deeply buried in the core, surrounded by a horseshoe-like array of α -NGF and γ -NGF subunits, and this fact might explain the lack of activity of β -NGF in the complex. The two α -NGF subunits bind on opposite sides of the β -NGF dimer, whereas the two γ -subunits interact with each other

around the twofold axis of the 7S complex, and are positioned below the β -NGF dimer, as depicted in fig. 1.2.2 (PDB entry: 1sgf).

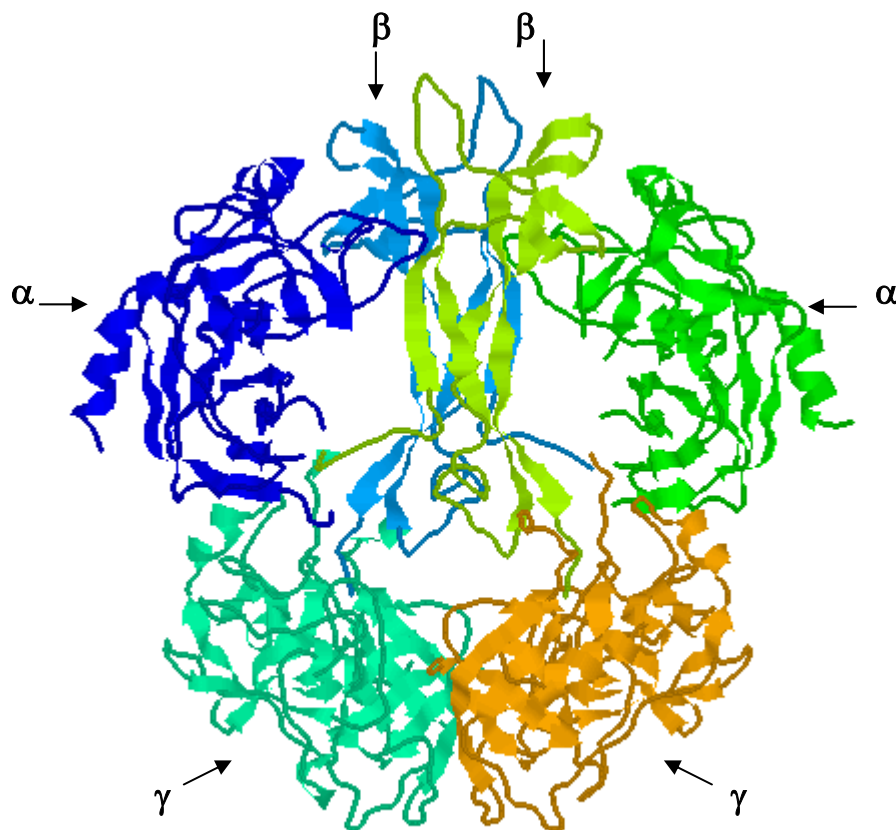


Figure 1.2.2 – The 7S NGF complex. The crystallographic structure of the 7S NGF complex (PDB entry 1SGF); the figure was generated with the program VMD. The Greek letters with the arrows indicate the position of the various subunits, α , β , γ

1.3 Biological function of NGF

NGF is a protein with pleiotropic actions *in vivo*, as briefly summarized in the following paragraphs.

The role of NGF *in vivo* has been defined to be trophic, differentiative and tropic (Calissano *et al.*, Exp. Cell Res., 1984): the trophic effect of NGF explicits in the feature that it is necessary for sensory and sympathetic cells; the differentiative effect is due to the role in differentiation of the same cells to mature nerve cells; finally, the tropic effect of NGF resides in its ability of guiding the growing axons or collaterals along its own concentration gradient.

Another important feature of NGF is the retrograde transport: this neurotrophin, in fact, was shown to be retrogradely transported within neurons *in vivo*, during physiological conditions (revised in Reynolds *et al.*, Brain Res. Rev., 2000), allowing the “communication” of the cell body with the nerve terminal. The retrograde transport is a composite mechanism, involving a series of complex events, like the release of the neurotrophin by the post-synaptic target cell, followed by receptor binding on the nerve terminal pre-synaptic membrane. Subsequently, the protein must be internalized, targeted for transport and propelled along the axon towards the cell body; finally, upon reaching it, the neurotrophins signals the nucleus.

The vital role of NGF has been demonstrated from the very beginning, when it was proven that the use of anti-NGF antibodies cause a severe reduction of the number of sympathetic neurons (Levi-Montalcini and Booker, PNAS, 1960; reviewed in Levi-Montalcini, Scientific American, 1979).

NGF also plays an important role in the Central Nervous System (CNS). Indeed, NGF, as well as its coding mRNA, are present in brain and especially hippocampus, a target area of forebrain cholinergic neurons. Accordingly, NGF has been found to promote the survival of forebrain cholinergic neurons after axonal transection (Hefti, J. Neurosci., 1986); NGF, indeed, promotes the survival and regulates the function of cholinergic neurons of the basal forebrain (reviewed in Counts and Mufson, J Neuropath. Exp. Neurol., 2005). NGF is secreted by neurons in the CNS in both constitutive and activity-dependent pathways (reviewed in Thoenen, Science, 1995), thus suggesting a role for the neurotrophins as synaptic modulators, with a role in neuronal plasticity (reviewed in Thoenen, Science, 1995; Poo, Nature Rev. Neurosci., 2001).

Along with the growth of the studies on NGF and of the repertory of the available investigation techniques, the role of this neurotrophins has grown incredibly, and it is now well established that NGF acts as a modulator of the neuro-endocrine-immune triad (reviewed in Levi-Montalcini, The Saga of the Nerve Growth Factor, 1997). It has been endowed with well defined roles also in the immune system, autoimmune disease, tissue inflammation, psychological stress, lactation and more recently also in the AIDS syndrome (reviewed in Levi-Montalcini *et al.*, J. Neurol. Sci., 1995). One other link to the immune system is given by the fact that natural autoantibodies against NGF were found to be present in both normal and pathological human sera,

and one of the most intriguing hypothesis is that these autoantibodies might act as carriers of NGF (Dicou and Nèrrière, J. Neuroimm., 1997).

As well defined by Levi-Montalcini: *“At physiological concentrations, NGF alone might not directly activate cells of immune lineage, but instead modulate their sensitivity to other triggering stimuli. (...) Circulating NGF might function as a general “alerting” signal utilized by the brain in conditions of stress and anxiety to “prime” the immune system against external noxious perturbations.”*

After more than fifty years from NGF discovery, still many open questions need to be answered before completely elucidating its function in the organism. In particular, the open questions raised by Levi-Montalcini during her Nobel Lecture in 1986 remains still without a complete answer: *“Are other biologically active peptides coded for by the NGF gene? What is the significance of different splicing in different cells of NGF messenger RNA? Is the processing of pre-pro-NGF identical in all neuronal and non-neuronal cells or, as in other peptides, do alternative processing pathways result in the production of peptides endowed with different biological functions?”*

2. The receptors of Nerve Growth Factor

The response of neurons to NGF is governed by two types of cell surface receptors: p75^{NTR}, a member of the tumour necrosis factor (TNF) receptor superfamily, and p140^{trk} (referred as TrkA) receptor tyrosine kinase (Teng and Hempstead, CMLS, 2004).

The dimerization of Trk receptor upon binding of neurotrophin leads to trans-autophosphorylation and to the activation of intracellular signalling cascades (reviewed in Chao, Nature Rev. Neurosci., 2003).

The p75^{NTR} receptor, as other members of the TNF superfamily, was demonstrated to modulate apoptotic responses, while on the contrary the survival signaling predominantly reflects TrkA activation. Classic signalling modules, such as the Ras-mitogen-activated protein (MAP) kinase cascade and the phosphatidylinositol-3 (PI-3)-kinase-Akt pathway, have been identified as downstream cellular events induced by TrkA activation. When p75^{NTR} and TrkA are expressed in the same cell, however, survival signalling dominates (Teng and Hempstead, CMLS, 2004).

Historically p75^{NTR} was the first receptor of NGF to be identified (Chao *et al.*, Science, 1986), but a lack of readily identifiable signal transduction modules within its cytoplasmic sequence led to the hypothesis that the function of p75^{NTR} was primarily to augment TrkA signalling, as also stated below (Hempstead *et al.*, Nature, 1991; reviewed in Teng and Hempstead, CMLS, 2004).

The molecular determinants of the binding between NGF and its receptors have been widely studied through mutational approaches to probe the specificity of certain amino acid residues (reviewed in McDonald and Chao, JBC, 1995). In this way it was proven that the difference in the binding surface of NGF toward p75^{NTR} and TrkA, respectively, is quite large: many more contacts are involved in the interaction with the latter receptor.

The study of the receptor binding and specificity has gained a wealth of information from the alanin- and homologue-scanning mutagenesis of variable regions of neurotrophins. In NGF, the determinants of binding to TrkA are distributed along the twofold axis of the molecule, following the interface between the two monomers (reviewed in Ibáñez, TINS, 1998). Moreover, the N-terminus of NGF is an

important binding determinant, since its replacement or deletion strongly diminish the binding. In the case of the binding to p75^{NTR}, the interaction surface has been proven to be much smaller, located mostly in a positive electrostatic patch on the surface of NGF, formed primarily by three Lysine residues from two of the hairpin loops. Replacement of these Lysines with Alanines compromises the binding to p75^{NTR}, but not to TrkA (reviewed in Ibáñez, TINS, 1998).

The kinetic analysis of the binding to the two receptors show a clear difference in the binding mechanism: whereas p75^{NTR} displays fast rates of association and dissociation with NGF, TrkA interacts with much slower on and off rates: as a consequence it is the high affinity receptor for NGF, with a K_d of 10^{-9} - 10^{-10} M. When TrkA and p75^{NTR} are co-expressed, the rate of the forward reaction is accelerated, producing the high affinity NGF binding site ($K_d=10^{-11}$ M) (reviewed in Chao and Hempstead, TINS, 1995; and in Neet and Campenot, Cell. Mol Life Sci., 2001). In addition to binding, p75^{NTR} seems also to influence signal transduction through TrkA, by enhancing TrkA autophosphorylation.

Many studies aimed to define the subdomains of the extracellular domain of TrkA which are involved in the binding to NGF. In particular, the subdomains are five: Cys-rich₁ (d1), Leu-rich motif (LRM) triad (d2), Cys-rich₂ (d3); IgGL₁ (d4) and IgGL₂ (d5), where IgGL refers to the immunoglobulin-like C2 folding motif (reviewed in Neet and Campenot, Cell. Mol. Life Sci., 2001).

More insights into the binding surfaces came after the crystallization studies of the human NGF/TrkA-IgGL₂ (d5) complex, which confirmed an extended surface interaction of this subdomain with NGF. By comparison of the structure of the mouse NGF alone, the structure of the human NGF in the complex with TrkA-IgGL₂ (d5) presents few differences. The majority of these differences resides in the sequence difference of certain residues. However, the most striking difference is however at the N-terminus, which is important for receptor binding. It was disordered in all the previously determined structures, while in this case it adopts a helical conformation. It forms an important part of the interface with TrkA-d5 (Wiesmann *et al.*, Nature, 1999), as it appears from fig. 2.1.

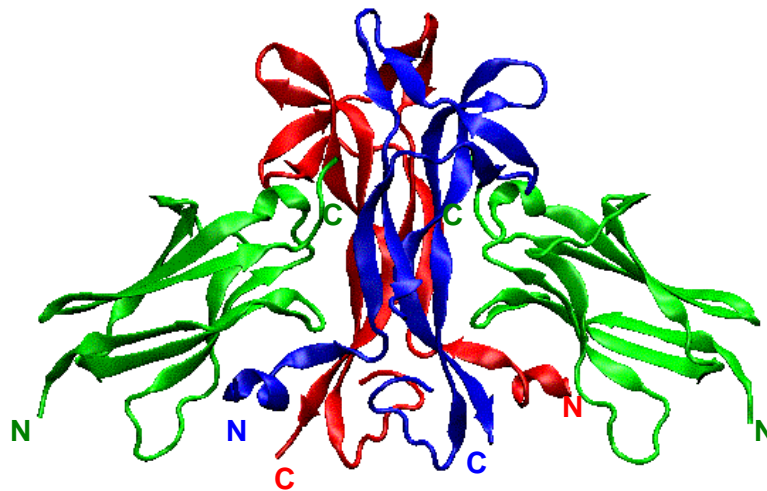


Figure 2.1 – Crystallographic structure of the complex of the TrkA-d5/NGF complex. The figure was generated with the program VMD using the PDB entry 1WWW. The blue and red traces represent the NGF monomers; the green structures are the TrkA-d5 domains. The N- and C-termini of all the components are indicated.

Moreover, the analysis of the structure of the complex allowed the authors to argue that the IgGL₁ (d4) subdomain is unlikely to be close enough to bind NGF. However, the hypothesis of the contribution of other subdomains to the binding cannot be completely excluded, since the crystal structure revealed the occurrence of a likely proteolytic cleavage between the IgGL₁ and IgGL₂ domains.

Thanks to these and other studies, it was possible to get the evidence that at least one, and maybe two IgG subdomains are the main responsible for the neurotrophin binding; the LRM might contribute to the interaction (reviewed in Neet and Campenot, Cell. Mol. Life Sci., 2001).

Also the receptor binding regions of p75^{NTR} has been extensively studied and although the data are somewhat conflicting, the consensus appears to support the second Cys-rich subdomain of p75^{NTR} as being the most important for neurotrophin binding, with the first subdomain being less important (reviewed in Neet and Campenot, Cell. Mol. Life Sci., 2001).

The crystallographic structure of the complex between NGF and p75^{NTR} extracellular domain has been recently determined at 2.4 Å resolution (He and Garcia, Science, 2004; comment by Zampieri and Chao, Science, 2004), helping the interpretation of the binding of this receptor. It is important to point out that the

structure of the complex NGF/p75^{NTR} presents an NGF-to-p75^{NTR} stoichiometric ratio of 2:1, which was also confirmed by size exclusion chromatography and isothermal titration calorimetry (ITC). This is quite a striking feature, since neurotrophins exists as biological dimers and it would be expected that the ligand dimer would bind a dimer receptor, much like the case of TrkA as determined by the crystal structure of the TrkA/NGF complex. In the structure, p75^{NTR} accomodates along a groove formed by the two monomers of NGF; many individual contacts are formed by electrostatic interactions between the positively charged residues on NGF and the negatively charged extracellular domain of p75^{NTR}. The big surprise in the structure was that the formation of the complex induces a conformational change in NGF that renders impossible the binding to a second receptor molecule. This asymmetry might allow the formation of multimeric complexes, formed by p75^{NTR} with various molecular partners, like for example two different neurotrophins, that could indeed induce the conformational changes.

A view of the structure is shown in fig. 2.2.

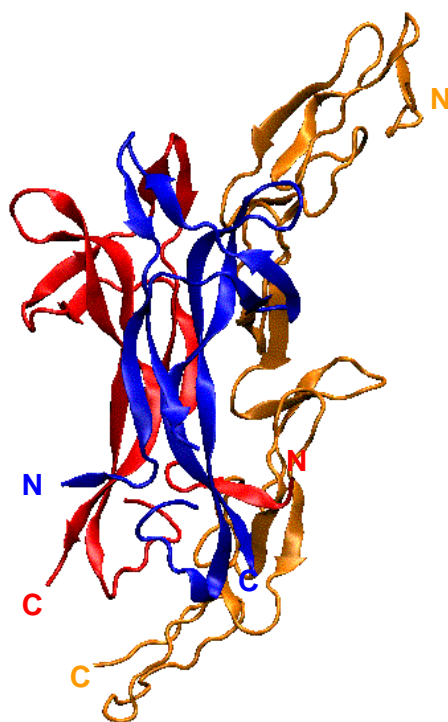


Figure 2.2 – Crystallographic structure of the complex of the p75^{NTR}/NGF complex.

The figure was generated with the program VMD using the PDB entry 1SG1. The blue and red traces represent the NGF monomers; the orange structure is the p75^{NTR} extracellular domain. The N- and C-termini of all the components are indicated.

More recently new insights into the p75^{NTR}/NGF binding enriched the investigation. In fact, the characterization of a symmetric complex of NGF and the ectodomain of p75^{NTR} was described (Aurikko *et al.*, JBC, 2005). The study was done in solution with human p75^{NTR} which included the four cysteine-rich domains of p75^{NTR} and the N-glycosylation site. In this case, at variance with the crystal structure, the Authors describe a binary complex with human NGF, proved by mass spectrometry and analytical ultracentrifugation data. The difference with the crystallographic complex might reside in the p75^{NTR} preparations, since they differ in the species (the crystallographic is from rat and the one used by Aurikko *et al.* is human) and in glycosylation. This symmetric complex was also characterized by solution X-ray scattering (SAXS) experiments which allowed a low-resolution molecular reconstruction of the complex. The outcome was the presence of a larger crowding around the periphery of the complex, if compared with the crystallographic structure, although the overall binding mode of the components was the same.

One still open question in the field of the binding NGF/receptors, is whether or not NGF can bind at the same time to TrkA and to p75^{NTR}. The evidence of the existence of the complex between p75^{NTR} and TrkA was supported by the results of cross-linking and immunoprecipitation experiments (reviewed in Chao and Hempstead, TINS, 1995; and in Neet and Campenot, Cell. Mol. Life Sci., 2001), but still the open question remains for the actual formation of the complex *in vivo*.

The availability of the crystal structures of the complexes of NGF with each one of the receptors and of the SAXS studies of the p75^{NTR}/NGF complex helps to advance toward an answer to the question. An interesting observation was that in the two structures, the receptors reveal an opposite orientation with respect to the membrane. If each C-terminus segment of the receptor extracellular domains was inserted in the membrane, the N- and C-termini of the elongated NGF molecule would be oriented away from the membrane in the case of the TrkA complex, and oriented toward the membrane in the case of p75^{NTR}. This can be easily observed by comparing figs. 2.1 and 2.2, where the N- and C-termini of the proteins are indicated. The crystal structure of the NGF/p75^{NTR} complex indeed confirmed the results already shown for the modelled structures of p75^{NTR} as to the relative orientation of the components (Chapman & Kuntz, Protein Sci., 1995; Shamovsky *et al.*, Protein Sci., 1999).

The comment to this particular observation was already made by Neet and Campenot (Cell. Mol. Life Sci., 2001), and recently reconsidered by Zampieri and Chao (Science, 2004) in the comment to the crystal structure of the complex NGF/p75. In particular, the biological significance of the opposite orientation of the receptors respect to NGF remains still unclear. For example, p75^{NTR} and TrkA may interact within the active complex, binding only a single NGF dimer to either TrkA or p75^{NTR} but not both at the same time (Neet and Campenot, Cell. Mol. Life Sci., 2001). Alternatively, Zampieri and Chao proposed that the binding of a heterodimer composed of p75^{NTR} and TrkA receptor binding to an NGF dimer could take place, preserving the opposite orientation of the two receptors, as shown in fig. 2.3. As explained by the Authors: *“although unconventional, this is nonetheless possible because p75 undergoes multiple cleavages that could release the extracellular ligand-binding domain. Moreover, changes in the conformation of TrkA also can occur”*.

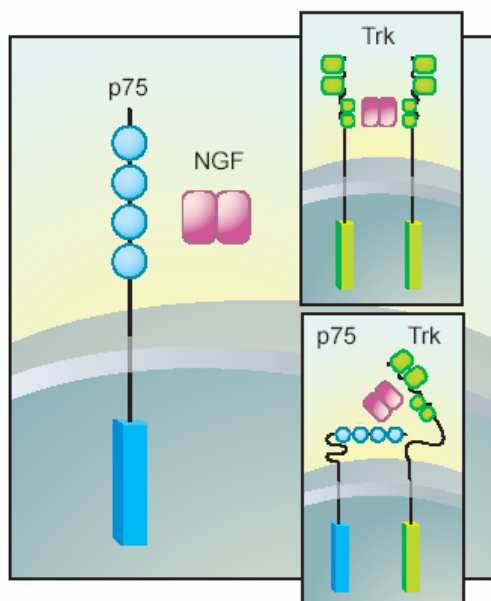


Fig. 2.3 – Models of NGF-receptor interactions. NGF binds a dimeric form of TrkA but a dimeric form of p75^{NTR}. A heterodimer of p75^{NTR} and TrkA would be possible, but would require a rearrangement of the receptors to accommodate the NGF molecule, as depicted in the figure, taken from Zampieri and Chao, Science 2004.

Recently, a new finding has added a further level of complexity to the field of NGF receptors. In fact, a novel p75^{NTR}-related protein, NRH2 was identified. This protein contains a similar transmembrane and intracellular domain as p75^{NTR}, but lacks the characteristic cysteine-rich repeats in the extracellular domain. It was shown that NRH2 is expressed in several neuronal populations that also express p75^{NTR} and TrkA receptors. Although NRH2 does not bind NGF, it was found to interact with TrkA

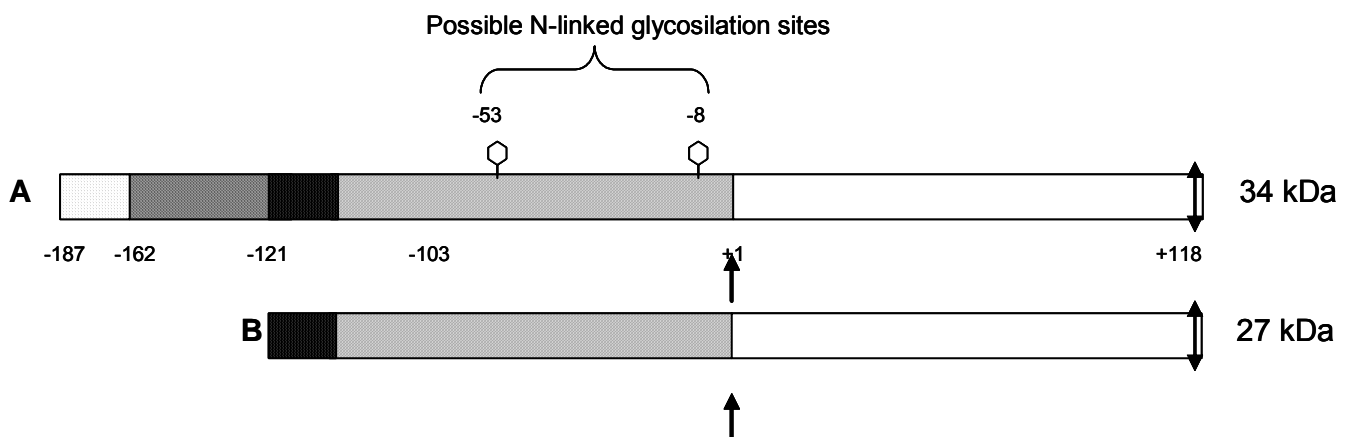
in immunoprecipitation experiments. Moreover, the coexpression of NRH2 and TrkA resulted in the formation of high-affinity binding sites for NGF. This protein, therefore, might be involved in the modulation of TrkA receptor binding properties (Murray *et al.*, J. Neurosc, 2004).

3. The precursor protein of Nerve Growth Factor: pre-proNGF

3.1 Identification and sequence

It was clear already from the identification of the 7S NGF complex, that the existence of an NGF precursor protein was plausible, especially due to the close proximity of the C-terminal Arginine residues of β -NGF with the γ -subunit, that led to the idea that the latter was involved in cleaving a propeptide that extended beyond the C-terminal Arginine residue (Hogue Angeletti and Bradshaw, PNAS, 1971). Indeed, the evidence for the existence of a precursor of β NGF was found (Berger and Shooter, PNAS, 1977) when another NGF-containing protein of about 22 kDa was isolated from submandibular glands, together with the expected 13 kDa β -NGF.

Once the sequences of both mouse and human NGF mRNA were determined (Scott *et al.*, Nature, 1983; Ullrich *et al.*, Nature, 1983), the existence and function of the NGF precursor became clearer. NGF is encoded by a single gene that is over 45 kilobases long (Selby *et al.*, Mol. Cell. Biol., 1987; Ullrich *et al.*, Nature, 1983). Two separate promoters and a total of four exons are alternatively spliced to yield two major and two minor transcripts with the coding sequence at the 3' end in exon four (Edwards *et al.*, Nature, 1986). NGF protein is translated from the two major alternatively spliced transcripts to produce 34 and 27 kDa pre-pro species, with translation initiation sites at amino acid position -187 and -121 respectively, as shown in fig. 3.1.1 (adapted from Fahnestock *et al.*, Progr. Brain Res., 2004).



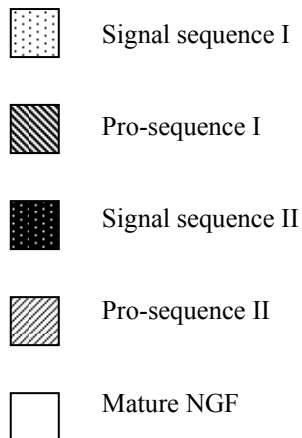


Figure 3.1.1 - Schematic representation of the major translation products arising from alternative splicing of the NGF transcript: the long pre-proNGF form of 34 kDa (**A**) and the short pre-proNGF form of 27 kDa (**B**). The two forms differ by the additional pro-sequence stretch I of 66 amino acids at the N-term of the long form A. Upon removal of the signal sequence, the two products give rise to two proNGF proteins: the long form of proNGF of 32 kDa and the short form of proNGF of 25kDa. The arrows mark the cleavage sites for furin, the double headed arrows represent the C-terminal processing site (post translational modification) and hexagons the potential N-glycosylation sites.

From the nucleotide sequencing of mouse NGF mRNA (Scott *et al.*, Nature 1983), it emerged that the mRNA (1176 nucleotides long) had a 5' untranslated region of 100 bases, a single open reading frame which starts at the first Methionine codon (nucleotides 96-98) and ends with the termination codon (nucleotides 1117-1119). In the sequence, an amino-terminal signal sequence for translocation was also predicted, by analogy with other secreted proteins, although the N-terminal region does not present highly hydrophobic stretches.

The complete nucleotide sequence of mouse pre-proNGF is shown in Appendix 1, while the amino-acid sequence is indicated in fig. 3.1.2, where all the different parts composing the pre-proNGF protein are indicated.

-180 -170 -160 -150
MLCLKPVKLGSLEVGHGQHGGVLACGRAVQGAGWHAGPK
 -140 -130 -120 -110
 LTSVSGPNKGFAKDAAFYTGRSEVHSV **MSMLFYTLITAFLI**
 -100 -90 -80 -70
GVQA EPYTDSNVPEGDSVPEAHWTKLQHSLDTALRRARSA
 -60 -50 -40 -30
 PTAPIAARVTGQTRNITVDPRLFKKRRLHSPRVLFSTQPPP
 -20 -10 +1 +10
 TSSDTLDLDFQAHGTIPFNRTH **RSKR** **SSTHPVFHMGFEFSVC**
 +20 +30 +40 +50
DSVS VWGDKTTATDIKGKEVTVLA EVNINNSVFRQYFFET
 +60 +70 +80 +90
KCRASNPVESGCRGIDSKHWNSYCTTHTFVKALTTDEKQ
 +100 +110 +120
AAWRFIRIDTACVCVLSRKATR **RC**

Figure 3.1.2 – Primary sequence of the whole pre-proNGF. The long precursor is indicated in red, with the putative signal sequence underlined. The signal sequence of the short pro-peptide is highlighted in green; the short pro-peptide is indicated in blue; the mature NGF is highlighted in cyan; the C-terminus amino-acids removed by post-translational modification are highlighted in blue. The consensus sequence for the furin cut is indicated in dark green and underlined.

The occurrence of the long and the short transcripts in different tissues has been investigated: the short one is the predominant one in mouse L cells, in hind limb at several stages of early development, in rat submandibular gland, in placenta and in the developing brain; the long transcript predominates in male mouse submandibular gland (Edwards *et al.*, Nature, 1986).

The different biological significance of the two proteins derived from the major transcripts is by far still not clear. One hypothesis came from Edwards and colleagues after the identification of the two transcripts (Nature, 1986). In particular, in the two proteins the position of the hydrophobic sequence would result different: in the long precursor it resides in the middle of the molecule and it might serve as a membrane anchor (signal sequence II in fig 3.1.1); in the short precursor it is at the

N-terminus, and might act as a signal peptide for secretion (signal sequence II in fig 3.1.1). The long transcript might therefore produce a form of NGF that is membrane-bound and could interact with high efficiency with a receptor on a contiguous cell thus providing cell-to-cell communication.

The precursor protein can be glycosylated and it was reported that trimming of the N-linked oligosaccharide chains was required for transport of proNGF from the endoplasmic reticulum to the *trans* Golgi, where the conversion to NGF occurred (Suter *et al.*, EMBO J, 1991; reviewed in Shooter, Ann. Rev. Neurosci., 2001). It was also reported that the oligosaccharide chains of the pro-segment of proNGF can be sulphated, although no known function for this post-translational modification has been attributed so far (Seidah *et al.*, Biochem. J., 1996). High molecular weight glycosylated NGF precursors, mostly of molecular weight 53 kDa (with other molecular weight bands of 42 kDa and 60 kDa also significantly present), have been identified both *in vitro* and *in vivo* (Reinshagen *et al.*, J. Neurochem, 2000). However, many tissues contain the unglycosylated form of proNGF (Fahnestock *et al.*, Mol. Cell. Neurosci., 2001).

Removal of the signal sequence in the endoplasmic reticulum reduces the translation products to two proNGF species of 32 and 25 kDa (Ullrich *et al.*, Nature 1983; Edwards *et al.*, Nature, 1986), which from now on will be termed as the “long-proNGF” and the “short-proNGF” forms respectively.

The presence of a pair of Arginine residues and of groups of dibasic amino acid residues (compare sequence in fig. 3.1.2), would suggest the presence of cleavage sites in those positions, giving rise to products with intermediate molecular weight of 27-29 kDa, 22-24 kDa and 18-19 kDa, thereby explaining the occurrence of products of these molecular weights in mouse and rat tissues (reviewed in Fahnestock *et al.*, Progr. Brain Res., 2004). The function of these intermediates is poorly understood.

Upon discovery of the proNGF sequence it was surprising to verify that the pro-peptide of NGF was localized at the N-terminus and not at C-terminus of NGF, as it was previously reported in the studies of the interaction with the γ -subunit. Indeed, a pro-sequence is present also at the C-terminus, but it is represented uniquely by a dipeptide Arg-Gly, that is actually cleaved by the γ -subunit. It is not clear whether this processing occurs in other tissues other than the mouse submandibular gland (Fahnestock *et al.*, Progr. Brain Res., 2004).

The processing of the precursor NGF protein to mature active NGF was also studied by *in vitro* and *in vivo* translation experiments on both major transcripts (Edwards *et al.*, JBC; 1988). The *in vitro* products of the two transcripts resulted to be wrongly folded and were degraded by the γ -subunit. On the contrary, the precursors synthesized *in vivo* via the vaccinia expression vector are similarly glycosylated and both were cleaved downstream of the signal peptide. Moreover, they were both effectively cleaved by the γ -subunit and also by trypsin to give active NGF.

The actual processing of the NGF precursor occurs at a four-residue basic site (see arrow in fig. 3.1.1), recognized by a protease of the prohormone convertase family, namely furin (Seidah *et al.*, Biochem. J., 1996). Furin appears to be a likely candidate for the cleavage of proNGF since it is ubiquitously expressed, including in cells that generate neurotrophins and it is produced early in embryonic development, before the appearance of neurotrophins. Furin selectively cleaves the consensus sequence Arg-X-(Lys/Arg)-Arg, which is indeed present just before the N-terminus of NGF. Indeed, co-localization of furin and NGF in granular convoluted tubule cells within submandibular glands of adult mice gave the final confirm that furin effectively processes proNGF (Farhadi *et al.*, J. Histo. & Cytochem., 1997). The fact that furin cleaves proNGF in the trans-Golgi network was also experimentally proven (Mowla *et al.*, J. Neurosci., 1999), corroborating the idea that NGF is processed and released in the constitutive pathway (reviewed in Thomas, Nature Rev.Mol.Cell.Biol., 2002).

Recently, both plasmin and matrix metalloprotease-7 (MMP-7) have also been shown to process the NGF precursor (Lee *et al.*, Science, 2001).

In solution, proNGF most likely is a dimer, as it was demonstrated by Rattenholl and colleagues (Eur. J. Biochem., 2001), who showed that recombinant human short proNGF (rh-proNGF), produced in *E. coli*, is a dimer, using a set of experiments including analytical ultracentrifugation, glutaraldehyde crosslinking followed by SDS-PAGE and gel filtration. Hence, cleavage of the pro-peptide is likely to occur *in vivo* after dimerization. Also the mouse long proNGF form, recombinantly produced in baculovirus, was shown to be a dimer in solution (Fahnestock *et al.*, J. Neurochem. 2004).

Both the long and the short form of proNGF are basic proteins, like NGF (Fahnestock *et al.*, Progr. Brain Res., 2004).

Circular dichroism (CD) spectroscopy experiments suggest that the structure of mature NGF is largely maintained in the presence of the pro-segment (Rattenholl *et*

al., Eur. J. Biochem., 2001), which, on the contrary, shows a limited amount of secondary structure. A further support came also from the digestion with trypsin, which demonstrated that the pro-peptide is readily cleavable and therefore the packing of the pro-peptide into secondary elements seems not to be very tight. The near-UV CD spectroscopic analysis of the recombinantly expressed human short proNGF (rh-proNGF) presented some fine structure, that was suggested to be due to the asymmetrical environment of a Tryptophane in the pro-peptide, probably associated to the mature part.

The biophysical properties of the pro-peptide of NGF in the isolated form have also been investigated and its stability and structure were compared to those of the entire proNGF. For these purposes, the pro-peptide has been recombinantly expressed and has been found to be monomeric in solution, contrary to the dimeric proNGF. The biophysical analysis suggests that the pro-peptide is stabilized by association to the mature part and that in absence of the latter the pro-peptide lacks stabilizing tertiary contacts (Kliemann *et al.*, FEBS, 2004).

It was demonstrated by several reports that in tissues other than submandibular gland (like prostate cells, hair follicles, primary sympathetic neurons, primary rat cortical astrocytes), NGF is likely secreted as proNGF. Accordingly, proNGF have also been found to be the most abundant form of NGF in many tissues, like brain, thyroid gland, retina, prostate, hair follicle, skin, colon and dorsal root ganglia (Fahnestock *et al.*, Progr. Brain Res., 2004). Recently, these results has also been confirmed in sympathetic and sensory ganglia and their target tissues (Bierl *et al.*, Neurosci. Lett., 2005).

A complete investigation of the distribution of proNGF in tissues of aged animals has been recently reported (Bierl *et al.*, Neurobiol. Aging, 2005). It was shown that mature NGF is only weakly expressed in peripheral targets of the aged rat, and that the higher molecular weight NGF forms are predominant in these tissues; most aged tissues showed an increase in the expression of the 25 kDa species, corresponding to the short form of proNGF.

3.2 Biological activity of NGF precursor protein

The pro-domain of NGF is highly conserved between species, and also quite conserved among the different neurotrophins of the family, suggesting an important role for this sequence. A sequence alignment of the long preproNGF of a selection of

species is shown in fig. 3.2.1. A complete sequence alignment of a wider number of species is shown in Appendix 1, together with a sequence alignment of the different pro-neurotrophins.

mouse	MLCLKPKVGLSGLEVGHGQGVLCAGRAVQGGAGWGHPKLTSVSGPNKGFAKDAAFYTRG	60
rat	-----MSALLHR-VLACGRAVQGGAGWHAGPKLTSVSGPNKGFAKDAAFYPGH	46
human	----GRVGAGS----RRGAQR-VLASGRAVQGGAGWHAGPKLTSSASGPNNSTFGAAFPYGH	52
	. . . : . *** . ***** : . * . * . * . * . * :	
mouse	SEVHSVMSMLFYTLITAFLLIGVQAEPYTDNSNVEGDSVPEAHWTKLQHSOLDALRRARS	120
rat	SEVHSVMSMLFYTLITAFLLIGVQAEPYTDNSNVEGDSVPEAHWTKLQHSOLDALRRARS	106
human	TEVHSVMSMLFYTLITAFLLIGVQAEPHSESNVPAGHTIPQVHWTKLQHSOLDALRRARS	112
	: ***** : ***** : : ***** * . : : . : *****	
mouse	PTAPIAARVTGQTRNITVDPRLFKKRRLHSPRVLFSTQPPPTSSDTLDLDFQAHGTIPFN	180
rat	PAEPIAARVTGQTRNITVDPKLFKKRRLRSPRVLFSTQPPPTSSDTLDLDFQAHGTISFN	166
human	PAAAIAARVAGQTRNITVDPRLFKKRRLRSPRVLFSTQPPREAADQLDDEFVGGAAPFN	172
	* : . ***** : ***** : ***** : ***** : : ** ***** : * : . **	
mouse	RTHRSKRSSSTHPVFHMGESVCDSSVSVWVGDKTTATDIKGKEVTVLAEVNNINNSVFRQYF	240
rat	RTHRSKRSSSTHPVFHMGESVCDSSVSVWVGDKTTATDIKGKEVTVLGEVNNINNSVFKQYF	226
human	RTHRSKRSSSHPIFHRGESVCDSSVSVWVGDKTTATDIKGKEVMVLGEVNNINNSVFKQYF	232
	***** : ** : * ***** ***** * * . ***** : **	
mouse	FETKCRASNVPESGCGRGIDSKHWSYCTTHTTFVKALTTDEKQAAWRFIRIDTACVCVLS	300
rat	FETKCRAPNVPESGCGRGIDSKHWSYCTTHTTFVKALTTDDKQAAWRFIRIDTACVCVLS	286
human	FETKCRDPNPVDSGCGRGIDSKHWSYCTTHTTFVKALTMDSGQAAWRFIRIDTACVCVLS	292
	***** . *** : ***** ***** * *****	
mouse	RKATRRG 307	
rat	RKAARRG 293	
human	RKAVERRA 299	
	*** **	

Although for a long time it was assumed that no specific biological function could be attributed to proNGF, the findings of the most recent years shed new light on this NGF form and helped to elucidate its function *in vivo*.

complete analysis on the *in vitro* renaturation of rh-proNGF (Rattenholl *et al.*, JMB, 2001). The method used to determine the pathway of re-oxidation is chemical labelling of the intermediates followed by mass spectrometry. Aliquots of the renaturation mixture withdrawn at different times during refolding process were alkylated with iodoacetamide as a thiol-blocking reagent. Thereby, the free SH groups could be trapped and the molecular mass of the intermediates increased allowing to identify those containing different numbers of disulfide bonds. The various intermediates were also identified by proteolytic digestion followed by MALDI-MS analysis. The outcome was that indeed the pro-region of proNGF facilitates refolding of NGF. In fact, both the yield and the rate of rh-proNGF folding were significantly enhanced when compared with the *in vitro* refolding of mature recombinantly expressed human NGF, rh-NGF. The proposed function for the pro-sequence would consist in acting as a specific scaffold during the structure formation of the Cystein knot motif of NGF. Once the native disulfide bonds are formed, the characteristic β -sheet structure is formed and two monomers can associate to form the rh-proNGF dimer. Alternatively, the pro-sequence of NGF could passively confer solubility to aggregation-prone folding intermediates by shielding hydrophobic patches and thus enhancing folding yields. It is interesting to note that addition of pro-peptide on *in vitro* refolding of rh-NGF did not enhance the low renaturation yields (Rattenholl *et al.*, JMB, 2001).

Regarding the biological role of proNGF, Lee and colleagues recently demonstrated that it promotes apoptosis. They produced a furin-resistant long proNGF protein by changing two conserved Arginine residues to Alanine (Lee *et al.*, Science, 2001) and isolated sufficient protein quantity for binding and functional analysis; the isolation of the material was somehow complicated by the fact that proNGF could be cleaved by various extracellular proteases despite the mutation for furin. The most striking finding was that proNGF bound to p75^{NTR} with an about five times stronger affinity than mature NGF (i.e. with a binding constant of 10^{-10} M); conversely, proNGF bound TrkA much less strongly than mature NGF. Moreover, proNGF was found to have a greater potency for activation of a p75-mediated cellular response, namely induction of apoptosis of smooth muscle cells.

These finding opened a completely new way of considering proNGF as a potential functional protein, and the NGF-mediated signalling in general (reviewed in Hempstead, Curr. Opin. Neurob., 2002; Chao and Bothwell, Neuron, 2002). For

example, in this view the definition of TrkA and p75^{NTR} as high- and low-affinity receptors lose part of the previous meaning. Moreover, the open question is addressed on the kind of structure adopted by the pro-neurotrophin and the features of the surface exposed to interaction with p75^{NTR}. Therefore, a new scenario for the role of neurotrophins has been indicated, where the balance between cell death and cell survival might be determined by the ratio of proNGF and mature NGF secreted by cells.

Indeed, the long form of proNGF was found to be the most abundant form of NGF in brain and to show increased levels in post-mortem samples of parietal cortex from Alzheimer's patients (Fahnestock *et al.*, Mol. Cell. Neurosci., 2001). This findings raise the possibility that p75^{NTR} activation may contribute to disease pathology.

On the contrary, experiments from various laboratories, have proven that the proNGF molecule did possess an activity, although lower than the one of mature NGF (Fahnestock *et al.*, Progr. Brain Res., 2004). Most recently, these results have been confirmed by a set of experiments in sympathetic cervical ganglion (SCG) neurons and PC12, that showed that the specific activity of the long proNGF form is approximately five-fold less than that of mature NGF (Fahnestock, J. Neurochem., 2004). These results suggest that some forms of proNGF might indeed be neurotrophic.

Moreover, certain peptides derived from the NGF precursor were found to possess biological activity: they could activate TrkA in PC12 cells, although they were unable to induce neurite outgrowth in PC12 cells (Dicou *et al.*, J. Cell Biol., 1997) and they were shown to enhance cholinergic enzyme activities *in vivo* (Clos & Dicou, Dev. Brain Res., 1997).

In light of these new findings, proNGF has also been defined as a "Jekyll-Hyde neurotrophin" (Ibáñez, TINS, 2002). A model for the receptor discrimination by mature NGF and proNGF has been proposed, depicted in fig. 3.2.2:

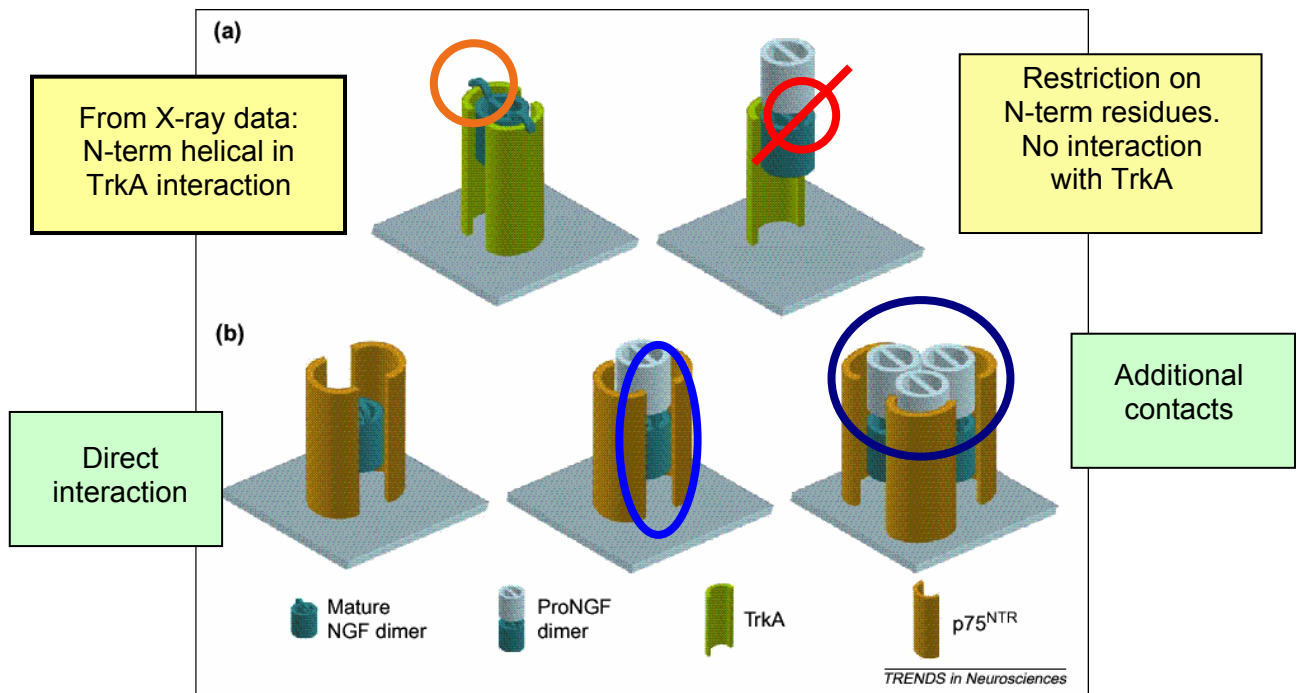


Figure 3.2.2 – Hypothesis of the binding mode of NGF and proNGF to the p75^{NTR} and TrkA receptors. The figure is taken from Ibáñez, TINS, 2002

In particular, the binding of proNGF to p75^{NTR} might be more efficient for two reasons: on one side, the pro-sequence could provide a more extended interaction surface with the receptor in comparison to NGF; on the other side an oligomerization process could take place through the pro-sequences and increase the affinity, giving rise to trimerization of proNGF dimers (Ibáñez, TINS, 2002).

Further support to the vision of proNGF as an apoptotic ligand came from a recent study, where upregulation of proNGF was found to be causally linked to p75^{NTR}-mediated oligodendrocyte death following spinal cord injury (Beattie *et al.*, Neuron, 2002).

Moreover, microglia-derived proNGF has been shown to promote photoreceptor cell death via p75^{NTR} (Srinivasan *et al.*, JBC, 2004).

Once again, a possible model was suggested, to re-interpret the available data on the neurotrophin signalling. In particular, mature neurotrophin would selectively bind Trk, whether it is expressed alone or complexed with p75^{NTR}, while pro-neurotrophins would bind selectively to p75^{NTR} but not to Trk, as depicted in fig. 3.2.3 (Teng and Hempstead, CMLS, 2004). Support to this hypothesis will come from a re-

evaluation of prior studies to assess the ratio of pro-neurotrophin *versus* mature neurotrophin which is released from cells for differential receptor activation. Moreover, the availability of specific pro-domain antisera will help to distinguish the pro- and mature forms.

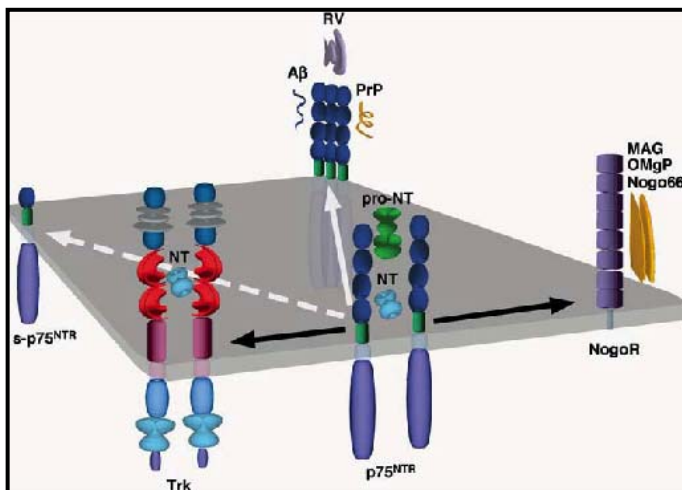


Figure 3.2.3 – Hypothesis on the NGF and proNGF signalling. Figure from Teng and Hempstead, CMLS, 2004

The presence of controversial data on the neurotrophic or apoptotic activity of proNGF as shown in the previous statements, makes it difficult to have a final vision on the actual role of proNGF *in vivo*.

One suggestion for the understanding of the problem came recently from Fahnstock and colleagues (Progr. Brain Res., 2004). The authors suggest that proNGF is responsible for the normal neurotrophic activity in most tissues, but that injury increases the processing of proNGF to NGF and thereby provides a rapid and local supply of the more neurotrophically-active mature NGF. However, the authors also point out a certain number of experiments still needed before claiming a clear understanding of the question. In particular, it is not clear whether both proNGF and NGF are internalized by cells or, if they do, whether they are internalized at the same rate; it is not known whether they are both retrogradely transported at the same rate, or if NGF-induced signal transduction pathways are similarly activated by proNGF. Since many of the experiments performed so far made use of recombinant proNGF, an important help for a better understanding of the authentic role of proNGF would come from the possibility of isolating native, full-length protein to a high degree of homogeneity and from its further characterization.

The field is continuously evolving, and indeed recent studies provided a new piece for the pro-neurotrophin puzzle. In particular, new findings in favour of the role of proNGF as the physiological ligand for p75^{NTR} under physiological conditions were reported, since secreted proNGF was found to be a pathophysiological death-inducing ligand after adult CNS injury. In this report it was for the first time demonstrated that proNGF can be detected in extracellular fluids, such as cerebrospinal fluid, suggesting a significant biological role for this protein in the adult brain after lesion (Harrington *et al.*, PNAS, 2004; commentary by Barde, PNAS, 2004). Moreover, in the same study, it was shown that intracortical infusion of proNGF-specific polyclonal antibody results in complete rescue of the lesioned corticospinal neurons, because of the antibody interference with the binding of proNGF to p75^{NTR}. These data revealed a potential target for pharmacological intervention in diseases in which neuronal death is a pathogenic factor.

The investigation of the functional role of proNGF is also open to other fields: it has been recently reported, for example, that accumulation of proNGF is detected in the rat uterus during pregnancy (Lobos *et al.*, Endocr, 2005).

3.3 The proNGF receptor

The field of pro-neurotrophins has gained an important new piece of information from a recent publication on the discovery of the specific receptor for proNGF: Sortilin. In fact, the binding of Sortilin to proNGF was found to be essential for proNGF-induced neuronal cell death (Nykjaer *et al.*, Nature, 2004). Sortilin is a sorting protein originally identified for its ability to interact with a receptor-associated protein (RAP) (reviewed in Mazella, Cell. Signall., 2001), which was found to bind the neuropeptide neurotensin with high affinity. Sortilin, together with the receptors SorLA and SorCS, forms a new receptor family, characterized by the presence of a luminal/extracellular region containing a Cystein-rich domain homologous to the yeast vacuolar sorting protein Vps10p and one transmembrane region preceding a short intracellular part bearing signals for rapid internalization. The peculiarity of this receptor family is the presence of at least one cleavage site for the protein convertase furin at the N-terminal sequence of their Vps10p domain. All the receptors of the family are present in the brain; Sortilin and SorLA are present particularly in the hippocampus, dentate gyrus and cerebral cortex.

In the paper by Nykjaer and colleagues (Nature, 2004), the authors found that Sortilin interacts with the pro-region of proNGF with high affinity and does not have affinity for mature NGF; the data were obtained both *in vitro* by BIAcore binding studies and *in vivo* through cell transfection. They proved that sortilin was essential for proNGF to induce cell death through p75^{NTR} in various cell types known to undergo apoptosis mediated by proNGF: in other words, proNGF simultaneously binds Sortilin (*via* the pro-sequence) and p75^{NTR} (*via* the mature NGF) and thereby acts as a crosslinker, creating a ternary complex (Nykjaer *et al.*, Curr Opin Neurobiol, 2005). Consequently, sortilin was found to be a third important receptor in neurotrophin signalling. The authors suggested that Sortilin serves as a co-receptor and molecular switch, enabling neurons expressing TrkA or p75^{NTR} to respond to a pro-neurotrophin and to initiate pro-apoptotic rather than pro-survival action. In the absence of Sortilin, a regulated activity of extracellular proteases may cleave proNGF to mature NGF, promoting Trk-mediated survival signalling, as depicted in the scheme in fig. 3.3.4.

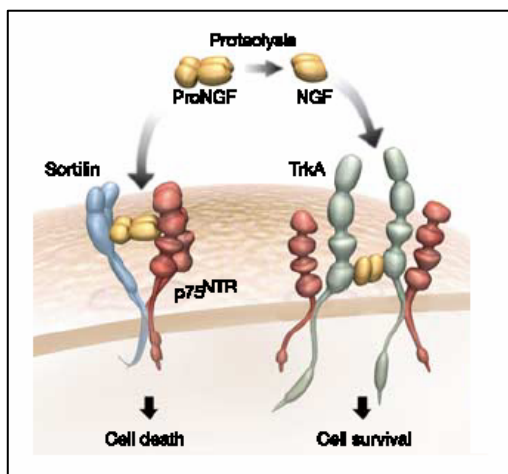


Figure 3.3.4 – Proposed mechanism for the signalling of NGF and proNGF, involving Sortilin receptor, besides the “traditional” receptors p75^{NTR} and TrkA. Figure from Nykjaer and colleagues, Nature 2004

To date, little is known about the signalling pathways elicited by Sortilin-p75^{NTR} complex, but several possibilities exist. Sortilin might simply function to facilitate proNGF binding to p75^{NTR}. Alternatively, its cytoplasmic tail might provide a template for adaptor proteins to modulate or even activate p75^{NTR} signalling. Some recent results seem to support this second hypothesis (Nykjaer *et al.*, Curr Opin Neurobiol, 2005).

These new findings help to better understand the functional role of proNGF *in vivo*, but also raise many questions, as stated in the comment to the paper by Kaplan

and Miller (Nature, 2004). The first question is if Sortilin is required for p75^{NTR}-induced cell death also in the whole organism, besides in cultured cells. Secondly, it is still not well understood what is the death signal that emanates from the p75^{NTR}-Sortilin complex, since Sortilin was first found to regulate protein movement within cells; maybe it could function as a chaperone for p75^{NTR} to specific compartment in cells to bind certain death-inducing proteins. Finally, there is little information available on the way the expression of proNGF and neurotensin is regulated during development and injury.

Recently, another protein of the Sortilin family, SorCS3 has been investigated as a putative receptor for proNGF, like Sortilin. Indeed, SorCS3 has been shown to bind proNGF with high affinity, but unlikely Sortilin, the binding strength is of the same order of magnitude also for NGF. Therefore, more studies will be necessary to validate the implication of Sortilin in pro-neurotrophin signalling (Westergaard *et al.*, FEBS, 2005).

A possible scenario for the way of action of Sortilin in pro-neurotrophin binding has been recently proposed, involving also the point of the cellular localization of the involved proteins (Bronfman & Fainzilber, EMBO reports, 2004). Indeed, it has been proposed that pro-neurotrophin/Sortilin interactions could commence intracellularly within the secretory pathway. Sortilin binding to the pro-domain of the neurotrophin in the Golgi apparatus protects it from proteolytic cleavage, and the molecules could then travel to the cell surface in a preformed pro-apoptotic p75-activating complex. Therefore, Sortilin regulation might be a way for the cell to possess a mechanism of active suicide. Alternatively, cell-surface cleavage of Sortilin could release a soluble Sortilin/pro-neurotrophin complex into the extracellular space. This kind of complex could represent a circulating reservoir of pro-neurotrophin protected from cleavage to the mature form and available for interaction with receptors on adjacent or distant cells. The representation of this proposed scenario is represented in fig. 3.3.5.

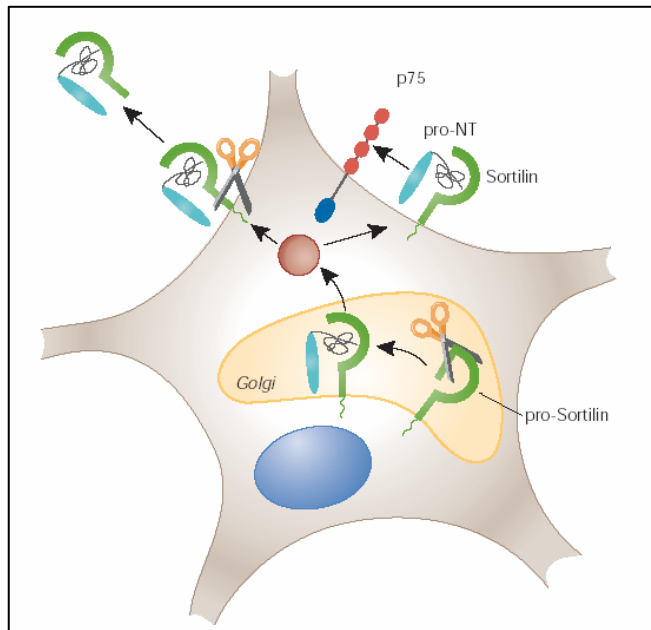


Figure 3.3.5 – Proposed ways to the Sortilin regulation. On the left side the extracellular release of the Sortilin/proNGF complex; on the right side, the cell surface complex. Figure from Bronfman and Fainzilber, EMBO reports, 2004

All these levels of complexity, and especially the new findings involving $p75^{\text{NTR}}$ and its partners, like sortilin, help in better understanding many mechanisms of the molecular functions of the nervous system, and, as stated recently by Barker (Neuron, 2004), mark the beginning of a new phase of neurotrophin receptor research. Indeed, in the review by Nykjaer and colleagues (Curr Opin Neurobiol, 2005), $p75^{\text{NTR}}$ appears to be a key character in the scene of regulation of neuronal survival, by interacting with different partners to promote life (mature neurotrophin and Trk receptor) or induce cell death (pro-neurotrophin and Sortilin). Of course, still much has to be done before reaching a complete comprehension of the problem, particularly as to the investigation of the basis of the choice of $p75^{\text{NTR}}$ of the proper partner to live or let die.

Besides proNGF, also the biological role of the other pro-neurotrophins has been recently investigated. Indeed, a recombinant cleavage resistance form of proBDNF has been found to be a pro-apoptotic ligand for cultured sympathetic neurons, *via* activation of a receptor complex of $p75^{\text{NTR}}$ and sortilin (Teng *et al.*, J. Neurosci., 2005). These results support the idea that pro-neurotrophins are true ligands with distinct physiological functions than mature neurotrophins, and not merely intracellular precursors.

4. NGF, proNGF and Alzheimer's disease

To understand the role played by NGF in Alzheimer's disease (AD), many different kinds of investigations have been carried out, aimed first of all to compare NGF levels in the normal and pathological state.

It was indeed found that NGF mRNA levels are the same in controls and AD, but the protein levels were slightly higher in AD patients *versus* normal individuals (Fahnestock *et al.*, Mol. Brain Res., 1996). These data supported the hypothesis of a reduced efficiency in the retrograde transport of NGF by degenerating basal forebrain cholinergic neurons. Besides the changes in NGF protein expression in various stages of AD, also the reduction of the TrkA protein has been observed. On the contrary, the p75^{NTR} protein levels are unchanged in AD. Therefore, the putative “off Trk” cycle of deficient NGF signalling may contribute to the selective degeneration of cholinergic neurons observed in AD (reviewed in Counts *et al.*, J Neuropath Exp Neuro, 2005).

In light of the discovery of the role of the neurotensin receptor Sortilin in the binding to proNGF (see previous paragraphs), the possible scenario for the role of neurotrophins in AD has slightly changed. Indeed, besides the finding that Sortilin might be binding partner of p75^{NTR} during cell death, preliminary findings suggest that cortical Sortilin levels are increased in AD patients compared with normal controls (reviewed in Counts *et al.*, J Neuropath Exp Neuro, 2005).

Indeed, proNGF isolated from human brain affected by Alzheimer's disease has been found to effectively induce neuronal apoptosis mediated by p75^{NTR} (Pedraza *et al.*, Am. J. Pathol., 2005). The authors also confirmed the increased levels of a 53 kDa form of proNGF in AD; as previously reported, this form is glycosylated and interestingly, a high degree of glycosylation in some proteins such as acetylcholinesterase, APP and tau has been reported in AD. Since glycosylation may protect from proteolytic hydrolysis, this could also provide an explanation for the predominance of glycosylated forms of proNGF in AD human brain samples.

In light of these results, a picture can be obtained to model the putative scenarios for proNGF/receptor complexing during the progression of AD, as shown in fig. 4.1, where signaling in cholinergic neurons changes from the pro-survival (A) to pro-apoptotic (B) as the TrkA levels decline; p75^{NTR} levels remain unchanged and proNGF levels rise in cortical projection sites during the progression of AD.

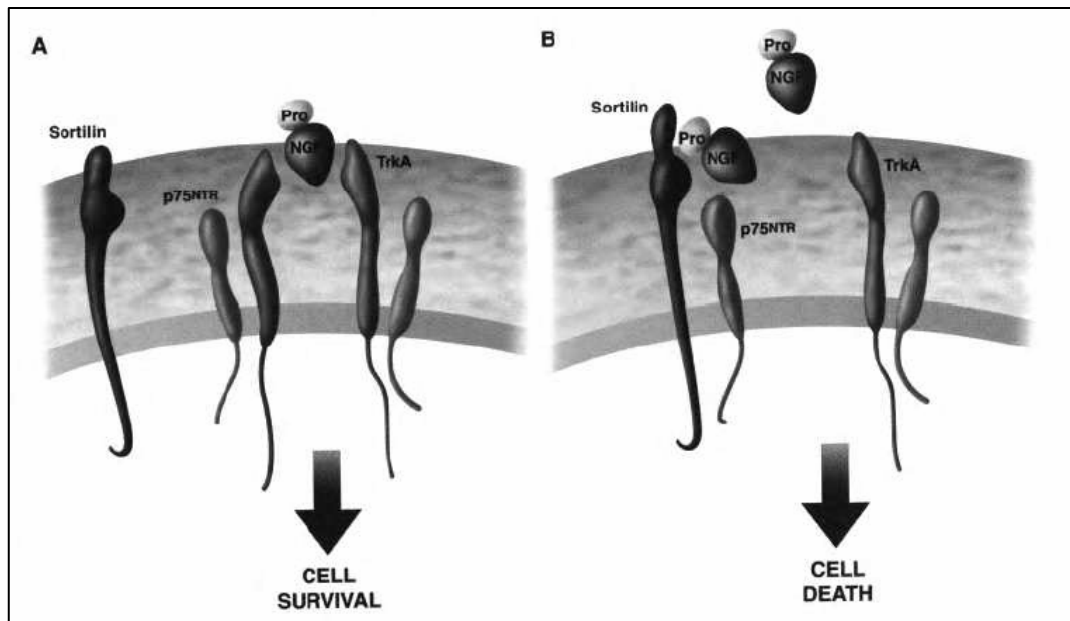


Figure 4.1 – (A) proNGF complexes with TrkA to activate cell survival mechanisms in the aged human healthy brain. This binding event is facilitated by the coexpression of p75NTR on the cell surface. (B) elevated levels of cortical proNGF in the face of reduced cortical TrkA results in increased binding of proNGF to p75NTR/sortilin complexes, enhancing the activation of pro-apoptotic mechanism during the evolvement of AD. Figure taken from Counts *et al.*, J. Neuropath. Exp. Neurol., 2005.

Many therapeutic applications of NGF have been investigated, given the wide spectrum of possible implications of this protein. Indeed, the studies performed on animals have shown that delivery of NGF reverses age-related and cholinergic lesion-induced spatial memory deficits (reviewed in Counts *et al.*, J. Neuropath. Exp. Neurol., 2005).

However, the drawbacks in the use of the intact protein, especially in the delivery methods, have prevented so far a wide clinical application of NGF (Longo and Massa, J. Alz. Dis., 2004). However, a new field comprises the development for therapeutic use of small molecule ligands for the neurotrophin receptor, retaining the biological activity of the natural protein, but presenting more advantages (Longo and Massa, J. Alz. Dis., 2004).

In light of the involvement of NGF in AD, an anti-NGF mouse model for AD was developed (Ruberti *et al.*, J. Neurosc., 2000): the AD11 mice express a recombinant antibody neutralizing NGF activity (mAb α D11). Because the levels of transgenic anti-NGF antibodies are three order of magnitude higher in adult than in newborn mice, effective inhibition of NGF actions occurs in adult animals only. Indeed, the level of free NGF in the brain of two-month old AD11 mice is less than half than in control mice. For this reason, the aged anti-NGF mice display, as a result of NGF deprivation, a progressive degeneration with phenotypic changes, presenting the histological hallmarks characteristic of AD, including neurofibrillary tangles, tau hyperphosphorylation, amyloid plaques, neuronal death, cholinergic deficits and selective behavioral impairments, closely resembling those found in AD (Capsoni *et al.*, PNAS, 2000; Capsoni *et al.*, Mol. Cell. Neuro., 2002). Recently, it has been reported that intranasal administration of NGF to AD11 mice in a well defined time window could revert recognition memory deficits (De Rosa *et al.*, PNAS 2005).

ABSTRACT OF THE THESIS

The aim of this Thesis was a structural and functional characterization of mouse proNGF, for an insight into the biological role of proNGF, especially for a comparison to the one of NGF. More in particular, one specific question addressed in this thesis was to ask whether and how the presence of the pro-domain changes the overall structure of the mature NGF moiety. The distinctive approach to gain some insight into this question was to perform a number of binding studies with well characterized molecules (soluble receptors or antibodies), that are used as “structural probes”. This is the novelty of the work performed in this thesis.

The results obtained in the investigation of the functional and structural role of rm-proNGF will be described, presented in two separate sections.

In the first one, the functional and structural experiments carried out on the recombinantly expressed m-proNGF will be presented; in the second one, the work on the selection and characterization of an anti-proNGF antibody in the form of scFv will be presented.

To achieve these results, the cDNA of the short form of proNGF was cloned by RT-PCR from submandibular glands of mouse, and the protein expressed *in vitro* in *E. coli*. The mature NGF moiety is characterized by the presence of a complex disulfide bridge net, that represents an obstacle when expressing the protein in the reducing environment of *E. coli*: in fact, in these conditions proNGF is not soluble and is stored into inclusion bodies, and the protein needs to be refolded *in vitro*. In this Thesis the same procedures were applied, that were already published for the refolding of the recombinant human proNGF. The *in vitro* produced protein (rm-proNGF) was carefully characterized, and the protein turned out to be correctly folded and functional, as emerged from the comparison of the biophysical properties with the human one. Moreover, the mature NGF was obtained by proteolytic cleavage from rm-proNGF, and it was verified by *in vitro* biological studies (PC12 cells differentiation and TrkA phosphorylation assay) that the mature neurotrophin was as active as the commercial protein, giving a further prove for the effective *in vitro* refolding of rm-proNGF.

As side studies, this thesis also aimed to an investigation of the difference between the two main proNGF forms, the short and the long one. Besides the short form of rm-proNGF, therefore, also the long variant was cloned and expressed, although the

purification protocols for the long m-proNGF needs still to be optimized. Moreover, two fusion proteins of the pro-peptide of proNGF with GST protein were generated, designed to obtain possible models for the study of the functional role of the pro-peptide *in vitro*.

The availability of high amounts of the purified rm-proNGF allowed to perform a whole series of experiments aimed to characterize the protein from the physico-chemical and structural point of view. The general question was addressed in this thesis, whether the proNGF had any functional difference in respect to NGF, arising from a different structural arrangement. To this aim, two different approaches were selected. On one side, a series of binding studies was carried out, using a panel of anti-NGF antibodies and the two NGF receptors, p75^{NTR} and TrkA, as structural probes; the binding studies were carried out with BIAcore. On the other side, the structural arrangement of rm-proNGF in solution was investigated by mean of SAXS (Small Angle X-ray Scattering). In both cases, the properties of rm-proNGF were compared to the ones of m-NGF in the same conditions. The whole approach represents the novelty of this thesis.

The high degree of flexibility of the pro-peptide gives rise to an intrinsic disorder, that renders proNGF a difficult protein to crystallize for structural purposes. For this reason, SAXS was chosen as the technique to investigate the structure and dynamic of m-proNGF in solution. Thanks to the SAXS measurements, it was possible to reconstruct two possible models for the tri-dimensional arrangement of rm-proNGF in solution, eventually describing the extremes of a dynamic equilibrium in solution. For the first time it was possible to get insights into the 3D structural arrangement of rm-proNGF and to design a structure-based hypothesis on the role of proNGF *in vivo*; in particular, a possible equilibrium in solution was hypothesized between a close and an open conformation, upon binding to different ligands, like receptors or specific antibodies.

Besides the structural investigations, a series of functional studies were performed, in order to unravel some of the properties of rm-proNGF and to look into the difference of its behavior in comparison with that of the mature m-NGF. In this Thesis, various types of studies were employed, to investigate the binding properties of the m-proNGF with various partners. In particular, the kinetics of binding with the two NGF receptors, *i.e.* TrkA and p75^{NTR}, were studied using BIAcore. With the same technique, the differential binding of m-proNGF and m-NGF versus a panel of anti-

NGF antibodies was investigated. In particular, a complete kinetic analysis was carried out with the α D11 anti-NGF antibody, (involved in the AD11 mouse model for AD), to investigate the possible influence of the different binding modes of the neurotrophins at the molecular level of the disease.

Besides the experiments *in vitro*, the comparison of the effect of proNGF and of NGF was carried out through functional assays on cell cultures.

To complete the approach on the structural and functional studies on proNGF, an important tool was developed: a novel anti-proNGF antibody was selected in the scFv format using a yeast two-hybrid system and characterized both from the biophysical-biochemical and from the functional point of view. It was possible to express it on large scale in *E. coli* and get information on its binding properties by mean of ELISA and BIAcore measurements. Moreover, a structural study of the scFv in solution through SAXS was carried out. A further development of this tool should allow a wider application on the study of the biological role of proNGF. In particular, this antibody represents a new tool for the investigation of the binding properties of proNGF and for its functional characterization.

EXPERIMENTAL SECTION

1. Materials

1.1. Chemicals and biochemicals

Acrylamide/bis-acrylamide (30% in water)	Fluka
Ampicillin	Sigma
L-Arginin	Ajinomoto and Sigma
dNTPs	Invitrogen
Glutathion (both oxidized ad reduced)	Fluka
Guanidinium hydrochloride, C-Grade (GdmCl)	Nigu Chemie
Guanidinium hydrochloride, ultra pure (GdmCl)	Fluka
Yeast extract	Difco/Becton Dickinson
Isopropyl-b-D-thiogalactopyranoside (IPTG)	Talent
Kanamycin	Sigma
Mineral oil for PCR	Sigma
N,N,N',N'-Tetramethylethylenediamine (TEMED)	Fluka
Trypton	Difco/Becton Dickinson
Developing solution for ECL	Kodak
Fixing solution for ECL	Kodak
BCIP (5-bromo-4-chloro-3 indolyl phosphate) for alkaline phosphatase staining (disodium salt, in 100% DMF)	Boehringer
NBT (nitrate blue tetrazolium) for alkaline phosphatase staining (in 70% DMF)	Boehringer

All the other chemicals used were mainly from Sigma and Fluka companies and had a technical purity grade.

For the preparation of all used buffers, bi-distilled water was employed.

1.2. Standards and kits

Amine Coupling kit for CM5 chip protein immobilization: from BIAcore

DNA ladders: Mass Ruler, Fermentas

DNA sequencing kit: LC SequiTherm Excel II. Epicentre Technologies
 ECL detection kit: Amersham Pharmacia
 Miniprep and Midiprep: QIAgen and Sigma
 Mutagenesis: QuickChange from Stratagene
 Protein Concentration: DC Protein Assay, Bio-Rad (according to Lowry)
 Protein Marker: Kaleidoscope prestained standard from Bio-Rad and wide-range
 prestained from Fermentas
 mRNA isolation: QIAgen – Oligotex. Direct mRNA protocol for polyA isolation
 from animal tissues – MINI KIT
 RT-PCR: access introductory system by Promega

1.3. Enzymes and other proteins

Alkaline Phosphatase (from calf) – CIAP	NEB
Bovine serum albumin (BSA)	Sigma
Dnase I	Fluka
EDTA-free protease inhibitor cocktail	Roche
Lysozyme	Sigma
NGF, human, recombinant from E. coli	generous gift from Dr. Elisabeth Schwarz (Halle)
proNGF, human, recombinant from E. coli	generous gift from Dr. Elisabeth Schwarz (Halle)
NGF, mouse, 2.5S	Alomone
p75 ^{NTR} , immunodhesin	generous gift from LLG
Pfu DNA Polymerase	Promega
Protein L, recombinant	PIERCE
Red Taq-DNA polymerase	Sigma
Restriction enzymes	NEB
RNase	Sigma
T4-DNA-Ligase	NEB
TrkA, immunoadhesin	generous gift from LLG
Trypsin	Roche Diagnostics
Furin	Sigma

1.4. Antibodies

α SV5: supernatant, prepared in the laboratory according to (Hanke *et al.*, J Gen Virol, 1992)

9E10: supernatant, prepared in the laboratory according to (Evan *et al.*, Mol Cell Biol, 1985)

α D11: supernatant, prepared in the laboratory according to (Cattaneo *et al.*, J Neurochem, 1988)

4C8: supernatant, prepared in the laboratory according to (Cattaneo *et al.*, J Neurochem, 1988)

27/21: supernatant, Korshing and Thoenen, 1987

α D11, 4C8, 27/21: purified monoclonal antibodies were a generous gift of dr. Sonia Covaceuszach, from LayLine Genomics (LLG)

YL anti-tubulin: supernatant, prepared in the laboratory according to Kilmartin *et al.* JBC, 1982

anti-GFP: polyclonal, affinity purified on GFP-coupled chromatographic column (F. Paoletti and K. Ainger, SISSA)

Anti-His tag antibody (from ascites): from Amersham Pharmacia

Anti-GST polyclonal antibody: from SIGMA

Anti- NGF polyclonal antibody: from SIGMA

Anti-proNGF polyclonal antibodies: from Alomone and from Chemicon

Anti-SV5 monoclonal antibody, HRP conjugated: from Invitrogen

Anti-SV5 monoclonal antibody: from SIGMA

All the HRP-conjugated secondary antibodies: from Dako

All the AP-conjugated secondary antibody: from SIGMA

1.5. Other materials

Dialysis tubes, Spectra-Por 8/10K and 12/14K	Spectrum
Nitrocellulose membrane	Amersham Pharmacia
Sterile filters (0.2 and 0.45 μ m)	Millipore
Filtration device (for buffers – 0,22 μ m)	Corning
Concentration device for proteins (MWCO 10000), 15 mL and 0.5 mL	Amicon and VivaScience
Photographic films	Amersham Pharmacia

1.6. Instruments

(Only the main instruments used are listed)

Centrifuge: Beckman Coulter

Cell-Homogenisator: Gaulin Micron Lab 40, APV Homogeniser

DNA sequencing: Li-COR system

FPLC chromatographic separation of proteins: ÄKTA system with P-900 pump, UPC-900 UV-Monitor, Frac-900 Fractions collector. Data recording and analysis with Unicorn Software. (Amersham Pharmacia)

Gel electrophoresis systems (both agarose and acrylamide): Amersham Pharmacia

Spectrofluorimeter: Perkin Elmer LS 50B luminescence spectrometer

Surface Plasmon Resonance: BIAcore 2000 and BIAcore 3000 from Biacore AB

Transfer apparatus: semi-dry system, from Amersham Pharmacia

Thermocycler (PCR): MJ Research PTC-100

Ultraturrax: T25, IKA

1.7. E. coli strands and plasmids

E. coli DH5 α F' (GIBCO) – used for all the cloning procedures of plasmid DNA

E. coli BL21 (DE3) (Novagen) – used for the expression of recombinant proteins in cytoplasm of *E. coli*

E. coli HB 2151 (GIBCO) - used for the expression of recombinant proteins in periplasm of *E. coli*

Plasmids

pET11a	Novagen
pETM-13	EMBL – Protein Expression and purification facility
pET41-a	Novagen
pGEX-4T-2	Amersham Pharmacia
pDAN	Sblattero <i>et al.</i> , Nature Biotech., 2000
scFv-cyto-SV5	gently provided by dr. Michela Visintin, LLG

1.8. Oligonucleotides

All primers used are from the company TIB MOLBIOL.

The primers for the RT-PCR reactions were initially prepared as 500 μ M stock solutions in TE buffer. The working solution was a 50 μ M solution in sterile water, used as 50 X for the RT-PCR reaction.

The primers for the PCR reactions were prepared as stock solutions as 100 μ M in TE buffer. The working solution was a 10 μ M in water, that was 20 X for the PCR amplification reactions.

Primers for RT-PCR reactions of m-proNGF short and long :

5'UTR (sense):

5' - GAG GGG AGC GCA TCG AG - 3'

PRE (sense):

5' - TCT ATA CTG GCC GCA GTG AG - 3'

3'UTR (antisense) :

5' - CAG GAT GCT TTG AAA ATT TAA TAA ATA ATG TC - 3'

PolyT (antisense):

5' - TTT TTT TTT TTT CA - 3'

Primers for cloning of m-proNGF (short and long) into pET11a vector:

FwPro-NGF (sense) – for short m-proNGF:

5' - CGG AAT TCC ATA TGG AAC CGT ACA CAG ATA GC - 3'

FwPro-NGF long (sense) – for long m-proNGF:

5' – CGG AAT TCC ATA TGC TGT GCC TCA AGC CAG – 3'

RevNGF (antisense) – for both constructs:

5' - CCG GAT CCT TAT CAT CTT GTA GCC TTC CTG CT - 3'

Primers for proNGF cloning into pEGFP-N3:

Long-Bam (sense):

5' – TAT AAT GGA TCC ATG CTG TGC CTC AAG C – 3'

5'-Bam (sense):

5' – TAT AAT GGA TCC GTA ATG TCC ATG TTG TTC TAC – 3'

GFP-Hind (antisense):

5' – TAT ATG CGA AGC TTG GCC TCT TCT TGT AGC CTT CC – 3'

Pro-GFP-Hind (antisense):

5' – TAT ATG CGA AGC TTG GCG CTT GCT CCG GTG AG – 3'

Pro-GFP-Hind-mut (antisense):

5' – TAT ATG CGA AGC TTG GCG CTT GCT CTG GTG AGT CC – 3'

Primers for mutagenesis of proNGF to proNGF P5A:

proNGF P5A for (sense):

5' – CGC TCA TCC ACC CAC GCA GTC TTC CAC ATG G – 3'

proNGF P5A back (antisense):

5' – CCA TGT GGA AGA CTG CGT GGG TGG ATG AGC G – 3'

Primers for cloning of the pro-GST (proNGF short pro-peptide into pET-41a vector):

pET Nde for (sense):

5' – TAT AAT GGA CAT ATG GAA CCG TAC ACA GAT AGC AAT G – 3'

pET Nde back (antisense):

5' – TAT TAA GGT CAT ATG GCG CTT GCT CCG GTG AG – 3'

Primers for cloning of the GST-pro (proNGF short pro-peptide into pGEX-4T-2 vector):

pGEX Bam for (sense):

5' – TAT AAT GCA GGA TCC GAA CCG TAC ACA GAT AGC AAT G – 3'

pGEX Eco back (antisense):

5' – TAT TAA TGG AAT TCC TCA GCG CTT GCT CCG GTG AG – 3'

Primers for DNA sequencing:

The primers used for DNA sequencing were stained at 5' with IRD 41 dye.

pGEX-sense ($T_{\text{anneal}} = 63.5^{\circ}\text{C}$):

5' - CCA CGT TTG GTG GTG GCG AC – 3'

T7 ($T_{\text{anneal}} = 53^{\circ}\text{C}$):

5' - TAA TAC GAC TCA CTA TAG GG – 3'

BTM116 for ($T_{\text{anneal}} = 50^{\circ}\text{C}$):

5' - GAA ATT CGC CCG GAA TT – 3'

1.9. Media, antibiotics and buffers

Media

LB-medium: 10 g/L Tryptone, 5 g/L Yeast Extract, 5 g/L NaCl

LB-Agar: LB-medium added to 15 g/L Agar Agar

SOB-medium: 20 g/L Tryptone, 5 g/L Yeast extract, 10mM NaCl, 2.5 mM KCl

SOC-medium (10 mL): 9.7 mL SOB-medium, 0.1 mL of 1 M MgCl_2 , 0.2 mL of 20% (w/v) Glucose

2-YT medium: 17 g/L Tryptone, 10 g/L Yeast extract, 5 g/L NaCl

Antibiotics

Ampicillin stock solution: 100 mg/mL in water

Kanamycin stock solution: 50 mg/mL in water

Chloramphenicol stock solution: 30 mg/mL in ethanol

All the antibiotics were sterile filtered after preparations and stocked into small volume aliquots at -20°C. They were used at a 1:1000 dilution in the media.

Buffers

All the buffers are prepared in bi-distilled water.

- TBE buffer for agarose gels: 45 mM Tris-Borate, 1mM EDTA
- Agarose gels for DNA separation: 0.75 – 1.5 % solutions of agarose in TBE, added with 0.5 $\mu\text{g/mL}$ Ethidium Bromide
- Loading buffer for samples on agarose gels (6X): 0.25% bromophenolblue, 0.25% xylene cianol, 30% glycerol
- Coomassie blue staining of protein gels: 40% (v/v) EtOH, 10% (v/v) CH_3COOH , 0.1% (w/v) Coomassie blue R250
- Destaining solution for protein gels: 40% (v/v) EtOH, 10% (v/v) CH_3COOH
- HIC buffer A: 50 mM Sodiumphosphate, pH 7.0, 1 M $(\text{NH}_4)_2\text{SO}_4$, 1mM EDTA
- HIC buffer B: 50 mM Sodiumphosphate, pH 7.0, 1mM EDTA
- IB-resuspension buffer: 100 mM Tris/HCl, pH 7; 1 mM EDTA
- IB-washing buffer (Triton-IB): 60 mM EDTA; 6% (v/v) Triton X-100; 1.5 M NaCl

- IB-washing buffer: 100 mM Tris/HCl, pH 7,0; 20 mM EDTA
- IB-solubilization buffer: 100 mM Tris/HCl, pH 8; 6 M GdmCl; 10 mM EDTA; 100 mM DTT
- IB-dialysis buffer: 6 M GdmCl, pH 4; 10 mM EDTA
- Refolding buffer for rm-proNGF: 100 mM Tris/HCl, pH 9.5; 1 M L-Arginina; 5 mM GSH; 1 mM GSSH; 5mM EDTA
- IEX-buffer A: 50 mM Sodiumphosphate, pH 7; 1 mM EDTA
- IEX-buffer B: 50 mM Sodiumphosphate, pH 7; 1 mM EDTA, 1 M NaCl
- Sample buffer for sample loading in SDS-PAGE acrylamide protein gels (4X): 200 mM Tris/HCl pH 6.8, 8% SDS, 0.4% bromophenole-blue, 40% glycerol, 100 mM DTT (freshly prepared)
- Sample buffer for sample loading in native protein gels (4X): 200 mM Tris/HCl pH 6.8, 0.4% bromophenole-blue, 40% glycerol
- Stacking gel for SDS-PAGE: acrylamide/bis-acrylamide 5%, 0.125 M Tris-HCl pH 6.8, 0.1 % SDS, 0.1 % APS, 0.1 % TEMED
- Stacking gel for native protein gels: like the one for SDS-PAGE, but without SDS
- Running gel for SDS-PAGE: acrylamide/bis-acrylamide at variable percentage (the most part of the displayed gels were at 12% or 15%), 0.4 M Tris-HCl pH 6.8, 0.1 % SDS, 0.1 % APS, 0.1 % TEMED
- Running gel for native protein gels: like for SDS-PAGE, but without SDS
- Running buffer for SDS-PAGE: 25 mM Tris-HCl, 250 mM Glycine, 0.1% SDS, pH 8.3
- Running buffer for native protein gels: 25 mM Tris-HCl, 250 mM Glycine, pH 8.3
- Transfer buffer for western blotting: 39 mM Glycine, 48 mM Tris base, 0.037% SDS, 20 % MeOH
- PBS: 173 mM NaCl, 27 mM KCl, 4.3 mM Na₂HPO₄, 1.4 mM KH₂PO₄
- TE buffer: 10 mM Tris-HCl pH8, 1mM EDTA
- Developing buffer for alkaline phosphatase western blot developing: 100mM NaCl, 5mM MgCl₂, 100 mM Tris-HCl pH 9.5
- RIPA buffer for immunoprecipitation: 50 mM Tris, pH 7.4, 150 mM NaCl, 1 % Triton X-100, 1 % Deoxycholate, 10 mM EDTA

- Homogenization buffer for animal tissues (same as in Fahnestock et al, Mol Cell Neur, 2001) : 0.5 M Tris-HCl, pH 7.5, 10 mM EDTA pH 8, 0.5% Tween 20, EDTA-free protease inhibitor cocktail
- PPB buffer for periplasmic preparation of recombinant proteins: 200mg/mL sucrose, 1mM EDTA, 30mM Tris-HCl pH8

2. Methods

2.1. rm-proNGF production – cloning procedures

2.1.1. Total RNA extraction from submandibular glands

The submandibular glands from adult mice were extracted from the animals and immediately frozen in liquid nitrogen after operation, and stored at -80°C until performing the experiments.

For total RNA extraction, 2 glands were chosen and separately treated. For the extraction, the protocol from the QIAgen – Oligotex - Direct mRNA protocol for polyA isolation from animal tissues – MINI KIT was followed. After extraction, the sample were precipitated overnight at in isopropanol -20°C. The day after, the samples were centrifuged at 14000 g for 40' at 4°C, the supernatant was carefully removed and at each sample 500 mL of 70% EtOH in DEPC-H₂O were added. The samples were centrifuged at 14000 g for 30' at 4°C, the supernatant was removed, and the samples were centrifuged at 14000 g for 1'. The samples were dried to remove ethanol, and resuspended in 10 µL of DEPC water. Finally, 2 mL were analyzed on a formaldehyde gel and the remaining sample was saved at -80°C.

2.1.2. RT-PCR for amplification of pre-proNGF cDNA

The RNA extracted from the submandibular glands was used as a template for RT-PCR amplification of the cDNA for both the long and the short pre-proNGF, using the RT-PCR: access introductory system by Promega.

The DNA region amplified with the indicated primers is numbered according to the following nucleotide sequence for m-proNGF (GenBank: M35075):

```

1   agagagcgcc tggagccgga ggggagcgca tcgagagtga ctttggagct ggccttatat
61  ttggatctcc cgggcagctt ttggaaact cctagtgaag atg ctg tgc ctc aag cca gt
121 g aaa tta ggc tcc ctg gag gtg gga cac ggg cag cat ggt gga gtt ttg gcc tgt ggt cg
181 t gca gtc cag ggg gct gga tgg cat gct gga ccc aag ctc acc tca gtg tct ggg ccc aa
241 t aaa ggt ttt gcc aag gac gca gct ttc tat act ggc cgc agt gag gtg cat agc gta at
301 g tcc atg ttg ttc tac act ctg atc act gcg ttt ttg atc ggc gta cag gca gaa ccg ta
361 c aca gat agc aat gtc cca gaa gga gac tct gtc cct gaa gcc cac tgg act aaa ctt ca
421 g cat tcc ctt gac aca gcc ctc cgc aga gcc cgc agt gcc cct act gca cca ata gct gc
481 c cga gtg aca ggg cag acc cgc aac atc act gtg gac ccc aga ctg ttt aag aaa cgg ag
541 a ctc cac tca ccc cgt gtg ctg ttc agc acc cag cct cca ccc acc tct tca gac act ct
601 g gat cta gac ttc cag gcc cat ggt aca atc cct ttc aac agg act cac cgg agc aag cg
661 c tca tcc acc cac cca gtc ttc cac atg ggg gag ttc tca gtg tgt gac agt gtc agt gt
721 g tgg gtt gga gat aag acc aca gcc aca gac atc aag ggc aag gag gtg aca gtg ctg gc
781 c gag gtg aac att aac aac agt gta ttc aga cag tac ttt ttt gag acc aag tgc cga gc
841 c tcc aat cct gtt gag agt ggg tgc cgg ggc atc gac tcc aaa cac tgg aac tca tac tg
901 c acc acg act cac acc ttc gtc aag gcg ttg aca aca gat gag aag cag gct gcc tgg ag
961 g ttc atc cgg ata gac aca gcc tgt gtg tgt gtg ctc agc agg aag gct aca aga aga gg
1021 c tga cttgcc tgcagcccc tccccacct gccccctcca cactctctg ggccccctcc
1081 tacctcagcc tgtaaattat tttaaattat aaggactgca tgataattta tegtattatac
1141 aattttaag acattattta ttaaatttc aaagcatcct gaaaaaaaaa

```

Legend:

underline: precursor-long

double underline: pre-sequence of the short precursor

italic: pro-sequence of the short precursor

bold: NGF

normal: 5' UTR & 3' UTR

The corresponding nucleotide sequence for m-proNGF is reported here:

MLCLKPVKLGSLVGHGQHGGVLACGRAVQGAGWHAGPKLTSVSGPNKGF	50
AKDAAFYTGRSEVHSVMSMLFYTLITAFILIGVQAEPYTDSNVPEGDSVPE	100
AHWTKLQHSLDTALRRARSAPTAPIAARVTGQTRNITVDPRLF <u>KKRR</u> LHS	150
PRVLFSTQPPPTSSDTLDLDFQAHGTIPFNRTHR <u>SKRS</u> STHPVFHMGES	200
VCDSVSVWVGDKTTATDIKGKEVTVLAEVNINNSVFRQYFFETKCRASNP	250
VESGCRGIDSKHWSYCTTTHTFVKALTTDEKQAAWRFIRIDTACVCVLS	300
RKATTRG*	

Legend:

double underline: consensus sites for furin cleavage

2.1.2.1. Pre-proNGF short

For the reaction, five samples were amplified. The primers used were described in the previous sections:

1. RNA 8, primers PRE+3'UTR (from bp 267 to bp 1181), annealing temperature: 64°C
2. RNA8, primers PRE+PolyT (from bp 267 to bp 1190), annealing temperature: 42°C
3. Positive control RNA with carrier (from the Kit – Kanamycin resistance gene mRNA by *in vitro* transcription with *E. coli* rRNA as carrier) + control primers, annealing temperature: 64°C (+C)
4. No RNA, primers PRE+PolyT (-C), annealing temperature: 42°C (-C)
5. No RNA, no primers (--C), annealing temperature: 42°C (- -C)

The following mixtures were prepared for the various samples:

Samples 1 and 2: 32 µL H₂O, 10 µL 5x buffer, 1 µL dNTP, 2 µL MgSO₄, 1 µL of reverse transcriptase, 1 µL DNA polymerase

Sample +C: 26.4 µL H₂O, 10 µL 5x buffer, 1 µL dNTP, 2 µL MgSO₄, 1 µL of reverse transcriptase, 1 µL DNA polymerase

Sample -C: 33 µL H₂O, 10 µL 5x buffer, 1 µL dNTP, 2 µL MgSO₄, 1 µL of reverse transcriptase, 1 µL DNA polymerase

Sample - -C: 35 μ L H₂O, 10 μ L 5x buffer, 1 μ L dNTP, 2 μ L MgSO₄, 1 μ L of reverse transcriptase, 1 μ L DNA polymerase

Then, the following tubes with the primers were prepared:

Sample 1: 1 μ L RNA, primers PRE+3'UTR 1 μ L+1 μ L

Sample 2 : 1 μ L RNA, primers PRE+PolyT 1 μ L+1 μ L

Sample +C : 2 μ L control RNA, 3.3 μ L+3.3 μ L control primers

Sample -C: only primers - PRE+PolyT 1 μ L+1 μ L

These tubes were incubated 94°C for 2'.

Then, to each tube, the corresponding RNA/primer mixture was added.

The following thermal cycles were used:

First strand transcription:

1 cycle: 42°C for 45'

1 cycle: 94°C for 2'

Second strand + amplification:

40 cycles: 94°C for 30''

- PRE-3'UTR 64°C for 1'

- PRE-PolyT 42°C for 1'

68°C for 2'

1 cycle: 68°C for 7'

1 cycle: 4°C soak

2.1.2.2. *Pre-proNGF long*

The same procedure was used for the amplification of the pre-proNGF long, except that the used primers were 5'UTR+3'UTR.

The samples amplified were:

RNA8, primers 5'UTR+3'UTR (from bp 19 to bp 1181)

+C of kit

no RNA, primers 5'UTR+3'UTR

no RNA, no primers

2.1.3. PCR amplification of pre-proNGF cDNA for cloning

The cDNA for both the long and the short pre-proNGF was used as a template for the subsequent PCR amplification reactions for the different cloning procedures.

The general protocol for the PCR reactions was the same in all the cases, changing only the annealing temperature used for the program.

The general procedure was the following:

- preparation of reaction mixture, containing DNA, dNTP 10X (from 10 mM total stock solution), 0.5 μ M primer (from 20X stock solution 10 μ M), Pfu DNA polymerase
- cycles for amplification:
 - a. 94°C for 5'
 - b. 94°C for 1'
 - c. T_{annealing} for 1'
 - d. 72°C for 2'
 - e. 25 times steps b-d
 - f. 72°C for 5'
 - g. 4°C

The amplified samples were the following, according to the numbering of the nucleotide sequence for the pre-proNGF described in previous section:

- proNGF short (cloned into pET11a vector – primers “FwPro-NGF” and “RevNGF”): from bp 353 to bp 1015
- proNGF long (cloned into pET11a vector – primers “FwPro-NGF long” and “RevNGF”): from bp 101 to bp 1015
- proNGF short P5A (cloned into pET11a vector – primers “FwPro-NGF” and “RevNGF”): from bp 353 to bp 1015, but with a mutation at bp 674-676, from CCA (Pro) to GCA (Ala), with primers “proNGF P5A for” and “proNGF P5A back”
- pro-GST (primers “pET Nde for” and “pET Nde back”): from bp 353 to bp 661
- GST-pro (primers “pGEX Bam for” and “pGEX Eco back”): from bp 353 to bp 661

2.1.4. Cloning procedure for the plasmids

The adopted cloning procedure was the same for the cloning of the different constructs, with variable parameters in the volumes of DNA used, depending on the concentration of the purification.

In general, after the PCR reaction, the amplification product was loaded on a preparative agarose gel, the band cut and the DNA extracted using the Gel-extraction kit from QIAgen.

Both the insert and the vector was digested using the required restriction enzymes; in both cases, the restriction was performed with a concentration of restriction enzyme of 2 U/ μ g DNA to cut and the required buffer according to manufacturer indications (enzymes and buffers from NEB). The restriction reaction was achieved by incubation of the mixture at 37 °C for 2 hours.

Before the ligation, the vector was always modified with the CIAP alkaline phosphatase enzyme from calf at a ratio of 0.5 μ L of CIAP (NEB, 25 U/ μ L) *per* sample.

The digestion product was always purified on a preparative agarose gel, followed by DNA extraction from the band excised from the gel.

Finally, the ligation reaction was conducted, with a 3:1 ratio of vector:insert, in presence of the T4-ligase enzyme and the proper ligase buffer conditions; the ligation reaction was generally carried out at 16 °C for 16 hours. In rare cases, the reaction was performed for 2 hours at 22°C.

The ligation product was used to transform bacterial cells DH5 α F', and grown on a solid agarose plate containing the antibiotic Ampicillin. From the many colonies grown, 10 colonies were picked and used for a colony PCR screening, using the suitable primers for the fishing of the clones containing the DNA of the desired construct. Of the positive clones, the minipreps were performed with the GenElute Plasmid Miniprep Kit from SIGMA, starting from 5 mL of liquid medium. From these, three to six clones, depending on the cases, were selected for DNA sequencing to check for the nucleotide sequence correctness.

2.1.5. Cells transformation

All the transformation of plasmids performed in this thesis, were performed with chemically competent cells, prepared according to the protocol by Sambrook manual (Molecular Cloning).

For the DNA experiments, DH5 α F' cells were used for all the cloning procedures, BL21 cells were used for the expression of recombinant protein in *E. coli*

cytoplasm, HB 2151 cells were used for the recombinant protein expression in *E. coli* periplasm.

2.1.6. DNA Sequencing

All the cloned constructs were checked for correct nucleotide sequence by sequencing with an Epicentre Sequitherm Excel II kit and analyzed on a LiCor 4000L automatic sequencer.

2.2. rm-proNGF - Protein chemistry methods

2.2.1. Recombinant proNGF production in *E. coli*

For the recombinant protein production of the rm-proNGF, the same protocol was employed, that was optimized by Rattenholl and colleagues (2001). The whole methodology will be described here.

For the recombinant protein production in *E. coli*, 4*5 L flasks containing 1 L of 2·YT medium with the appropriate antibiotic were inoculated 1:100 with an overnight culture. The cultures were grown at 37°C at 100 rpm until OD₆₀₀=0.5-0.8. Then, the cells were induced with 1 mM IPTG (for rm-proNGF P5A and rm-proNGF long) and 3 mM IPTG (for rm-proNGF). After 3-4 hours induction, the cells were pelleted by centrifugation at 15 min a 5000 rpm (Beckman JLA – 8.1000 rotor), and the humid cell mass was weighted. To check the expression levels of the protein, a 500 µL sample was taken from the flasks, centrifuged to pellet the cells and resuspended into denaturing sample buffer to be analyzed on SDS-PAGE.

For the expression of the rm-proNGF with a fermentation, only the basic indications of the protocol will be described. The pre-culture was an overnight grown culture (1 L of LB + Amp), inoculated with the clone to be expressed. This culture was used to inoculate 8 L of medium for the fermentation; the medium was initially only yeast extract, that was supplemented during time with glucose. During the fermentation procedure, the parameters for the O₂ saturation, pH and temperature were carefully monitored. The addition of both the glucose and the pre-culture was carried out at a 2 g/min with a peristaltic pump. The expression was induced at OD₆₀₀=35 with IPTG 2 mM and carried out for 3 hours. After the induction, the cells were harvested at 65000 rpm. The total weight of the humid mass was 500 g.

2.2.2. IB Preparation (according to Rudolph *et al.*, 1997)

The cell pellet was resuspended with resuspension buffer at 5 mL/g. Then, lysozyme was added at 1.5 mg/g, together with 3mM MgCl₂ and DNaseI 50µg/mL and the sample was incubated at 4°C for 30 minutes. Finally, the suspension was treated twice with a French Press (Pression: 1000-1200 bar).

Then, 0.5 times the volume of buffer Triton-IB was added, and the sample was incubated at room temperature for 30 minutes on a stirring plate, to disrupt the membrane elements.

The IB were then centrifuged for 10 minutes at 4°C at 2000 rpm (SS34 Rotor), resuspended in 20 mL of resuspension buffer + 10 mL of Buffer Triton-IB and incubated at room temperature for 30 minutes on a stirring plate.

The IB were then centrifuged for 10 minutes at 4°C at 2000 rpm and subsequently washed three other times, each one with 40 mL of washing buffer IB. The IB pellet was then stored at -20°C or immediately solubilized.

2.2.3. IB solubilization (according to Rudolph *et al.*, 1997)

The IB pellet was resuspended with solubilization buffer at a ratio of 5 mL/g and incubated for 2 h at RT on rocking platform. The, the pH was lowered to 3-4 by dropwise addition of HCl 1M or concentrated CH₃COOH, to avoid the oxidation of Cysteins to disulfide bridges in denaturing conditions.

The insoluble cellular elements were then removed by centrifugation at 13000 rpm and 4°C for 30 minutes.

Subsequently, the DTT was removed through a triple dialysis each one against 300 mL of Buffer Dialysis IB for twelve hours at 4°C.

The protein concentratio was estimated with the Protein Assay from BIO-RAD (Lowry system). The solute was immediately used for renaturation or stored at -80°C.

2.2.4. Pulsed renaturation

The protein was refolded by pulsed renaturation with the best protein folding buffer according to Rattenholl and colleagues (2001). The renaturation was performed in 1 L of buffer, at 6°C at a protein concentration of 50 µg/mL. Every hour 50 µg/mL of new protein were added to the buffer under vigorous stirring

and then the stirrer was switched off. The maximum sustainable concentration of GdmHCl was of 500 mM, to avoid loss of product. After 16-48 hours after the last addition, the sample was concentrated to a volume of approximately 200-300 mL, using a cross-flow filtration system or, alternatively, with an ultrafiltration device. Finally, the sample was dialyzed for 16 hours at 4°C against 8-10 L of IEX-A buffer. Smaller volumes were dialyzed, covered with PEG 35000 and left at 6°C until the desired volume was reached.

2.2.5. Purification of the refolded rm-proNGF through cation-exchange chromatography

The refolded, dialyzed sample was centrifuged for 30 minutes at 20000 rpm, to remove insoluble, unfolded protein. The supernatant was loaded on a SP-Sepharose column (24 mL – Amersham Pharmacia), equilibrated with IEX-A buffer. The sample was eluted with a linear gradient from 0 to 100% of IEX-B buffer, at 2 mL/min flow in 10 CV. Finally, the column was cleaned with IEX-B buffer and the non-native protein was eluted in denaturing conditions, with GdmHCl. The collected fractions were tested on SDS-PAGE to select the ones containing the clean protein.

2.2.6. Purification of the refolded rm-proNGF through Hydrophobic interaction chromatography

The fractions collected from the previous chromatographic step were pooled and dialyzed against 1 L of IEX-A buffer. Then $(\text{NH}_4)_2\text{SO}_4$ was added to the solute to reach a final concentration of 1 M. The insoluble material in these conditions was removed by centrifugation at 20000 rpm for 30 minutes. The supernatant was loaded on a Phenyl-Sepharose column Fast Flow (20 mL - Amersham Pharmacia), previously equilibrated with the HIC buffer A. The sample was loaded and the a-specific was washed with the same buffer. Then, the sample was eluted with a linear gradient from 0 to 100% of HIC-B buffer, at 2 mL/min flow in 10 CV. Finally, the column was cleaned with HIC-B buffer. The collected fractions were analyzed on SDS-PAGE and the ones containing the desired protein were dialyzed against IEX-A buffer.

2.2.7. Estimation of protein concentration

In all cases of the recombinantly expressed proteins, the concentration was evaluated using the Bio-Rad system for protein concentration, through the Lowry method.

In the case of the purified rm-proNGF and the P5A, the protein concentration was estimated through measurement of the absorbance at 280 nm. The extinction coefficient is calculated according to the coefficient of the Trp and Tyr residues and the disulfide bridges (Gill and von Hippel, 1989). In particular, the coefficients were calculated using the Expasy web server (ProtParam program), and resulted to be equal to:

rm-proNGF	$\epsilon_{280, \text{ox}}=26470$	$\epsilon_{280, \text{red}}=26845$
rm-proNGF P5A	$\epsilon_{280, \text{ox}}=26470$	$\epsilon_{280, \text{red}}=26845$

where ϵ is [1/(molxcm)]. The numbers refer to the monomer state.

The UV spectrum was always recorder from 240 to 340 nm, to check any contamination by DNA (abs at 260 nm) or aggregates (abs at 300 nm).

2.2.8. SDS-PAGE and native protein gels. Staining.

For the SDS-PAGE, the discontinuous system was composed by a 6 % (w/v) stacking and a 12 % or 15 % running (dimensions: 10 cm X 14 cm X 1mm). The samples were heated for 3 minutes at 100°C, centrifuged for 1 minutes at 12000 rpm in a table centrifuge and loaded on the gel. The gel was run at 15 mA for 2 hours.

The native gels were prepared in the same way of the SDS-PAGE, except the fact that the SDS was removed from all the buffers and that the samples were not heated before loading. No marker was used.

Both kind of gels were stained with Coomassie blue for 2-3 hours and then destained for several hours.

2.2.9. Isoelectric focusing

The isoelectric focusing (IEF) presented in the data was performed with the Phast system from Amersham Pharmacia. A Phast gel IEF 3-9 was used, with a 8/1 comb; a broad calibration kit from Amersham Pharmacia was used a marker for the pI.

The experiment was conducted according to manufacturer's instructions.

2.2.10. Enzyme-Linked ImmunoSorbent Assay (ELISA)

The ELISA assay was employed throughout the thesis for the estimation of the binding properties of the purified proteins towards different antibodies.

The general strategy will be briefly described here and should be retained valid for all the experiments displayed, unless otherwise indicated in the "Results" section.

In this test a microtiter 96 wells plate (Falcon) was used. In the different kinds of experiments, the antigen or the antibody were immobilized on the plate, using the same strategy. In all cases, the functionalization of the plate (called *coating* step) was obtained in same way, by dissolving the protein of interest in a solution 100 mM NaHCO₃ pH 9.6, with a concentration of 10 µg/mL; in every well, 100 µL of the protein solution were displayed. In all the cases, a negative control was used, with a coating with the buffer alone, without protein, to check for a-specific interactions of the protein with the plastic surface. After coating, the plate was incubated for 16 hours at 4°C, and subsequently washed twice with PBS.

Before the incubation with the interacting partners, the a-specific sites on the coated protein were "blocked" with a solution of 3 % non-fat dry milk in PBS (called M-PBS) for 1 hour at room temperature.

After two washes with PBS, the next step were carried out.

Depending on the cases, the first incubation step was represented by the primary antibody (if the antigen was coated on the plate) or by the antigen (if the antibody was coated on the plate). In both cases, the protein of interest was diluted in a M-PBS solution and dispensed at 100 µL *per* well. The concentration of the protein used in the incubation step is indicated in the single ELISA results displayed in the text. In all the cases, the incubation time for this step was of 90 minutes at room temperature.

The general dilution of the antibodies was the following: all surnatants at 1:2, anti-NGF polyclonal at 1:8000, anti-proNGF polyclonal (both from Chemicon and from Alomone) at 1:1000, anti-GST polyclonal at 1:2000, anti-GFP polyclonal at 1:1000, αD11 (purif.) at 1:4000, anti-SV5 (purif.) at 1:2000.

After that, the plate was washed with T-PBS (a PBS solution containing 0.05 % of Tween-20 detergent) and PBS for three times each.

In the most complex ELISA formats described in the text, a second incubation step was used, to check for the interaction of two proteins “in solution”. The same procedure of the previous step was followed for this additional incubation step.

Finally, the secondary antibody was used in the incubation: this antibody is conjugated with horse-radish peroxidase (HRP) and is used for a colorimetric assay for the recognition of the primary antibody. The kind of secondary antibody was different depending on the source of the primary antibody. In the various experiments, three kinds of secondary antibodies were employed: anti-mouse, anti-rabbit and anti-rat, all HRP conjugated; all of them were used at a 1:1000 dilution in M-PBS (except for the anti-rabbit that was used at a 1:2000 dilution), in a 1 hour incubation at room temperature.

After wash with T-PBS and PBS, the developing step was carried out, using the TMB 3,3',5,5'-tetra-metil-benzidina (TECNA) as a developing agent for the HRP. After sufficient incubation time (ranging from 1 minute to 30 minutes, depending on the efficiency of the binding), the reaction was stopped with a 0.1 M solution of H₂SO₄.

The intensity of the colorimetric signals were analysed with a spectrophotometer at 450 nm using an ELISA Reader (Spectra).

2.2.11. Surface Plasmon Resonance using BIAcore

The experiments presented in the thesis were all performed with a BIAcore 2000 machine, except from the Protein L experiments, performed with a BIAcore 3000 machine.

In all the cases, the experiments were performed on CM5 chips, with amine coupling, performed with the specific kit for coupling purchased at BIAcore.

The coupling reaction was performed according to manufacturer's instructions.

The flow used in the experiments was of 30 µL/min, unless otherwise indicated.

The regeneration of the chip was performed in all the cases with a pulse (10 µL) of 10mM Glycine pH 1.5.

2.2.12. Immunoprecipitation

The immunoprecipitation experiments described in the thesis were all performed following the same protocol.

For the precipitation, Protein G Sepharose (Amersham) was used.

At first, the Protein G resin was equilibrated in RIPA buffer; for each sample, 5 μ L of resuspended resin were used. 0.5 mL of RIPA buffer were added to the resin, that was subsequently centrifuged for 2 minutes at 6000 rpm in a table centrifuge. The wash was repeated twice. Finally, the resin was resuspended in a volume corresponding to 10 μ L for each sample to be analyzed.

The samples to be immunoprecipitated were treated in the following way. The antigen was incubated with the antibody in RIPA buffer, for 90 minutes on a rocking wheel at 4°C. In the described cases, 5 μ g of the α D11 purified monoclonal antibody were used for each sample. Then, the resin was added to the mixture and the sample was incubated for 90 minutes on a rocking wheel at 4°C.

In the case of the immunoprecipitation with the scFv anti-proNGF, the procedure was slightly different: the scFv was first incubated with the proNGF at a 2:1 molar ratio (2 μ g of scFv with 1.5 μ g of rm-proNGF); on the same time, the anti-SV5 antibody was incubated with the resin. Finally, the two samples were pooled and incubated together for 90 minutes on a rocking wheel at 4°C. Then, the sample was washed for three times with RIPA buffer. Every centrifugation step was of 2 minutes at 6000 rpm in a table centrifuge, the supernatant was carefully removed with an insulin needle syringe and the sample resuspended in 0.5 mL of RIPA buffer.

Finally, the sample was resuspended in 20 μ L of 1X sample buffer for SDS-PAGE and loaded on a gel for subsequent western blot analysis.

2.2.13. Western blotting analysis

The western blotting analysis displayed in the thesis were analyzed with two alternative methods, according to the specific needs: ECL and alkaline phosphates.

In both cases, however, the blotting procedure and the incubation steps were the same.

First of all, the SDS-PAGE was transferred to the nitrocellulose membrane, with a semi-dry system, for 45 minutes under the conditions of 100 mA and 5-10 volts.

After removal of the membrane from the blotting system, the membrane was incubated for 1 hour at room temperature in 10 % blocking solution of non-fat dry milk in PBS.

Then, the membrane was incubated with the primary antibody, at the different concentrations indicated in the “Results” section, but always in 10 % M-PBS, for 16 hours at 4°C.

After washing with T-PBS and PBS, the membrane was incubated with the secondary antibody, that was conjugated with HRP or with AP (Alkaline Phosphatase) depending on the developing method used. In both cases, however, the solution was prepared in 10 % M-PBS and the incubation time was of 1 hour at room temperature.

After washing again with T-PBS and PBS, the developing was carried out.

In the case of ECL, the membrane was briefly dried and incubated for 1 minute with the developing solution (mix solution A and B of the Amersham kit); the films were exposed for different time frames.

In the case of AP, the membrane was washed with the developing buffer and then incubated with the BCIP/NBT solution until the desired staining intensity was reached. Finally, the reaction was stopped with a solution of 100 mM TrisHCl pH 7.5, the membrane washed with water, dried and saved.

2.2.14. HPLC separation of rm-proNGF and m-NGF

Both the rm-proNGF and the m-NGF cut from it were run on an HPLC column before Mass Spectrometric analysis, on a Dionex machine. The chromatogram was recorded at 280 nm.

The sample loaded was of the order of 25 µg and it was loaded on a C4 RP-HPLC column. The elution was performed with a stepwise gradient from 0 to 100 % of buffer B, where buffer A was 0.1 % TFA in water and buffer B was 0.08 % TFA in 80 % acetonitrile.

2.2.15. Mass Spectrometry analysis of the proteins

All the displayed mass spectra were recorded at the Martin-Luther University thanks to Dr. Angelika Schierhorn, using a MALDI-TOF (Brucker) and an ESI Triple-quadrupole (Fisons) instruments.

2.2.16. Limited Proteolysis of rm-proNGF using Trypsin and Furin

The analytical limited proteolysis on rm-proNGF was initially carried out according to the protocol described by Rattenholl et al, 2001.

62.5 µg of rm-proNGF (in 50 mM Tris/HCl, pH 8) were incubated on ice with 0.25 µg of trypsin (from a 0.5 mg/mL stock solution in 10mM CaCl₂, 1mM HCl, pH 2-3) in a total volume of 500 µL (buffer: 50 mM Tris/HCl, pH 8). At certain time points, every 30 minutes, a sample was taken and the reaction was stopped by addition of the loading buffer for SDS-PAGE. By control, a sample of rm-proNGF was incubated in the same conditions without trypsin. The samples were loaded on an SDS-PAGE to check for the proteolysis progression.

The same 1:250 trypsin:rm-proNGF ratio was used for the preparative digestion with trypsin. In this case, 281.2 µg of rm-proNGF were incubated for 2 hours on ice with 1.125 µg of trypsin; the total reaction volume was of 2.25 mL. The reaction was stopped by addition of the EDTA-free protease inhibitor cocktail, and the sample was then loaded on a HiTrap SP column (5 mL – Amersham). The cut rm-NGF was eluted in the same conditions described for the rm-proNGF.

For the proteolysis with Furin, no protocol was available, except a previously described experiment (Leighton, JBC, 2003), performed with a different furin protein. Therefore, according to the data available, the reaction was initially performed with a ratio of 1µg proNGF : 0.25 U furin, using 4 µg of rm-proNGF and 10 U of furin (from the commercial 2 U/µL), in a total reaction volume of 100 µL. The buffer used was 50mM TrisHCl pH 7.5, 1 mM CaCl₂ and the incubation time was of 24 hours at room temperature. At certain time points, the reaction was stopped by addition of the loading buffer for SDS-PAGE.

2.2.17. Fluorescence spectroscopy

The spectroscopic properties of rm-proNGF reside in the presence of aromatic residues. In particular, the protein contains 4 Trp, 3 Tyr and 11 Phe, of which 1 Trp, 1 Tyr and 4 Phe are localized in the pro-peptide.

Fluorescence measurements were performed with the Spectrofluorimeter F-4500 from Hitachi (Japan) with a thermostated ($T=20^{\circ}\text{C}$) cuvette-holder. The slits for excitation and emission were 5nm wide. The measurements were done in 0.5 mL cuvettes (Hellma) – $d=1\text{cm}$. The protein concentration was $10\mu\text{g/mL}$. The fluorescence emission spectra were recorded from 300 to 400 nm, at a speed of 60 nm/min, using an excitation wavelength of 295 nm. All spectra were corrected against the corresponding buffer. To establish the denaturation rate of rm-proNGF, the sample was measured both in native and denaturing conditions. The protein solution has been prepared both in the native buffer (50mM Na-Phosphate, pH 7.0, 1mM EDTA) and in the denaturing one (6M Guanidinium Chloride in 50mM Na-Phosphate, pH 7.0, 1mM EDTA). The fluorescence maximum for the rm-proNGF in native and denatured state was 335nm and 354nm respectively.

2.2.18. Denaturing buffer –dependent transitions

The dependence of the denaturing curve of the rm-proNGF from the denaturant concentrations was evaluated by incubation of the protein in serial dilutions of 8 M GdmHCl in the IEX-A buffer. The samples were incubated at room temperature for 12 hours and then measured, with an excitation wavelength of 280 nm.

The precise concentration of GdmHCl in the sample was evaluated by refractive index measurement, as described in the PhD Thesis of Anke Rattenholl (University of Halle, 2001).

2.2.19. Circular dichroism measurements

CD measurements were carried out with a JASCO J-810 circular dichroism spectrometer at 20°C in 50mM Na-phosphate pH 7.0. Far-UV CD (190-250 nm) spectra were recorded at protein concentration of 0.5 – 1.0 mg/mL in a 0.02 cm cell, averaged over 10 accumulations (acquisition time: 2 s). Near-UV (250 nm – 350 nm) spectra were determined at 0.3 mg/mL, in a 1 cm cuvette

(Hellma). Spectra were buffer corrected. Mean ellipticity values were calculated according to Schmid, 1997:

$$[\Theta]_{\text{MRW}} = \frac{\Theta \cdot 100 \cdot M_r}{c \cdot d \cdot N_A}$$

where:

Θ = the measured ellipticity in degrees

c = protein concentration in mg/mL

d = cuvette path in cm

M_r = Molecular weight of the protein in g/mol

N_A = number of amino acids of the protein

MRW = mean residue weight – average molecular weight of a general amino acid

2.2.20. Dynamic Light Scattering

DLS measurements were performed with 6.5 mg/ml proNGF in 50mM Sodium-phosphate, pH 7, at 25°C on a DynaPro MS/X instrument (Protein Solutions). Samples were filtered through a 0.02µm Anodisc membrane using the NanoFilter kit (Wyatt Technology) to remove precipitate or dust particles and then injected in a 12µl quartz microCUVETTE (Wyatt Technology). Data collection and deconvolution were performed using the DYNAMICS 6.2.05 software (Protein Solutions). The laser power during measurement was equal to 75 %; the model used for protein parameters evaluation was that for a globular protein.

2.2.21. Expression and purification of the fusion proteins GST-pro and pro-GST

400 mL of LB + Ampicillin were inoculated with an overnight culture at 1:100 ratio. The cultures were grown at 37°C until an OD_{600} =0.5-0.6 and then induced with IPTG 0.5 mM or 1 mM for 4.5 hours at 30°C.

The cells were harvested at 5000 rpm (Beckman) and the pellet were saved at -80°C.

The pellet was resuspended in 5 mL/g of PBS, lysozyme was added at 1.5 mg/g, together with 3mM MgCl₂ and DNaseI 50µg/mL and the sample was incubated at 4°C for 60 minutes.

The cells were disrupted by sonication, with 3 pulses of 45 seconds each at 13000 micron intensity, each one followed by a 1 minute incubation on ice.

The insoluble material was removed by centrifugation for 30 minutes at 4°C at 10000 rpm and the supernatant used for the further purification.

In both cases of the two proteins, the first purification step consisted of an affinity purification over a GST-Trap column (5 mL, Amersham Pharmacia). The column was operated on a peristaltic pump at 1 mL/min speed, except during the sample loading, where the speed was of 0.3 mL/min. The a-specifically bound protein was removed with PBS, and the GST-fusion protein was eluted in PBS supplemented with 10 mM GSH. The occurrence of the protein peak was followed by spectrophotometric reading at 280 nm.

After the elution, the sample was dialyzed against 50 mM sodium-phosphate 50 mM pH 7, to remove the GSH.

The second purification step was different for the two proteins.

The GST-pro was loaded on a cation exchange chromatography column, HiTrap SP-Sepharose (Amersham Pharmacia), equilibrated with IEX-A buffer and eluted with a linear gradient from 0 to 100 % of IEX-B buffer. Subsequently, the sample was loaded on a size exclusion chromatography column, Superdex 75 (Amersham Pharmacia) and eluted in PBS, at 0.6 mL/min.

The pro-GST sample, on the contrary, was dialyzed against 50mM CH₃COONa, pH 5.6 (A buffer) and loaded on a HiTrap SP-Sepharose (Amersham Pharmacia), and eluted with a linear gradient from 0 to 100 % of B buffer (A buffer + 1 M NaCl).

2.3. Structural methods and modelling

2.3.1. Small-Angle X-ray Scattering (SAXS) and Data Processing

Synchrotron radiation X-ray scattering data were collected on the X33 beam line and camera (Koch, M. H. J. & Bordas, J. (1983). Nucl. Instrum. Methods; Boulin, C. J. (1988). Nucl. Instrum. Meth. A) at the Hamburg EMBL Outstation

(on the DORIS III storage ring, at DESY). Solutions of full-length rm-proNGF in 50 mM Na-phosphate pH 7.0, 1 mM EDTA were measured at protein concentrations of 3.2, 6.4 and 12.8 mg/ml using a MAR345 image plate at sample-detector distance 2.4 m and wavelength $\lambda = 1.5 \text{ \AA}$, covering the momentum transfer range $0.012 < s < 0.45 \text{ \AA}^{-1}$ ($s = 4\pi \sin(\theta)/\lambda$ where 2θ is the scattering angle).

To check for radiation damage two 2-minute exposures were compared; no radiation effects were observed (2mM DTT was added to the sample). The data were averaged after normalization to the intensity of the incident beam, corrected for the detector response, and the scattering of the buffer was subtracted. The difference data were extrapolated to zero solute concentration following standard procedures. All data manipulations were performed using the program package PRIMUS (Konarev, P. et al., (2003). J. Appl. Crystallogr.).

The maximum particle dimension Dmax was estimated using the orthogonal expansion program ORTOGNOM (Svergun, D. I. (1993). J. Appl. Crystallogr.). The forward scattering $I(0)$ and the radius of gyration R_g were evaluated using the Guinier approximation (Guinier, A. (1939). Ann. Phys. (Paris)) assuming that at very small angles ($s < 1.3/R_g$) the intensity is represented as $I(s) = I(0) \exp(-1/3(R_g s)^2)$. These parameters were also computed from the entire scattering patterns using the indirect transform package GNOM (Svergun, D. I. (1992). J. Appl. Crystallogr.). The molecular mass (MM) of the solute was evaluated by comparison of the forward scattering with that from reference solutions of bovine serum albumin (MM = 66 kDa). The excluded volume of the hydrated particle (the Porod volume) was computed using the equation (Porod, G. (1982). Small-angle X-ray scattering,):

$$V = 2\pi^2 I(0) / \int_0^\infty s^2 I_{\text{exp}}(s) ds \quad (1)$$

Prior to this analysis, an appropriate constant was subtracted from each data point to force the s^{-4} decay of the intensity at higher angles following the Porod's law for homogeneous particles. This "shape scattering" curve was further used to generate a low resolution ab initio model of full-length proNGF

by the program DAMMIN, which represents the protein by an assembly of densely packed beads. Simulated annealing was employed to build a compact interconnected configuration of beads inside a sphere with the diameter Dmax that fits the experimental data $I_{exp}(s)$ to minimize the discrepancy:

$$\chi^2 = \frac{1}{N-1} \sum_j \left[\frac{I_{exp}(s_j) - cI_{calc}(s_j)}{\sigma(s_j)} \right]^2 \quad (2)$$

where N is the number of experimental points, c is a scaling factor and $I_{calc}(s_j)$ and $\sigma(s_j)$ are the calculated intensity and the experimental error at the momentum transfer s_j , respectively.

The scattering from the crystal structure of dimeric mature m-NGF (1BET) [33] was calculated using the program CRY SOL (Svergun, D. I., Barberato, C. & Koch, M. H. J. (1995). J. Appl. Crystallogr.). To construct a model of full-length rm-proNGF dimer in solution, the N-terminal segment missing in the mature m-NGF structure was represented by interconnected chains composed of dummy residues (Petoukhov, M. V., et al., (2002). Biophys J). The structure of the truncated mature m-NGF dimer was rotated so that the 2-fold axis coincided with Z-axis, and fixed at this position. A simulated annealing protocol implemented in the program BUNCH was employed to find a native-like configuration of the N-terminal fragment without steric clashes, fitting the scattering from the full-length protein. Both reconstructions using DAMMIN and BUNCH were performed assuming two-fold symmetry axis and also without the symmetry restrictions.

2.3.2. Modelling

The crystallographic structures of the NGF/Ig-like domain d5 of TrkA (PDB code 1WWW) and of the NGF/p75^{NTR} receptor (PDB code 1SG1) complexes have been superimposed with the proNGF SAXS-derived models (crab model and extended model) using SUPERIMPOSE (Diederichs, Proteins, 1995). The figures have been produced using O (Jones *et al.*, Acta Crystallogr. Sect. A, 1991).

2.4. Cell biological experiments

2.4.1. TrkA phosphorylation assay on 3T3 TrkA cells

Western blot: BALB/C 3T3-transfected cells (3T3 TrkA cells), expressing 106 human TrkA molecules per cell (kindly provided by Stefano Alema Consiglio Nazionale delle Ricerche (CNR) Institute of Cell Biology, Roma, Italy), were maintained in DMEM medium (Life Technologies, Milano, Italy), supplemented with 10% fetal calf serum. 3T3 TrkA cells were plated in 35 mm Petri dishes at a density of 106 cells per dish. The next day, 3T3 TrkA cells were washed and incubated with serum-free medium supplemented with 0.05% BSA for 60 min at 37°C. Equimolar serial dilutions of m-NGF and rm-proNGF were added for 10 min at 37°C. After washing with PBS, cells were scraped in 250 µl of cold RIPA buffer supplemented with phosphatases and protease inhibitors (50 mM Tris pH 7.4, 150 mM NaCl, 1% Triton X100, 1% Na deoxycholate, 10 mM EDTA, protease inhibitor cocktail purchased by Roche, 1 mM sodium orthovanadate, 50 mM NaF, 1 mM okadaic acid). Insoluble material was removed by a 5 min, 10000 rpm centrifugation. Extracts were separated on SDS polyacrylamide 10% gels and transferred to nitrocellulose. After blocking in PBS (5% nonfat dry milk) for 1 h at room temperature with gentle agitation, the filters were incubated over night at 4°C with both the anti-phosphotyrosine TrkA antibody (Cell Signalling) diluted 1:1000 and anti-tubulin monoclonal antibody Y0L 1/2, followed respectively by anti-rabbit and anti-rat secondary antibodies, coupled to horseradish peroxidase HRP diluted 1:1000 for 1h at room temperature. After washes with PBST (0.1% Tween 20) and PBS at room temperature with gentle agitation, the HRP conjugates were detected by the electrochemiluminescence protocol developed by Amersham Corp.

Sandwich ELISA assay - Sandwich ELISA assay was performed by coating a 96 well plate with anti-TrkA monoclonal antibody MNAC13 (10 µg/ml) (Cattaneo et al., J. Neurosci. 1999). After blocking in PBS (3% non fat dry milk) for 1 hour at room temperature, each cell extract was incubated in PBS (3% non fat dry milk) for 3 hours at room temperature. Following the anti-phosphotyrosine TrkA antibody (Cell Signalling) diluted 1:1000 in PBS (3% non fat dry milk), acting as primary antibody, the anti-rabbit antibody peroxidase conjugated was used as a secondary antibody. After incubating

with TMB substrate (TECNA) and blocking the reaction with 0.1 M H₂SO₄, the intensity of each colorimetric signal was measured at 450 nm by an ELISA Reader (Spectra).

2.4.2. PC12 cells differentiation bioassay

PC12 cells (Green and Tischler, PNAS, 1976; from CNR, Roma, Italy) were grown as monolayer cultures in RPMI 1640 supplemented with 10 % Fetal Calf Serum in a humidified atmosphere of 5 % CO₂ at 37°C.

For use in bioassay, medium was changed to RPMI supplemented with 50 ng/mL of NGF or 100 ng/mL proNGF. After 48 hours the medium was changed and free medium + proteins was supplied.

Finally, pictures under the light microscope were taken on the living cells.

2.4.3. Immunofluorescence on primed PC12 cells

The cells were cultivated as in the previous paragraph, except that before the priming procedure, they were grown on coverslips.

The cells were fixed in 4 % paraformaldehyde for 20 minutes at room temperature and then washed 3-4 times with PBS.

Then, they were permeabilized for 5 minutes in 0.1 % IGEPAL in PBS and washed three times with PBS.

A blocking step in 10 % Fetal Calf Serum (FCS) was then performed for 20 minutes at room temperature.

Then, the primary antibody anti-tubulin (YL – as supernatant) was applied, at a 1:10 dilution in 10 % FCS, for 60 minutes at room temperature.

After rinsing three times with 5 % FCS, the secondary antibody, anti-rat TRITC conjugated was applied, at a 1:500 dilution in 10 % FCS for 30 minutes at room temperature.

Then, the cells were washed and the DAPI (Boehringer) was applied at 1:1000 in PBS (from a stock solution of 2 mg/mL) for 5 minutes at room temperature.

Finally, the cells were rinsed in PBS and the coverslips mounted in 90 % glycerol/1,4-Diazabicyclo[2,2,2]octane (DABCO).

The Immunofluorescence was observed with a Zeiss Axioplan microscope. Images were acquired with Nikon Coolpix 990 digital camera.

2.5. Other techniques

2.5.1. Homogenization of mouse tissue

For the homogenization of the submandibular glands from mouse, the glands were homogenized in a mortar in liquid nitrogen, until a fine powder was obtained. Then, the powder was transferred into an eppendorf tube in the homogenization buffer, at 5 mL/g tissue. The homogenates were incubated on ice for 15 minutes and then the insoluble debris was removed by centrifugation at 14000 g for 15 minutes at 4°C.

The total protein concentration in the samples was measured with the Bio-Rad protein assay.

For the direct loading on the SDS-PAGE, 160 µg of homogenate were used; for the immunoprecipitation, 200 µL of sample were used (total protein concentration: 16 µg/µL according to Lowry assay for protein concentration).

2.6. IAC selection of the scFv anti-proNGF

The detailed methodology for the selection of the scFv with the IACT technology, improved with the SPLINT, is described in the publications by Visintin and colleagues (Visintin et al, JMB, 2002, Visintin et al, JIM, 2004) and will not be described here. The selection was performed in collaboration with dr. Michela Visintin and Isabella Cannistraci from LayLine Genomics SpA.

Only the constructs used for the selection will be reported here.

2.6.1. Mutants of m-proNGF and fusion constructs with lexA

To select the best domain of m-proNGF to be used for the in vivo selection on the SPLINT library, a series of deletion mutants of m-proNGF was created, that will be reported here. The numbering of the constructs refers to the nucleotide sequence of m-proNGF reported in the previous sections. The proteins were fused in the same reading frame of the lexA binding domain. The expression level of the described fusion proteins was evaluated by western blot analysis, using polyclonal antibodies anti-lexA. The constructs were cloned in the polylinker at C-terminus of lexA as PCR product cut with the restriction enzymes BamHI-PstI, in the pMICBD1 vector cut in the same way.

The baits used for the SPLINT selection were:

1. **proNGF**: the whole pro-peptide, from bp 348 to 698 (pro-peptide + first 14 amino acids of mature NGF). Used primers:

pro Bam for:

5' TAT AAT GGG ATC CGT GAA CCG TAC ACA GAT AGC AAT G 3'

pro Pst back:

5'TGT ATA TGT ACT GCA GGT CAC ACT GAG AAC TCC CCC ATG 3'

2. **proNGFmut**: the whole pro-peptide, from bp 348 to 698 (pro-peptide + first 14 amino acids of mature NGF), with a mutation in the consensus sequence for furin: site KKRR mutated into KEAR (see protein sequence in previous sections). The mutation was carried out using the protocol from the QuikChange Site-Direct Mutagenesis Kit (Stratagene), using the primers:

M-bait for:

5' CCC AGA CTG TTT AAG GAA GCG AGA CTC CAC TCA CCC 3'

M-bait back:

5' GGG TGA GTG GAG TCT CGC TTC CTT AAA CAG TCT GGG 3'

3. **pro**: Only the pro-peptide, without the NGF. Sequence from bp 348 to bp 656. With the mutation. Used primers:

pro Bam for:

5'TAT AAT GGG ATC CGT GAA CCG TAC ACA GAT AGC AAT G 3'

pro-only-Pst-back:

5' TGT ATA TGT ACT GCA GGT CAG CGC TTG CTC CGG TGA G 3'

4. **pro-10**: only the pro-peptide, with a deletion of 10 amino acids at the C-terminus. Sequence from bp 348 to bp 626. With mutation. Used primers:

pro Bam for:

5' TAT AAT GGG ATC CGT GAA CCG TAC ACA GAT AGC AAT G 3'

C-term-10:

5' TGT ATA TGT ACT GCA GGT CAG ATT GTA CCA TGG GCC TGG
3'

5. **pro-20:** only the pro-peptide, with a deletion of 20 amino acids at the C-terminus. Sequence from bp 348 to bp 596. With mutation. Used primers:

pro Bam for:

5' TAT AAT GGG ATC CGT GAA CCG TAC ACA GAT AGC AAT G 3'

C-term-20:

5' TGT ATA TGT ACT GCA GGT CAC AGA GTG TCT GAA GAG
GTG G 3'

6. **pro-30:** only the pro-peptide, with a deletion of 30 amino acids at the C-terminus. Sequence from bp 348 to bp 566. With mutation. Used primers:

pro Bam for:

5' TAT AAT GGG ATC CGT GAA CCG TAC ACA GAT AGC AAT G 3'

C-term-30:

5' TGT ATA TGT ACT GCA GGT CAG GTG CTG AAC AGC ACA
CGG 3'

7. **pro-41:** only the pro-peptide, with a deletion of 41 amino acids at the C-terminus. Sequence from bp 348 to bp 533. With mutation. Used primers:

pro Bam for:

5' TAT AAT GGG ATC CGT GAA CCG TAC ACA GAT AGC AAT G 3'

C-term-41:

5' TGT ATA TGT ACT GCA GGT CAC GCT TCC TTA AAC AGT CTG
GG 3'

8. **pro N-10:** only the pro-peptide, with a deletion of 10 amino acids at the N-terminus. Sequence from bp 378 to bp 656. With mutation. Used primers:

N-term-10:

5' TAT AAT GGG ATC CGT GGA GAC TCT GTC CCT GAA G 3'

pro-only-Pst-back:

5' TGT ATA TGT ACT GCA GGT CAG CGC TTG CTC CGG TGA G 3'

2.7. Cloning and expression of scFv anti-proNGF for periplasmic preparation

The selected scFv obtained from the IACT selection was cloned by restriction with the enzymes BssHII/NheI into the pDAN vector for periplasmic expression of the

protein. The vector allows the expression with two tags at the C-terminus: an SV5 tag and a His tag.

2.7.1. Periplasmic expression of scFv anti-proNGF

400 mL of 2*YT medium + Ampicillin were inoculated with an overnight culture at 1:100 ratio. The cultures were grown at 37°C until an OD₆₀₀=0.5-0.6 and then induced with IPTG 1 mM for 4.5 hours at 30°C.

The cells were harvested at 5000 rpm (Beckman) and the pellet were saved at -80°C.

The pellet was resuspended in 10 mL of cold PPB buffer, and incubated on ice for 20 minutes.

Then, the sample was centrifuged at 5000 rpm for 15 minutes and the supernatant was transferred in a new tube.

The pellet was resuspended in 10 mL of 5 mM MgSO₄ buffer and incubated on ice for 20 minutes.

Then, both preparation were centrifuged at 10000 rpm for 15 minutes, the supernatant was collected and dialyzed against PBS.

2.7.2. Purification of the scFv from periplasm

The purification of the scFv expressed in the periplasm of *E. coli* was achieved through affinity purification on the Ni-NTA resin (QIAGEN). The procedure was the one indicated by the manufacturer.

2.8. Cloning and expression of the scFv in the cytoplasm of *E. coli*

2.8.1. Cloning of the scFv

The scFv anti-proNGF selected from SPLINT was sub-cloned into the vector pETM-13 for cytoplasmic expression in *E. coli*.

The whole scFv, with the SV5 and the His tags was cloned by PCR, using the primers:

Anti-pro for (sense):

5' – TAT AAT GGA TCC ATG GAT GCC GAA ATT GTT CTC ACC – 3'

Anti-pro back (antisense):

5' – TGT ATA TGT AGC GGC CGC AGT ACT ATC CAG GCC CAG C
– 3'

The amplified region is highlighted in the “Results” section.

2.8.2. Expression of the scFv in the cytoplasm of *E. coli*

400 mL of 2*YT medium + Kanamycin were inoculated with an overnight culture at 1:100 ratio. The cultures were grown at 37°C until an OD₆₀₀=0.7-0.8 and then induced with IPTG 0.5 mM for 4.5 hours at 37°C.

The cells were harvested at 5000 rpm (Beckman) and the pellet were saved at -80°C.

2.8.3. IB preparation and solubilization

The same protocol was adopted, already described for the preparation of IB for rm-proNGF. The only difference was in the cell disruption, performed *via* sonication (three pulses of 45 seconds each at 13000 micron, followed by 1 minute incubation on ice) instead that using the Franch Press.

Also the IB solubilization was carried out in the same way already described for the rm-proNGF

2.8.4. Refolding of scFv anti-proNGF

The optimization of the pulsed refolding of the scFv anti-proNGF is described in the “Results” section.

The general, technique, however, is the same already described for the rm-proNGF.

At the best of the optimized refolding conditions, the refolding was performed into a 1 L of refolding buffer: Tris 100mM pH 8.5, 400mM Arg, 375uM GSSG, 5mM EDTA. The pulses were done every hour, with a protein concentration of 35 µg/mL. After the last pulse, the refolding solution was left at 4°C for 48 hours.

After volume reduction by ultrafiltration, the sample was dialyzed against Tris 20mM pH8, and the sample was purified.

2.8.5. Purification of refolded scFv anti-proNGF

The purification of the refolded scFv anti-proNGF was achieved through two subsequent steps: an anion exchange chromatography and a size-exclusion chromatography.

The anion exchange chromatography was performed on a HiTrap Q column (5 mL – Amersham Pharmacia), equilibrated with 20 mM Tris, pH 8 as A buffer. The elution of the sample was achieved with a linear gradient from 0 to 70 % of B buffer (A buffer + 1 M NaCl).

The sample was then dialyzed against PBS and purified on a size exclusion chromatography column, a Superdex 75 (Amersham Pharmacia), equilibrated with PBS.

2.9. Cloning of scFv into scFv-cyto-SV5 vector

The cDNA of the scFv anti-proNGF was subcloned by restriction with enzymes BssHII/NheI into the vector scFv-cyto for mammalian cells transfection, cut with the same enzymes.

The subsequent transfection of the HEK 293 cells was performed with standards methods, using FuGene to transfect the cells, according to manufacturers instructions.

RESULTS

PART 1:

BIOCHEMICAL CHARACTERIZATION

AND

STRUCTURAL INSIGHTS

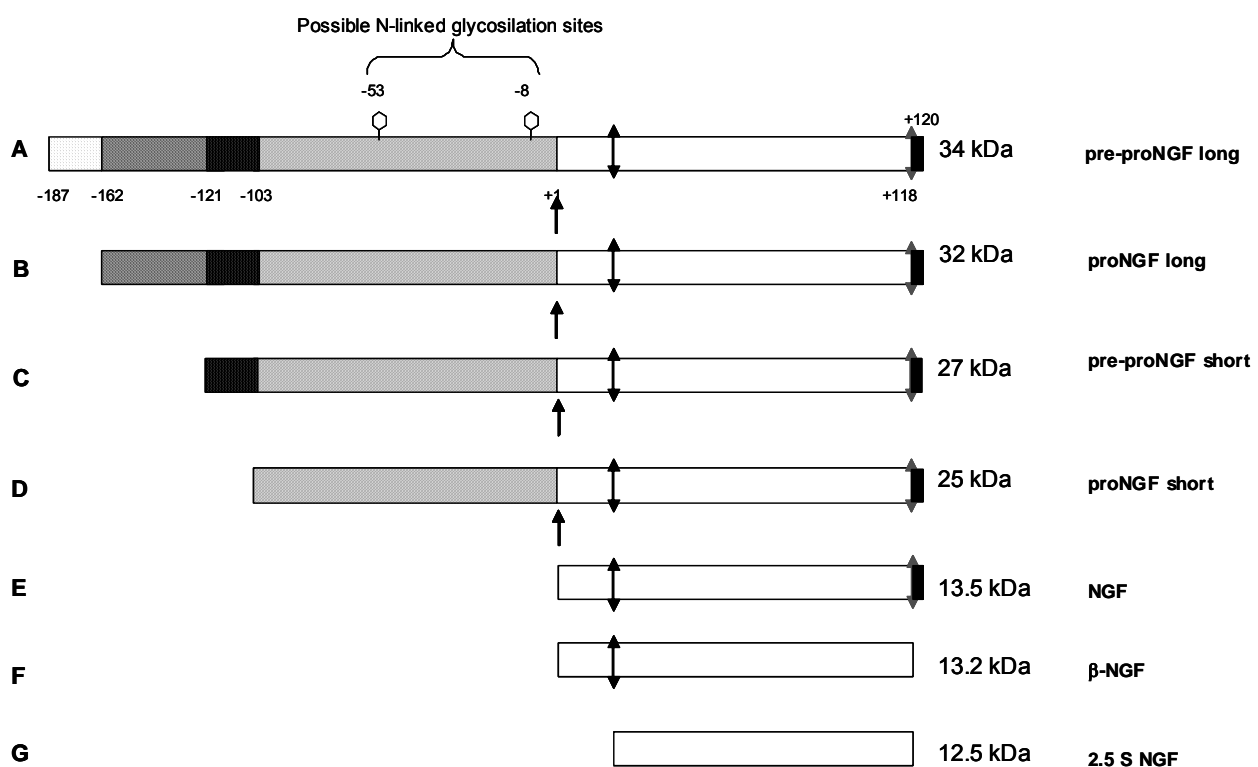
OF M-PRoNGF

IN ITS DIFFERENT FORMS

The different recombinant proNGF proteins that will be presented in this part of the Results will be described referring to the following scheme and table.

Summary of the main products of the transcripts of NGF precursor

The following scheme represents the transcripts products of the NGF precursor. The figure was adapted from Fahnestock *et al.*, Progr. Brain Res., 2004).



Summary table of the abbreviations used in the text

Abbreviation	Extended description
m-NGF	Mouse NGF, commercial
h-NGF	Human NGF
rm-NGF	Recombinant mouse NGF
rh-NGF	Recombinant human NGF
m-proNGF	Mouse proNGF, short precursor of NGF, without signal peptide; transcript D in scheme
rm-proNGF	Recombinant mouse proNGF, short precursor of NGF, without signal peptide; transcript D in scheme
h-proNGF	Human proNGF, short precursor of NGF, without signal peptide; transcript D in scheme
rh-proNGF	Recombinant human proNGF, short precursor of NGF, without signal peptide; transcript D in scheme
pre-proNGF long	Long precursor of NGF, with signal peptide; transcript A in scheme
pre-proNGF short	Short precursor of NGF, with signal peptide; transcript C in scheme
proNGF long	Long precursor of NGF, without signal peptide; transcript B in scheme
proNGF short	Short precursor of NGF, without signal peptide; transcript D in scheme
rm-proNGF P5A	Recombinant mouse proNGF, short precursor of NGF, without signal peptide; transcript D in scheme. With mutation Proline to Alanine on position 5 on NGF.
GST-pro	Fusion construct of GST protein to the N-terminal of the short pro-peptide of m-proNGF
pro-GST	Fusion construct of GST protein to the C-terminal of the short pro-peptide of m-proNGF

1. rm-proNGF expression in *E.coli*: a tool for large-scale production of m-NGF and rm-proNGF

SUMMARY

In this chapter of the thesis I will described the employment of an *in vitro* expression system for m-proNGF in order to produce a well characterized protein for biophysical, biochemical and cell biology studies.

ProNGF is not a soluble protein when expressed in *E.coli*, due to the presence of a complex disulfide bridge connection in the NGF moiety (see the Introduction, p.5). Therefore the protein is sent to inclusion bodies (IB) when expressed in *E.coli* and needs to be subsequently refolded *in vitro*.

In this thesis, the cDNA of the protein was amplified by RT-PCR from the submandibulary glands of mouse. The cDNA was subsequently cloned into a vector suitable for recombinant protein production in *E.coli*, and the protein could be successfully expressed, refolded and purified, according to the protocols established for the rh-proNGF. A full biochemical/biophysical analysis on the protein was carried out, to verify the correct folding and the specific biochemical parameters.

For a further structural and functional analysis of the protein, other proteins were cloned and expressed: that is, a point mutation clone, P5A, and two fusion protein of the pro-peptide of m-proNGF with the GST protein, namely GST-pro and pro-GST.

1.1 RT-PCR and cloning

The cDNA used for the expression of recombinant mouse proNGF (rm-proNGF) in this thesis was obtained by RT-PCR from the RNA extracted from submandibulary glands of mouse, known to be a rich source of NGF.

In particular, two glands of adult mice were homogenized, and total RNA was subsequently prepared as described in the experimental section. The total RNA preparation resulted to be of good quality as shown in fig.1.1.1, representing an agarose gel of the RNA preparation.

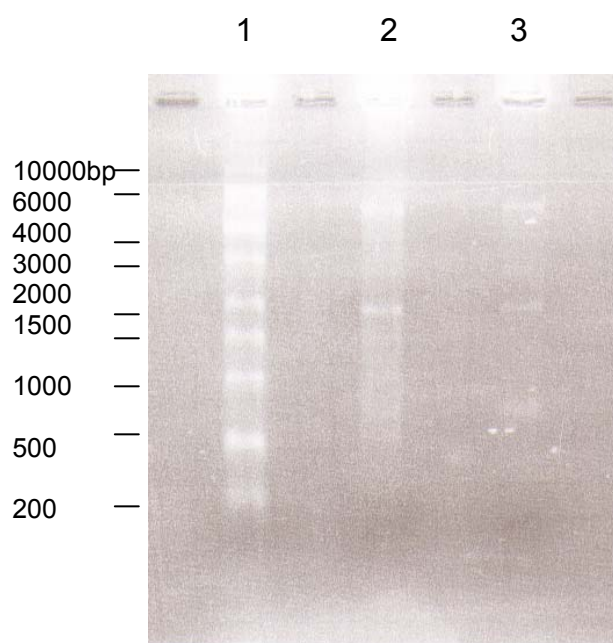


Figure 1.1.1 – Agarose gel for RNA preparation analysis. Lane 1: RNA marker for molecular weight (SIGMA 7020); lane 2 and 3: two different RNA preparations.

From the total RNA preparation, the mRNA corresponding to the proNGF was fished out using an RT-PCR with the specific primers PRE (at 5' end) and 3'UTR (at 3' end), described in the experimental section. With these primers, the cDNA corresponding to the so called "short" pre-proNGF was considered, according to the nomenclature described in the Scheme at p.74 for the possible NGF forms. The amplification reaction resulted to be clean enough to only amplify the expected band corresponding to 917 bp (see fig. 1.1.2 – lane 2); the controls resulted to be all good: the positive control amplified a band of 320 bp as expected (fig. 1.1.2 – lane 5), and the two negative controls were clean (fig.1.1.2 – lane 6 - control A: no addition of RNA; fig.1.1.2 – lane 7 - control B: no addition of RNA and primers). A second RT-PCR reaction was also performed, using a different primers pair, namely the PRE at 5'-end and the polyT at 3'-end, for the amplification of the cDNA up to the polyA tail. But as is clear from the picture in fig.1.1.2 – lane 3, this reaction didn't give rise to any well defined amplification product.

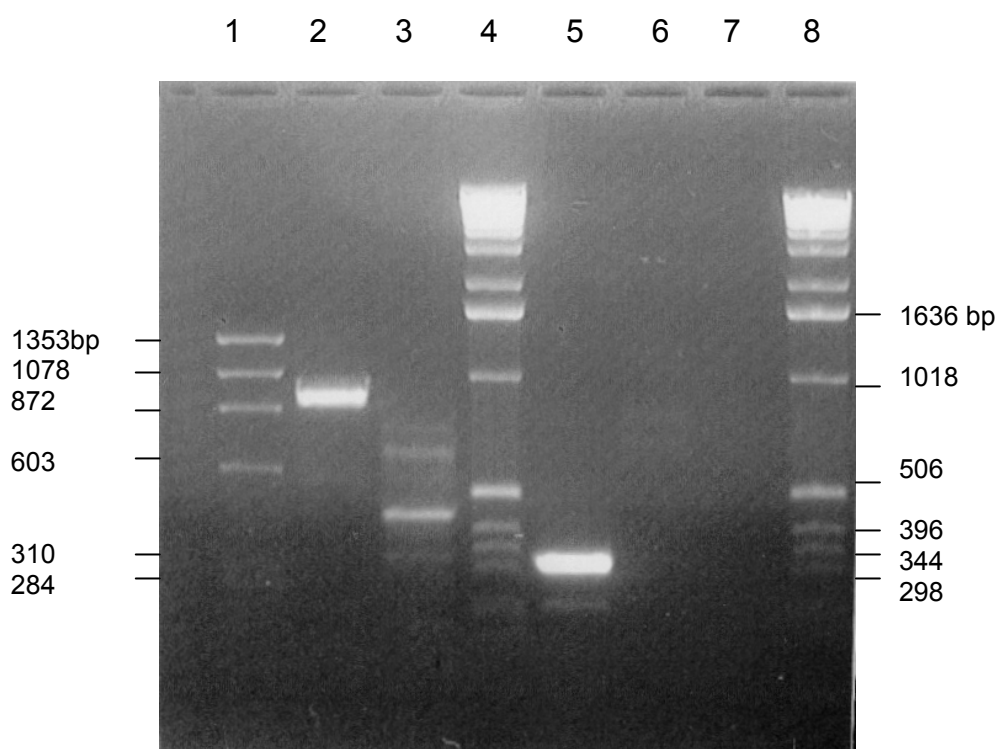


Figure 1.1.2 – Agarose gel with the samples of the RT-PCR reaction for the amplification of the cDNA of m-proNGF. Lane 1: DNA marker; lane 2: RT-PCR with primers PRE and 3'UTR; lane 3: RT-PCR with primers PRE and polyT; lane 4: Marker 1kb for DNA dimension; lane 5: Positive control from the kit (see Experimental Section); lane 6: Negative control A; lane 7: Negative control B; lane 8: Marker 1kb

The amplification product was purified on a preparative agarose gel, the band corresponding to the interesting cDNA was cut and the cDNA extracted using the Gel-extraction kit.

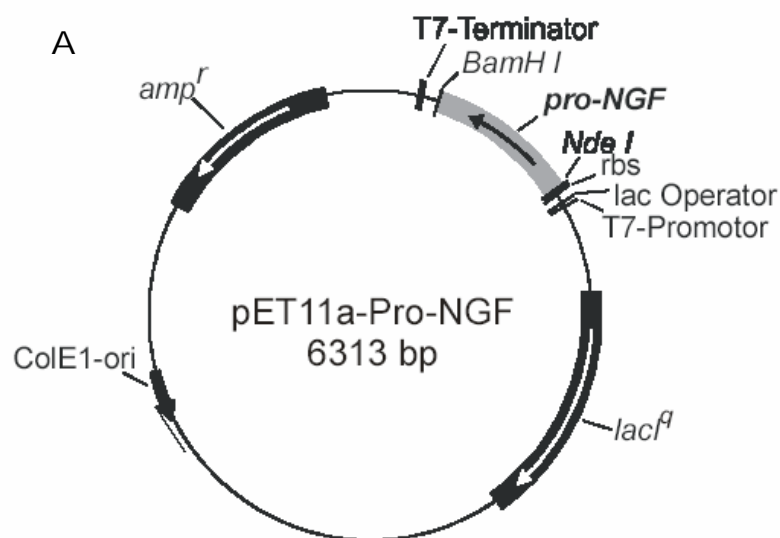
The cleaned band needed to be subsequently cloned into a suitable vector for the expression of the protein.

In the search for the best conditions for the expression of the protein in *E.coli*, various options were considered, selecting a series of vectors suitable for *in vitro* protein expression. For this purpose, the amplification product from RT-PCR was used as a template for a PCR reaction to isolate a cDNA containing at the termini the suitable restriction sites for the cloning into the expression vectors. In this case, the DNA corresponding exclusively to the short proNGF was amplified, excluding from the amplification the signal peptide, not only because it is a very hydrophobic

peptide, and therefore not suitable for expression in *E.coli*, but also because this peptide is normally cleaved *in vivo* after targeting of the translation product in the Endoplasmic Reticulum (ER), and is therefore not present when the protein is secreted to perform its biological function; it's not necessary, therefore, for the functional studies using the recombinantly produced m-proNGF. Moreover, the last two amino acids at the C-terminus were excluded, since they are physiologically removed after protein expression (see Scheme at p.74).

The m-proNGF cDNA was successfully cloned in the following vectors: pETM-13 (EMBL), pET11a (Promega), pTrcHis (Invitrogen); in this last case also the cDNA corresponding to the short pre-proNGF was cloned. In each case, clones were selected after DNA sequencing to check the correctness of the nucleotide sequence. An expression trial was performed with each of the prepared constructs, and the best one resulted to be the m-proNGF cloned into pET11a, as also reported by the previous studies on the expression and *in vitro* refolding of rh-proNGF (Rattenholl *et al.*, Eur. J. Biochem., 2001) (data not shown).

The constructed plasmid is shown in fig. 1.1.3 A, and the corresponding amplified amino acid sequence of m-proNGF is shown in fig. 1.1.3 B.



B

```

      -100      -90      -80      -70
M E P Y T D S N V P E G D S V P E A H W T K L Q H S L D T A L R R A R S A
      -60      -50      -40      -30
P T A P I A A R V T G Q T R N I T V D P R L F K K R R L H S P R V L F S T Q P P P
      -20      -10      +1      +10
T S S D T L D L D F Q A H G T I P F N R T H RSKR S S T H P V F H M G E F S V C
      +20      +30      +40      +50
D S V S V W V G D K T T A T D I K G K E V T V L A E V N I N N S V F R Q Y F F E T
      +60      +70      +80      +90
K C R A S N P V E S G C R G I D S K H W N S Y C T T T H T F V K A L T T D E K Q
      +100      +110      +118
A A W R F I R I D T A C V C V L S R K A T R

```

Figure 1.1.3 – Plasmid construct pET11a-m-proNGF for the cytoplasmic expression of rm-proNGF in *E. coli* (Panel A) and primary sequence of the cloned proNGF (Panel B). The figure in panel **A** was taken from the PhD thesis of A. Rattenholl (University of Halle). In panel **B**, the short pro-peptide is indicated in blue; the mature NGF is highlighted in cyan. The consensus sequence for the furin cut is indicated in dark green and underlined. The starting Methionin, in red, was added during the cloning procedure.

1.2 Expression, refolding and purification of rm-proNGF

The m-proNGF cloned into pET11a vector, was used to transform the *E.coli* strain BL21, suitable for expression of recombinant proteins.

The expression of the protein was made both in shaking flasks and in fermentation facility. From 1L of culture, around 400mg of inclusion bodies pellet could be restored, containing almost entirely the rm-proNGF (fig.1.2.1 – red arrow).

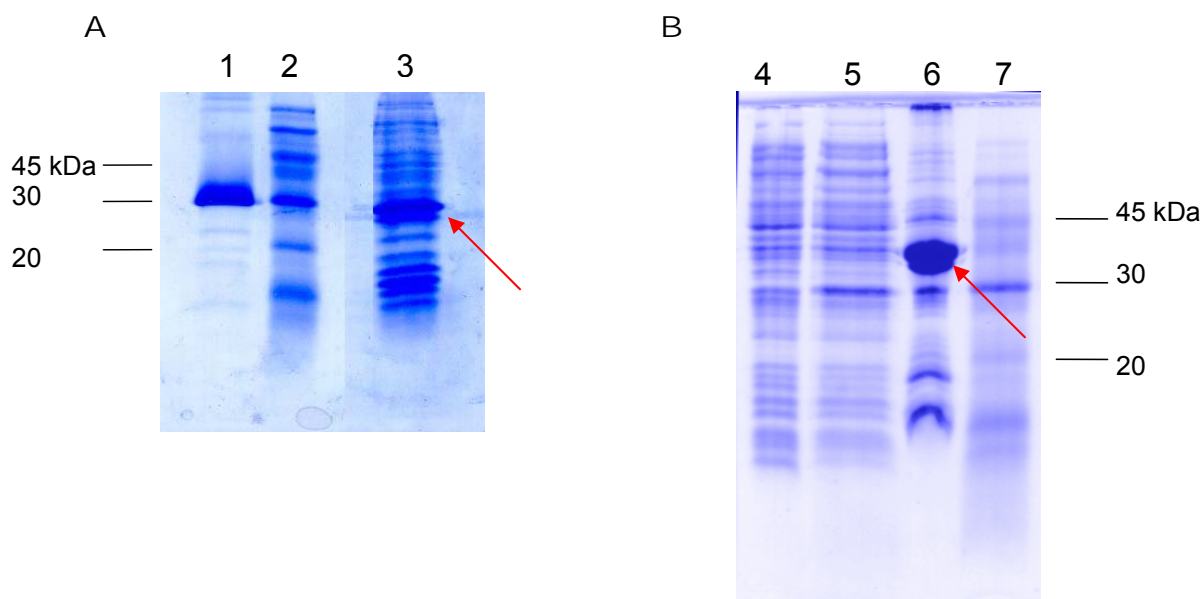


Figure 1.2.1 – SDS-PAGE with the samples of rm-proNGF IB in shaking flasks (panel A) and in fermentation facility (panel B). Lane 1: h-proNGF as reference; lane 2: molecular weight marker; lane 3: m-proNGF IB preparation; lane 4: pre-induction control; lane 5: post-induction control; lane 6: m-proNGF IB preparation; lane 7: molecular weight marker

The inclusion bodies (IB) pellet was treated according to the previously described protocol (Rattenholl *et al.*, Eur. J. Biochem. 2001). Briefly, the IB pellet was solubilized in denaturing conditions and the protein refolded in presence of Arginine as stabilizing agent and the redox shuffling system composed by an adequate mixture of reduced and oxidized Glutathion; the overall pH of the refolding buffer is alkaline.

Although the major part of the protein in the IB is the rm-proNGF, the protein needed to be purified by contaminating proteins and non-native rm-proNGF.

The basic isoelectric point of the protein, makes it suitable for purification the use of a cation exchange chromatography. In particular, in the case of rm-proNGF, the column SP-Sepharose (Amersham Pharmacia) was used and the purification was carried out in phosphate buffer at neutral pH, with a linear gradient of NaCl. The profile of the purification chromatography is represented in fig. 1.2.2.

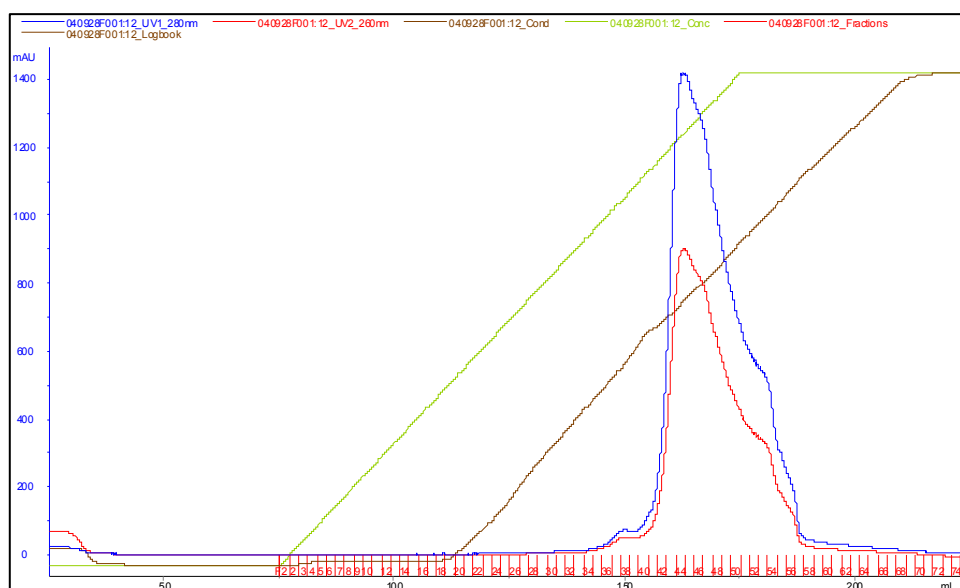


Figure 1.2.2 – Chromatographic profile of the purification of rm-proNGF by ion-exchange chromatography. The blue curve represents the absorbance at 280 nm, while the red one the absorbance at 260 nm. The green curve represents the gradient change in % of salt; the brown curve represents the change in the conductance of the system during the gradient.

For a further purification of the protein, a second chromatographic step was introduced, namely a step of a hydrophobic interaction chromatography, using a Phenyl Sepharose column (Amersham Pharmacia) and a linear decreasing gradient in ammonium sulfate content. The profile of this chromatographic purification step is shown in fig. 1.2.3.

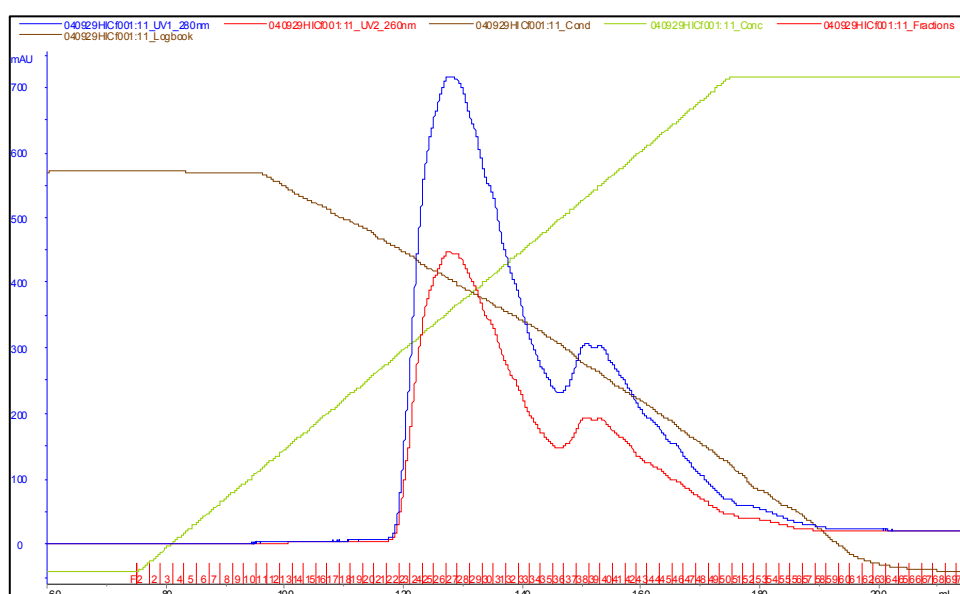


Figure 1.2.3 – Chromatographic profile of the purification of rm-proNGF by hydrophobic interaction chromatography. The blue curve represents the absorbance at 280 nm, while the red one the absorbance at 260 nm. The green curve represents the gradient change in % buffer without ammonium sulfate; the brown curve represents the change in the conductance of the system during the gradient.

After the purification steps, the protein results to be clean by more than 90%, according to a Coomassie Blue staining of an SDS-PAGE polyacrylamide gel (fig. 1.2.4), also after gel overloading. The final yield was of 30 mg of pure rm-proNGF *per* litre of bacterial culture.

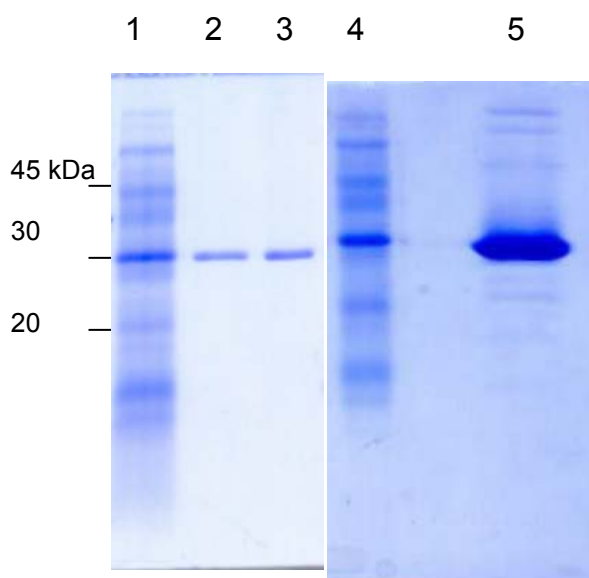


Figure 1.2.4 – SDS-PAGE stained with Coomassie Blue. Lanes 1 and 4: molecular weight marker; lane 2 and 3: two different amounts of purified rm-proNGF; lane 5: overloaded gel for rm-proNGF

The apparent molecular weight of the protein on an SDS-PAGE is around 30 kDa, value that is slightly higher than the expected 25 kDa (from theoretical calculation from Expasy web-server). This is probably due to the isoelectric point (pI) of rm-proNGF, which is 9.6 according to the theoretical calculations of the Expasy web-server, and this makes the protein highly positively charged at the usual pH of 8.8 of the running buffer of the SDS-PAGE, assuming more negative charges than it would be for a positive or neutral protein of the same molecular weight.

The anomalous run of the protein could be avoided by loading the protein on an SDS-PAGE in oxidative conditions, *i.e.* in absence of the reductive agent DTT. As

shown in fig.1.2.5, in fact, in these conditions the protein was running around 25 kDa as expected.

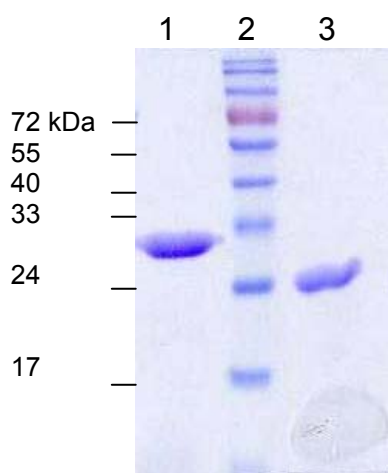


Figure 1.2.5 – SDS-PAGE stained with Coomassie Blue. Lane 1: m-proNGF loaded with addition of DTT; lane 2: molecular weight marker; lane 3: m-proNGF loaded without addition of DTT

The run on an SDS-PAGE in oxidizing conditions allowed also to exclude the presence of wrong inter-chain disulfide bridges among the two monomers of the rm-proNGF dimer. Indeed, as shown in fig. 1.2.5, the rm-proNGF runs on an SDS-PAGE as monomer, both in reducing and in oxidizing conditions.

1.3 Characterization of rm-proNGF

The estimation of the molecular weight of rm-proNGF and of its multimeric state in solution was evaluated by a run on size-exclusion chromatography, in particular using a Superdex 75 column. The protein eluted as a single peak and the retention time corresponds to a molecular weight of around 50 kDa (according to the calibration of the column), as expected for a dimeric state of the protein (fig. 1.3.1). It should be noted that the protein rm-proNGF interacts very tightly with the column matrix, and therefore a small amount of the protein is actually eluting from the column, if one considers the amount loaded.

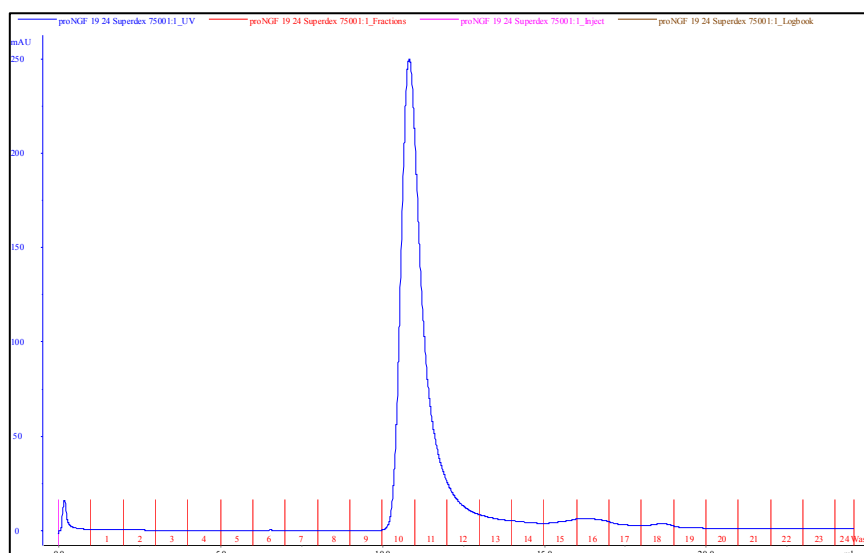


Figure 1.3.1 – Size exclusion chromatography profile of purified rm-proNGF. The chromatographic run was performed on a Superdex 75 (Amersham Pharmacia) column. The chromatogram represents the elution profile of rm-proNGF detected by the absorbance at 280 nm.

The precise molecular weight of the purified rm-proNGF was established by mass spectrometry. The protein was first loaded on a C4 column for RP-HPLC, in order to change the buffer of the system and make it suitable for mass spectrometry. The protein resulted to be reasonably clean (see fig. 1.3.2), since one main peak eluted from the column, at the expected retention time for rm-proNGF (compare to the rh-proNGF in PhD thesis from Rattenholl, 2001).

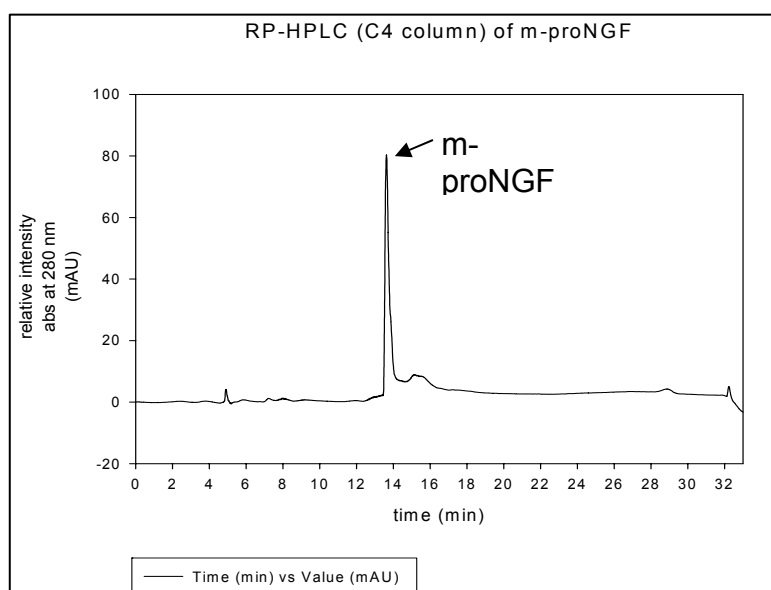


Figure 1.3.2 – Elution profile of the RP-HPLC on the purified rm-proNGF. The rm-proNGF (100 μ g) was loaded on a C4 RP-HPLC column and eluted with a discontinuous gradient of acetonitrile. The chromatogram was recorded at 280 nm.

After the elution from HPLC column, the sample was analyzed using electron-spray mass spectrometry (ESI-MS). The theoretical value for the molecular weight of rm-proNGF with oxidized Cysteins is 24'990 Da, and the measured value results to be of 24'987 Da (fig. 1.3.3), in optimal accordance with the expected one.

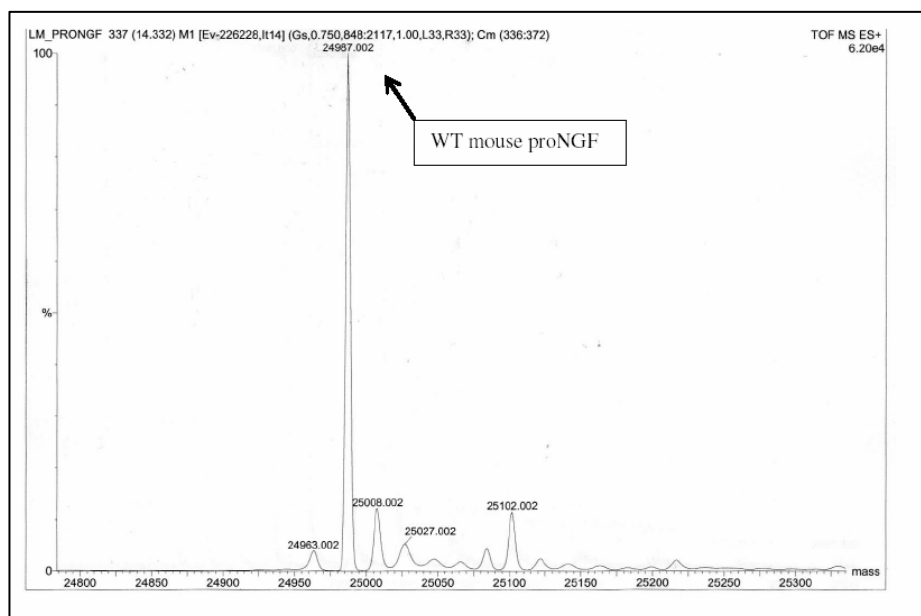


Figure 1.3.3 – Mass Spectrometry analysis on the purified rm-proNGF. The molecular weight deconvolution spectrum is shown. The arrow indicates the molecular weight of rm-proNGF.

Although the protein is eluting as a single peak in RP-HPLC, this is still not the proof for the correct folding of the protein. The spectral properties of the recombinant rm-proNGF were therefore used to verify the correct folding of the protein; in particular, rm-proNGF contains four Tryptophanes (Trp), three Tyrosines (Tyr) and eleven Phenylalanines (Phe), of which one Trp, one Tyr and four Phe are localized in the pro-sequence.

The UV-absorption spectrum of the sample resulted to correspond to the one expected from the rm-proNGF protein, if compared to the one published for the rh-proNGF (see Rattenholl *et al.*, Eur.J.Biochem. 2001); the emission maximum is correctly localized at 280 nm (fig.1.3.4). The absorption of the Phenylalanine is difficult to be recognized in the range between 255 and 275 nm; although there are Phenylalanines present in rm-proNGF, their absorption is small, and is than the one of Tyrosine and Tryptophane, that have an extinction coefficient of one order of

magnitude bigger than the one of Phenylalanines. The maximum at 280 nm and the shoulder at 290 nm should be attributed to the Tryptophane.

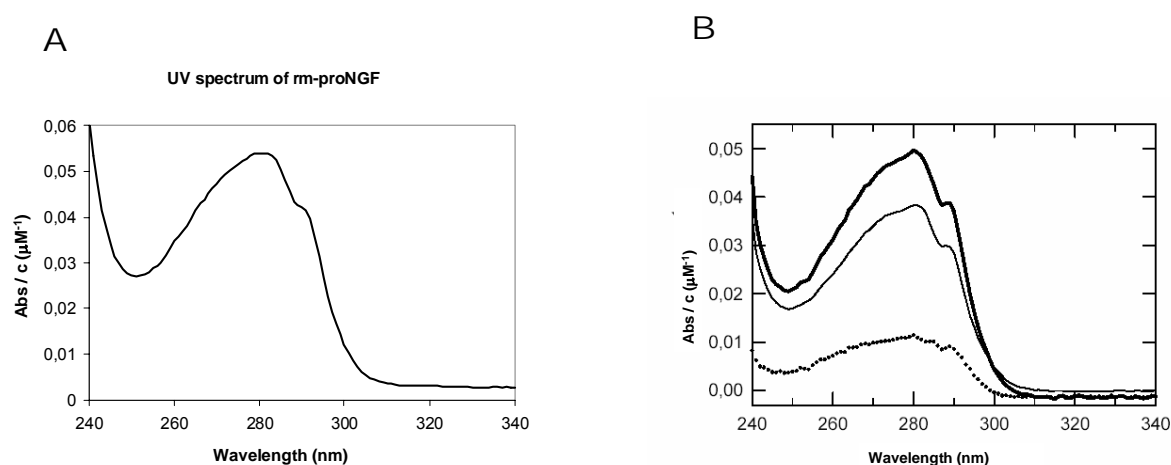


Figure 1.3.4 – UV absorption spectrum for rm-proNGF (panel A) and for rh-proNGF (panel B). The recorded UV-spectrum for rm-proNGF is compared to the one of rh-proNGF presented by Rattenholl and colleagues (2001). In both cases the spectra were corrected for the concentration and buffer subtracted. In panel B, the thin line represents the spectrum for rh-NGF, the thick line represents the spectrum for rh-proNGF and the dotted line represents the difference spectrum of the two proteins. All spectra were recorded at 22°C in 50 mM Sodium-phosphate, pH 7.0.

The fluorescence emission spectra of purified rm-proNGF in native and denatured conditions were recorded (fig.1.3.5), in order to compare it to the previously published one for rh-proNGF. The selected excitation wavelength was 280 nm. The fluorescence of Phenylalanine was not taken into consideration, due to its low sensitivity and the energy transfer to Tyrosines and Tryptophanes (Schmid, 1997).

The fluorescence maximum of native rm-proNGF is 335 nm, almost the same value recorded for the rh-proNGF (337 nm).

In denaturing conditions (fig. 1.3.5, panel A, dotted line) the spectrum was looking substantially different from the native conditions, as it is expected to be: the maximum is shifted towards higher wavelengths (354 nm) and the fluorescence intensity is decreased. Overall, the fluorescence spectra allowed to confirm that the

protein was in its native conformation, according to the comparison to the previously reported data for the human protein (reported in fig. 1.3.5, panel B).

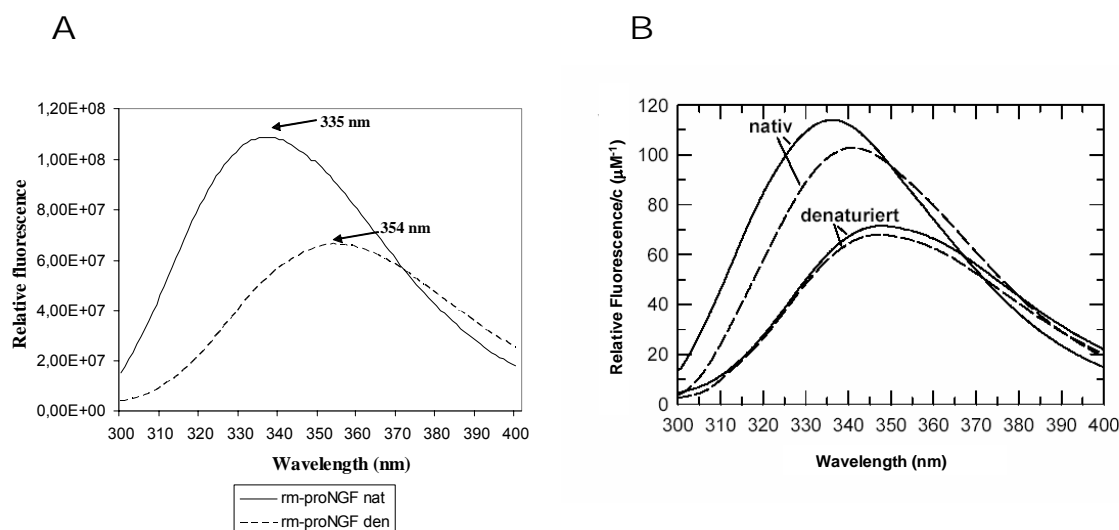


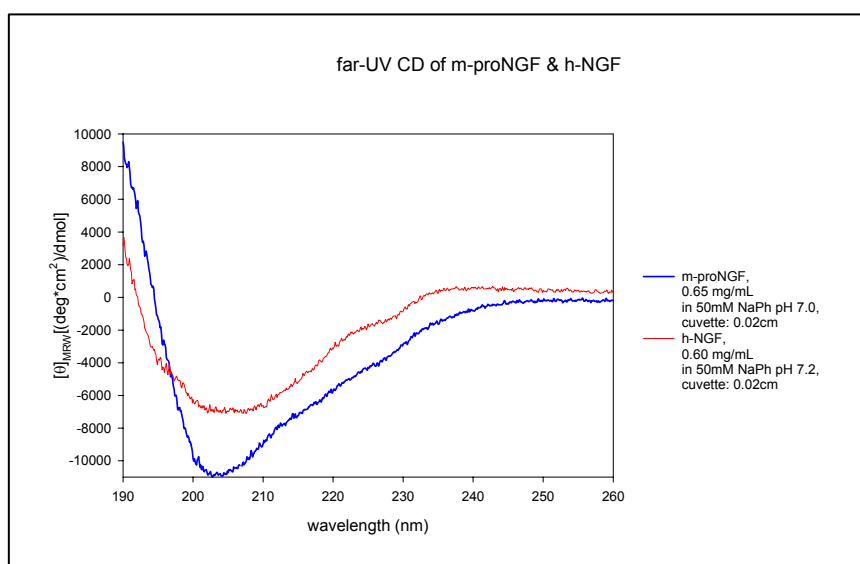
Figure 1.3.5 – Fluorescence emission spectra of m-proNGF (panel A) and for rh-proNGF (panel B). The recorded fluorescence emission spectrum for rm-proNGF is compared to the one of rh-proNGF presented by Rattenholl and colleagues (2001). In both cases the spectra were buffer subtracted; in panel B the fluorescence intensity was concentration corrected. In Panel A, the black curve indicates the spectrum for rm-proNGF in native conditions, while the dotted line represents the one in denaturing conditions. In panel B, the dotted line represents the spectrum for rh-NGF, the solid line represents the spectrum for rh-proNGF, both in native and denatured conditions as indicated by the arrows. All spectra were recorded at 20°C in 50 mM Sodium-phosphate, pH 7.0, 1mM EDTA; for the denaturing conditions, 6 M GdmHCl was added to the solution.

To verify the secondary structure composition of the purified rm-proNGF, the Circular Dichroism (CD) spectra of the native protein were recorded, both in the far-UV (190-250 nm) (fig.1.3.6 – panel A) and in the near-UV (250-350 nm) (fig.1.3.6 – panel B). The spectra were then compared with both the corresponding spectra for mature h-NGF and for rh-proNGF. The far-UV spectrum of the purified rm-proNGF (fig.1.3.6 – panel A) is overall resembling the one of the rh-proNGF, showing the same secondary structure composition. In particular, it presents a decrease of the signal between 235 and 210 nm, due to the β -sheet structure. From there on, it has a

deep minimum around 205 nm (compare also Timm & Neet, Prot. Sc., 1992; Narhi *et al.*, JBC, 1993). The spectrum of native rm-proNGF in the far-UV is comparable to the one of mature h-NGF in the region between 235 and 210 nm, but presents a deeper minimum around 202 nm. This feature is typical from non-structured protein, and allows therefore to conclude that the contribution of the pro-sequence to the secondary structure is mainly the one of a protein that does not present a definite secondary structure.

The near-UV spectrum (fig.1.3.6 – panel B) presents a fine structure in the range between 280-300 nm, that is not present in the mature protein. This finding allows to state that the Tryptophane residues in the pro-sequence are present in an asymmetric environment in the rm-proNGF protein.

A



B

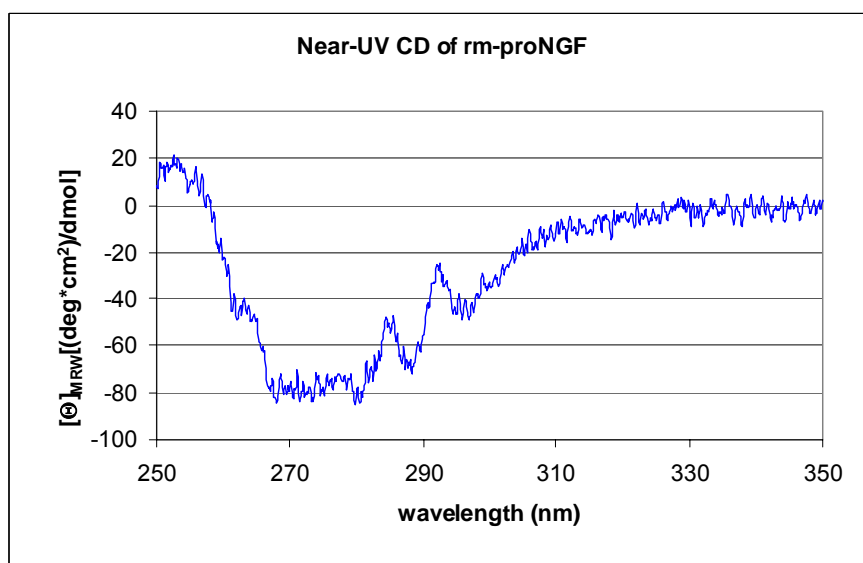


Figure 1.3.6 – Far-UV (Panel A) and Near-UV (Panel B) circular dichroism spectra of rm-proNGF. The mean ellipticity values were calculated. In the panel A, the blue trace represents the spectrum of rm-proNGF, while the red one indicates the spectrum of NGF by comparison. Both kinds of spectra were recorded in 50 mM Sodium phosphate. Panel A (far-UV spectra): of 0.6 mg/mL in a 0.02 cm cell, averaged over 10 accumulations (acquisition time: 2 s). Panel B (Near-UV spectrum): protein concentration of 0.3 mg/mL, in a 1 cm cuvette. Spectra were buffer corrected.

The experimental isoelectric point of the purified rm-proNGF was evaluated by mean of an isoelectric focusing gel. In particular, the protein was loaded on a gel with a wide range of pH and after the run it was possible to establish that the protein has indeed a very basic pI. It's not possible to calculate the precise value, due to the fact that the protein is more basic than the maximum possible value allowed from the pre-cast gel, *i.e.* pI=9 (fig.1.3.7).

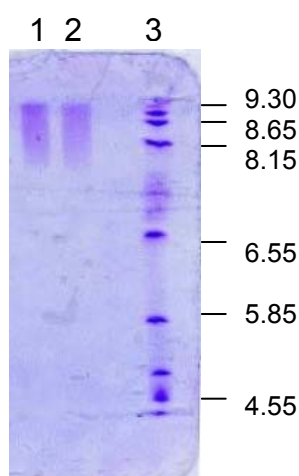


Figure 1.3.7 – Pre-cast gel for isoelectric focusing. Lane 1 and 2: m-proNGF; lane 3: pH marker. Performed with with the Phast system from Amersham Pharmacia.

The polydispersity in solution of the purified rm-proNGF was proven by measuring the Dynamic Light Scattering parameters (table 1.3.1). These DLS measurements indicated a molecular hydrodynamic radius of 3.5 nm (the distribution of the radius is shown in fig.1.3.8) and a typical solution poly-dispersity of 26% (see table 1.3.1).

Table 1.3.1

<i>Type of plot</i>	<i>R (nm)</i>	<i>% Pd</i>	<i>MW</i>	<i>% Int</i>	<i>% Mass</i>	<i>Model</i>
Int/Rad	4	27.5	87	95.1	100	
Mass/Rad	3.5	26.9	63	95.1	100	coils
Mass/Rad	3.3	25.7	54	95.1	100	spheres

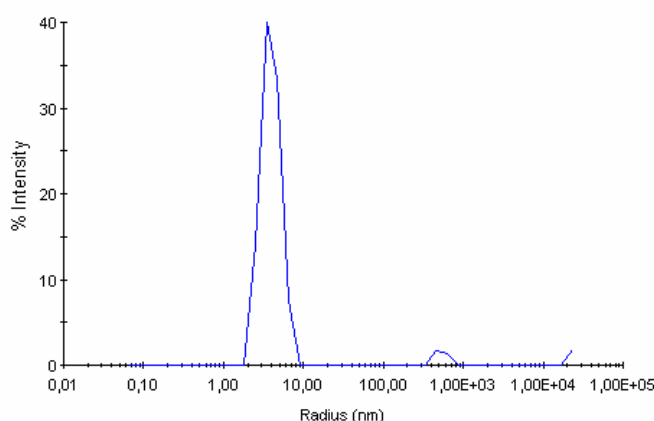


Figure 1.3.8 - dynamic light scattering measurements on rm-proNGF. The distribution of the hydrodynamic radius of the protein sample. The used protein concentration was of 6.5 mg/mL.

1.4 Limited proteolysis of rm-proNGF to release mature m-NGF

The correct folding of the recombinant rm-proNGF was further proven by an indirect technique: limited proteolysis. In fact, if the folding of the protein is correct, it is possible to release the mature m-NGF from its precursor in an active form, as previously shown for rh-proNGF (Rattenholl *et al.*, 2001). *In vivo* the mature NGF is released by its precursor through the cut by specific proteases of the furin family (see Introduction – p.19). *In vitro*, the same result can be obtained both by processing pre-proNGF with stoichiometric quantities of γ -NGF from submandibular glands from mouse and with catalytic quantities of trypsin (Edwards *et al.*, JBC, 1988).

In the present case, rm-proNGF was treated both with trypsin and with recombinant furin, in separate experiments.

The proteolysis with trypsin was optimized according to the already existing protocols (Rattenholl *et al.*, Eur. J. Biochem., 2001 and Experimental Section): rm-proNGF was treated with trypsin and samples at certain time points were taken; the digestion of the samples was stopped by addition of the SDS-PAGE loading buffer, and the samples were analyzed on an SDS-PAGE. The results are shown in fig.1.4.1: after 2h of digestion intact rm-proNGF was converted to mature rm-NGF (the band correspond to the one of the rh-NGF used as control) and no further proteolysis of the rm-NGF took place.

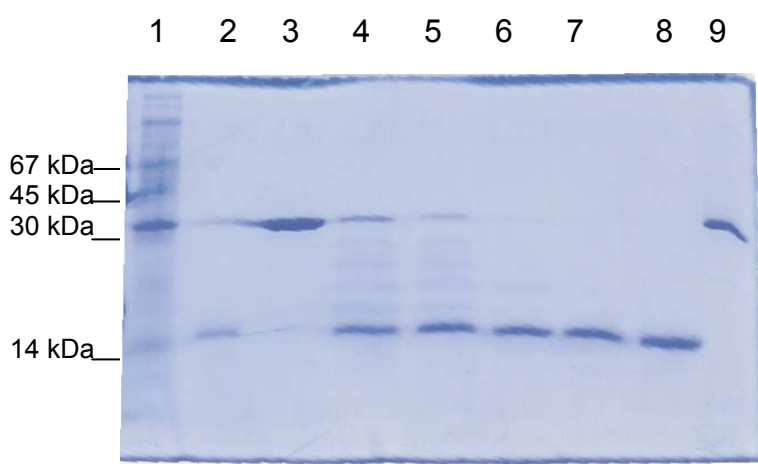


Figure 1.4.1 – SDS-PAGE with the samples of the time-course of the proteolysis of m-proNGF with trypsin. Lane 1: molecular weight marker; lane 2: reference NGF; lane 3: m-proNGF without trypsin; lanes 4 and 5: 15 and 30 minutes trypsin incubation respectively; lanes 6,7,8: 1 hour, 2 hours, 3 hours trypsin incubation; lane 9: reference m-proNGF

The best conditions for the limited proteolysis used for trypsin, were also employed for a preparative processing of rm-proNGF to rm-NGF. The obtained mature rm-NGF was purified by cation-exchange chromatography (SP-Sepharose), in order to separate the mature rm-NGF from the peptide fragments released during the cleavage process. As shown by the chromatogram on fig.1.4.2 and by the SDS-PAGE in fig.1.4.3, where the fractions of the chromatographic separation were loaded, there is a main peak containing mature rm-NGF, that can be completely separated from the other contaminants.

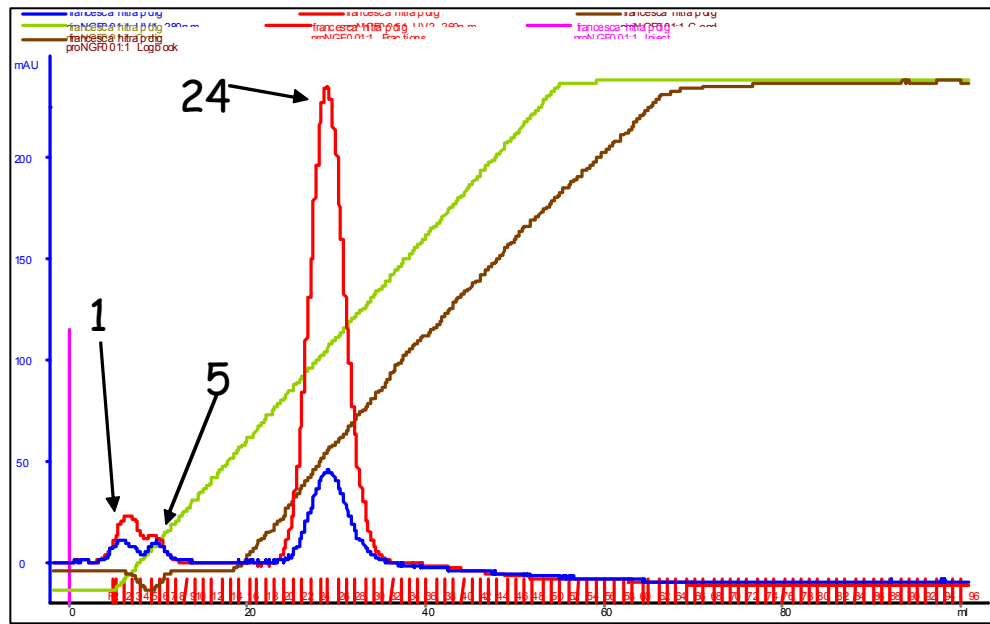


Figure 1.4.2 – Ion exchange chromatography separation of m-NGF released from rm-proNGF. Both the absorptions at 280 nm (red trace) and at 260 nm (blue trace are indicated). The linear gradient for the elution is indicated by both the percentage change in the elution buffer (green trace) and by the change in the conductance of the buffer. The arrows indicate the position and the corresponding numbers of the fractions analyzed on SDS-PAGE (see fig. 1.4.3).

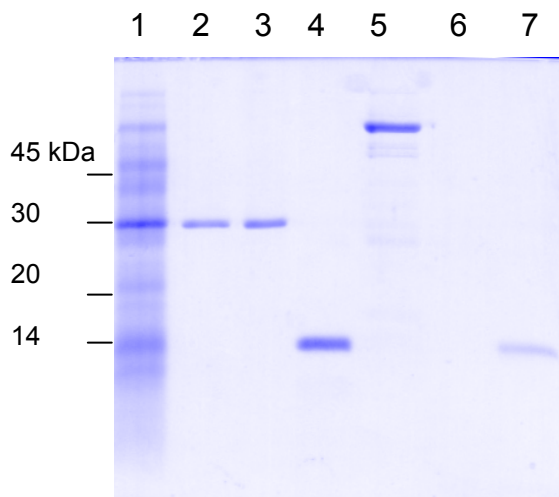


Figure 1.4.3 – SDS-PAGE with the fractions eluted from the ion-exchange column of the m-NGF cut from m-proNGF. Lane 1: molecular weight marker; lane 2 and 3: m-proNGF uncut (different amounts); lane 4: reference NGF; lane 5: fraction 1 of IEX; lane 6: fraction 5 of IEX; lane 7: fraction 24 of IEX

The rm-NGF release by cleavage from the rm-proNGF was also analyzed by liquid chromatography followed by mass spectrometry (LC-MS), for the assessment of the correct molecular weight. After separation on RP-HPLC with the same method

already described for rm-proNGF, the protein resulted to be eluting at the correct retention time and one single peak was detected (see fig.1.4.4).

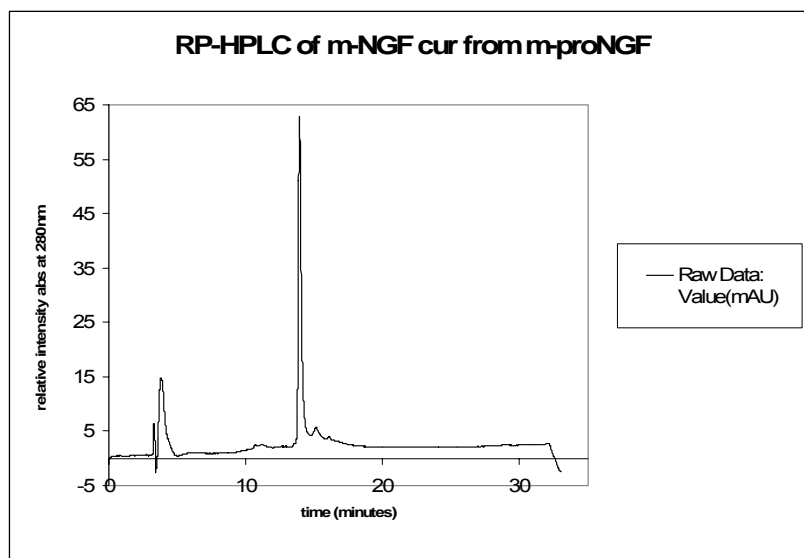
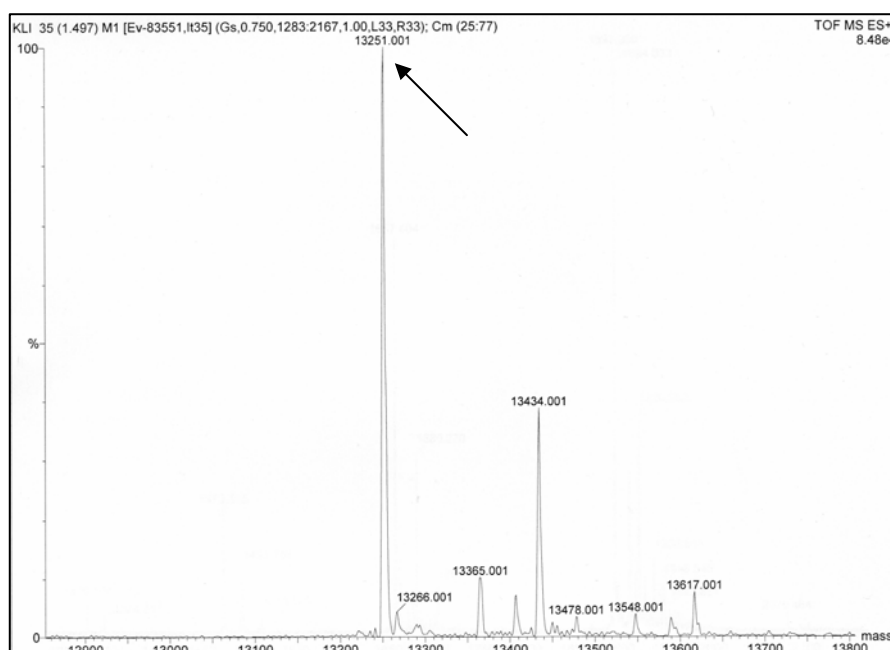


Figure 1.4.4 – RP-HPLC on purified m-NGF from trypsin digestion of m-proNGF. The elution profile recorded at 280 nm is shown.

The sample from HPLC was subsequently analyzed by mass spectrometry (both Ion-spray and MALDI) and as shown in fig.1.4.5 (panel A and B), the experimental value is equal to 13.251 kDa, in perfect agreement with the theoretical value of 13.252 kDa, for the monomeric m-NGF with all oxidized Cysteins. This finding is also a further confirmation that the trypsin proteolysis was giving rise to the intact, complete, mature m-NGF and that no further cleavage took place.

The rm-NGF released by cleavage from rm-proNGF was also tested in bioassay and was shown to be functionally active (data shown later).



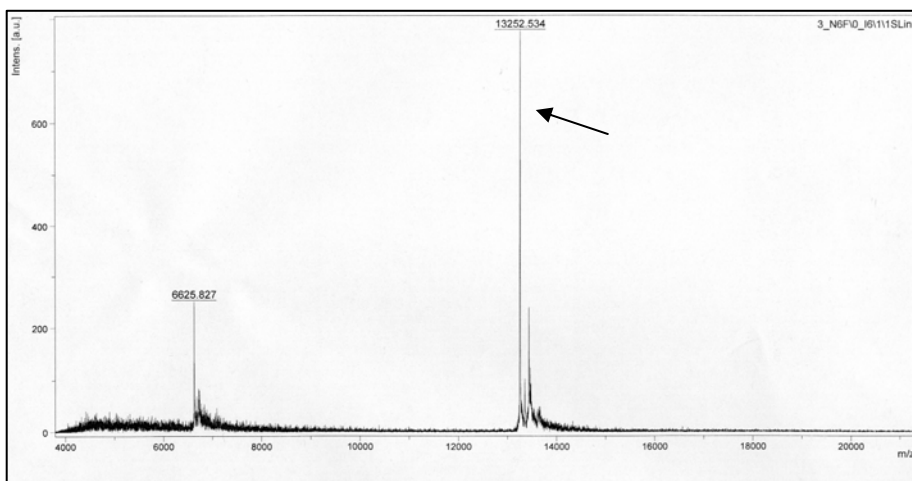


Figure 1.4.5 – Mass spectrometry on the m-NGF released by trypsin digestion from rm-proNGF. Panel A: ion-spray mass spectrometry; Panel B: MALDI-TOF MS. The peak corresponding to the MW of m-NGF in both spectra is indicated by an arrow.

The possibility of releasing mature rm-NGF from rm-proNGF was also tested using recombinant furin as a proteolytic enzyme. In this case there was no protocol available, besides an experiment (Leighton *et al.*, JBC, 2003) reporting proteolysis overnight at 37°C with a ration of 2.5-5 U of furin/ μ g of protein. Since the protein used in the published protocol was different from proNGF, in the case of the latter the reaction was carried out at room temperature instead of 37°C for a more careful analysis; at various time points a sample was extracted and stopped by addition of the SDS-PAGE loading buffer. The samples were finally analyzed on an SDS-PAGE (fig.1.4.6) and surprisingly it was possible to notice that already after 30 min of furin treatment, the protein is completely processed to mature rm-NGF. The appearance of two bands is probably due to the specificity of the protease, which gives rise to two parts: the intact propeptide (expected MW = 11.5 kDa) and the mature rm-NGF.

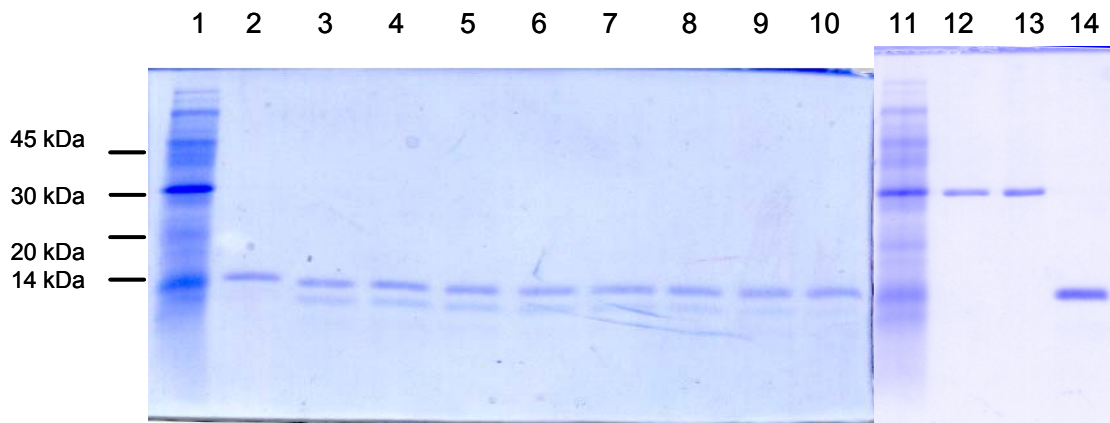


Figure 1.4.6 – SDS-PAGE with the samples of the time-course furin proteolysis of rm-proNGF. Lanes 1 and 11: molecular weight marker; lanes 2 and 14: reference NGF; lanes 3, 4, 5, 6, 7, 8, 9: 30 minutes, 1 hour, 2 hours, 4 hours, 6 hours, 8 hours, 10 hours incubation respectively; lane 10: overnight incubation; lane 12: rm-proNGF, 10 hours incubation without furin; lane 13: rm-proNGF, overnight incubation without furin

The reaction was furthermore changed to find out better cleavage conditions. The protocol needs still to be optimized: even changing the ratio of furin:protein and the reaction time, in fact, furin is digesting the sample very quickly. On the contrary, by lowering the furin concentration too much, an incomplete digestion is achieved, driving to a ladder of products (fig.1.4.7).

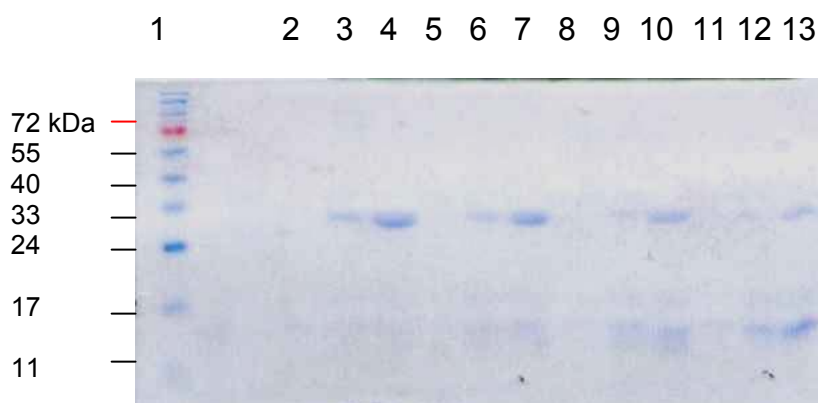


Figure 1.4.7 – SDS-PAGE of a scouting of proteolysis conditions for the furin cut of m-proNGF. Lane 1: molecular weight marker; lanes 2, 5, 8 and 11: ratio 1 μ g/m-proNGF: 0.25U of furin at 30 minutes, 1 hour, 2 hours, 3 hours incubation respectively; lanes 3, 6, 9, 12: ratio 1 μ g/m-proNGF: 0.05U of furin at 30 minutes, 1 hour, 2 hours, 3 hours incubation respectively; lanes 4, 7, 10, 13: ratio 1 μ g/m-proNGF: 0.25U of furin at 30 minutes, 1 hour, 2 hours, 3 hours incubation

1.5 Guanidinium-dependent denaturation of rm-proNGF

The stability of rm-proNGF was tested using a Guanidinium-dependent denaturation and by measuring the fluorescence values. The experiment was conducted as previously described (Rattenholl, PhD Thesis, 2001); in particular, rm-proNGF was incubated overnight (12 hours) at room temperature (22°C) in increasing Guanidinium concentrations. The results are shown in fig.1.5.1. The curve presents two transition points, deriving by the unfolding of the pro-sequence (between 0 and 2 M GdmCl) and of mature NGF (around 3.5 M GdmCl). The trend of the denaturation is not changing significantly after a longer incubation (7 days at room temperature – data not shown).

In fig. 1.5.1 the curve for the rm-proNGF is compared to the one previously described for the rh-proNGF. In the measurement of the rm-proNGF, the plateau is less clear than in the case of the rh-proNGF, and this should be ascribed to the lower number of experimental points measured around the plateau region.

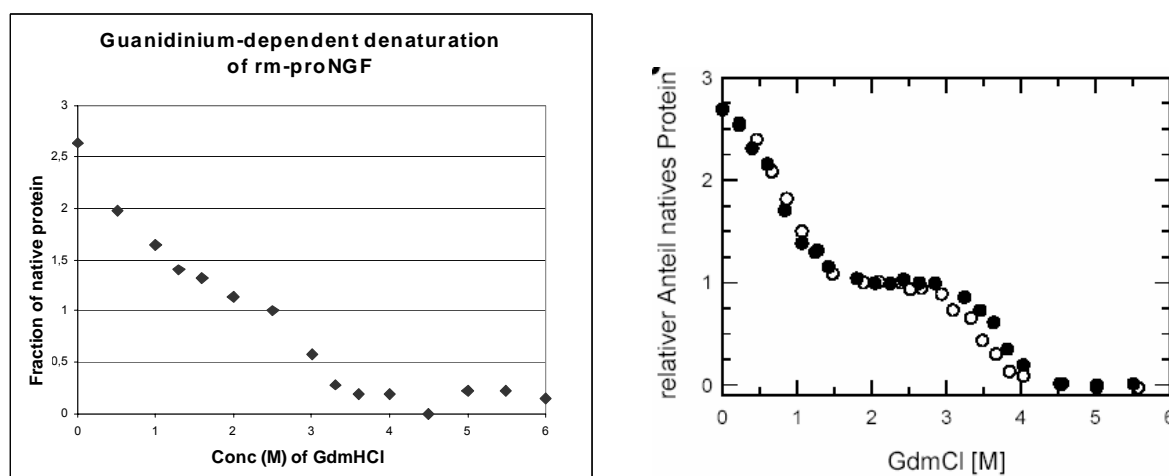


Figure 1.5.1 – Guanidinium-dependent denaturation of rm-proNGF (panel A) and rh-proNGF (panel B). The fraction of native protein resides in the mature NGF part, as demonstrated by Rattenholl (PhD thesis, University Halle), therefore the relative fraction of native protein is displayed on the y-axis, assuming 1 to be the native NGF part. The proteins were incubated in 50 mM Sodium-phosphate buffer, pH 7.0, 1mM EDTA with the indicated GdmHCl concentrations for 12 hours at 22°C. The samples were analyzed at 20°C with a 280 nm excitation and the emission intensities measured at 333 nm. In panel A the experiment for rm-proNGF is displayed. By comparison, in panel B, the experiment for the rh-

proNGF performed by A. Rattenholl (PhD thesis, University Halle) is displayed (black circles, rh-proNGF after 10 hours, white circles, after eight days incubation).

1.6 Looking for a functional mutation in rm-proNGF

To unravel the structural arrangements of rm-proNGF, a mutant was created to try getting insights into the structure of rm-proNGF. The selected mutant was chosen to mutate a Proline in position 5 on NGF sequence (see Introduction – p.18); this position appears to be critical in the arrangement of the protein. Looking into the crystallographic structure of the complex between NGF and the d5 Ig-like domain of TrkA receptor, in fact, this Proline is situated in the N-terminal region of NGF that is involved in the binding with the TrkA receptor (fig.1.6.1). Taking into account that the biological data available for proNGF (Lee *et al.*, Science 2001) indicate a reduced interaction of proNGF with TrkA, one hypothesis is that the Proline in position 5 is functioning as a sort of tilting junction and switch from one conformation to the other (cis/trans) going from proNGF to NGF.

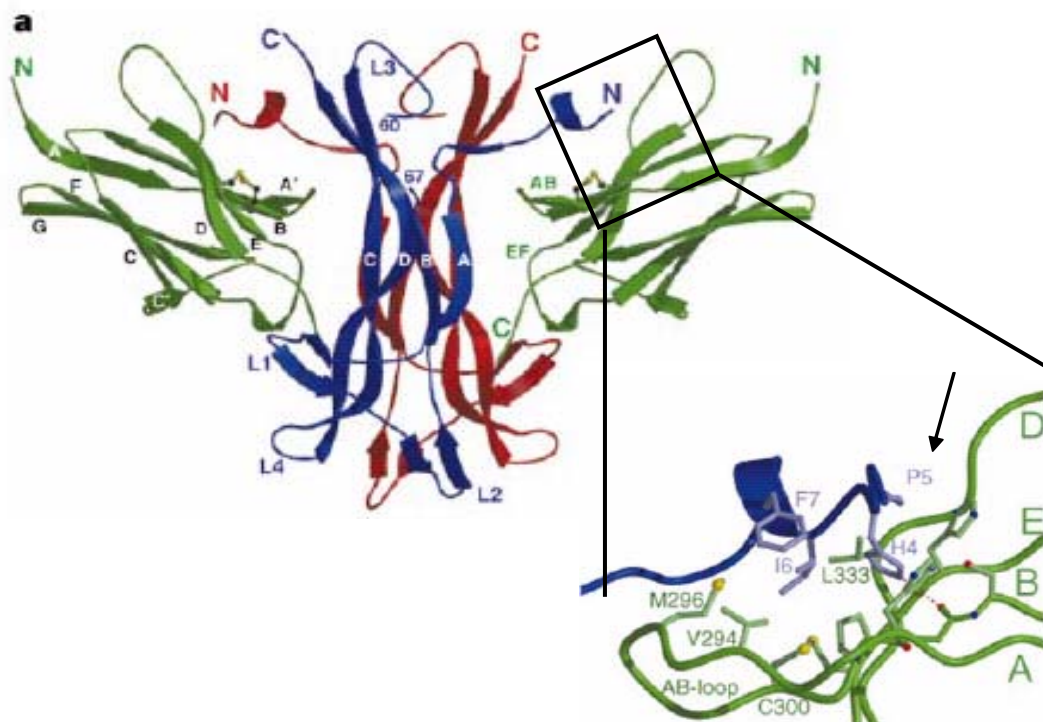


Figure 1.6.1 – Crystallographic structure of the complex NGF/TrkA (according to Wiesmann, 1999). In the enlargement of the bottom right side, the Proline 5 on NGF is indicated by an arrow.

Therefore, the mutant with this Proline changed into Alanine was created, using site directed mutagenesis with PCR. The template used has been the clone of the wild-type rm-proNGF in the vector pET11a, described in the previous paragraph 1.2. After mutagenesis, the clone was sequenced to prove it correctness.

The mutant, named P5A, was expressed in IB and refolded, using the previously described protocols. The purification procedure was the same already proven to be efficient for the wild-type protein, namely a step of cation exchange chromatography (SP Sepharose) followed by a step of hydrophobic interaction (Phenyl Sepharose). At the end of the purification process, the protein resulted to be clean at 95%, according to Coomassie Blue staining of SDS-PAGE (fig.1.6.2).

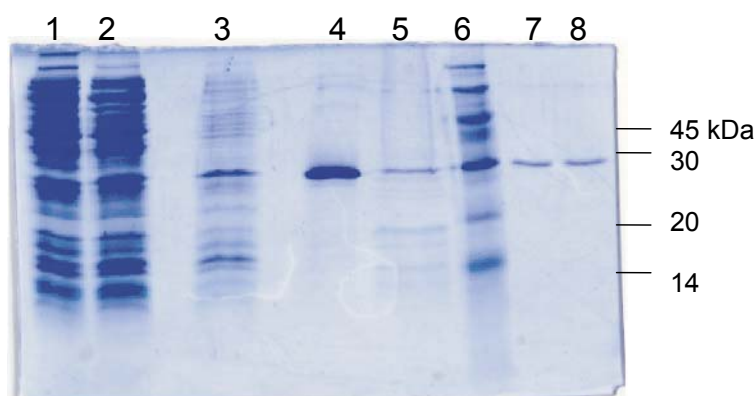


Figure 1.6.2 – SDS-PAGE with samples of various steps of the purification of P5A protein. Lane 1: pre-induction control; lane 2: post-induction control; lane 3: IB preparation; lane 4: sample before IEX step; lane 5: sample before HIC step; lane 6: molecular weight marker; lanes 7,8: Purified P5A

The mutant protein was also characterized by biophysical methods, namely fluorescence spectroscopy and CD, to be compared to the wild-type rm-proNGF.

The fluorescence emission spectrum was recorded both in native and denatured conditions, and resulted to be completely overlapping with the wild-type one (fig.1.6.3), with a maximum in emission at 337 nm in native conditions and at 354 nm in denaturing ones.

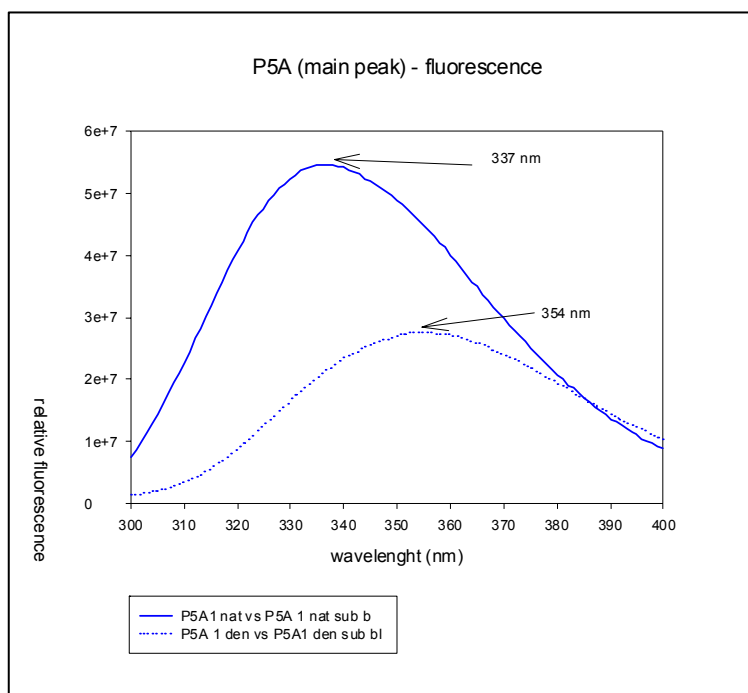


Figure 1.6.3 – Fluorescence emission spectrum of P5A. The blue, solid trace represents the spectrum in native conditions, while the blue dotted one the spectrum in denaturing conditions.

Regarding the secondary structure composition, too, the mutant presents a behaviour analogue to the one of the wild-type, as it appears from the far-UV CD spectra of the two proteins, that are completely overlapping (fig.1.6.4).

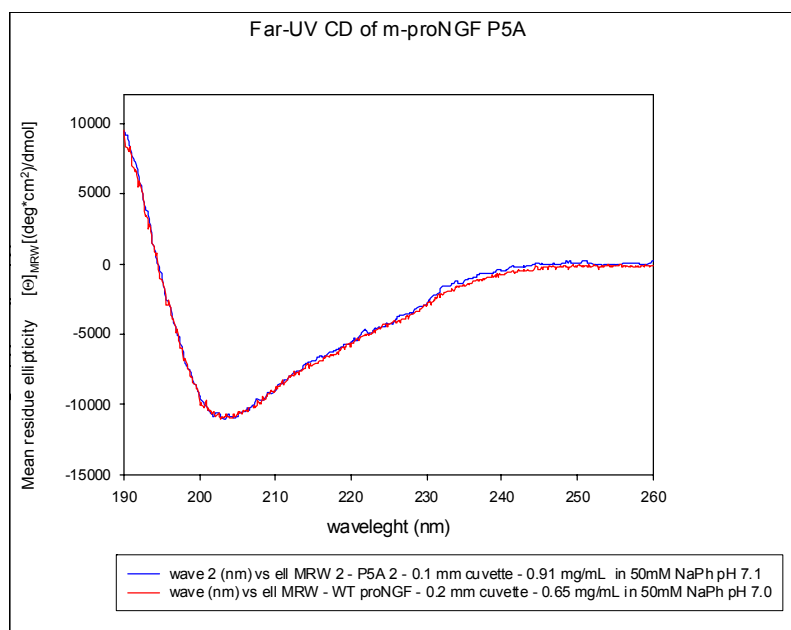


Figure 1.6.4 – Far-UV CD of P5A proNGF. The blue line represents the far-UV CD spectrum of P5A. By comparison, the far-UV CD spectrum of wild-type m-proNGF is represented by the red line.

The isoelectric point of the mutant P5A was evaluated experimentally by an isoelectric focusing gel, described in the previous section for the wild-type rm-proNGF,

and also in this case the protein resulted to be very basic (pI higher than 9 – see fig.1.6.5).

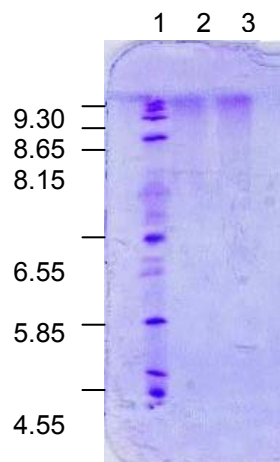


Figure 1.6.5 - Pre-cast gel for isoelectric focusing. Lane 1: pH marker; lanes 2 and 3: P5A rm-proNGF

From the whole experiments described in this section, one can conclude that the mutant P5A behaves in the same way as the wild-type protein, at least as far as its biophysical properties. However, the biophysical measurement might not be the best ones to evaluate if the selected mutation has functional effect. For this reason, bioassays and binding studies will be necessary for a detailed analysis.

1.7 Looking for the role of the pro-peptide of rm-proNGF

The biological function of the pro-region of proNGF is still not completely understood. The pro-peptide alone was expressed and purified by Kliemann and colleagues, and its properties investigated (Kliemann *et al.*, FEBS, 2004); it was demonstrated that it is not a stable protein and that it has no clear secondary structure.

Therefore, to derive reagents that might help to get insights into the function of the pro-peptide and to study its properties independently from the mature NGF, two fusion constructs were prepared, using GST as a fusion partner for the pro-peptide, to obtain a soluble product in the cytoplasm of *E.coli*. In particular, the considered fusion proteins are: GST-pro and pro-GST. In the first case, the partner protein GST is fused at the N-terminus of the pro-peptide of m-proNGF, as the usual way for the fusion proteins with GST; in the second case, the opposite fusion order is obtained, trying to reproduce the physiological role of the pro-peptide, namely its function at the

N-terminus of the protein NGF; moreover, GST is known to dimerize in solution (Dirr *et al.*, Eur. J. Biochem., 1994), as it is also the case of NGF; the fusion construct could therefore represents a model for the proNGF protein.

In both cases the m-pro-peptide for the cloning was amplified by PCR from the DNA of the wild-type m-proNGF.

The GST-pro fusion protein was expressed in soluble form in *E.coli*, and purified by affinity, on a GST-Trap column, and by size-exclusion chromatography, with a Superdex 75 column. The protein eluted as a single peak in gel-filtration (fig.1.7.1) and the apparent molecular weight of around 70 kDa is in agreement with the expected value of 75.6 kDa (two homodimers of 37.8 kDa each) for the dimeric state of the protein in solution. After purification the protein was clean by 90% according to Coomassie Blue staining on SDS-PAGE (fig.1.7.1) and run on the gel well separated from the GST alone (molecular weight: 25.6 kDa), although with an apparent molecular weight slightly lower than the expected one, *i.e.* around 33 kDa instead of the theoretical 37.8 kDa.

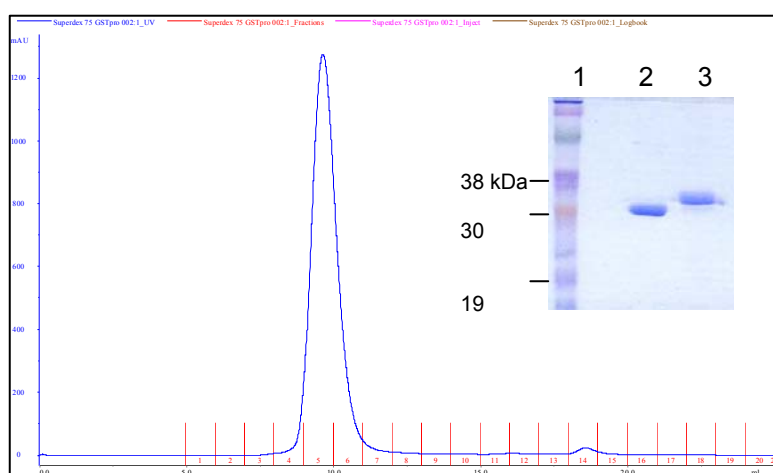


Figure 1.7.1 – Size exclusion chromatography on GST-pro and SDS-PAGE. A Superdex 75 column was used. The absorbance profile at 280 nm is represented. On top-right, SDS-PAGE of GST-pro. Lane 1: molecular weight marker; lane 2: purified GST; lane 3: purified GST-pro

The pro-GST protein was also expressed as soluble in *E.coli*, and the first purification step was an affinity chromatography on a GST-trap column; the protein, however resulted to be quite dirty after the affinity chromatography, mainly by a contamination of a lower molecular weight band, most likely to be GST alone. The protein sample was running on the SDS-PAGE with an apparent molecular weight of

35 kDa, reasonably lower than the expected one, of 47.4 kDa for the monomeric protein. This could be due to a cleavage by instability at the end of the GST sequence, releasing a stretch of the vector by itself; the released protein product would have a molecular weight of 37.5 kDa.

Therefore, a second purification step was necessary, by ion-exchange chromatography. The theoretical value of the isoelectric point of the protein (the cleaved one) is equal to 8.19 (calculated with program MW/pI On Expasy web server) and therefore a cation exchange chromatography on SP-Sepharose column was employed, to reduce the binding of the possible contaminant GST (theoretical pI equal to 5.91). However, it was impossible to get an adequate separation from the other contaminants (fig.1.7.4), among which the main one is GST alone (see SDS-PAGE in fig. 1.7.5).

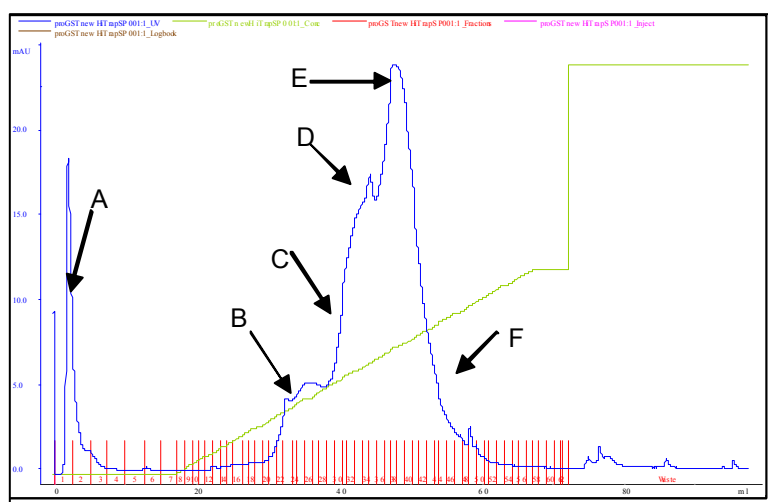


Figure 1.7.4 – Ion-exchange chromatography on pro-GST. The blue trace represents the elution of pro-GST. In green, the gradient trend of the elution. The arrows with the letters indicate the samples of the SDS-PAGE in fig 1.7.5

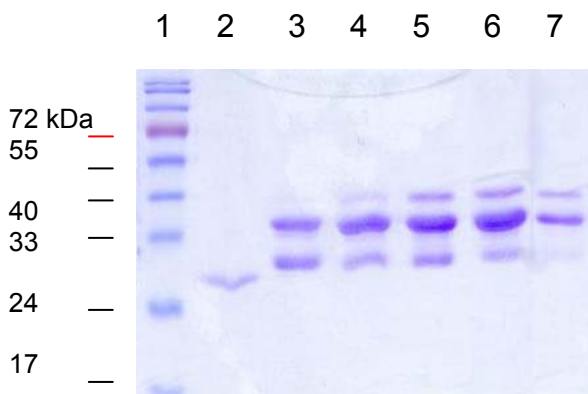


Figure 1.7.5 – SDS-PAGE with the samples from the ion-exchange chromatography. The names of the samples refer to the indications in fig. 1.7.4. Lane 1: molecular weight marker; lane 2: sample A (fractions 1-3); lane 3: sample B (fractions 21-29); lane 4: sample C (fractions 30-33); lane 5: sample D (fractions 34-36); lane 6: sample E (fractions 37-41); lane 7: sample F (fractions 42-51).

To check for the actual “identity” of the two fusion proteins GST-pro and pro-GST and for their purity, a western blot was performed, loading on the same gel the two purified proteins and the GST alone as reference; the primary antibody used is a polyclonal anti-GST. As its clear from fig.1.7.7, in both cases the fusion proteins are present, although their apparent molecular weight results once again lower than the expected, probably arising from an unusual overall charge distribution on the proteins’ surfaces.

Regarding the purity, the GST-pro was quite clean, while the pro-GST presented two major components: the pro-GST at higher molecular weight, and GST alone at lower molecular weight. This could be due either to co-expression of the GST together with the fusion protein, or to instability of the pro-GST product. In fact it was reported (Kliemann *et al.*, FEBS, 2004) that the pro-peptide of proNGF requires NGF to have its functional role in helping the correct folding of the mature protein. It could be concluded, therefore, that the pro-GST is expressed and the pro-peptide helps the correct folding of the GST fused at its C-terminus; but maybe the pro-peptide does requires the presence of NGF at the C-terminus to be stable enough, and in the presence of a difference fusion partner it could be more prone to degradation or cleavage.

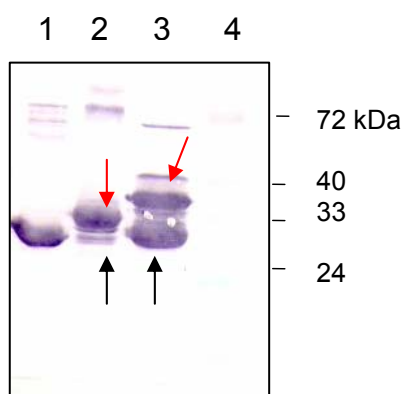


Figure 1.7.7 – Western Blot of the fusion proteins GST-pro and pro-GST. Lane 1: purified GST; lane 2: purified GST-pro (expected product: red arrow; GST from degradation: black arrow); lane 3: purified pro-GST (expected product: red arrow; GST from degradation: black arrow).

SUMMARY AND CONCLUSION

In this chapter, the expression, refolding and purification of rm-proNGF was described, according to the procedure established for the rh-proNGF. The protein was also characterized by a physico-chemical point of view. The yields for the purified rm-proNGF were encouraging, being equal to 30 mg/L of culture.

Moreover, the rm-proNGF was cleaved with both trypsin and furin proteases to give rise to mature rm-NGF. In the case of trypsin, a purification procedure was optimized for the achievement of mature rm-NGF. The yield was promising, being around 40% in mass of the rm-proNGF used.

Besides the rm-proNGF, three other proteins were cloned and expressed, namely a point mutation clone (rm-proNGF P5A) and two fusion constructs, GST-pro and pro-GST.

For the expression and purification of the P5A, the same procedure was used, already established for the rm-proNGF wild-type. The yield in this case was even better than in the previous one, being equal to 30 mg/L of culture.

The fusion constructs were purified by taking advantage of the GST fusion partners. Both proteins could be successfully expressed and purified, although in the case of the fusion protein pro-GST it was not possible to achieve a complete purification of the desired product. A more detailed work will be needed in the future to achieve a productive purification procedure for the pro-GST protein, that could be a useful tool for the analysis of the function of the pro-peptide. Moreover, a deeper investigation on the oligomeric state of this fusion constructs, *i.e.* if GST dimerizes or not, could help in a better understanding of the role of the pro-peptide in the dimerization of NGF.

These proteins were used in the experiments described in the following chapters in the frame of a wider analysis on the structure and function of the pro-peptide of m-proNGF.

2. m-pre-proNGF: a long-short equilibrium of different forms of the protein

SUMMARY

In this chapter, the experiments performed on the long form of m-pre-proNGF will be presented: it is of great interest, in fact, to analyze deeper the properties of the long form of the pre-proNGF and to compare it to the short one. So far, there are no clear evidences of the different biological function of the two forms of the protein, although it's known that they both exist *in vivo*.

The m-pre-proNGF-long was recombinantly expressed in *E.coli*, starting from a cDNA amplified by RT-PCR and cloned into suitable vectors for recombinant protein production. This protein will be named m-pre-proNGF-long to distinguish it from the “short” proNGF, that will be always indicated as m-proNGF.

In this case, however, the expression and purification of the protein was significantly more complicated than in the case of the short form of the protein. One of the next objectives will be therefore to start a more detailed work to achieve the best refolding and purification procedure for the expression of this protein form, in order to be able to produce enough material for a complete comparative analysis of the two main existing forms of proNGF.

RESULTS

The cDNA for the m-pre-proNGF-long was fished out by RT-PCR from a total RNA preparation from submandibular glands with the specific primers 5'UTR for the 5'-end and 3'UTR for the 3'-end, using the same protocol presented for the m-proNGF short. The RT-PCR did not give a very clean amplification, and besides the expected product of 1163 bp, others amplification products were detected as presented in fig.2.1.

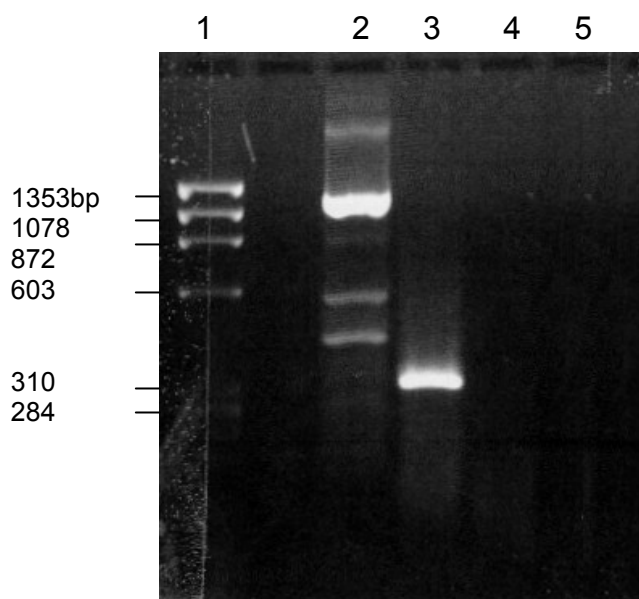


Figure 2.1 – Agarose gel with the samples resulting from the RT-PCR reaction. Lane 1: DNA marker; lane 2: RT-PCR product with 5'UTR-3'UTR primers; lane 3: Positive control from the kit (see Experimental Section); lane 4: Negative control A; lane 5: Negative control B

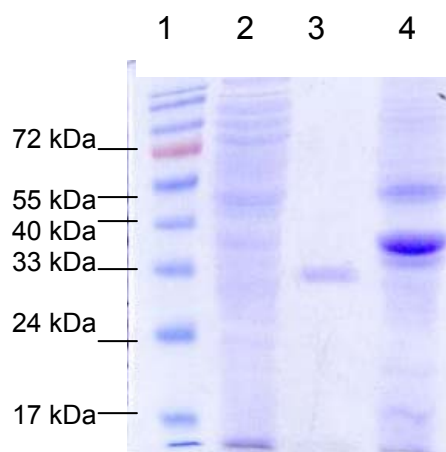
The amplified cDNA was subsequently cloned into pET11a vector for expression in *E.coli*. The protein was expressed in IB and needed to be refolded.

In this case the whole cDNA of the m-pre-proNGF long was cloned, since no clear signal peptide was identified so far at the N-terminal of this NGF precursor.

There is no protocol available for the refolding of m-pre-proNGF-long from *E.coli* so far; therefore the first attempt for the refolding was done using the same refolding conditions optimized for the rm-proNGF.

The protein was expressed, although it was not easy to distinguish a band of the expected molecular weight of 32 kDa in an SDS-PAGE with the controls before and after induction (data not shown). The IB preparation was carried out, and from SDS-PAGE it was possible to verify that the major part of the protein was present into IB (see fig.2.2).

Figure 2.2 – SDS-PAGE showing the IB preparation of m-proNGF-long. Lane 1: molecular weight marker; lane 2: cytoplasmic fraction of proNGF long; lane 3: m-proNGF; lane 4: IB of m-proNGF-long



Before proceeding to the purification of the protein, a western blot analysis was performed, to establish the “identity” of the protein present in the IB. The membrane was challenged with a polyclonal anti-NGF and polyclonal anti-pro-peptide antibodies. From fig.2.3, it is possible to conclude that the m-pre-proNGF-long does indeed contain a protein with the pro-peptide of proNGF (lane 5 in fig.2.3) and of a higher molecular weight than the rm-proNGF. However, the IB (lane 3) include a whole range of anti-NGF-reacting proteins. The result is anyway encouraging, since the protein is at least expressed and has the expected molecular weight.

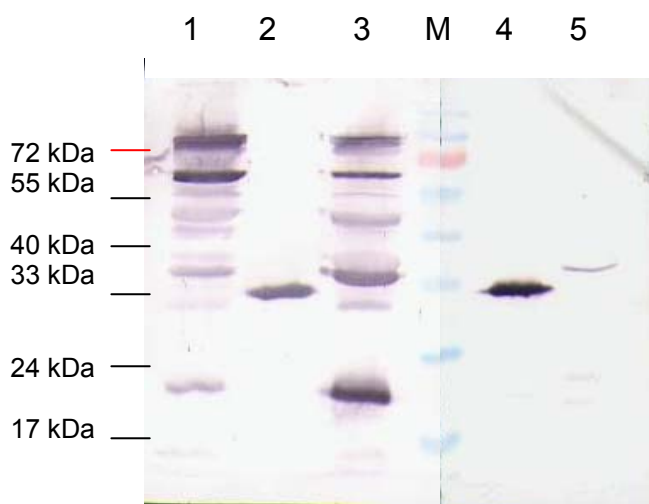


Figure 2.3 – Western Blot analysis on the IB preparation of m-proNGF-long. Lane 1: cytoplasmic fraction of m-proNGF-long; lane 2: m-proNGF; lane 3: IB of m-proNGF-long; lane 4: m-proNGF; lane 4: IB of m-proNGF-long. Lanes 1-3 were probed with a polyclonal anti-NGF antibody (from SIGMA); lanes 4-5 with an anti-proNGF one (from Chemicon).

For the refolding and purification of the protein from the IB, the same conditions established from the rm-proNGF were used, giving that m-pre-proNGF-long, has a theoretical pI value of 9.6, similar to the one of the short construct.

After refolding, a purification on ion-exchange chromatography on an SP-Sepharose column was carried out, but in this case, the protein was mainly not binding to the column (fig.2.4), as it was clear by SDS-PAGE analysis.

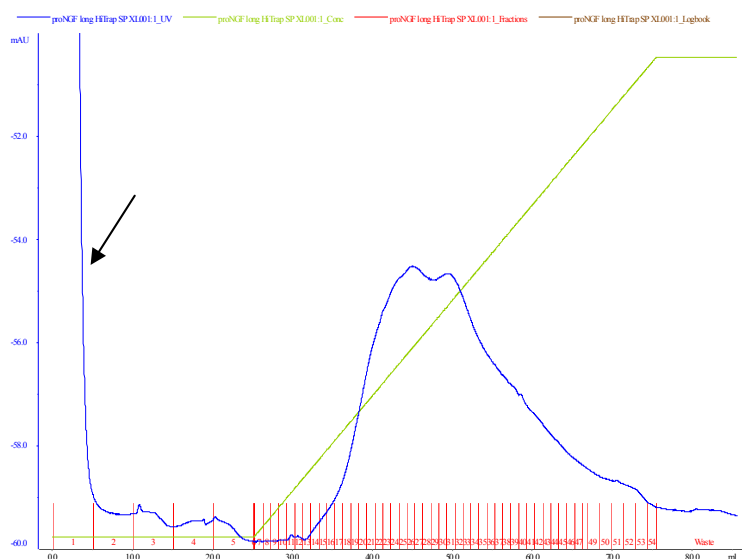


Figure 2.4 – Ion-exchange profile and relative SDS-PAGE of m-proNGF-long.

The elution profile shows a very low intensity and not single peak. The arrow marks the flow through, that analyzed on the SDS-PAGE did show the presence of the protein.

The cytoplasmic fraction left during the IB preparation was also loaded on the same column, and the chromatogram was presenting a clean peak. A careful analysis of the collected fractions on an SDS-PAGE, however, demonstrated that no interesting protein was actually eluting in those fractions. This was a further confirmation, that the m-pre-proNGF long, too, cannot be expressed as soluble protein in *E.coli*.

Due to the fact that the protein was not binding the cation exchange column, it was decided to load the flow-through on a Q-Sepharose as anion exchange column, with a buffer of pH=7.5. The chromatogram looked encouraging, but once the fractions are loaded on an SDS-PAGE, it appeared that the major peak eluting from the column was indeed only a “ghost” peak, not containing any protein. The result was also confirmed by a western blot using the anti-NGF antibody, where no band could be detected (data not shown).

The failure with these first attempts to purify the m-pre-proNGF-long from IB of *E.coli* in a productive way, makes it necessary to develop new approaches towards the problem. Indeed, the optimization of this purification is currently ongoing.

One of the possible approaches could be to remove the first twenty amino-acids from the construct used for the pre-proNGF, assuming to have also in the case of the long construct a signal peptide that could make the expression in *E.coli* more difficult.

3. effect of rm-proNGF on living cells

SUMMARY

In the present chapter, the effect of rm-proNGF on living cells is presented: the experiments were performed to check the biological function of the recombinant m-proNGF. For this purpose, two kinds of experiments were performed: the differentiation of PC12 cells upon addition of rm-proNGF and the TrkA phosphorylation assay.

3.1 Differentiation experiment on PC12 cells

The first experiment was a differentiation experiment on PC12 cells (Green and Tischler, PNAS, 1976). This cell lineage has the property of undergoing differentiation in neuron-like cells upon treatment with NGF. In the present case, the PC12 cells were used to check the ability of rm-proNGF to act as a trophic factor and to compare its ability to differentiate the cells to that of the mature m-NGF.

For this purpose, PC12 were grown and treated with rm-proNGF and m-NGF, as described in the experimental section. After 48 hours of treatment, the cells were observed under the optical microscope, and pictures were taken to qualitatively compare the results for the two cases. The rm-NGF arising from proteolytic digestion with trypsin (described in chapter 1) was also used; BSA was used as a control for a protein not inducing differentiation; the negative control was a dish of untreated cells. For comparison to rm-proNGF, also rh-proNGF was used, that was expressed in the same way.

The pictures shown in fig.3.1.1 describe quite clearly that rm-proNGF, as well as rh-proNGF, are able to induce a neurite outgrowth in PC12 comparable to the one given by m-NGF, both the commercial and the recombinant ones, and rh-NGF. What can also be stated, is that cells didn't dye due to the addition of proNGF to the medium, although a proper death test should be performed to verify if proNGF is

inducing apoptosis, as suggested by the paper of Lee and colleagues (Science, 2001). It should be pointed out, however, that the cell culture conditions were different from the ones reported in the cited paper (both in terms of culture conditions and of protein concentration), as well as the proteins used, and this might account from the difference in the overall result.

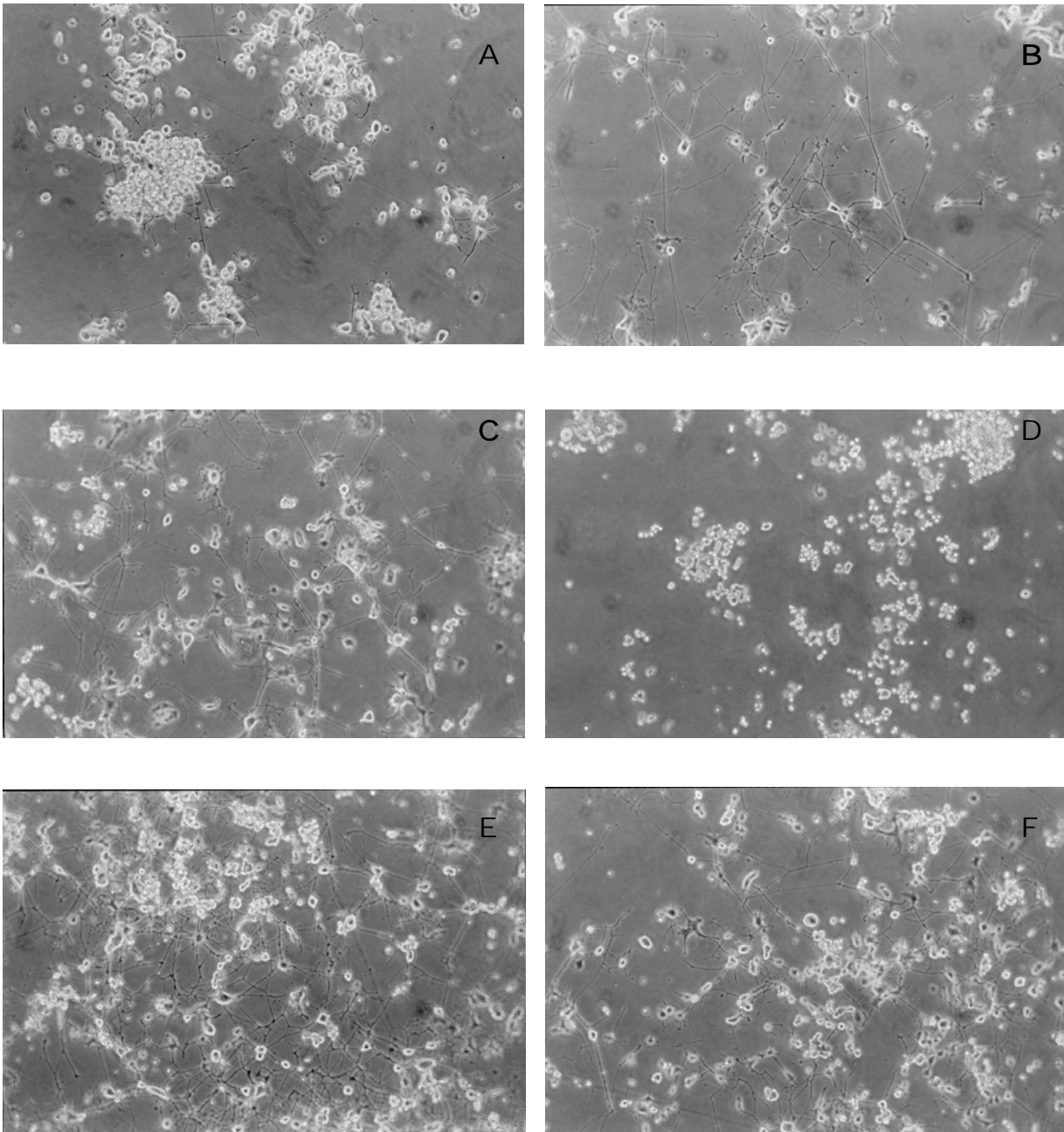


Figure 3.1.1 – Life-images of PC12 cells treated with different protein samples.

All pictures were taken with a traditional camera, using a 10x enlargement. Panel A: commercial m-NGF (50 ng/mL); panel B: h-NGF (50 ng/mL); panel C: m-NGF cut from rm-proNGF (50 ng/mL); panel D: BSA (100 ng/mL); panel E: rm-proNGF (100 ng/mL); panel F: rh-proNGF (100 ng/mL).

Also, an immunofluorescence experiment was carried out; the primary antibody anti-tubulin YL was employed, and the fluorescently labelled secondary antibody anti-rat TRITC was used to stain the cells. As a control, a staining of the cells with DAPI for the nucleus was carried out, and by looking at the staining under the microscope it was possible to exclude that the cells were sick.

By looking at the pictures in fig.3.1.2, it appears clearly that the recombinant proNGF, both mouse and human, are able to give nice neurites in PC12 cells, like the NGFs; on the contrary, the cells remained undifferentiated when BSA was used as a control.

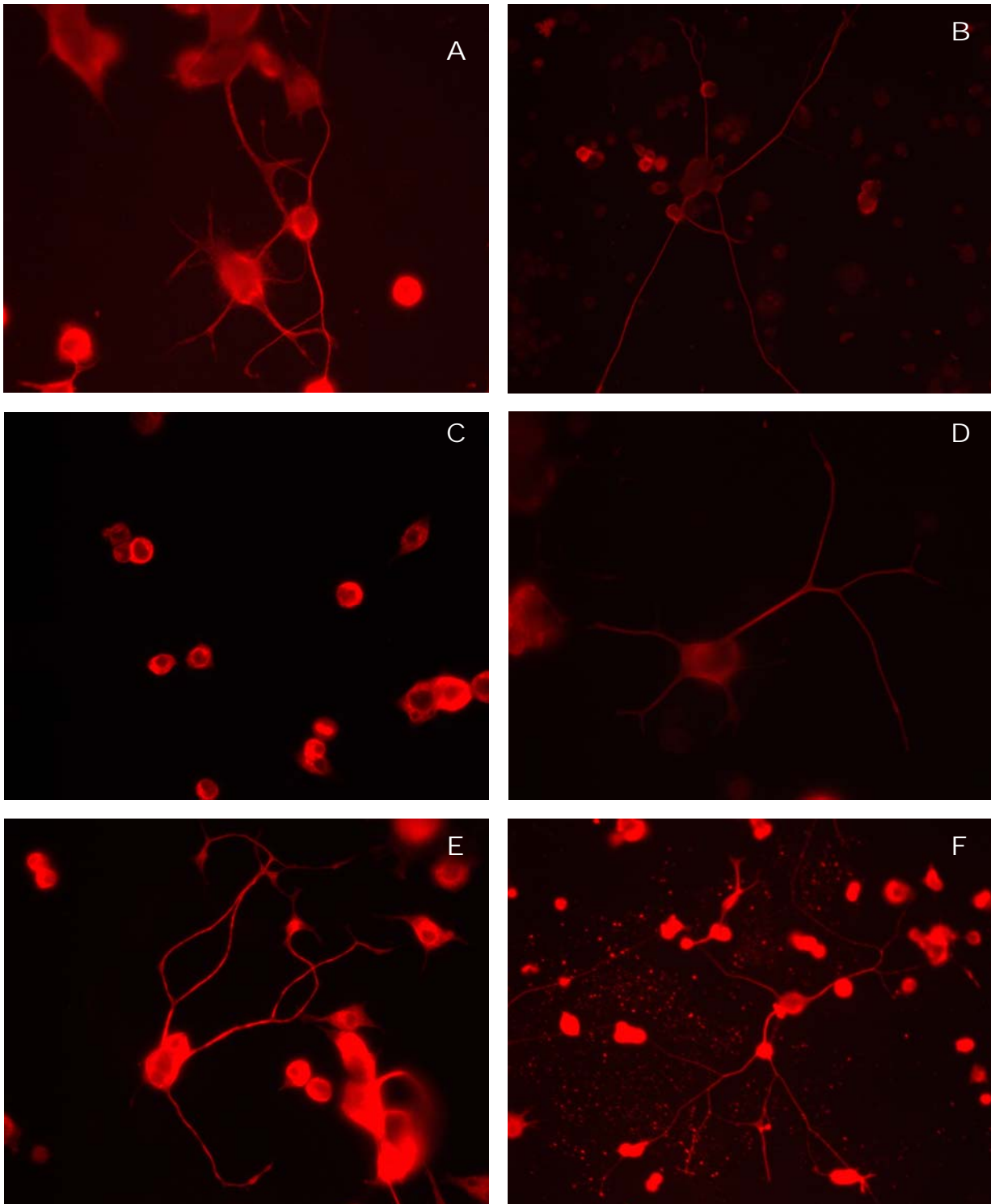


Figure 3.1.2 – Immunofluorescence of PC12 cells treated with various protein samples. All images were taken with a digital camera on an optical microscope, using a 100x enlargement (except the one in panel D, taken with a 20x enlargement). Panel A: h-NGF; panel B: m-NGF; panel C: BSA; panel D: m-NGF cut from rm-proNGF; panel E: rh-proNGF; panel F: rm-proNGF.

It's not possible, however, to formally exclude that the effect on the differentiation of cells is arising from a release of NGF from the rm-proNGF proteins due to a proteolytic cut of endogenous proteases. Therefore, to exclude this possibility, two controls experiments were performed.

In the first case, the cells were plated and treated in absence of serum (the major source of proteases). In these conditions, however, the cells are suffering, and die quicker than in the normal case. However it's still possible to compare the treated cells to the untreated ones, and check that rm-proNGF is able to induce cells differentiation, from a qualitative point of view (fig.3.1.3).

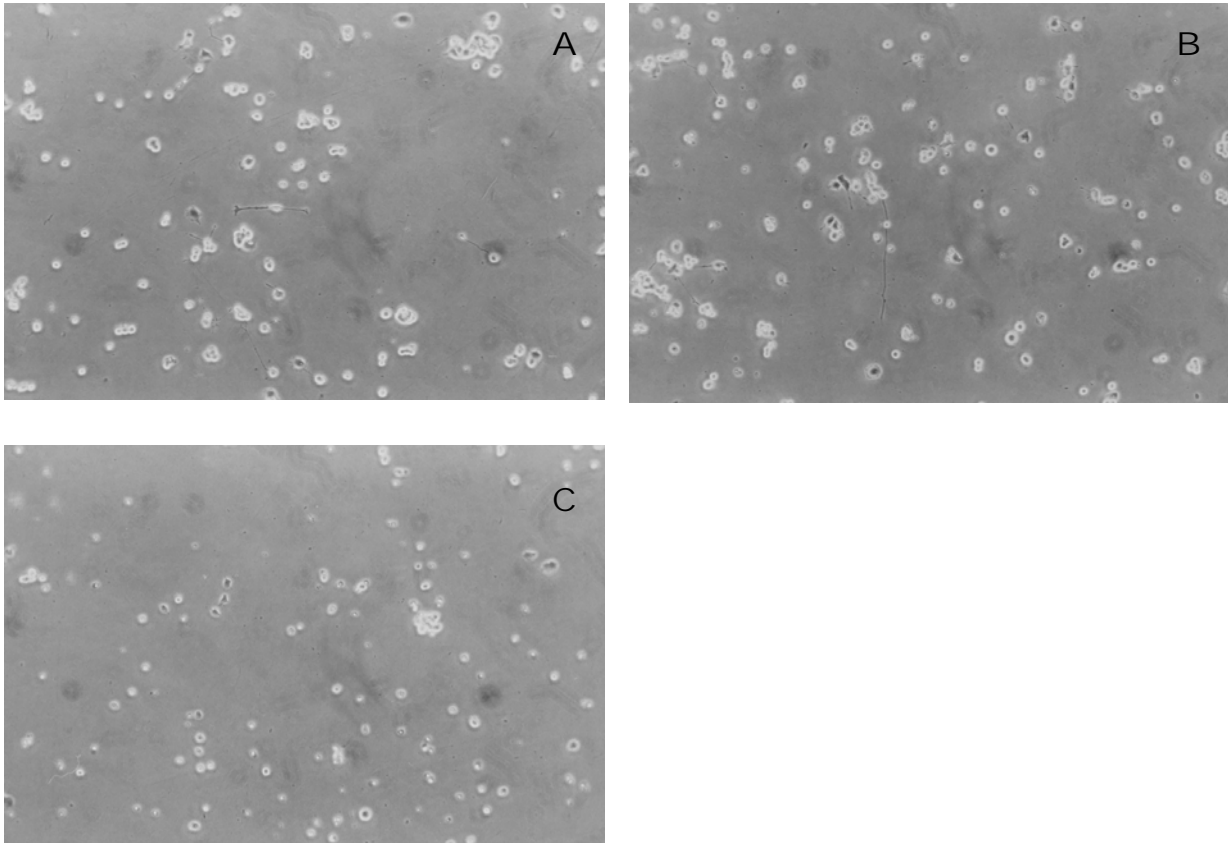


Figure 3.1.3 – Life images of PC12 cells treated with various protein samples in a serum-free medium. All pictures were taken with a traditional camera, using a 10x enlargement. Panel A: commercial m-NGF (50 ng/mL); panel B: rm-proNGF (100 ng/mL); panel C: control – no addition.

In the second control experiment, the PC12 cells were grown in normal conditions with serum, but during the treatment, a protease inhibitor cocktail was added to the serum, to decrease the protease activity. The cells are healthy in this case, as its clear from the controls pictures of fig.3.1.4 – panel C. And once again, the proNGF, both mouse and human, give neurite outgrowth in PC12 (fig.3.1.4).

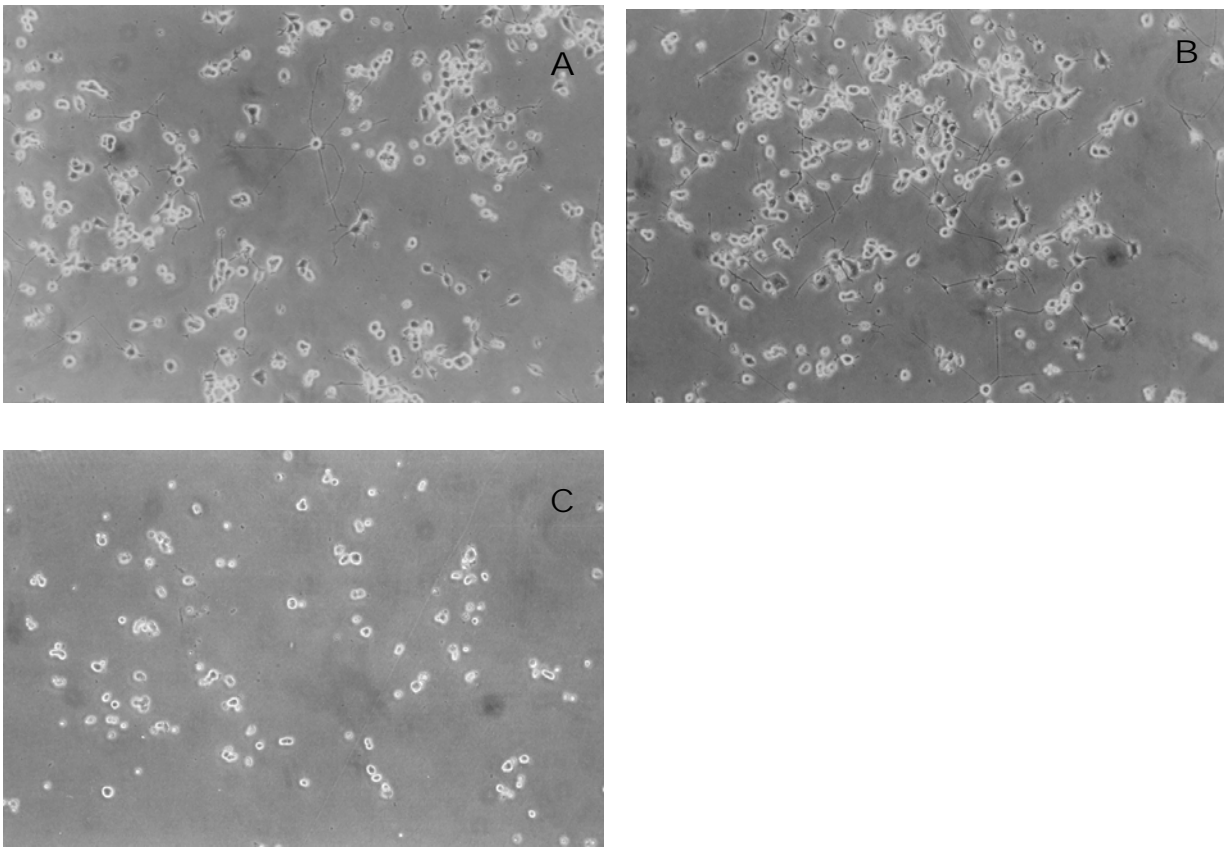
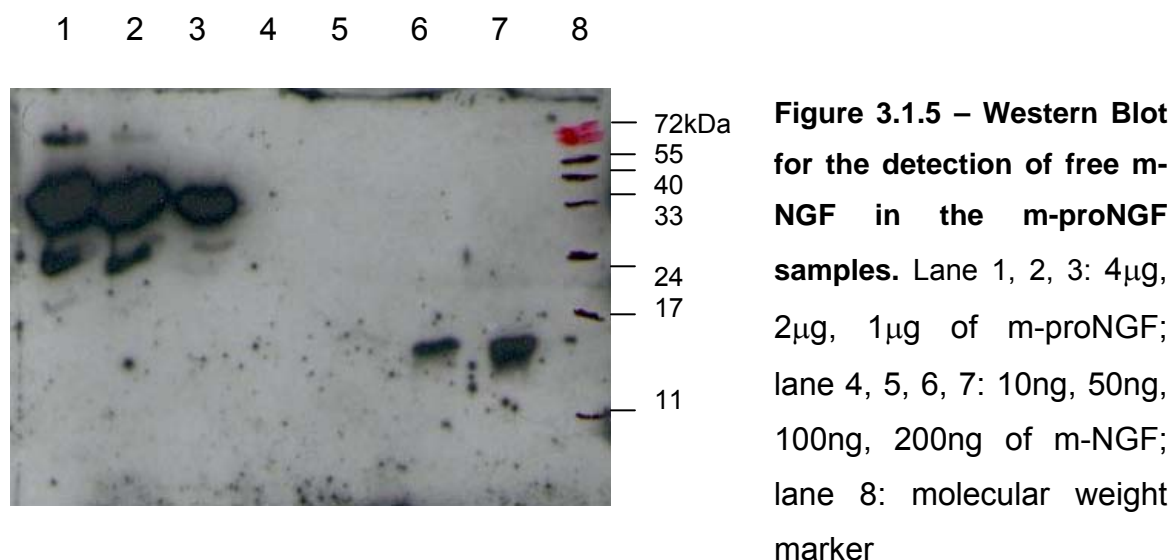


Figure 3.1.4 – Life images of PC12 cells treated with various protein samples in a medium treated with protease inhibitors. All pictures were taken with a traditional camera, using a 10x enlargement. Panel A: commercial m-NGF (50 ng/mL); panel B: rm-proNGF (100 ng/mL); panel C: control – no addition.

A further control for the absence of free NGF in the PC12 experiments, was done analyzing the supernatants, with both immunoprecipitation, followed by Western Blot analysis, and ELISA assay.

First of all an experiment was performed to check that there was no free m-NGF present in the rm-proNGF preparation used during the differentiation experiments, due to contaminations in the purification procedure or due to partial degradation. In particular, equi-molar amounts of m-NGF and rm-proNGF were loaded on an SDS-PAGE and immunoblotted, and the western blot was challenged with a primary antibody anti-NGF. As it is very clear from the fig.3.1.5, no free rm-NGF is present in the rm-proNGF preparations, even at very high concentrations, more than ten-fold higher than the ones used in the differentiation experiment.



Then, the supernatants of the experiments on PC12 in absence of serum and in presence of protease inhibitors were analyzed, to check for the presence of NGF and proNGF in the samples.

For the immunoprecipitation, the supernatants were treated with the α D11 anti-NGF monoclonal antibody, immunoprecipitated with Protein G Sepharose and the final product was loaded on an SDS-PAGE and immunoblotted on a nitrocellulose membrane, challenged with a polyclonal anti-NGF antibody. Unfortunately the method is not reaching the required sensitivity and it was therefore impossible to

detect any NGF in the samples, both in the case of proNGF and in the NGF ones (data not shown).

For a further control, the supernatants were probed in an ELISA assay experiment: the ELISA plate was coated with a suitable amount of α D11 anti-NGF antibody, than the supernatants were incubated and finally the “sandwich” was probed with both a polyclonal anti-NGF and a commercial polyclonal anti-proNGF. In parallel, a calibration curve was done, with a series of incubation samples containing either NGF or proNGF or a mixture of the two, to establish the sensitivity of the experiment.

From the controls made to establish the antibodies' properties (fig.3.1.6) it appears clearly that the polyclonal anti-NGF antibody is recognizing NGF much better than the proNGF, while the commercial polyclonal anti-proNGF is having a high specificity for the pro-peptide, but has a very low sensitivity.

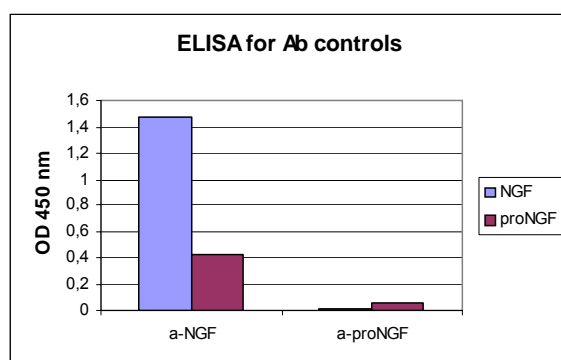


Figure 3.1.6 – ELISA assay for the control on the antibody efficiency.

The blue bars represent the m-NGF sample and the violet ones, the m-proNGF. The used antibodies are indicated on the x-axis. The coating was performed at 10 μ g/mL.

Regarding the calibration curve, it was possible to get a good curve for m-NGF with the anti-NGF antibody, and the same is also true for the rm-proNGF with the anti-NGF, although with lower absorbance values than for m-NGF; anyway, in both cases, it was possible to reach a good sensitivity in the low concentrations range (until 50 ng/mL for m-NGF and 200 ng/mL for rm-proNGF). Unfortunately the same is not true for the rm-proNGF probed with the anti-proNGF antibody, with which is not possible to detect less than 800 ng/mL (data not shown).

The overall result of the calibration experiment, allows to say that it should be possible to distinguish between m-NGF and rm-proNGF only according to the intensity of the response of the anti-NGF antibody; it's not possible, in fact, to get an absolute value due to the lack of sensitivity of the signal of the anti-proNGF antibody.

In this respect, the availability of a sensitive anti-proNGF antibody would be very important, to overcome to lack of sensitivity of the commercially accessible antibodies.

After establishing the sensitivity of the system, the experiment on the supernatants was performed. The anti-proNGF antibody was not able to detect any proNGF in the sample; on the contrary, the result given by the anti-NGF antibody was quite encouraging: the signal given by the supernatants of cells treated with m-NGF was very high, while the one arising from the supernatants of the rm-proNGF was very low (Fig.3.1.7).

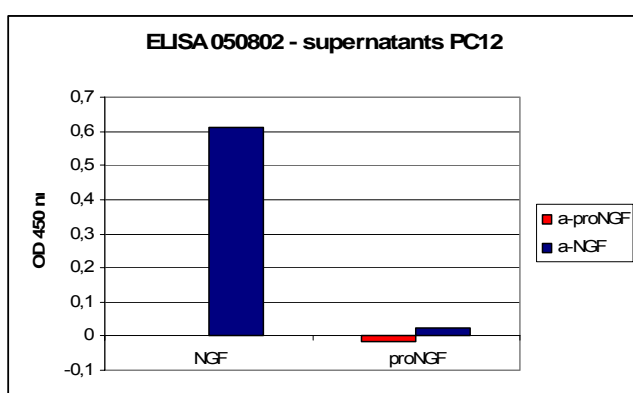


Figure 3.1.7 – ELISA assay for the detection of NGF and proNGF in treated PC12 cells. The supernatants of the PC12 treated with the neurotrophins samples were tested by ELISA assay with two different antibodies: anti-NGF (blue bars) and anti-proNGF (red bars). The detected neurotrophin is indicated on the x-axis.

In conclusion, one could say that rm-proNGF is actually able to induce cell differentiation in PC12 cells, although a quantitative dose/response assay would be necessary for a quantification of the effect. The presented result, is in agreement with the recent findings by Fahnestock and colleagues (J. Neurochem., 2004), who reported an analogue PC12 cells differentiation by proNGF; it is interesting to notice that in this last case, the used construct was the long m-pre-proNGF. Therefore, it would be interesting deeply investigate the problem, in order to really check the difference between the short and the long constructs of m-proNGF.

However, the PC12 bioassay is not sensitive enough, as a read-out, to clarify this issue. Therefore a TrkA receptor activation assay was performed.

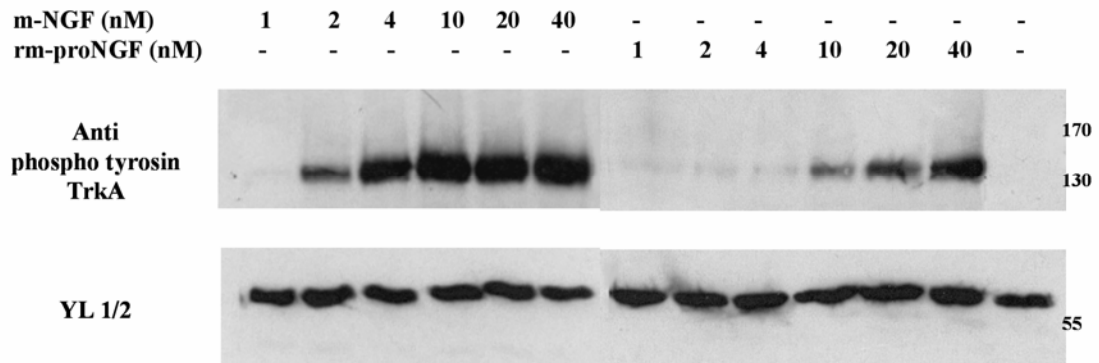
3.2 TrkA – receptor activation assay on 3T3 and PC12 cells

The ability of rm-proNGF and m-NGF to activate the TrkA receptor was evaluated in cell culture, using 3T3 TrkA cells (ectopically expressing human TrkA receptor, but not expressing p75^{NTR} receptor). In this experiment the 1-40 nM range of neurotrophin concentration was tested, to check for the concentration-dependence of the TrkA activation, and to overcome possible limitations in the anti-phosphotyrosine-TrkA antibody sensitivity. In previously reported experiments, with the long form of proNGF, the 0.04 –1 nM (Lee et al., Science, 2001) and 0.04-8 nM (Fahnestock et al., J. Neurochem., 2004) range of concentrations were considered.

As shown by Western-blot analysis of TrkA phosphorylation (Fig.3.2.1 – panel A), rm-proNGF is able to activate the TrkA receptor, although to a lesser extent than mature m-NGF at equimolar concentrations. Furthermore sandwich ELISA assays (Fig.3.2.1 – panel B) were performed to compare quantitatively the difference in the activation; for a given concentration, the activation level induced by rm-proNGF was the same observed with a ten times lower concentration of m-NGF.

Appropriate control experiments were carried out to ensure that no NGF was present in the rm-proNGF preparation. Contaminations by mature NGF could be caused by proteolytic cleavage of proNGF during the bioassay or by the presence of NGF in the proNGF sample. The former could be excluded by a short incubation interval and the use of serum free medium. A Western-blot analysis (shown in the previous section) demonstrated that the proNGF sample did not contain any trace of mature NGF.

A



B

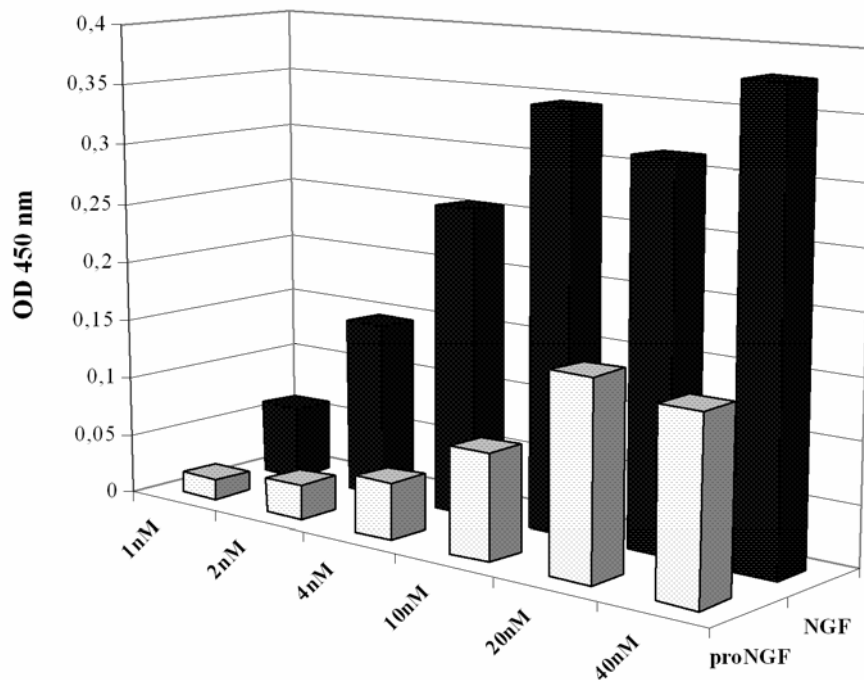


Figure 3.2.1 - TrkA phoshorylation assay. Panel A: Western blot: 3T3 TrkA cells were incubated with the indicated concentrations of m-NGF and rm-proNGF. Cell lysates were separated on a 10% SDS-polyacrylamide gel and tyrosine phosphorylation detected using anti phospho tyrosin TrkA antibody. The ubiquitous band of tubulin (detected by YL 1/2 antibody) serves as gel loading control. Panel B: ELISA assay was performed on 3T3 TrkA cells lysates, using anti TrkA MNAC13 monoclonal antibody coating (10ug/ml) and anti phosphor-tyrosin TrkA antibody, to obtain quantitative data.

The TrkA phosphorylation assay on 3T3 cells was also carried out with the rm-NGF obtained by proteolytic digestion from rm-proNGF and the result was showing that the protein behaves in a comparable way to the commercial m-NGF (data not shown).

The same kind of experiment was also carried out on PC12 cells, which express the endogenous TrkA receptor, as well as p75^{NTR} receptor. In this case, too, the activation of the TrkA receptor by rm-proNGF could be observed, as shown by the western blot analysis performed on cell-lysates (fig.3.2.2), and again, this was significantly lower than the activation induced by mature NGF.

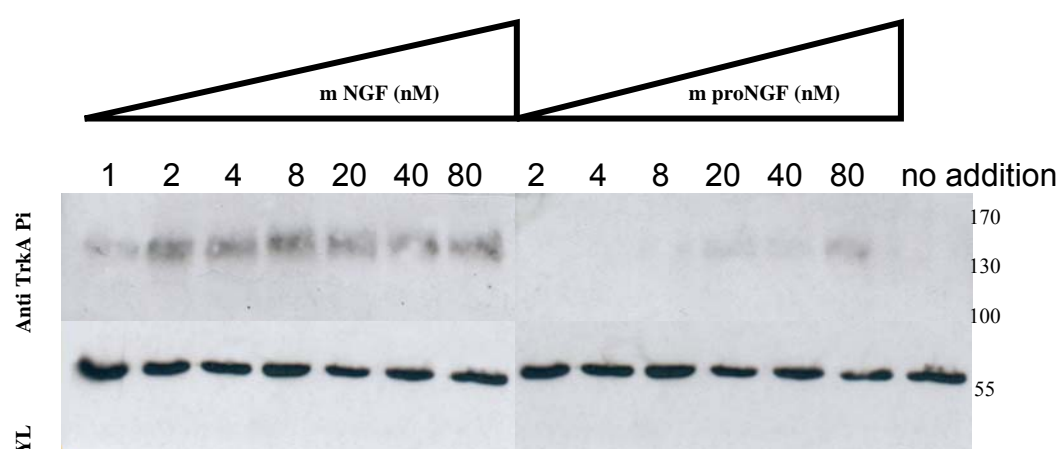


Figure 3.2.2 - TrkA phosphorylation assay on PC12 cells - Western blot. PC12 cells were incubated with the indicated concentrations of m-NGF and rm-proNGF. Cell lysates were separated on a 10% SDS-polyacrylamide gel and tyrosine phosphorylation detected using anti phospho tyrosin TrkA antibody. The ubiquitous band of tubulin (detected by YL 1/2 antibody) serves as gel loading control.

In conclusion, the activation experiments on TrkA receptor, performed with rm-proNGF, demonstrated that the protein is still able to activate the signalling pathway involving this receptor, both in presence and in absence of the “partner” receptor p75. However, its potency is at least ten fold lower than that of mature NGF.

Therefore, the signalling way of m-proNGF still remains open and deserves further interpretation, also to help understanding the contradictory findings by the publications of Lee and colleagues (Science, 2001) and Fahnstock and colleagues (J. Neurochem., 2004). It is worthy of note, however, that the results presented here

where the first ones to be carried out using the short m-proNGF, in contrast to the other available results, obtained with the long human pre-proNGF. It will be interesting, in the future, to go deeper into the understanding of the function of these two different protein forms, to make clear if they have a distinct role in the cell and what this role is.

CONCLUSION

In these chapter, a set of bioassays was performed, in order to verify the correct folding and the biological activity of the rm-proNGF that was expressed and purified as described in the previous chapter.

In particular, two assays were carried out: a PC12 differentiation and a TrkA phosphorylation assay. In both cases it was possible to achieve interesting results.

In the PC12 differentiation experiment, it was verified that rm-proNGF is able to induce cell differentiation, in a similar way like m-NGF. It should be pointed out that the proteins concentrations used were saturating, and this might be an explanation for the result. Controls were also performed, allowing to exclude that the differentiation is due to NGF released from rm-proNGF during the assay.

To exclude more certainly also the cleavage of rm-proNGF by various classes of proteases, however, a more careful analysis should be carried out.

The survival activity of rm-proNGF was confirmed by the TrkA phosphorylation assay: it emerged that rm-proNGF is able to induce the signalling cascade through TrkA activation, although to a lesser extent than NGF.

These results, taken together, are in quite good agreement with the published ones. It should be noted, moreover, that the presented results were conducted with the short proNGF form, while the published ones did employ the long form of the protein.

In any extent, these results obtained by challenging the protein in cellular assays, demonstrated that the recombinantly expressed protein is fully functional.

4. differential interaction of rm-proNGF and m-NGF with the receptors TrkA and p75^{NTR} and with a panel of anti-NGF antibodies

SUMMARY

In this chapter, the interaction of proNGF with different partners will be presented, and compared to the behaviour of NGF.

The biological role of m-proNGF *in vivo* appears to be distinct from the one of the mature m-NGF. This is likely to be due to structural differences between proNGF and NGF and one of the way to probe their structural differences is to use a panel of well characterized anti-NGF antibodies as structural probes. Exploring how the two proteins interact with a panel of antibodies anti-NGF allows to check if the pro-peptide is affecting somehow the way of binding of the NGF moiety. Here, this experiment was performed, by selecting three anti-NGF antibodies and exploring their binding towards rm-proNGF and m-NGF. The antibodies selected for this experiments are three very well characterized monoclonal anti-NGF antibodies: α D11 and 4C8, obtained in the group of prof.Cattaneo (Cattaneo *et al.*, J. Neurochem, 1988), and the well known 27/21 antibody (Korshing and Thoenen, 1987). These antibodies were selected due to the fact that they are very well characterized, both from the functional and the structural point of view. In particular, the α D11 antibody was recently crystallized in the Fab format and its 3D-structure solved at high resolution (Covaceuszach *et al.*, Acta D, 2004). More recently, the structural determinants of the α D11/NGF complex were also determined (Covaceuszach *et al.*, manuscript in preparation), and this allows an interpretation of the binding results in light of the structural features.

In fig. 4.1 a schematic representation of the epitopes of the different antibodies on NGF is presented. The mapping of the interaction regions of α D11 was deeply studied also from a structural point of view (Covaceuszach *et al.*, manuscript in preparation); the mapping of 4C8 and 27/21 was also performed in the group of prof. Cattaneo (PhD thesis of S. Gonfloni and manuscript in preparation).

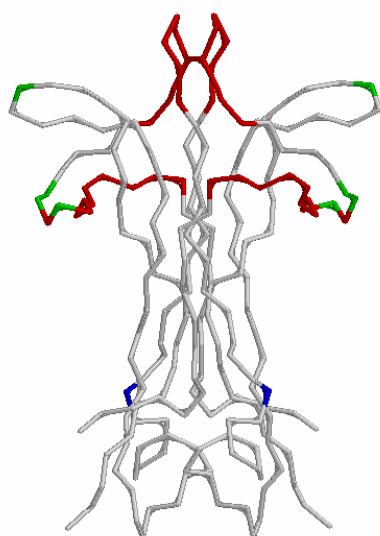


Figure 4.1 – Schematic representation of the epitope mapping of the regions of m-NGF recognized by the panel of anti-NGF antibodies. The represented structure is the crystallographic one of m-NGF (PDB: 1bet). The regions recognized by aD11 antibody are in red (loops I and II), the ones recognized by 27/21 in green (on loops I and V), and the amino acid needed for the 4C8 binding is represented in blue (Ser 61).

Concerning the panel of antibodies, a complete analysis could be performed, and by mean of BIAcore experiments the kinetic parameters could also be calculated. The most interesting result was achieved for the α D11 antibody, that is particularly interesting when thinking that is the one at the basis of the transgenic mouse AD11, model for the study of AD. As far as the results presented in this chapter, it can be surely affirmed that proNGF is characterized by a complete different binding kinetic versus α D11 antibody when compared to the NGF one.

Two techniques were chosen to look at the different way of binding: ELISA assay and Surface Plasmon Resonance using BIAcore.

Besides antibodies, the different binding mode of NGF and proNGF was also investigated through the measurement of the interaction with the two receptors TrkA and p75^{NTR}. The receptors were used in the immunoadhesin format, that allows to have them available in a useful format for solution experiments (Cattaneo *et al.*, J. Neurosc., 1999; Chamow and Ashkenazi, TIBTECH, 1996). Immunoadhesins are recombinant antibody-like molecules, obtained by combining framework sequences from a mAb with sequences from a protein that carries a target-recognition function. In the most common case, this fusion proteins combine the hinge and the Fc regions of an immunoglobulin (Ig) with domains of a cell-surface receptor that recognize a specific ligand (Chamow and Ashkenazi, TIBTECH, 1996).

A schematic representation of a general immunoadhesin is given in fig. 4.2.

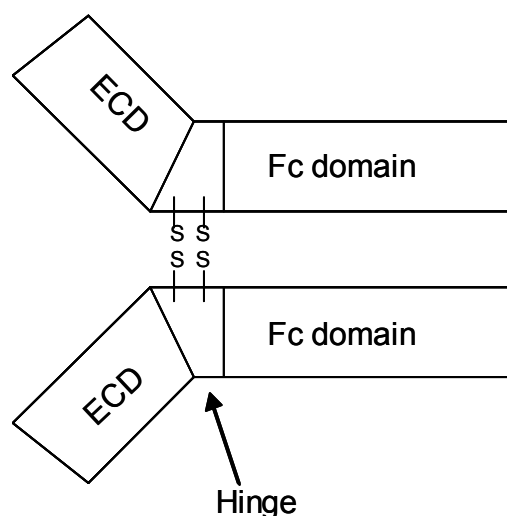


Figure 4.2 – Schematic representation of a prototypic immunoadhesin. In a typical immunoadhesin, the variable regions of the antibody molecule are replaced by the ligand-binding region of a receptor (ECD in the drawing, for extracellular domain of the receptor), while the antibody Fc region is retained, as indicated in the scheme. The hinge region (see arrow) is retained to provide conformational flexibility. (adapted from Chamow and Ashkenazi, TIBTECH, 1996)

Thanks to their versatility, the immunoadhesins too can be used as structural probes to get insights into the difference in the binding mechanism of NGF and proNGF to their partners.

The results obtained with the different approaches will be presented in the following sections.

RESULTS

4.1 Kinetic analysis on the binding of m-NGF and rm-proNGF to their receptors p75^{NTR} and TrkA

Using BIAcore, an analysis was performed, to evaluate the kinetics of binding of m-NGF and rm-proNGF to their receptors TrkA and p75^{NTR}, and be able, therefore, to compare the different binding properties.

The experiment was previously published for the human NGF and proNGF proteins (Nykjaer *et al.*, Nature, 2004; Woo *et al.*, Prot. Sci., 1998), and will be here presented for the corresponding mouse proteins. Moreover, the preparation of the

receptor is different in the experiment presented here when compared to the previously reported data. In particular, in our case, the protein used are immunoadhesins, presenting the extracellular domains of the two receptors on the scaffold of a camel immunoglobulin (Cattaneo *et al.*, J. Neuroscience, 1999).

The experiments was conducted in the following way: TrkA and p75^{NTR} were immobilized on a CM5 chip, in such a way, to obtain two comparable surfaces, taking in account the difference in the molecular weight of the two proteins. Subsequently, m-NGF and rm-proNGF were injected as analytes in a serial dilution mode (from 4 nM to 500 nM), in order to be able to perform a complete kinetic analysis. All the data were subtracted the blank, represented by a blank surface of the CM5 chip.

In fig.4.1.1, the kinetic analysis of m-NGF binding to TrkA is presented.

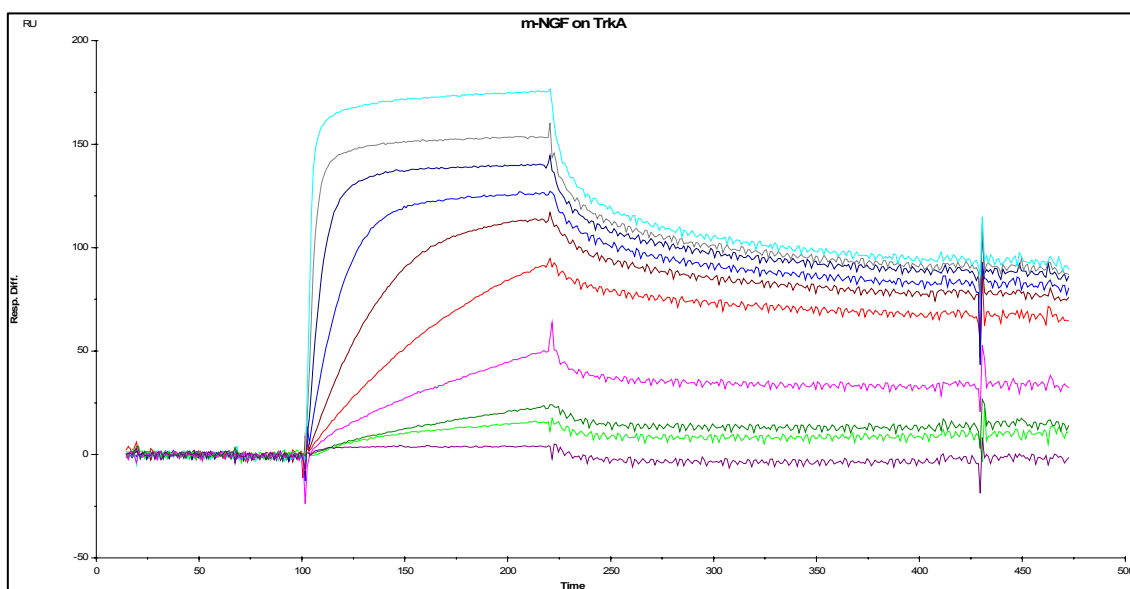


Figure 4.1.1 – BIAcore kinetic analysis of the binding of m-NGF over a TrkA receptor surface. TrkA immunoadhesin was immobilized on the CM5 chip at 8000 RU on Fc2, while Fc1 was left as a blank. Subsequently m-NGF was injected. The used concentrations were ranging from 2 to 500 nM by 1:1 serial dilutions. The corresponding curves are displayed in the figure; the lowest curve represents the buffer. All curves were blank subtracted.

In particular, a complete fitting analysis on the data was performed, in order to calculate the kinetic and affinity parameters. The binding of NGF to TrkA is characterized by a relatively slow association rate ($k_a = 1 \cdot 10^6 \text{ M}^{-1} \text{ s}^{-1}$) and a quite slow

dissociation rate ($k_d = 2 \cdot 10^{-3} \text{ s}^{-1}$). Therefore, the dissociation of m-NGF for TrkA can be described with a 2 nM value, and the association with a $0,5 \text{ nM}^{-1}$ ($\chi^2 = 0,28$), both consistent to the previously reported values for similar BIAcore analysis (Nykjaer *at al.*, Nature, 2004). These data are consistent to the previously reported data for the binding of NGF to TrkA, that is a “low affinity” binding (using the historical definition of high and low binding, with high binding defined with a K_d of 10^{-11} M and low affinity with a K_d of 10^{-9} M) when the binding towards the single receptor is calculated *in vitro* (Chao and Hempstead, TiNS, 1995; Neet and Campenot, CMLS, 2001).

The same kind of experiment and calculations were carried out for the binding of m-NGF to $p75^{\text{NTR}}$. The overall plot of the sensogram for the serial dilutions is shown in fig.4.1.2.

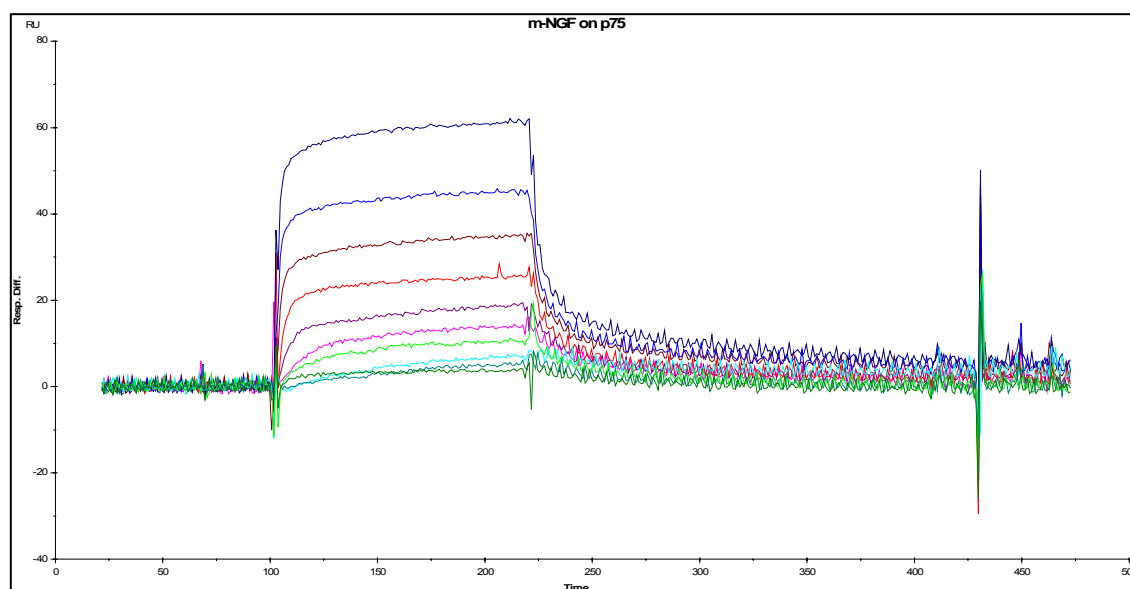


Figure 4.1.2 - BIAcore kinetic analysis of the binding of m-NGF over a $p75^{\text{NTR}}$ receptor surface. $p75^{\text{NTR}}$ immunoadhesin was immobilized on the CM5 chip at 8000 RU on Fc2, while Fc1 was left as a blank. Subsequently m-NGF was injected. The used concentrations were ranging from 2 to 500 nM by 1:1 serial dilutions. The corresponding curves are displayed in the figure; the lowest curve represents the buffer. All curves were blank subtracted.

A detailed analysis of the kinetic data was conducted in this case too. The binding of NGF to TrkA is characterized by a relatively slow association rate ($k_a = 4 \cdot 10^6 \text{ M}^{-1} \text{ s}^{-1}$) and a slow dissociation rate ($k_d = 3 \cdot 10^{-2} \text{ s}^{-1}$). The equilibrium association constant was reported to be of 0.1 nM^{-1} ($\chi^2 = 0,09$) and the dissociation one can be evaluated to be of 8 nM , therefore four times higher than the dissociation from the TrkA receptor. Again, these values are in agreement with the previously reported values for the binding of m-NGF to its receptor p75^{NTR}, that report it to be a low affinity ligand for NGF, according to the historical definition of the binding mode.

By comparison, the same kinetic analysis was performed on the rm-proNGF data, both for the binding at TrkA and at p75^{NTR}.

The sensograms for the TrkA/proNGF binding are presented in fig.4.1.3, and a qualitative analysis of the data shows that the affinity is lower than in the case of m-NGF, as also previously reported (Nykjaer *et al.*, Nature, 2004). Indeed, the kinetic and equilibrium constants were the following:

$$k_a = 8.9 \cdot 10^5 \text{ M}^{-1} \text{ s}^{-1}$$

$$k_d = 4 \cdot 10^{-3} \text{ s}^{-1}$$

$$K_A = 0.2 \text{ nM}^{-1}$$

$$K_D = 4.5 \text{ nM}$$

$$\chi^2 = 0.95$$

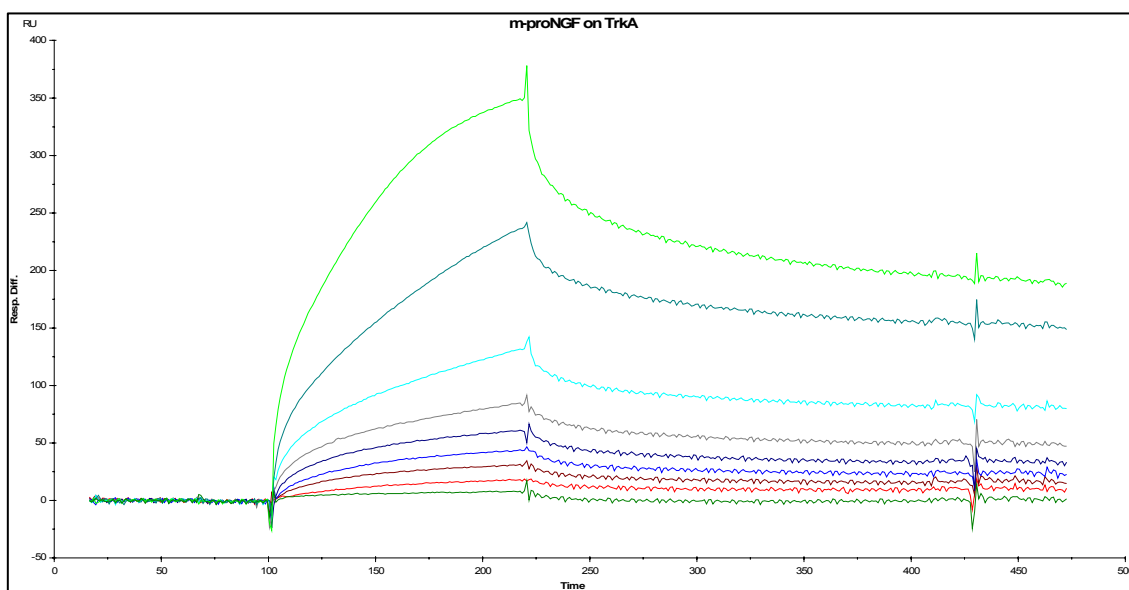


Figure 4.1.3 – BIAcore kinetic analysis of the binding of rm-proNGF over a TrkA receptor surface. TrkA immunoadhesin was immobilized on the CM5 chip at 8000 RU on

Fc2, while Fc1 was left as a blank. Subsequently rm-proNGF was injected. The used concentrations were ranging from 2 to 500 nM by 1:1 serial dilutions. The corresponding curves are displayed in the figure; the lowest curve represents the buffer. All curves were blank subtracted.

A similar data analysis was performed for the binding of rm-proNGF to the p75^{NTR} receptor. The sensograms obtained by the kinetic analysis with a serial dilution of protein, summarized in fig.4.1.4, show that the affinity of the p75^{NTR} receptor is not very different to the one versus TrkA.

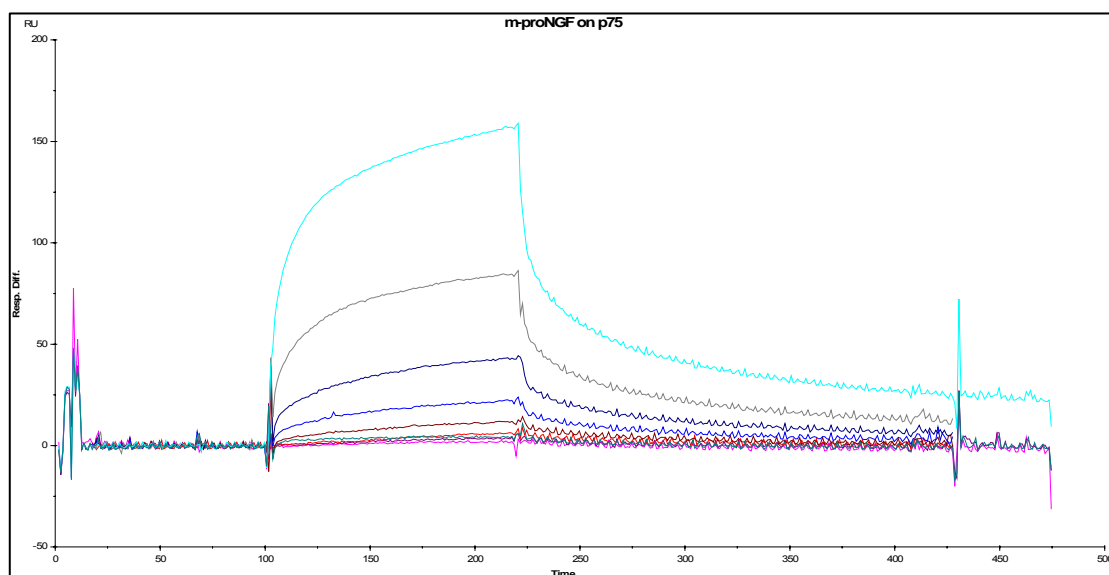


Figure 4.1.4 – BIAcore kinetic analysis of the binding of rm-proNGF over a p75^{NTR} receptor surface. p75^{NTR} immunoadhesin was immobilized on the CM5 chip at 8000 RU on Fc2, while Fc1 was left as a blank. Subsequently rm-proNGF was injected. The used concentrations were ranging from 2 to 500 nM by 1:1 serial dilutions. The corresponding curves are displayed in the figure; the lowest curve represents the buffer. All curves were blank subtracted.

The detailed calculation of the parameters, in fact, clearly shows that the difference in the binding of rm-proNGF to p75^{NTR} and TrkA is not so remarkable. In particular, calculated parameters are:

$$k_a = 0.4 \cdot 10^6 \text{ M}^{-1}\text{s}^{-1}$$

$$k_d = 9 \cdot 10^{-3} \text{ s}^{-1}$$

$$K_A = 0.05 \text{ nM}^{-1}$$

$$K_D = 26.8 \text{ nM}$$

$$\text{Chi}^2 = 0.35$$

Summary of all the measured binding constants for NGF and proNGF towards p75 and TrkA receptors.

	TrkA (kinetic)	TrkA (equilibrium)	p75 ^{NTR} (kinetic)	p75 ^{NTR} (equilibrium)
m-NGF	$k_a = 1 \cdot 10^6 \text{ M}^{-1}\text{s}^{-1}$ $k_d = 2 \cdot 10^{-3} \text{ s}^{-1}$	$K_A = 0.5 \text{ nM}^{-1}$ $K_D = 2 \text{ nM}$	$k_a = 4 \cdot 10^6 \text{ M}^{-1}\text{s}^{-1}$ $k_d = 3 \cdot 10^{-2} \text{ s}^{-1}$	$K_A = 0.1 \text{ nM}^{-1}$ $K_D = 8 \text{ nM}$
rm-proNGF	$k_a = 8.9 \cdot 10^5 \text{ M}^{-1}\text{s}^{-1}$ $k_d = 4 \cdot 10^{-3} \text{ s}^{-1}$	$K_A = 0.2 \text{ nM}^{-1}$ $K_D = 4.5 \text{ nM}$	$k_a = 0.4 \cdot 10^6 \text{ M}^{-1}\text{s}^{-1}$ $k_d = 9 \cdot 10^{-3} \text{ s}^{-1}$	$K_A = 0.05 \text{ nM}^{-1}$ $K_D = 26.8 \text{ nM}$

CONCLUDING REMARKS

Concluding, one can tell that our BIAcore data were confirming the previously reported data for both the binding of NGF and proNGF towards p75^{NTR} and TrkA receptors, carried out with different techniques and protein samples than the ones presented in this study.

Overall, the BIAcore data point out that the affinity of proNGF for p75^{NTR} is not higher than the one for TrkA, and this might appear contradictory to the reported data that p75 is a high affinity receptor for proNGF (Lee *et al.*, Science, 2004). However, as also reported by Nykjaer and colleagues (Nature, 2004), the observed behaviour is different when one considers the separate receptors or their co-expression. Indeed, the affinity of proNGF for p75^{NTR} was reported to be increased by the co-expression of sortilin. Indeed, one should also consider that the BIAcore experiment is carried out *in vitro*, in an “artificial system”; *in vivo*, therefore, the behaviour of the proteins could be very different, due to the involvement of many more biological components in the interaction.

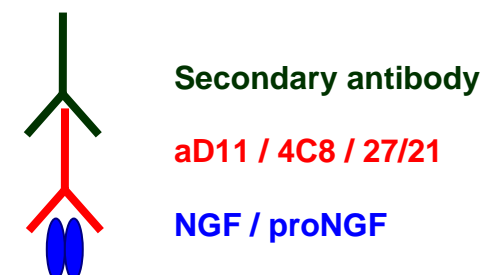
These data also contribute to the interpretation of the TrkA phosphorylation assays: in that experiment, described in a previous chapter, the level of activation given by proNGF was almost ten times lower than that of NGF, while by BIAcore the affinity was shown to be only three times lower. Probably, also in this case, the involvement of other partners during the protein-protein interactions *in vivo* might contribute to the change in the behaviour of proNGF if compared to the *in vitro* situation.

4.2 Interaction of NGF and proNGF with a panel of anti-NGF antibodies

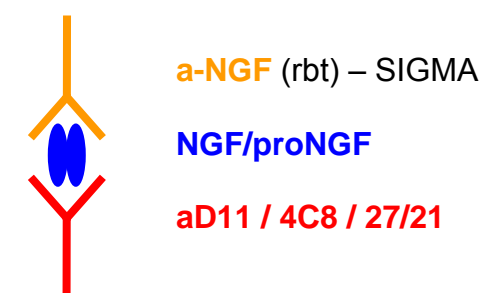
4.2.1 Analysis using ELISA assay

The ability of NGF and proNGF (both the mouse and the human forms) to differentially bind a panel of monoclonal anti-NGF antibodies was tested by ELISA assay and the results were compared. For this reason, equimolar concentrations of NGF and proNGF were tested, using three different configurations in the ELISA test:

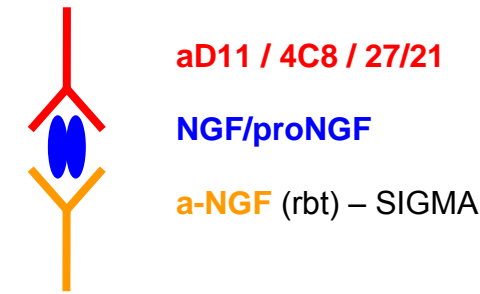
- immobilization on the plastic surface of ELISA plates of NGF and proNGF and subsequent incubation with the antibodies in solution (configuration A)



- immobilization on the plastic surface of the monoclonal antibodies, incubation of NGF and proNGF in solution and subsequent use of a polyclonal anti-NGF antibody as a primary antibody (configuration B)



- immobilization on the plastic surface of the polyclonal anti-NGF antibody, incubation of NGF and proNGF in solution and subsequent use of the monoclonal antibodies as primary antibodies (configuration C).



The results of the different experiments are summarized by the following figures.

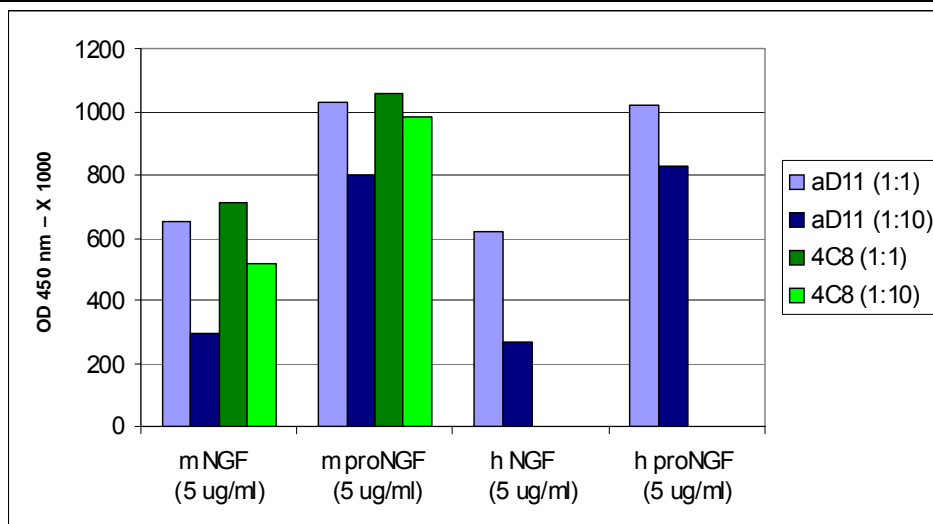
In particular, panel A and B in fig.4.2.1.1 depict the results of configuration A; on top the results of the use of hybridomas supernatants of the monoclonal antibodies are reported, and on bottom, the same result for the purified antibodies is reported. A first clear result is that the α D11 is able to recognize mouse and human NGF forms with the same intensity. Moreover, it is noteworthy that intensity of the signal arising from the proNGF samples is almost 30% higher than the corresponding NGF signal: this is clearly a sign that the α D11 is able to detect also proNGF samples, as well as the most proper antigen NGF. These results are true both for the use of antibodies' supernatants (panel A) and purified antibodies (panel B); in both cases, the antibody response is concentration-dependent. A possible explanation for this behaviour might reside in an increased ability of proNGF to adhere to the plastic surface of the ELISA plate with the pro-peptide, in order to somehow “expose” the mature NGF epitope to the antibody.

In the same panels, the experiment performed with the other antibodies is shown. In particular, with the 4C8 antibody only the experiment with the supernatants was conducted (Panel A) and with the 27/21 antibody only the experiment with the purified antibody was carried out (Panel B). Concerning the 4C8 antibody, the first result is that this antibody is only able to interact with the mouse antigens, but has no affinity for the human ones, as also previously described (PhD Thesis – S.Gonfloni). For 4C8 too, like for α D11, the intensity of the response is higher for rm-proNGF than

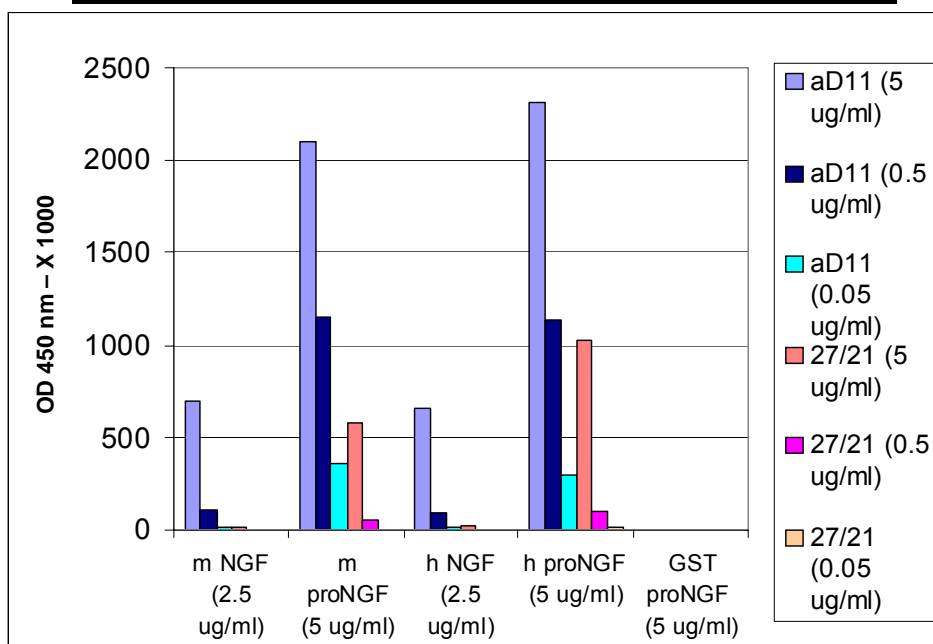
for m-NGF. The same behaviour is observed with the 27/21 antibody, as is clear from Panel B; like α D11 antibody, however, and on the contrary of 4C8, 27/21 can interact with both the mouse and the human antigens.

Finally, Panel C in fig.4.2.1.1 indicates a control experiment conducted using as a primary antibody a polyclonal, commercial anti-NGF antibody. The main result of this experiment is that the response is positive for both NGF and proNGF, and for both mouse and human antigens. The slightly higher response observed for the mouse antigens could be ascribed to the fact that the antibody has been raised against the mouse NGF.

Panel A: WITH SUPERNATANTS OF MONOCLONAL ANTIBODIES



Panel B: WITH PURIFIED MONOCLONAL ANTIBODIES



Panel C: with polyclonal anti NGF 1:8000 (CONTROL)

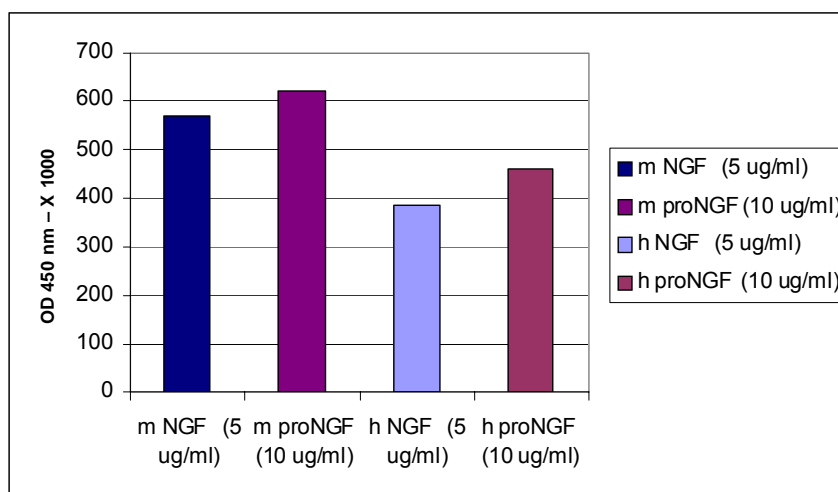


Figure 4.2.1.1 – ELISA assay of the differential binding of NGF and proNGF towards a panel of anti-NGF antibodies. The experiment with the immobilization on the plastic surface of ELISA plates of recombinant NGF and proNGF and subsequent incubation with the antibodies in solution (configuration A) is shown. The data represent an average of two measurements; all data were blank subtracted. Panel A: experiment performed with the supernatants of the indicated antibodies: α D11 (blue bars) and 4C8 (green bars). Panel B: experiment performed with the purified antibodies: α D11 (blue bars) and 27/21 (pink bars). Panel C: experiment performed with the commercial polyclonal anti-NGF antibody.

The ELISA format with the configuration B described previously, is represented in fig.4.2.1.2. The experiment was only performed for the α D11 and the 27/21 antibodies immobilized on the plastic plates. The most striking result is that the 27/21 antibody gives no response at all, neither with NGF, nor with proNGF. On the contrary, the result is positive for the α D11 antibody. In particular, in this case, two important features can be underlined. First of all, this format of the experiment present an opposite behaviour in comparison to the configuration A regarding the affinity for NGF and proNGF: in this case, where the neurotrophins are incubated in solution, the binding of the α D11 antibody is much higher for NGF than for proNGF, both for the mouse and in the human antigens. Moreover, it should be noted that in this case the response of the mouse antigens is much higher than the one for the human ones.

PURIFIED MONOCLONAL ANTIBODIES COATING (10ug/ml)

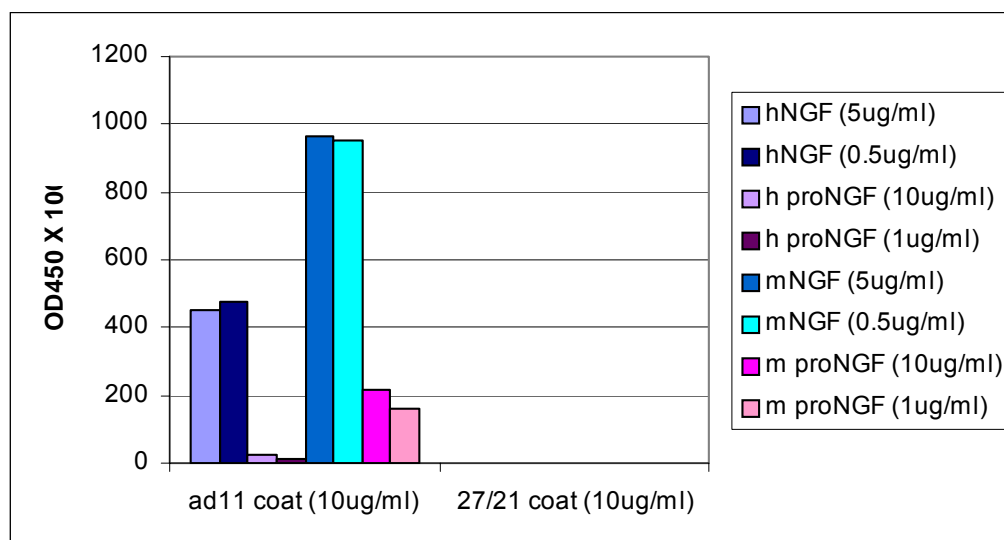


Figure 4.2.1.2 – ELISA assay of the differential binding of NGF and proNGF towards a panel of anti-NGF antibodies. The experiment with the immobilization on the plastic surface of the monoclonal antibodies, incubation of recombinant NGF and proNGF in solution and subsequent use of a polyclonal anti-NGF antibody as a primary antibody (configuration B) is shown. The legend to the different neurotrophins used in the incubation is shown on the right side. The data represent an average of two measurements; all data were blank subtracted.

These results described for the configuration B, could also be confirmed by the experiment with the configuration C, with the polyclonal anti-NGF antibody used as coating on the plate. The summary of the result is depicted in fig.4.2.1.3.

POLYCLONAL ANTIBODY COATING (15ug/ml)

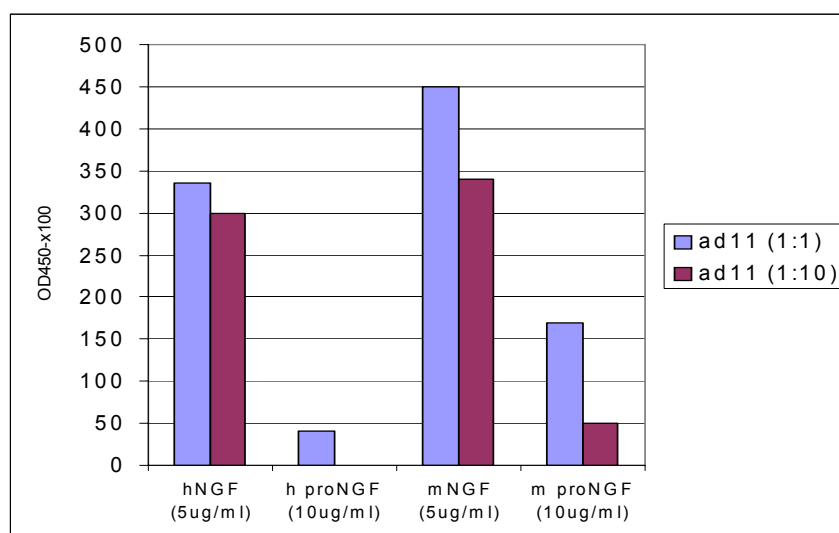


Figure 4.2.1.3 – ELISA assay of the differential binding of NGF and proNGF towards a panel of anti-NGF antibodies. The experiment with the immobilization on the plastic surface of the polyclonal anti-NGF antibody, incubation of NGF and proNGF in solution and subsequent use of the monoclonal antibodies as primary antibodies (configuration C) is shown. Two different dilution of the α D11 antibody were used as primary antibody, as indicated on the right side. The data represent an average of two measurements; all data were blank subtracted.

It is strange to observe the opposite behaviour in the response intensity of NGF and proNGF in the ELISA configuration A if compared to the B and C. In particular, two explanations are possible for this behaviour. The first one can be ascribed to the characteristic of proNGF: when coated on the plastic surface of the plate (like in configuration A ELISA), the pro-peptide could bind the plastic more than the NGF moiety, therefore presenting the mature protein to the antibody in solution. The increased binding in the configuration A could be therefore contingent to an experimental artefact and not reflect a true structural difference between NGF and proNGF. The second reason for the different binding behaviour could reside in the fact that in the configuration B of the ELISA, the neurotrophins are presented in solution to the antibody bound on the plastic surface, and therefore the proteins are more free to move and expose in the best possible way the epitope to the antibody; in solution, the pro-peptide of the proNGF could partially hinder the epitope and give rise to a decreased response in comparison to NGF. This would be a structural equivalent of the differential interactions of proNGF and NGF to their receptors.

4.2.2 Surface Plasmon Resonance using BIAcore

The qualitative result of the different binding mode of NGF and proNGF towards a panel of monoclonal anti-NGF antibodies, was also confirmed and further analysed using Surface Plasmon Resonance with BIAcore.

All the antibodies were analysed with this technique, although a more thorough kinetic analysis was carried out only with the α D11 antibody, due to the importance of this antibody in the AD11 transgenic mouse model for Alzheimer's Disease, based on this antibody.

Section 1: *Comparative analysis for the binding of proNGF and NGF to a panel of anti-NGF antibodies*

The first experiment was conducted using m-NGF and rm-proNGF as ligands immobilized at equimolar concentrations on a CM5 chip, while the different monoclonal antibodies were employed as analytes. The summary of the results is presented in fig.4.2.2.1 Already from a first look at the result, it is clear that the response of the antibodies is much higher for m-NGF than for rm-proNGF, especially taking in account that the neurotrophins were immobilized at equimolar concentrations on the chip.

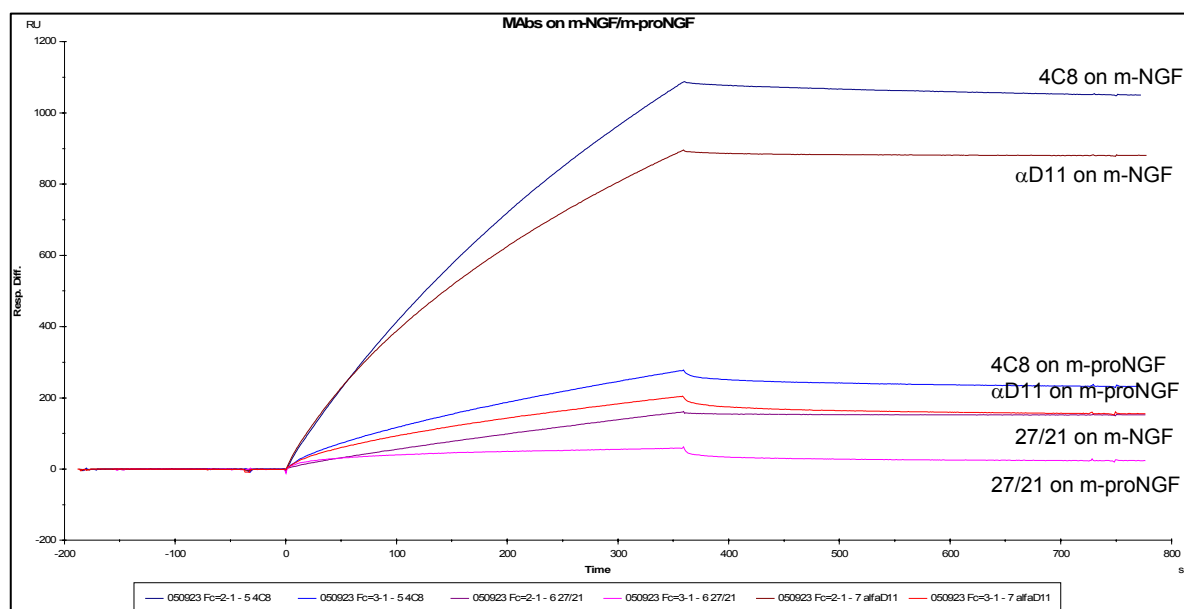


Figure 4.2.2.1 – BIAcore analysis of the binding of a panel of anti-NGF antibodies to m-NGF and rm-proNGF. The neurotrophins m-NGF and rm-proNGF were immobilized on the Fc2 and Fc3 respectively, while the Fc1 was left as a blank. The immobilization was of 1700 RU for m-NGF and of 2700 RU for rm-proNGF. The mAbs were injected at a 50 nM concentration.

A more detailed analysis of the results can be done by a separated plot of the binding curves on m-NGF (fig.4.2.2.2) and rm-proNGF (fig.4.2.2.3) respectively; the curves are the same of the previous plot.

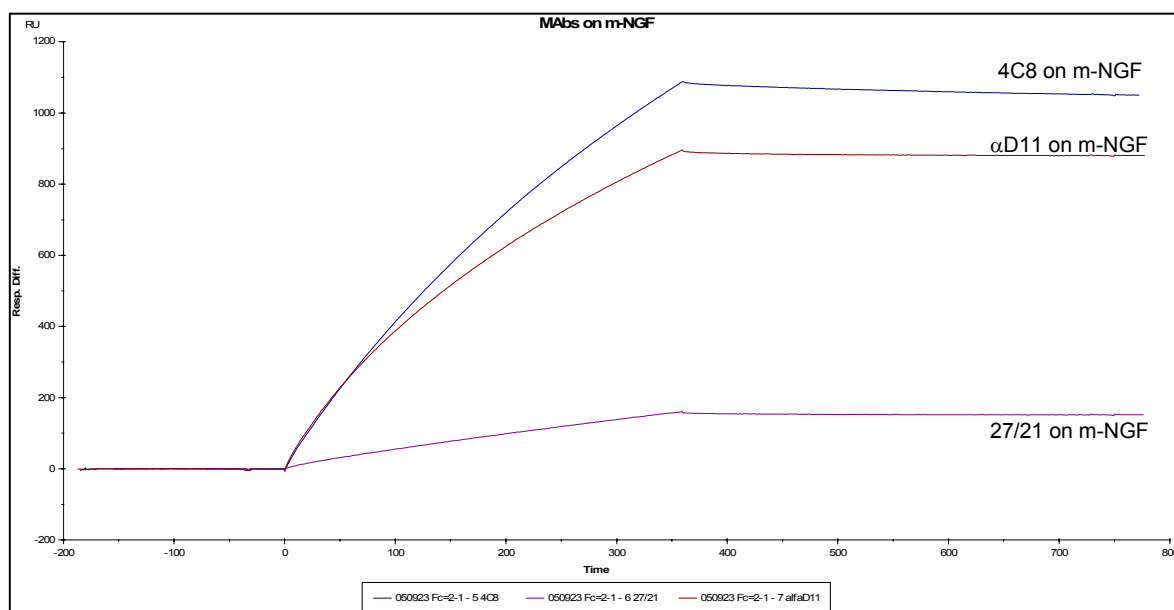


Figure 4.2.2.2 – BIAcore analysis of the binding of a panel of anti-NGF antibodies to m-NGF.

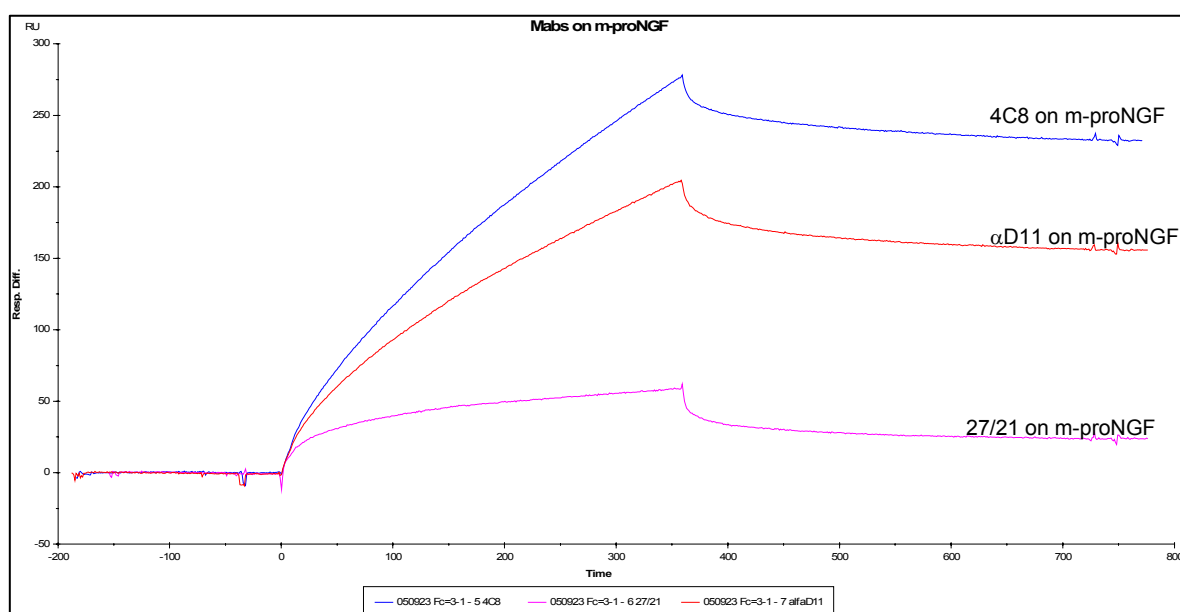


Figure 4.2.2.3 – BIAcore analysis of the binding of a panel of anti-NGF antibodies to rm-proNGF.

A closer look in the separated plot of the differential binding of the antibodies on the m-NGF and rm-proNGF proteins, makes it possible to address some

considerations. First of all, it is clear that 4C8 and α D11 antibodies have quite a similar binding mode towards their antigen: in fact, the intensity and the shape of the curves for the two antibodies is similar in the case of m-NGF as well as in the case of rm-proNGF. On the contrary, the 27/21 antibody has quite a different behaviour, as inferred from the shape of the curve both in the case of m-NGF and m-proNGF, that appears to be quite different from the ones of 4C8 and α D11; this antibody is also characterized by a lower intensity in the signal when compared to the other two. Moreover, for all three antibodies, it appears that the affinity of the antibodies is higher for m-NGF than for m-proNGF, as it can be assumed by looking at the association and dissociation curves in the two cases. In particular, the difference is much more remarkable in the dissociation part of the curves.

Although a precise kinetic analysis of the binding is not possible in this experiment due to the fact that the monoclonal antibodies used as analyte cannot be analysed with simple kinetic equations, it's still possible to evaluate a value for the dissociation constant. In particular, the fitting has been done on the various curves and it was possible calculate the following values:

	<i>αD11</i>	<i>4C8</i>	<i>27/21</i>
<i>k_d (1/s) for m-NGF</i>	$5e^{-5}$	$1e^{-4}$	$2e^{-4}$
<i>k_d (1/s) for rm-proNGF</i>	$1e^{-3}$	$1e^{-3}$	$3e^{-3}$

Therefore, it is possible to conclude that indeed in all the cases the antibodies have an increased affinity for m-NGF than for rm-proNGF, and that among all the antibodies, the one with the highest affinity is α D11.

In conclusion, the pro-peptide of pro-peptide is probably interfering with the binding of NGF to the different antibodies, maybe by a partial masking of the epitopes of the antibodies on the NGF protein.

Overall, the results are in agreement with the ones obtained by ELISA assay as described in the previous chapter.

Section 2: *Kinetic analysis on the α D11 antibody binding to m-NGF and rm-proNGF*

Due to the interest in the α D11 antibody from a structural and functional point of view, as pointed out in the introductory section to this part, and due to its high binding properties, a more detailed kinetic analysis was performed with this antibody, for a complete analysis on the differential binding to NGF and proNGF. In this case, both human and mouse neurotrophins were taken into account.

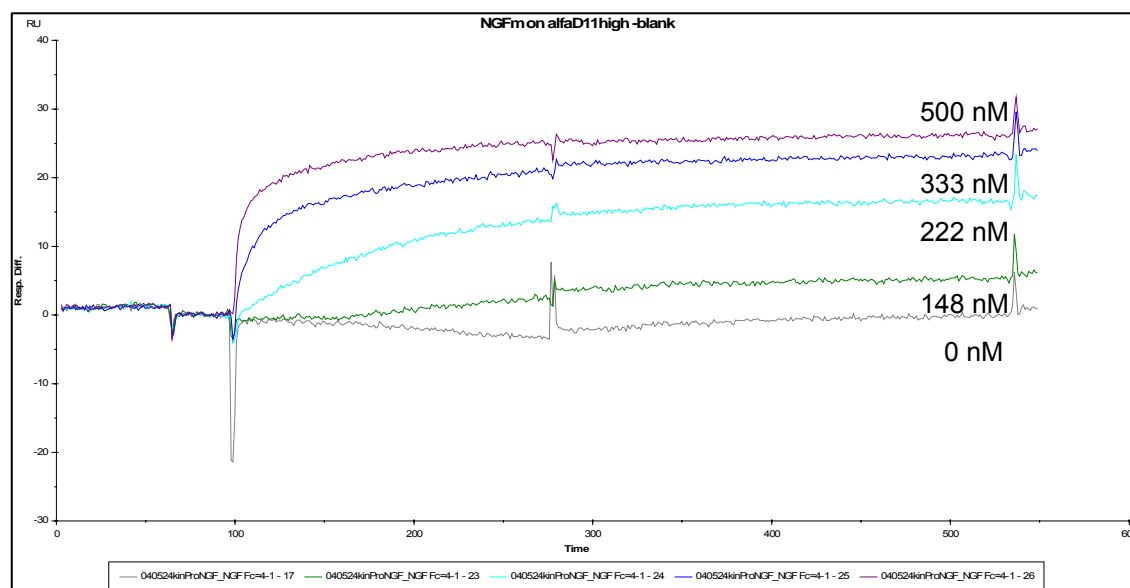
The format used for this experiment was the opposite than in Section 1: in particular, in this case, α D11 monoclonal antibody was immobilized as a ligand on the surface of a CM5 chip, and the neurotrophins were injected in solution as analytes.

A first difficulty encountered was due to the intrinsic stickiness of the pro-peptide of proNGF towards different materials. Therefore, the kinetic analysis on the rm-proNGF protein was complicated by a high background due to the aspecific binding of proNGF, both mouse and human, to the CM5 surface and to the antibody on aspecific sites. Moreover, α D11 was found to be a very high affinity antibody for NGF and the dissociation appeared to be very slow, probably even slower than the maximum allowed for the BIAcore instrument. However it was possible to perform a complete kinetic analysis on both NGF and rm-proNGF, and both in the human and in the mouse forms, and to evaluate the complete kinetic parameters.

The results are summarized in fig.4.2.2.4 for m-NGF, fig. 4.2.2.5 for rh-NGF, fig. 4.2.2.6 for rm-proNGF and fig. 4.2.2.7 for rh-proNGF.

Regarding the binding kinetic to NGF, the first result to be noted, both in the case of the mouse and of the human protein, is the rapid association and the very slow dissociation, as it clearly emerges from fig. 4.2.2.4 (panel A) for m-NGF and fig. 4.2.2.5 (Panel A) for rh-NGF. The result does not change if the association time for the experiment is shortened, as it appears from fig. 4.2.2.4 (panel B) for m-NGF and fig. 4.2.2.5 (Panel B) for rh-NGF.

A



B

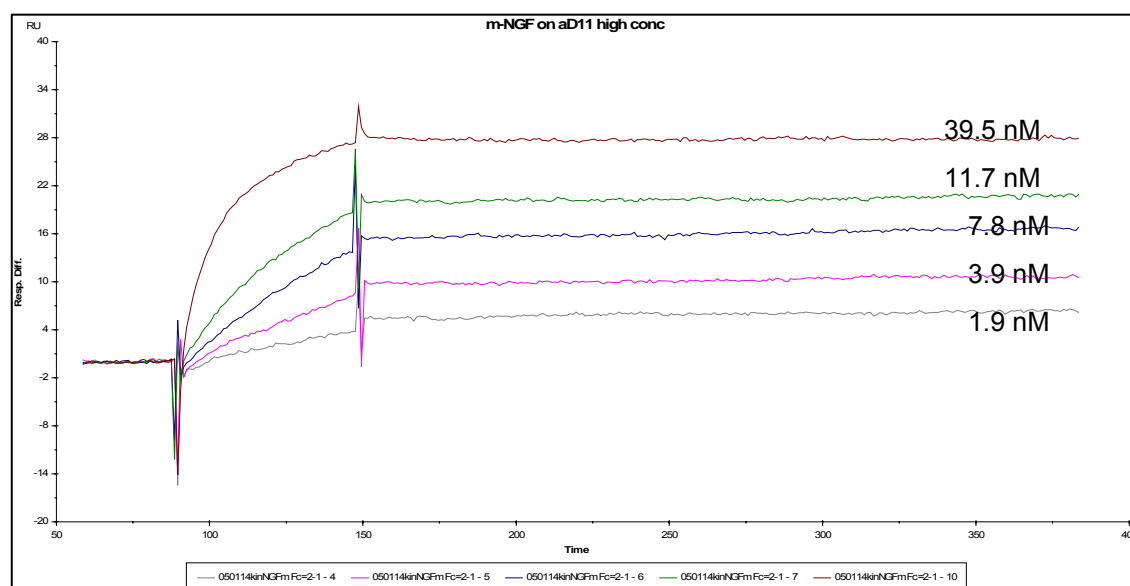


Figure 4.2.2.4 – BIAcore analysis of the binding of the α D11 anti-NGF antibody to m-NGF. The α D11 anti-NGF antibody was immobilized on the Fc2, while the Fc1 was left as a blank. The immobilization was of 3000 RU in the experiment of panel A and of 6000 RU in the experiment of panel B. The injected concentrations of the m-NGF are indicated on top of each curve. The curves were blank subtracted.

Already by looking at the curves, it is possible to affirm that the dissociation constant for NGF from α D11 is very small. From a complete analysis of the data, the affinity parameters were evaluated, and resulted to be the following:

$$K_A = 3,55 \cdot 10^{11} \text{ M}^{-1}$$

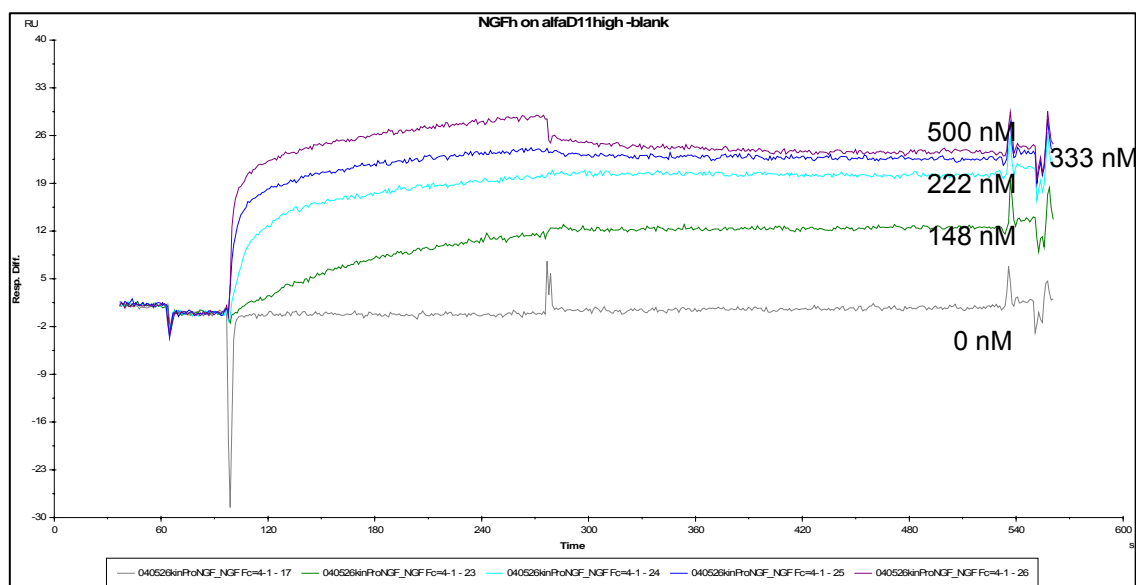
$$K_D = 2,81 \cdot 10^{-12} \text{ M}$$

With a χ^2 value of 0.123.

The kinetic analysis for the binding to α D11 antibody was also carried out with the rm-NGF obtained by proteolytic digestion from rm-proNGF. The protein demonstrated to behave in the same way as the commercial m-NGF (data not shown).

A completely analogue treatment of the data was performed on the binding curves of rh-NGF to α D11, as it emerges from the following figures.

A



B

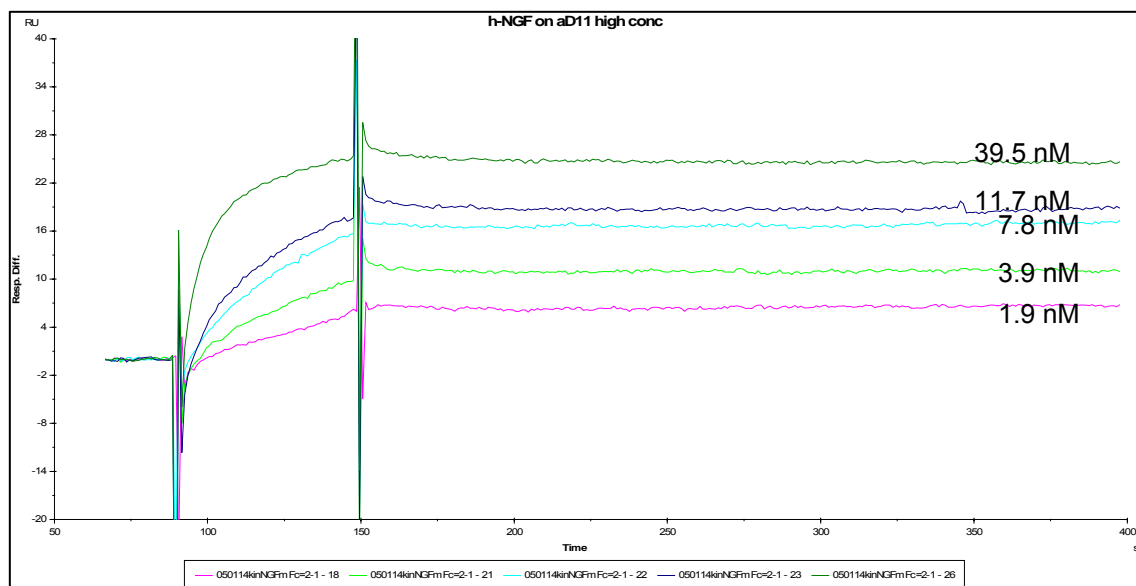


Figure 4.2.2.5 – BIAcore analysis of the binding of the α D11 anti-NGF antibody to h-NGF. The α D11 anti-NGF antibody was immobilized on the Fc2, while the Fc1 was left as a blank. The immobilization was of 3000 RU in the experiment of panel A and of 6000 RU in the experiment of panel B. The injected concentrations of the m-NGF are indicated on top of each curve. The curves were blank subtracted.

The kinetic analysis of the data was giving comparable results to the m-NGF ones, although the affinity resulted to be decreased in the case of the human protein, as it emerges from these values:

$$K_A = 2,84 \cdot 10^9 \text{ M}^{-1}$$

$$K_D = 3,53 \cdot 10^{-10} \text{ M}$$

With a χ^2 value of 0.265.

The same kind of experiments was carried out also for proNGF, both for the human and for the mouse recombinant proteins.

The results were quite interesting, and already a qualitative evaluation of the data was enough to demonstrate a difference in the binding kinetics of the proNGF if compared to the ones of NGF, resulting in a decreased affinity for proNGF. Fig. 4.2.2.6 for rm-proNGF and fig. 4.2.2.7 for rh-proNGF summarize these results.

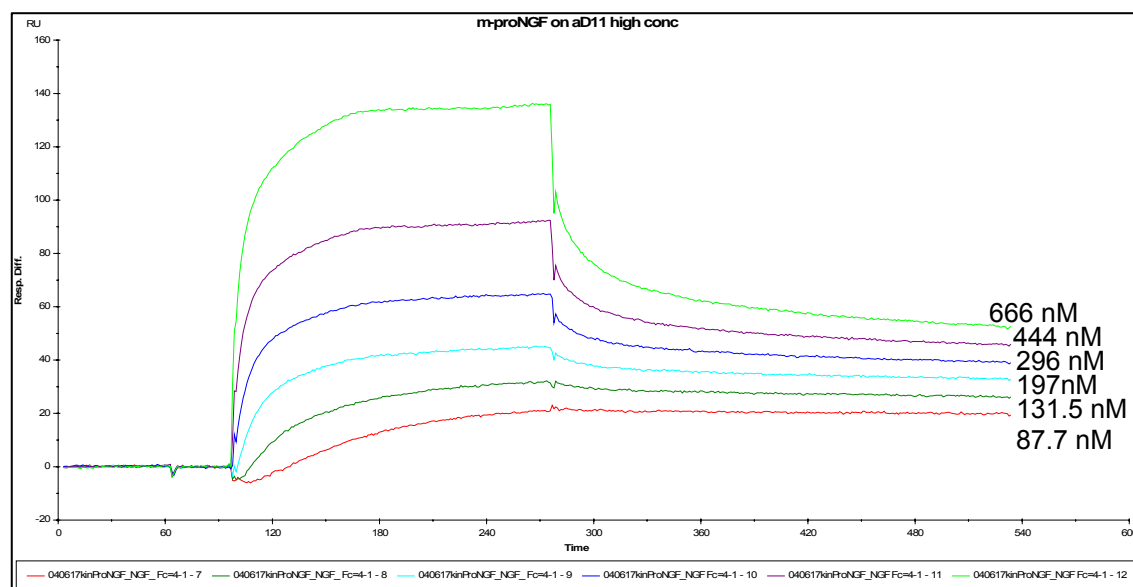


Figure 4.2.2.6 – BIAcore analysis of the binding of the α D11 anti-NGF antibody to rm-proNGF. The α D11 anti-NGF antibody was immobilized on the Fc2, while the Fc1 was

left as a blank. The immobilization was of 3000 RU. The injected concentrations of the rh-proNGF are indicated on top of each curve. The curves were blank subtracted.

Although the bulk effect recorded on the proNGF was very high, it was possible to perform a kinetic analysis of the data, that allowed to evaluate the following parameters:

$$K_A = 1,2 \cdot 10^9 \text{ M}^{-1}$$

$$K_D = 1,9 \cdot 10^{-9} \text{ M}$$

With a χ^2 value of 0.09.

Also in the case of the rh-proNGF the general behaviour was the same as for the mouse protein, as it can be observed from the sensograms represented in fig. 4.2.2.7.

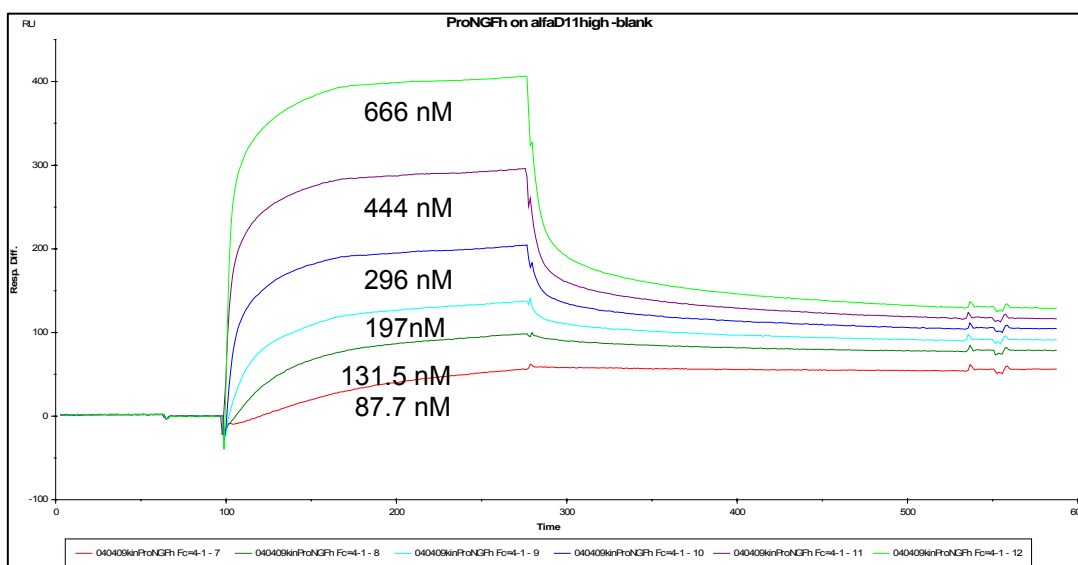


Figure 4.2.2.7 – BIAcore analysis of the binding of the α D11 anti-NGF antibody to rh-proNGF. The α D11 anti-NGF antibody was immobilized on the Fc2, while the Fc1 was left as a blank. The immobilization was of 3000 RU. The injected concentrations of the rh-proNGF are indicated on top of each curve. The curves were blank subtracted.

Also in this case a high bulk effect was recorded; nevertheless, the kinetic parameters were calculated:

$$K_A = 7,8 \cdot 10^8 \text{ M}^{-1}$$

$$K_D = 4,1 \cdot 10^{-9} \text{ M}$$

With a χ^2 value of 0.38.

It is possible to summarize the obtained data for the binding of the aD11 antibody in the following table:

	m-NGF	rm-proNGF	h-NGF	rh-proNGF
$K_A \text{ (M}^{-1}\text{)}$	$3.55 \cdot 10^{11}$	$1.20 \cdot 10^9$	$2.84 \cdot 10^9$	$7.80 \cdot 10^9$
$K_D \text{ (M)}$	$2.81 \cdot 10^{-12}$	$1.90 \cdot 10^{-9}$	$3.53 \cdot 10^{-10}$	$4.10 \cdot 10^{-9}$

Table 4.2.2.1 – Summary of the equilibrium binding constants of the aD11 antibody towards the different NGF and proNGF samples.

In conclusion, it is possible to say that the α D11 antibody binds with different kinetics on NGF and proNGF. In particular, the very small dissociation constant from NGF is representative of a very tight binding of the antibody for its antigen, and is quite a unique example among antibodies binding kinetics; it represents therefore a very important property of this antibody.

Moreover, by comparison of the α D11 antibody binding to NGF and to proNGF, it is possible to affirm that in the latter case the affinity is around two orders of magnitude lower. It is important here to point out that it was not easy to record the sensograms for the proNGF binding, due to a high bulk effect on the curves even after blank subtraction (as it clearly emerges from the curves shown in the figures). This is a clear evidence of a stickiness of the protein, that binds aspecifically to the chip surface.

The control for the stickiness of rm-proNGF was indeed performed using as an antibody the monoclonal anti-SV5. It is clear from the sensogram in fig.4.2.2.8 that the rm-proNGF has a high binding also to an unrelated antibody, maybe due to the interaction with the Fc portion of the immunoglobulin. However, an evaluation of the kinetic parameters of this binding of the proNGF the anti-SV5 antibody, gives rise to

different parameters indicating a much lower affinity. Therefore, the previously evaluated parameters for the proNGF binding to α D11 should be considered as specific.

$$K_A = 4,1 \cdot 10^6 \text{ M}^{-1}$$

$$K_D = 2,7 \cdot 10^{-7} \text{ M}$$

With a χ^2 value of 0.66.

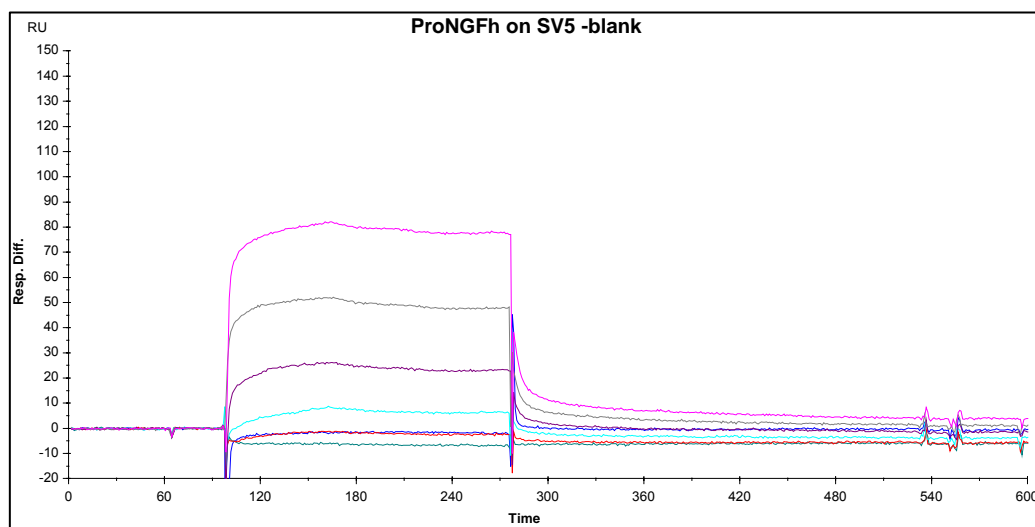


Figure 4.2.2.8 – BIAcore sensogram of the binding of rh-proNGF over the aspecific anti-SV5 antibody surface. The anti-SV5 antibody was immobilized on the Fc2, while the Fc1 was left as a blank. The immobilization was of 3000 RU. The injected concentrations of the rh-proNGF are indicated on top of each curve. The curves were blank subtracted.

The solution to the problem of the stickiness of proNGF to the CM5 chip is not easy to be solved, although some attempts were made in this direction.

A first approach was to try to use a stabilizing buffer for the BIAcore analysis, by adding at the running buffer compounds known to be stabilizing agents for flexible proteins, such as Na_2SO_4 , glycerol, sorbitol. The experiment was performed with the same format of the one previously described, *i.e.* α D11 antibody was bound on the CM5 chip surface, and rm-proNGF was subsequently injected as an analyte. The result, however, was not very encouraging, since the bulk of the system was not substantially decreased (data not shown).

Therefore, the optimization of the binding analysis of proNGF to α D11 MAb was not completely solved, and the problem is still under investigation.

Section 3: *Kinetic analysis on the α D11 antibody binding to m-NGF and rm-proNGF – an alternative approach*

The results presented in the previous section demonstrated that the α D11 antibody presents a very tight binding to its antigen NGF: if this is an important property of the antibody, on the other side its affinity for NGF cannot be calculated very precisely, due to experimental limitations in the BIAcore measurements. Moreover, it is not easy to calculate the kinetic parameters for the binding of α D11 to proNGF, due to an intrinsic “stickiness” of the latter, that gives rise to a high background and to a big bulk effect on the system.

To overcome these experimental limitations and to be able to calculate the affinity parameters with higher accuracy, a completely new strategy was developed. In particular, a “spacer” was selected for the immobilization on the CM5 chip: Protein L. This Protein is a bacterial protein characterized by the ability to bind through kappa light chains of immunoglobulins without interfering with antibody's antigen-binding site; it also binds to scFv and Fab fragments. Protein L binds to all classes of Ig of different mammalian species, including rat, the specie of α D11 antibody (Svensson *et al.*, Eur. J. Biochem., 1998; Svensson *et al.*, Biochemistry, 2004).

In this study, for the first time, Protein L was used in a BIAcore application: the strategy was the same already described for similar applications using other Ig-binding proteins from bacterial sources, like Protein A and Protein G (Svensson *et al.*, Eur. J. Biochem., 1998; BIAcore application note 38).

Initially, Protein L was immobilized on a CM5 chip by traditional procedure; subsequently, the monoclonal antibody α D11 was injected into the system and finally, m-NGF was injected as an analyte. In this way a sandwich assay is obtained, where the neurotrophin binds the antibody on a spacer to the chip surface, represented by Protein L. To verify any possible interference, NGF was also injected directly over Protein L, but no binding was recorded (data not shown).

The optimal α D11 concentration to be used has been selected after a concentration scouting to reach saturation of Protein L (see fig.4.2.2.9): the saturation of the system was reached at around 8000 RU. In the actual experiment, the α D11 was loaded on a single injection, after the selection of an appropriate injection time to reach saturation.

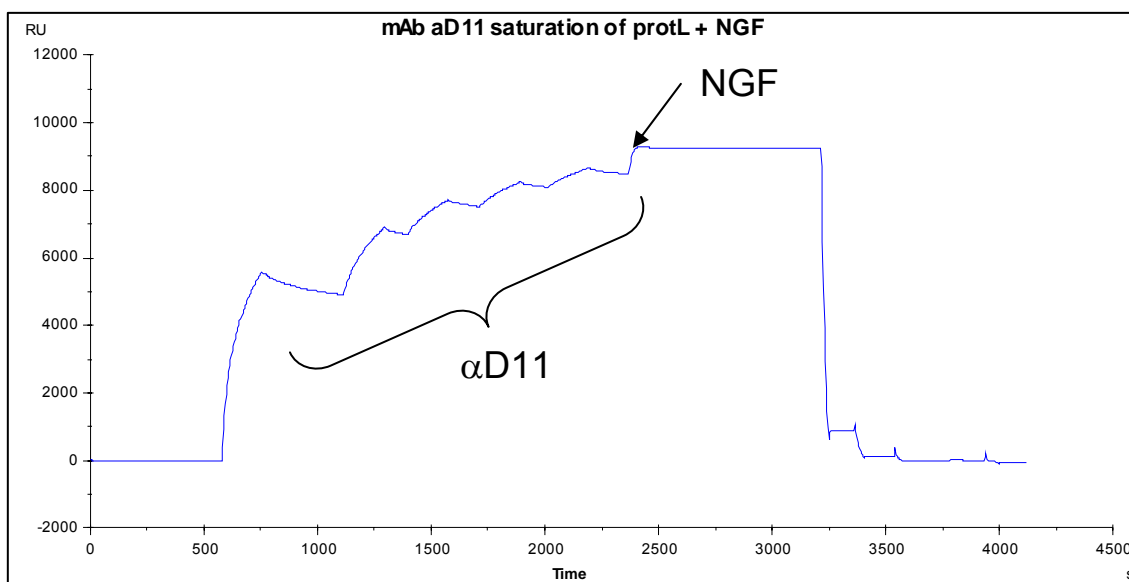


Figure 4.2.2.9 – BIAcore sensogram of the saturation of the Protein L surface with subsequent injections of α D11 antibody. Protein L was immobilized on the system at 3000 RU, and aD11 antibody at 1 μ M concentration was injected several times to evaluated when the saturation of the system could be reached. At that point, an injection of NGF at 100 nM was performed, as indicated in the figure. The system was finally regenerated by three injections of 10 mM Glycine, pH 1.5.

The second variable to be optimized has been the regeneration conditions between one measurement and the following: for this purpose, a selection of regeneration solutions have been employed. The final conclusion was that no regeneration was possible by removal of the solely NGF, but it was necessary to remove at every cycle both NGF and α D11. Therefore, in the experiment, the regeneration was made after each injection of NGF protein over the α D11 antibody, and after regeneration a new injection of α D11 and NGF was necessary.

Once the system has been optimized, the experiment was performed, making a whole kinetic series of injections of m-NGF. The overall final result is shown in fig.4.2.2.10.

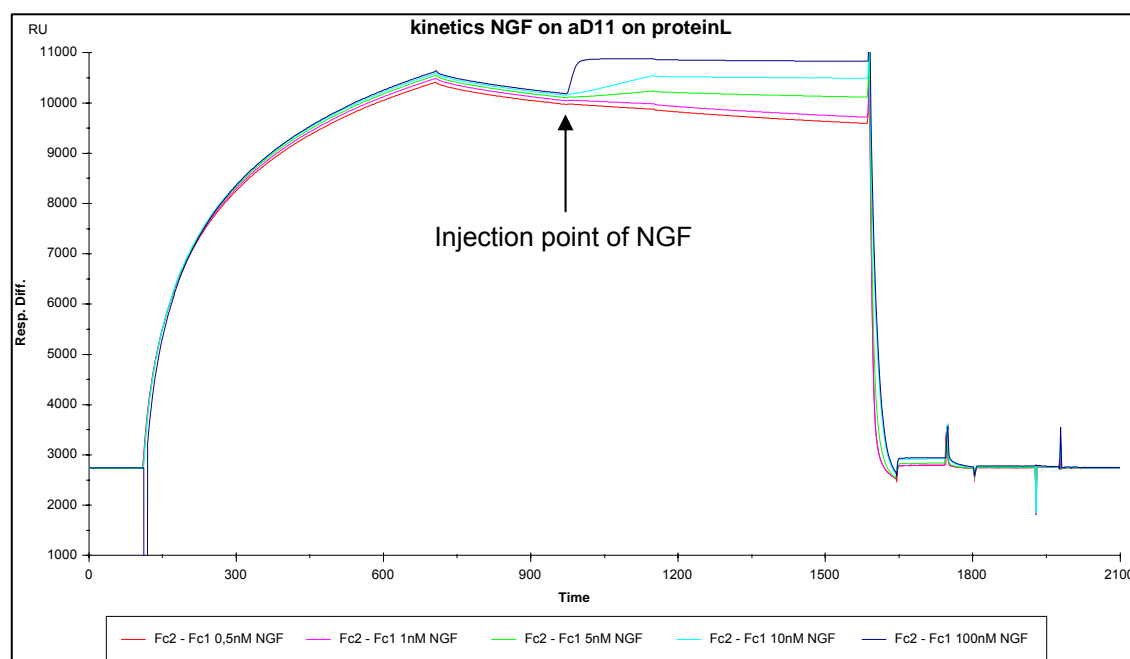


Figure 4.2.2.10 – BIAcore sensograms of the kinetic analysis of the binding of m-NGF to α D11 antibody bound on a surface of Protein L. Immobilization surface: 3100RU proteinL on CM5 chip (Biacore3000 at ScilProteins)

From a first look at the sensogram, one can observe that the binding of α D11 antibody at the Protein L was not very stable, because the R_{\max} value of α D11 over Protein L was increasing over time, maybe due to a partially incomplete regeneration of the system. Moreover, a large drift of the baseline of m-NGF association/dissociation can be observed, due to the dissociation of α D11 MAb from Protein L. This fact can be detected even more clearly in fig.4.2.2.11, where an enlargement of the solely m-NGF kinetic is shown. The shape of the curves is quite correct, although the kinetic analysis of the system is complicated by the fact that at lower concentrations a positive dissociation of m-NGF from α D11 is observed. The concentrations of m-NGF used in the experiment were: 0.5 nM, 1 nM, 5 nM, 10 nM, 100 nM.

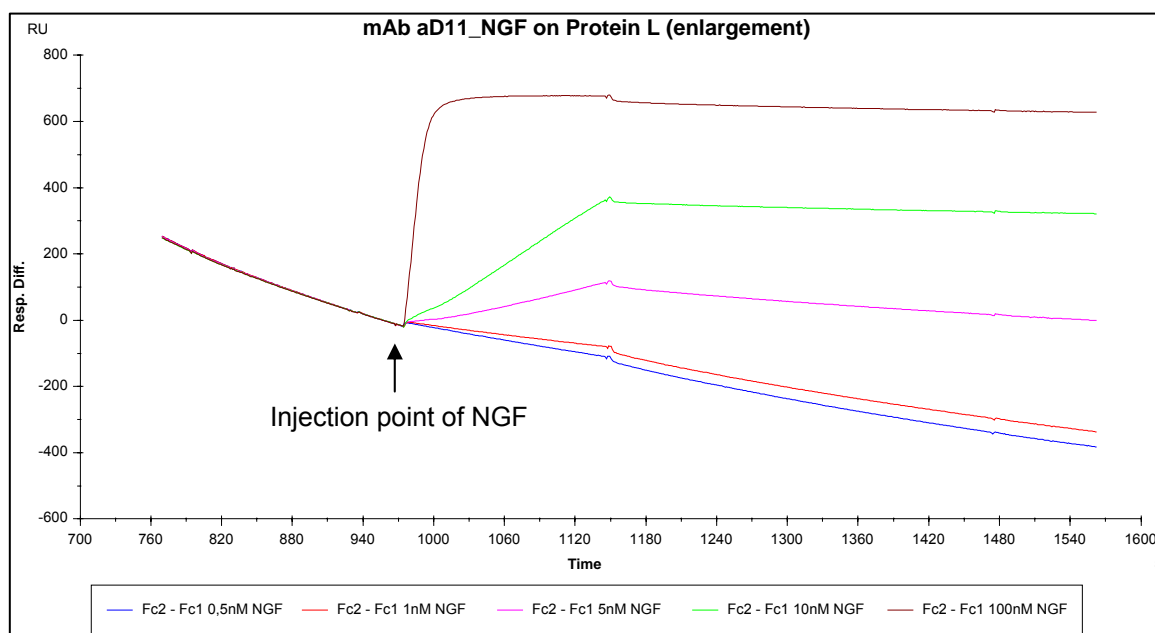


Figure 4.2.2.11 – Kinetic analysis of the BIAcore data of the binding of m-NGF over αD11 antibody. The figure is an enlargement of fig. 5.2.2.8, considering only the sensograms starting from the point of the injection of NGF.

Although the system is not optimized yet, it was possible to perform a first fitting on the data using only the three lowest concentrations, that gave the following parameters:

$$K_A = 2,3 \cdot 10^{13} \text{ M}^{-1}$$

$$K_D = 4,4 \cdot 10^{-14} \text{ M}$$

With a χ^2 value of 4,41.

Once again, it clearly emerges that the dissociation constant is very small, even more than it could be evaluated.

Regarding the kinetic analysis of the binding of rm-proNGF to αD11 antibody, an attempt was done to use the same approach, of using Protein L as a spacer on the CM5 chip, trying to reduce the α-specific binding of rm-proNGF to the chip surface.

Unfortunately, it was not possible to apply to rm-proNGF the same strategy used with m-NGF. In fact, a preliminary experiment to assess the proper conditions for the kinetic, showed that rm-proNGF binds α-specifically Protein L on the CM5

chip, unlikely NGF. In the sensogram in fig.4.2.2.12 this result is clearly explained: Protein L was immobilized on the CM5 chip, and α D11 was injected as an analyte; immediately after, without any regeneration, rm-proNGF was injected over the α D11 and a sensogram was detected. After regeneration of the surface, under the same conditions already used for the m-NGF experiment, a control injection was done. In particular, rm-proNGF was directly injected over the surface, and as it is clear from the second part of the sensogram, the response of the rm-proNGF is comparable to the one over the α D11 antibody, showing that there is an a-specific interaction with the surface of the CM5 chip coated with the Protein L.

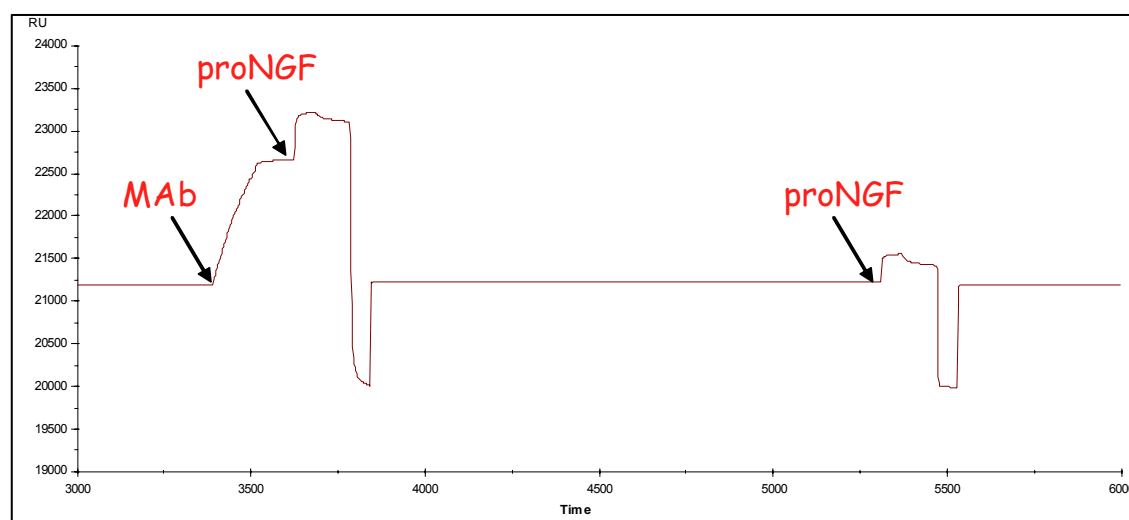


Figure 4.2.2.12 – BIAcore analysis on the binding of rm-proNGF over the experimental surface coated with Protein L. The chip surface was coated with Protein L at 3500 RU. The mAb α D11 was injected first (200 nM, flow: 10 μ L/min), and the rm-proNGF immediately after (250 nM, flow: 20 μ L/min), as indicated by the arrows. After the regeneration, the rm-proNGF was injected directly on the surface.

An attempt was done to try to ameliorate the situation and decrease the stickiness of rm-proNGF versus the BIAcore surfaces.

In particular, different strategies were employed, which are summarized in fig.4.2.2.13. The three represented sensograms, represent three subsequent injections of rm-proNGF directly on the Protein L surface: the first curve is the injection in the normal running buffer; in the second injection, the pH of the system

was raised, taking in account that rm-proNGF is a basic protein; the last injection was run in presence of Arginine as a stabilizing agent for the flexible pro-peptide. It can be concluded that it is indeed possible to decrease the aspecific response of the rm-proNGF over the chip surface. Unfortunately, in the best conditions for a decreased response, the binding of the MAb α D11 to Protein L was also decreased (data not shown), vanishing the attempts of getting an improvement in the conditions to run the rm-proNGF experiment in the sandwich format.

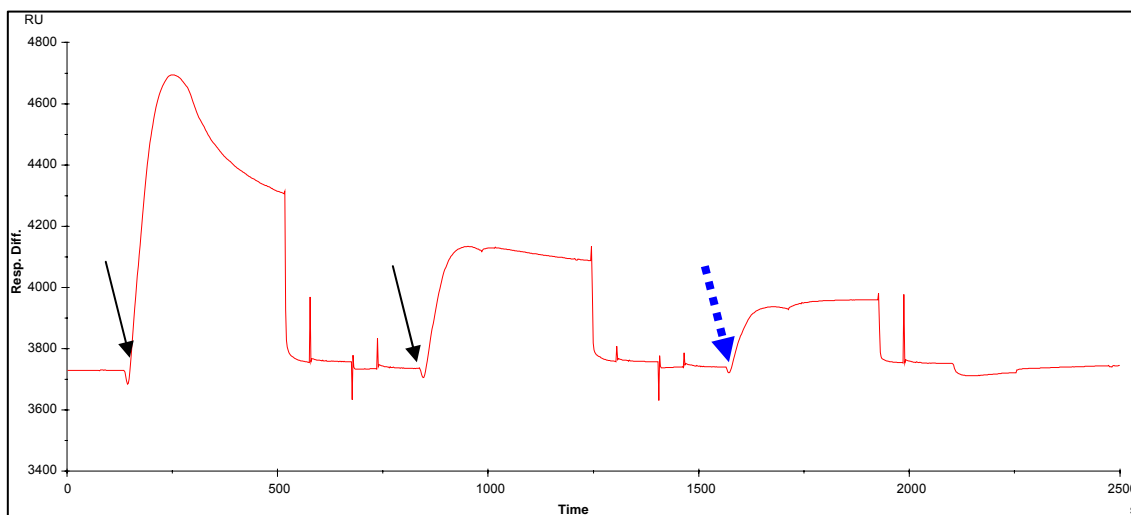


Figure 4.2.2.13 – Attempts to reduce the aspecific binding of rm-proNGF to the CM5 surface coated with Protein L. The chip surface was coated with Protein L at 3500 RU. The arrows mark the injections of the rm-proNGF (25 mM) directly on Protein L, after dilution in a buffer at different pH (7.5 the first and 8.0 the second) or added with 100 mM Arginine (the dotted arrow). After each injection, the surface was regenerated with a pulsed injection of 10 mM Glycine.

The strategy of the use of Protein L as a spacer was therefore abandoned in the analysis of the kinetic of the binding of rm-proNGF to the α D11 MAb.

On the contrary, the presented approach was a proof that the use of a spacer for the analysis of the binding of m-NGF to the α D11 antibody could be a useful methodology, although Protein L might not be the best one, due to the quite quick dissociation of α D11 antibody. Alternatively, an antibody anti-rat could be used as a spacer, to bind more tightly the α D11 MAb on the chip surface.

Overall, it is possible to conclude that the binding of m-NGF to the α D11 antibody is so strong, that it is not easy to be analysed even with a sensitive technique like BIAcore, although it is possible to estimate that the equilibrium K_D has a value between 10^{-12} and 10^{-15} M for m-NGF, showing in any way a very strong affinity of the antibody. Moreover, it was also possible to demonstrate that the kinetic of binding of the antibody versus rm-proNGF was around two orders of magnitude lower than in the case of NGF, being of the range of 10^{-9} - 10^{-10} M.

5. Structural characterization of rm-proNGF and of its complex with the anti-NGF antibody α D11

One of the aims of my work for this Thesis was the structural characterization of the rm-proNGF, to have a molecular base for the interpretation of the function of proNGF *in vivo*, through the analysis of the interaction with various molecular partners.

As such, the essential prerequisite is the availability of a well characterized, scalable expression system for rm-proNGF. The thorough biophysical and cell biological characterization of the protein produced in *E. coli* (as described in the previous chapters) confirmed that this protein can indeed be used for structural studies.

At first, the approach was to get a high resolution structure using X-ray crystallography.

I undertook initial attempts of obtaining suitable conditions for rm-proNGF crystallization that were performed with a high throughput screening on both the rm-proNGF alone and the complex between proNGF/ α D11 Fab, hoping that the antibody could stabilize the rm-proNGF. But no results could be achieved so far. Attempts are still underway.

The most likely reason for the difficulty in obtaining crystals of rm-proNGF can be attributed to the intrinsic biochemical properties of the protein. The pro-peptide of proNGF (both human and mouse), in fact, is highly flexible, and is characterized by an intrinsic disorder, as indicated by the circular dichroism analysis (see section 1 – p.87) and also predicted by the analysis on the aminoacid sequence by FoldIndex© web server: the fig.5.1 clearly indicates that no clear folding element can be attributed to the pro-peptide of rm-proNGF.

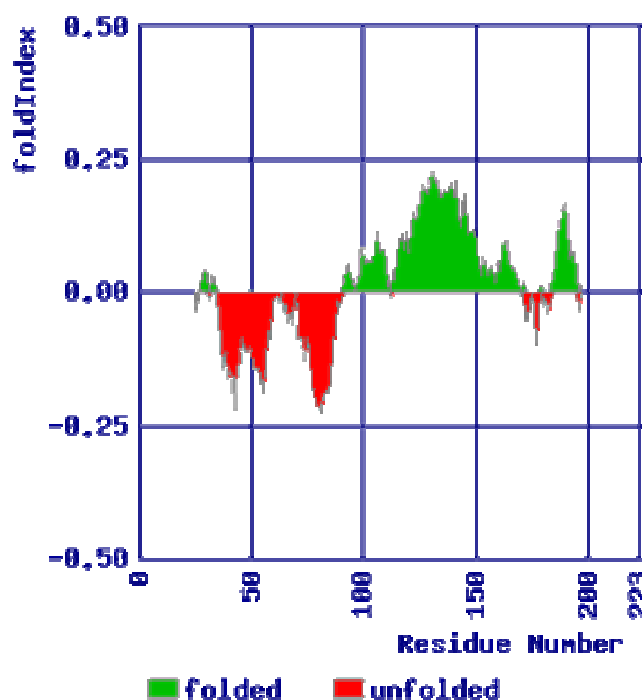


Figure 5.1 – FoldIndex Plot.

FoldIndex plot with window size 51 for the short form of mouse proNGF. Regions coloured in green and red correspond to the protein sequence predicted to be foldable and unfoldable (intrinsically disordered) respectively.

This particular feature of rm-proNGF made it impossible to achieve a positive score in the crystallization screening assay.

Therefore, Small Angle X-ray Scattering (SAXS) was chosen as the most suitable technique to obtain information on the structure and dynamic of the proNGF protein in solution.

A short introduction to the relevant aspects of the SAXS technique is presented hereafter giving an abridged version of the review by Svergun and Koch (Curr. Op. Str. Biol, 2002).

“Introduction - Small-angle scattering (SAS) of X-rays (SAXS) is a fundamental tool in studies of the solution structure of biological macromolecules with sizes ranging from a few kilo-Daltons to several mega-Daltons.

In a scattering experiment, a solution of macromolecules is exposed to X-rays (wavelength $\lambda \approx 0.15$ nm). The scattered intensity, $I(s)$, is recorded as a function of the momentum transfer s ($s = 4\pi \sin\theta/\lambda$, where 2θ is the angle between the incident and scattered radiation) and the solvent scattering is subtracted. The random positions and orientations of particles result in an isotropic intensity distribution, which, for monodisperse solutions of non interacting particles, is proportional to the scattering from a single particle averaged over all orientations.

The information content of SAXS data is qualitatively illustrated in Figure 5.2, which shows X-ray patterns from proteins with different folds and molecular masses. At low angles (2–3 nm resolution), the curves are very different, rapidly decaying functions of s essentially determined by the particle shape. At medium resolution (2–0.5 nm), the differences are already less pronounced and, above 0.5 nm resolution, all the curves are very similar. SAXS thus contains information about gross structural features — shape, and quaternary and tertiary structure — but it is not suitable for the analysis of atomic structure.

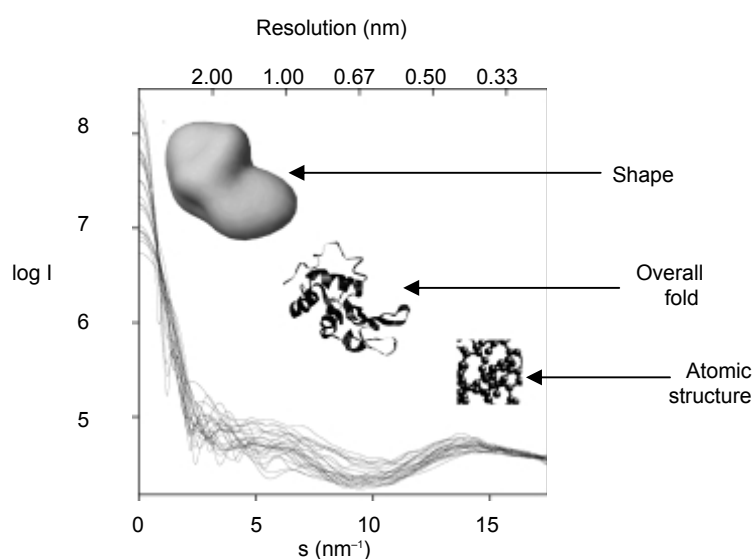


Figure 5.2 - X-ray solution scattering curves computed from atomic models of 25 different proteins with molecular masses between 10 and 300 kDa. The scattering intensities are plotted on a logarithmic scale, the upper axis displays the spatial resolution ($\Delta r = 2\pi/s$) and the labels indicate the levels of structural organisation characteristic of this resolution.

Shape determination - The aim of *ab initio* analysis of SAXS data is to recover the three-dimensional structure from the one-dimensional scattering pattern. Except for the trivial case of a spherical particle, the solution is clearly not unique and many different models could yield the same SAXS curve. To constrain the solution, homogeneous models assuming a constant scattering density within the particle are often used. This drastic simplification is reasonable in the analysis of the low-angle part of the scattering patterns from single component particles at sufficiently high contrasts, such as proteins in solution. In the past, low-resolution models were built

by trial and error using *a priori* information from electron microscopy or other methods. The low-resolution shape is thus defined by a few parameters—the coefficients of this series—that fit the scattering data. It was demonstrated that, under certain circumstances, a unique envelope can be extracted from the scattering data. The use of such envelopes is limited to globular particles with relatively simple shapes and without significant internal cavities. More detailed models can be constructed *ab initio* using different types of Monte Carlo searches. A sphere with diameter equal to the maximum particle size, D_{\max} , which is directly determined from the scattering data, is filled with a large number, M , of densely packed beads.

Domain structure analysis - For all its simplicity, the assumption of particle homogeneity is a severe limitation. In a more general approach, the beads may belong to different components, so that the shape and internal structure of multicomponent particles (e.g. nucleoproteins) can be reconstructed by simultaneously fitting scattering data at different contrasts. A new approach represents a protein by an assembly of dummy residues (DRs) and uses simulated annealing to build a locally 'chain compatible' DR model inside a sphere of diameter D_{\max} . The *ab initio* approach allowing one to build protein models using X-ray SAXS data up to 0.5 nm resolution. The search model is an assembly of DRs centred at the $C\alpha$ positions. The number of DRs is usually known from the DNA or protein sequence, whereas their coordinates are initially randomly distributed inside a sphere of diameter D_{\max} . During simulated annealing, a randomly chosen DR is moved to a point 0.38 nm (typical distance between adjacent residues) away from another randomly selected DR. The final model is constrained to be locally 'chain compatible' (in particular, each DR should have two neighbours at a distance of 0.38 nm). The efficiency of the method is illustrated by the reconstruction of several proteins, with known and unknown crystal structure, from experimental scattering data. The method substantially improves the resolution and reliability of models compared to *ab initio* shape determination.

Adding missing loops or domains - Inherent flexibility and conformational heterogeneity in proteins often result in the absence of loops and even entire domains in crystallographic or NMR models. Such missing fragments still contribute to the SAXS intensity and their probable configurations can be found by fixing the known part of the structure and adding the missing parts to fit the SAXS pattern from the entire particle.

Rigid-body modelling - Solution scattering patterns from multidomain proteins and macromolecular complexes can also be fitted using models built from high-resolution structures of individual domains or subunits, assuming that their tertiary structure is preserved. The 'automated constrained fit' procedure generates thousands of possible bead models in an exhaustive search for the best fit.

Conclusions - Many successful applications of new data analysis methods during recent years have further illustrated how much the popular view that solution scattering yields only the molecular mass and radius of gyration of a particle is a misconception."

SUMMARY

Through SAXS, as described in detailed in the next sections, it was possible to obtain, for the first time, an insight into the structural arrangement of rm-proNGF in solution. SAXS measurements revealed that rm-proNGF is dimeric in solution and appears to be very anisometric if compared to the highly compact structure of the NGF dimer. Two structural models, i.e. globular "crab-like" and elongated "rod-like" shape, yielded equally good fits to the scattering data; these models help interpreting the bioassays on TrkA binding and activation, and are also in agreement with the reported interaction between NGF and the p75^{NTR} receptor, as observed both in the crystal structure and in the SAXS studies of the NGF-p75^{NTR} complex. The two derived models may represent two extremes of a range of conformations characterizing an intrinsic disorder of the pro-peptide region. Accordingly, proNGF may be considered as a moonlighting protein that exposes different interacting/binding regions to its partners, depending on the physiological cellular conditions.

5.1 Structural arrangement of rm-proNGF in solution using SAXS

In order to assess the conformation of the N-terminal part of rm-proNGF in solution, SAXS experiments were performed on the full-length short rm-proNGF construct. SAXS is well known to be suited to study flexible macromolecules in solution (Svergun and Koch, Rep. Progr. Phys. 2003); it could then be of particular

help in the structural investigation of the N-terminal part of rm-proNGF even if the latter would predominantly take up an unfolded conformation.

The experimental SAXS curve from the full-length rm-proNGF is displayed in Figure 5.1.1.

The SAXS data were recorded also for the mutant P5A (see section 1 – p.96), to check if there was an influence of the mutation in the overall spatial arrangement of the two proteins in solution. From the experimental data, however, the SAXS pattern of the mutant resulted to be completely overlapping with the one of the wild-type protein. It can be therefore concluded that, at least at the resolution typical of SAXS experiments, there is no significant difference in the structural arrangement of the mutant P5A rm-proNGF in respect to the normal protein.

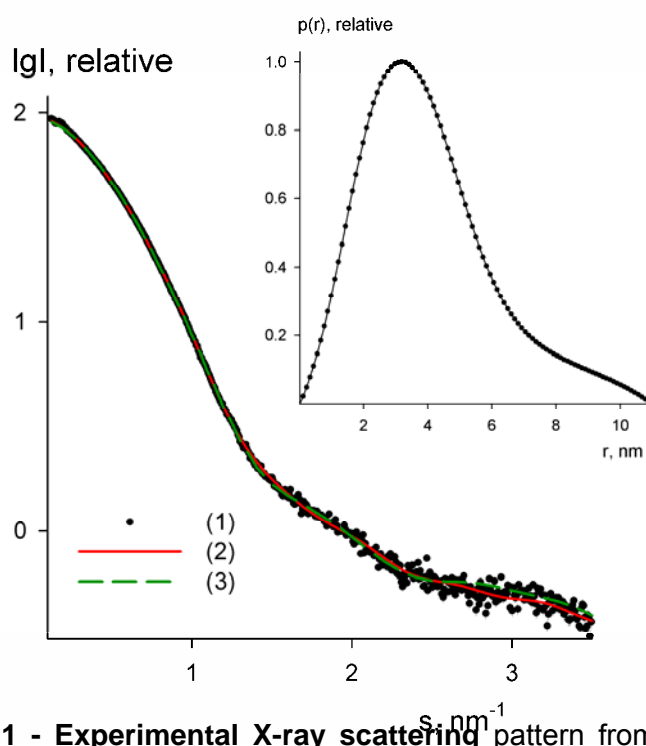


Figure 5.1.1 - Experimental X-ray scattering pattern from rm-proNGF (dots with error bars, blue), scattering from typical *ab initio* model computed by DAMMIN (Svergun, D. I. Biophys J, 1999) (full line, red) and from the crystallographic model with added C-terminal loop obtained by BUNCH (Petoukhov, M. V. & Svergun, D. I., Biophys J 2005) (discontinuous line, green). The models were restored using P2 symmetry. The plot displays the logarithm of the scattering intensity as a function of momentum transfer $s = 4\pi \sin(\theta)/\lambda$ where 2θ is the scattering angle and $\lambda = 0.15$ nm is the X-ray wavelength.

The distance distribution function is displayed in the inner window on top right.

The MM of the solute (45 ± 5 kDa), estimated from the relative forward scattering intensity ($s=0$), suggests that the protein is dimeric in solution, as expected (Rattenholl *et al.*, Eur.J.Biochem., 2001). This finding is further corroborated by the excluded (Porod) volume of the particle in solution of $(98\pm10) \times 10^3 \text{ \AA}^3$. This is in agreement with the empirical finding that for globular proteins the hydrated volume in \AA^3 should numerically be about twice the MM in Da. The experimental radius of gyration R_g and maximum size D_{max} ($31.5\pm0.5 \text{ \AA}$ and $110\pm10 \text{ \AA}$, respectively) point to an extended particle structure. The low resolution shape of rm-proNGF was reconstructed *ab initio* using the simulated annealing bead modeling program DAMMIN (Svergun, Biophys. J., 1999). Several reconstructions performed without symmetry restrictions yielded anisometric elongated structures, and a typical model presented in Figure 5.1.2 (silver model), neatly fits the experimental data with discrepancy $\chi=0.98$. Using the P2 symmetry constrains, two types of models can be obtained, a “crab-like” shape with the two-fold axis perpendicular to the longer particle axis (crab model, blue - Fig. 5.1.2 – panel A), and an elongated model with the two-fold axis parallel to the long axis (extended model, blue - Fig.5.1.2 – panel B). The two P2 models and the P1 all nicely fit the experimental data and show a similar overall shape (see overlap of P1 model with both P2 models in Figure 5.1.2).

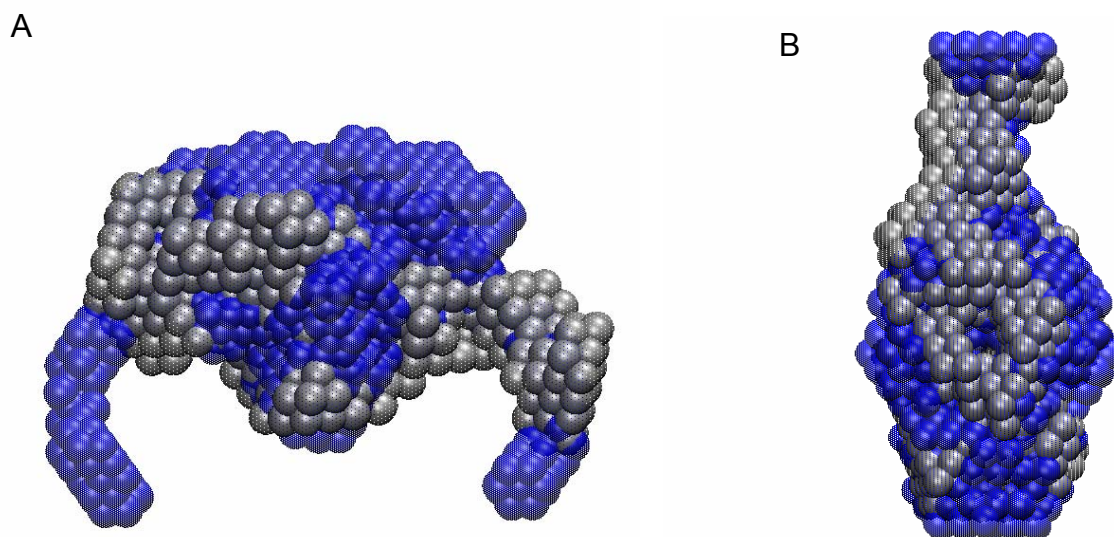


Figure 5.1.2 - *Ab initio* models for the shape determination of rm-proNGF. Panel A: DAMMIN model P1 (silver) overlapped with the DAMMIN P2 model for model 1 (blue). Panel B: DAMMIN model P1 (silver) overlapped with the DAMMIN P2 model for model 2 (blue). In the overlap of P1 and P2 models of model 1, the P1 model is rotated by 90° in

comparison to the model 2. The figures were generated using the program VMD (Humphrey et al., J.Mol Graph., 1996)

To obtain further information about the structure of the full-length rm-proNGF, the N-terminal portion, not present in the crystallographic model of mature NGF (PDB: 1bet), was built using the program BUNCH (Petoukhov and Svergun, Biophys. J., 2005). The two missing N-terminal regions were added to the known structure of dimeric NGF to fit the observed scattering from the full-length protein, yielding two types of solutions, both fitting the scattering data with discrepancy $\chi=1.5$. The first type (crab model - Fig.5.1.3 – panel A) depicts a structure where the C α chains of the two pro-peptides are oriented far away from the barrel scaffold of the NGF dimer. This model overlaps well with the symmetric “crab-like” *ab initio* shape (Fig. 5.1.2 – panel A). The other solution (extended model - Fig.5.1.3 – panel B), in which the two pro-peptides are protruding outwards on the opposite side of the N- and C-termini of NGF, can be well superimposed with the *ab initio* elongated model. Fig.7.1.3 displays the BUNCH-generated models using P2 symmetry, overlapped with the corresponding DAMMIN-generated models.

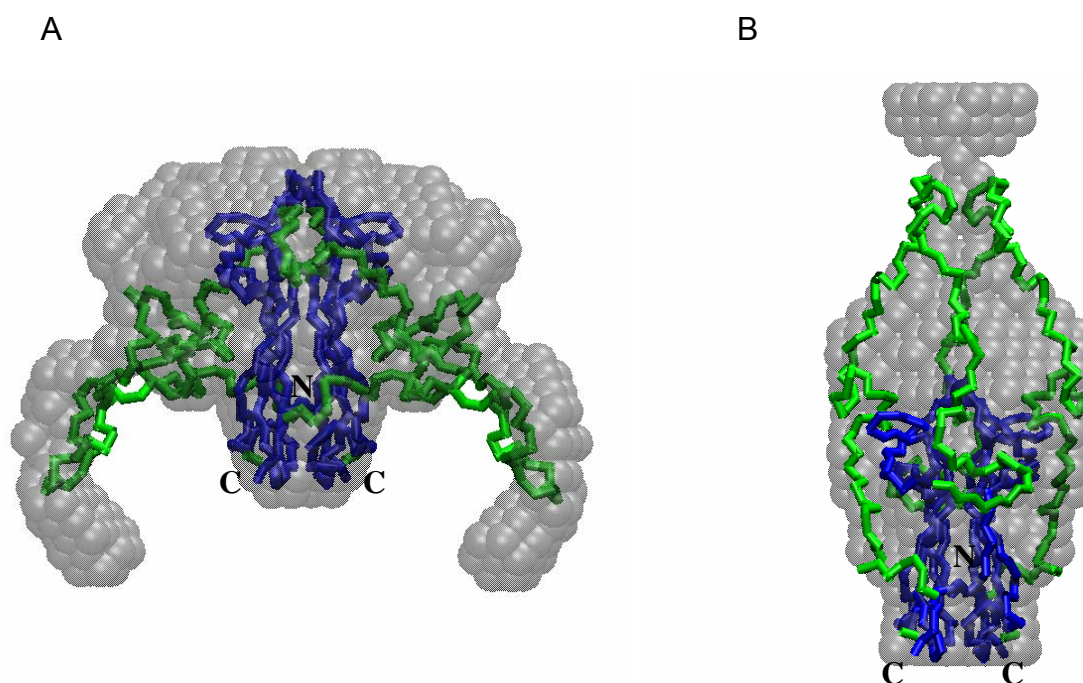


Figure 5.1.3 - *Ab initio* models for the shape determination of rm-proNGF superimposed to the simulated annealing models for addition of missing chains. Panel A: C α

traces obtained with BUNCH (NGF in blue; pro-regions in green) superimposed to the model obtained by DAMMIN (silver dots) for model 1. Panel B: C α traces obtained with BUNCH superimposed to the model obtained by DAMMIN for model 2;. The N- and C-termini of mature NGF are indicated. The figures were generated using the program VMD

Building of the N-terminus pro-region without imposing symmetry restrictions yielded models close to either of the two types (“crab” or elongated, see fig.5.1.4 – panel A for the “crab” and panel B for the elongated).

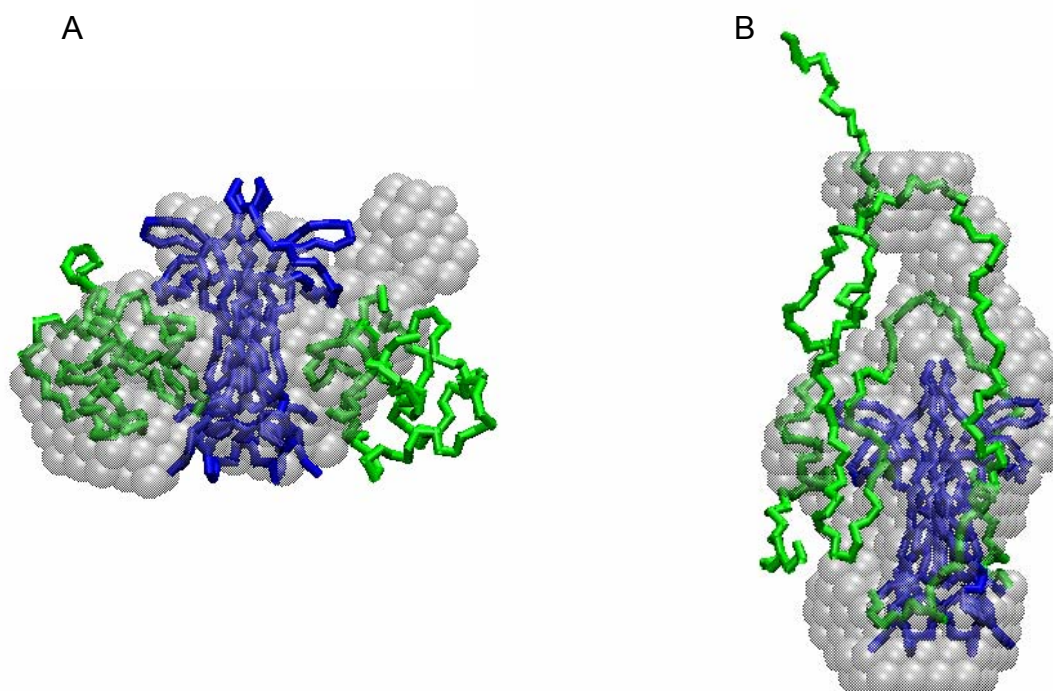


Figure 5.1.4 - Simulated annealing models for addition of missing chains – models without P2 symmetry. Panel A: C α traces obtained with BUNCH (NGF in blue; pro-regions in green) superimposed to the model obtained by DAMMIN (silver dots) for model 1. Panel B: C α traces obtained with BUNCH superimposed to the model obtained by DAMMIN for model 2;. The N- and C-termini of mature NGF are indicated. The figures were generated using the program VMD

5.2 Solution scattering experiment on h-NGF

For a validation of the results obtained by SAXS for rm-proNGF, the same kind of experiment was performed on NGF, which 3D crystal structure is known.

Due to the availability of the protein, the human NGF instead of the mouse form was used.

The solution scattering on h-NGF was performed, according to the procedure already described in the previous chapter for rm-proNGF.

The most striking result obtained from the SAXS measurements, was that the estimated molecular weight of the h-NGF solute (54 ± 5 kDa) suggested that the protein was tetrameric in solution and not dimeric as expected. This finding was further corroborated by the excluded (Porod) volume of the particle in solution ($(70 \pm 10) \text{ nm}^3$) noting that for globular proteins the hydrated volume in \AA^3 should numerically be about twice the molecular mass in Da, but for hollow particles it can be corrected to the lower values. The experimental radius of gyration R_g and maximum size D_{max} (3.10 ± 0.05 nm and 12.0 ± 1.0 nm, respectively) pointed to an extended particle structure.

In light of these results, therefore, it was not possible to reconstruct a model for NGF that could be used for a direct comparison with the ones obtained for rm-proNGF.

5.3 Structural insights into the complex rm-proNGF/Fab α D11

Once a low resolution structural model for rm-proNGF was obtained, it was decided to go further in the structural characterization, and the structural arrangement of the complex between rm-proNGF and the Fab fragment of the monoclonal anti-NGF antibody α D11 was investigated using SAXS.

To investigate the stable complex formation in solution and to determine its stoichiometry, a preliminary experiment was conducted using size exclusion chromatography.

Unfortunately, rm-proNGF does sticks aspecifically to the resin of the Superdex 75 column used for gel-filtration chromatography, rendering therefore very difficult to conduct a quantitative analysis. It was possible, however, to get an indirect indication on the stable complex formation by running on the column a known amount of Fab and subsequently the same amount of Fab previously incubated with a known amount of rm-proNGF. In particular, assuming a stoichiometry of 1:1 (one

Fab fragment bound to each rm-proNGF monomer), a mixture was prepared, containing a 2:1 composition, with an excess of Fab.

The samples were subsequently run on a Superdex 75 column for gel filtration and the result is shown in fig.7.3.1: in the sample with the mixture, the intensity of the peak corresponding to the Fab resulted to be decreased of almost 30% when compared to the equal injection of Fab alone (red peak in comparison to blue peak), suggesting that the rest of the protein is forming a complex with the rm-proNGF, that is not eluting from the column due to the stickiness of the rm-proNGF. It was not possible, however, to estimate the stoichiometry of the complex.

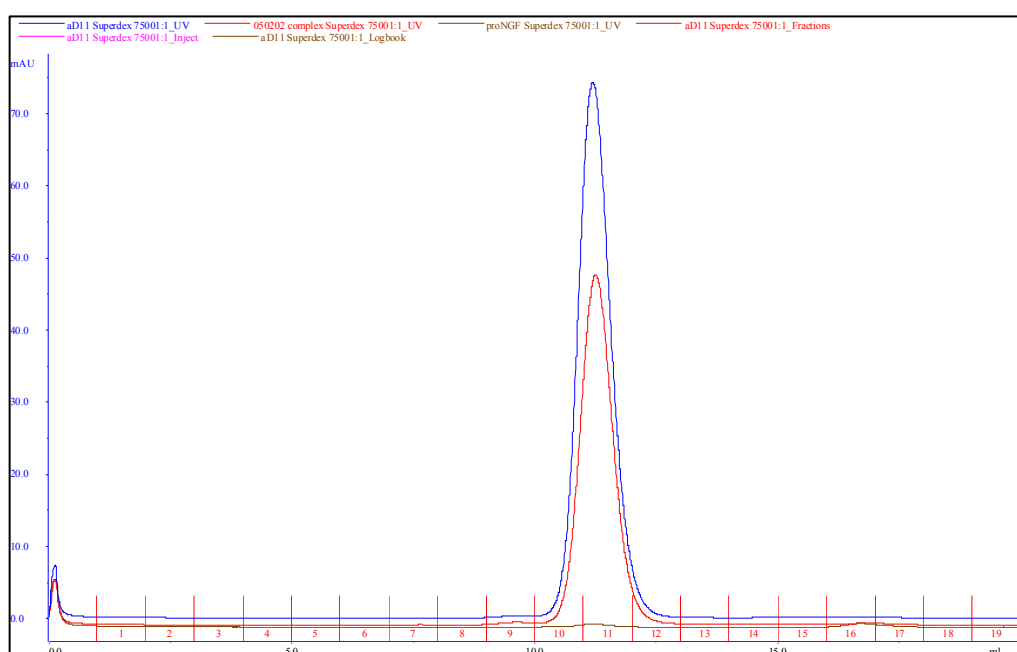


Figure 5.3.1 – Gel filtration of the complex α D11/proNGF. The blue peak represents the Fab fragment alone; the red peak represents the complex; the brown trace represents the proNGF injection. For this experiment, 120 μ g of purified Fab α D11 were used, and 60 μ g of rh-proNGF.

A second method was used to confirm the presence of the complex in solution: a native SDS-PAGE was carried out.

The highly basic properties of rm-proNGF, however, render it difficult to achieve a nice separation of the protein on this kind of gels: as it appears from the picture in fig.5.3.2, in lane 1, where the rm-proNGF was loaded, no band can be detected.

However, by comparison of all the samples loaded on the gel, it was possible to detect the appearance of a band of different properties than the Fab and the m-proNGF alone (see black arrow), and this fact allowed to confirm the presence of a complex in solution, although it was not possible to establish the correct stoichiometry of the complex (see fig.5.3.2). It should be noted, however, that the sample was heterogeneous, and more than one band could be detected, suggesting probably the formation of more than one complex specie in solution.

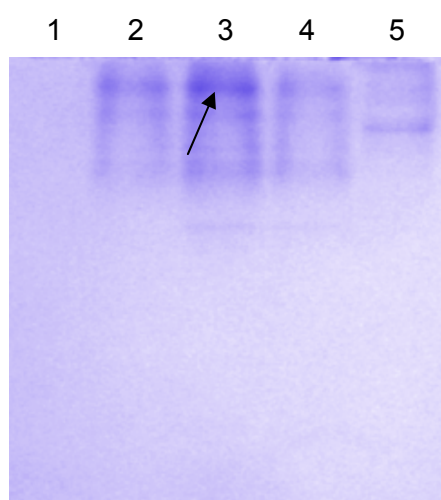


Figure 5.3.2 – Native gel of the complex α D11/proNGF at different stoichiometric ratios. Lane 1: m-proNGF; lane 2: stoichiometry 1:1 Fab:proNGF; lane 3: stoichiometry 2:1 Fab:proNGF; lane 4: stoichiometry 1:2 Fab:proNGF; lane 5: Fab α D11. The red arrow indicates the band corresponding to the Fab; the black arrow marks the position of the putative band corresponding to the complex.

It was finally possible to perform SAXS measurement on the complex m-proNGF/Fab α D11 in solution.

The SAXS measurement on the Fab fragment alone was also carried out, and the outcoming results were in nice agreement with the crystallographic parameters available for the α D11 Fab (PDB: code 1ZAN - Covaceuszach *et al.*, Acta D, 2001).

From the SAXS data, the estimated MM of the α D11 Fab fragment sample (50 ± 5 kDa) coincides with the theoretical value of homodimer 50 kDa, and the experimental scattering pattern calculated from the crystallographic model gives a good fit to the experimental data with $\chi=1.46$ (Figure 5.3.3).

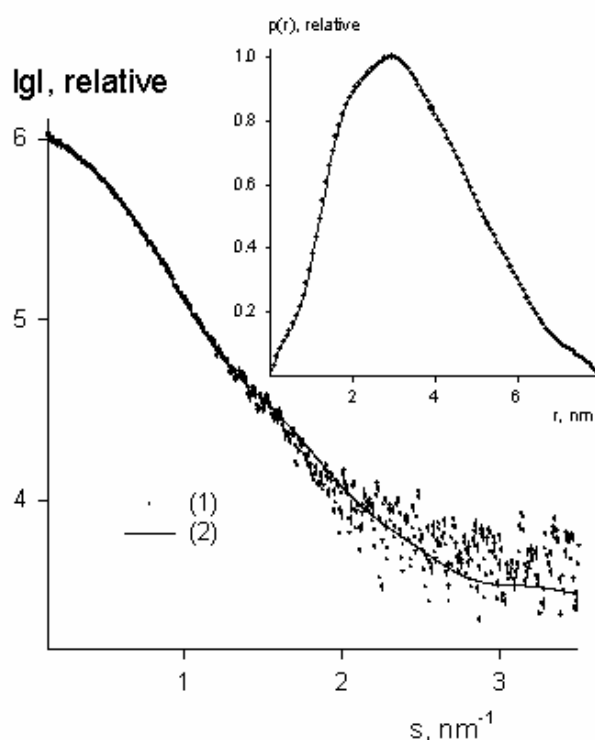


Figure 5.3.3 - Experimental X-ray scattering pattern from α D11 Fab fragment (dots with error bars), scattering from crystallographic dimeric model (PDB code 1ZAN) computed by CRY SOL (solid line). The plot displays the logarithm of the scattering intensity as a function of momentum transfer $s = 4\pi \sin(\theta)/\lambda$ where 2θ is the scattering angle and $\lambda = 0.15$ nm is the X-ray wavelength. The distance distribution function is displayed on top right.

It was then possible to proceed to the SAXS measurements for the complex between α D11 Fab and rm-proNGF. Due to the lack of information on the precise stoichiometry of the complex, different ratios of the components were tested, and indeed, in the case of a 1:1 ratio it was possible to obtain a good scattering curve, corresponding to a protein of molecular mass in solution of the same value of the expected 1:1 complex (see fig.5.3.4).

The experimental SAXS curve from the complex of rm-proNGF with α D11 Fab fragment prepared with stoichiometry of 1:1 is displayed in Figure 5.3.4. The estimated molecular weight of the solute (125 kDa) suggests that the complex has the stoichiometry of 1:1 and contains two α D11 dimeric Fab fragments bound to one rm-proNGF dimer. The excluded (Porod) volume of the particle in solution is equal to 155 nm^3 ; for globular proteins this value should be numerically almost twice the molecular mass in Daltons, but the presence of a hollow structure (the Fab fragment), the value becomes smaller. The experimental radius of gyration R_g and maximum size D_{max} (4.9 nm and 18.0 nm, respectively) point to an extended particle structure.

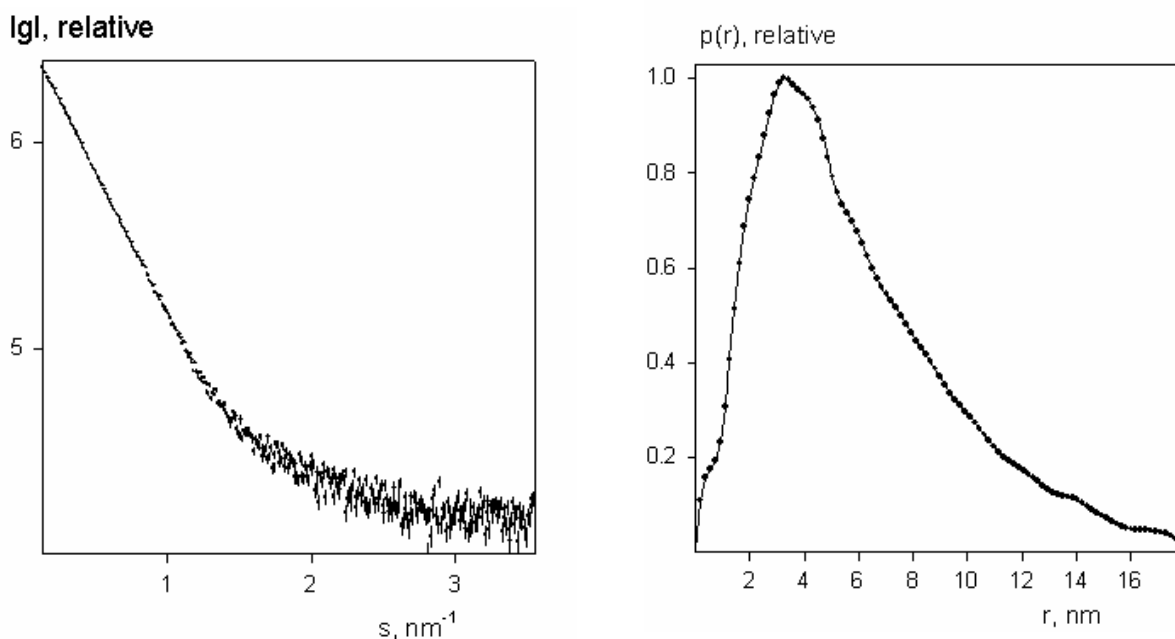


Figure 5.3.4 - Experimental X-ray scattering pattern from the complex rm-proNGF and α D11 Fab fragment with stoichiometry 1:1 (dots with error bars). The plot displays the logarithm of the scattering intensity as a function of momentum transfer $s = 4\pi \sin(\theta)/\lambda$ where 2θ is the scattering angle and $\lambda = 0.15$ nm is the X-ray wavelength. The distance distribution function is displayed on the right.

A complete analysis of the data is still ongoing, since the modelling of the complex Fab α D11/rm-proNGF is not an easy task, due to the lack of high resolution information on the rm-proNGF.

However, due to the fact that the SAXS measurements were conducted also on the complex Fab α D11/m-NGF and that it was possible to reconstruct the overall structural arrangement of this complex (Covaceuszach *et al.*, manuscript in preparation), it would be possible to reconstruct the structural arrangement also for the rm-proNGF complex. In this last case, moreover, a further level of complexity is given by the fact that the rm-proNGF was shown to exist in a flexible conformation in solution.

CONCLUDING REMARKS

Overall, the data presented in this chapter, aimed to a structural characterization of rm-proNGF and of its complex with the Fab fragment of the α D11 anti-NGF antibody.

The intrinsic flexibility of the pro-peptide region in the rm-proNGF made it difficult to achieve positive results for the crystallization of the protein, in the attempts made so far. Therefore, SAXS was chosen as the best technique to get insights into the structure and dynamics of the protein in solution.

Indeed, it was possible to reconstruct the possible model for the protein. Due to the flexibility of the protein, two models for its structural arrangement in solution were reconstructed, equally nicely fitting to the experimental data, *i.e.* a “crab-like” and an “elongated” models: they might represents the two extremes of a range of possible conformations in solution.

The outcome of the SAXS investigation are interesting, not only because it is the first time, as far as we know, that it was possible to get a structural information on proNGF, but also because the reconstructed models allow the interpretation of the available biological data for proNGF, as it will be discussed more deeply in the Discussion part.

RESULTS
PART 2:
SELECTION,
BIOCHEMICAL CHARACTERIZATION
AND
STRUCTURAL INSIGHTS
INTO A NOVEL
ANTI-PRONGF SCFV ANTIBODY

INTRODUCTION

Antibodies as molecular tools for protein-protein interactions studies

In the realm of molecular investigations on the functional role of a protein, in my case m-proNGF, one important tool is represented by the use of antibodies, in various formats, that allow a detailed analysis of the protein-protein interactions of the partners involved in a given pathway, both in normal and pathological state. Moreover, the interest in the use of antibodies was further enriched by the range of possible applications, also as therapeutic agents (reviewed in Holliger and Hudson, Nat. Biotech., 2005; Miller and Messer, Molecular Therapy, 2005).

1. Natural and synthetic antibodies

Intact antibodies of the various classes (IgG, IgM, IgA, IgE) are highly specific targeting reagents and provide us with the defence against pathogens and toxins. IgG class represent the main serum antibodies and the most widely used type of therapeutic antibodies. It is formed by an Y-shaped multidomain protein, with the antigen-specific binding sites located at the two Fab tips; the recruitment of effector functions is mediated by the stem Fc domain (see fig. 1.1) (reviewed in Holliger and Hudson, Nat. Biotech., 2005).

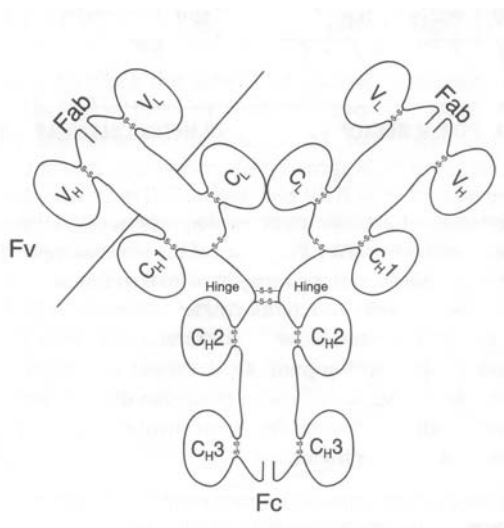


Figure 1.1 – Schematic representation of a whole antibody molecule. Figure from Biocca and Cattaneo, TiCB, 1995.

IgG antibodies are bivalent and this ability to bind two antigens greatly increases their functional affinity and confers high retention times (a property called avidity). The Fc domain provides long serum half-lives. However, this property is sometimes undesirable, and for this reason, IgG have been dissected into constituent domains, initially through proteolysis (with such enzymes as papain or pepsin) and later

genetically engineered into either monovalent (Fab, scFv, single variable VH and VL domains) or bivalent fragments (diabodies, minibodies, ecc.). For a schematic representation of some of these forms, see fig. 1.2. Single chain Fvs (scFv) are a format in which the VH and VL domains are joined with a flexible polypeptide linker preventing dissociation. Antibody Fab and scFv fragments usually retain the specific, monovalent, antigen-binding affinity of the parent IgG, while showing improved pharmacokinetics for tissue penetration (reviewed in Holliger and Hudson, Nat. Biotech., 2005).

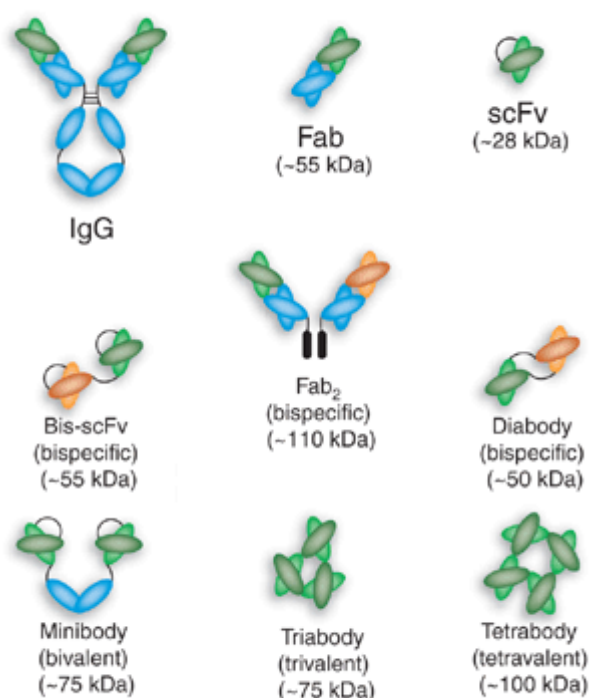


Figure 1.2 – Schematic representation of different antibodies formats. The usual intact IgG molecule is shown, together with a variety antibody fragments, including Fab, scFv and multimeric formats like minibodies and diabodies. (reviewed in Holliger and Hudson, Nature Biotech, 2005).

Due to their properties, antibodies in various formats have been exploited for a wide range of applications, both *in vivo* and *in vitro*. One of the possible applications *in vitro* is the use of antibodies to study protein-protein interactions, and this property has been exploited in this Thesis.

2. Intracellular antibodies, their selection and applications

For a widening of the use of antibodies, one approach has been to engineer immunoglobulin genes to express the antibodies in non-lymphoid cells, and to target them to the cytosol or to other intracellular compartments of mammalian cells, as well as of yeast cells, to block biological functions or confer new phenotypic traits. This procedure has been described as “intracellular immunization” (Biocca and Cattaneo,

TiCB, 1995). Both whole antibodies, as well as scFvs have been chosen for intracellular targeting. Antibodies are secreted proteins that enter the exocytic pathway by virtue of their N-terminal hydrophobic leader sequences that are cleaved after translocation across the endoplasmic reticulum (ER) membrane. Removal of this sequence or its substitution with a hydrophilic sequence prevents translocation of the antibodies in the ER and restrict it to the cytosol. If a nuclear localization signal or mitochondrial targeting signal is incorporated, these antibodies can also be localized to the nucleus or to the mitochondria. Therefore, antibody chains can be targeted to a wide spectrum of intracellular compartments.

Indeed, it was demonstrated that by using the intracellular antibody technology, the function of many intracellular antigens has been successfully inhibited (reviewed in Cattaneo and Biocca, TIBTECH, 1999). The intracellular antibody technology can be effectively used to interfere with the function of a protein *in vivo* and eventually to inhibit its functionality, giving rise to a protein knock-out. However, notwithstanding the success, some problems persist in relation to the folding stability, cellular half life, stability in the absence of disulfide-bond, affinity and introduction of effector functions.

Among the strategies used to optimize the selection of antibodies stable and soluble under conditions of intracellular expression, one should mention the use of the yeast two-hybrid system. The developed technology has been named IACT (Intracellular Antibodies Capture Technology) (Visintin *et al.*, PNAS, 1999; Visintin *et al.*, JMB, 2002; Visintin *et al.*, Methods, 2004). With this technology it is possible to effectively select, within the panel of all the possible antibodies against a certain target, those that are active *in vivo* in the intracellular environment. In this context, an antibody library has been created, to express antibodies directly in the two-hybrid format. Accordingly, the procedure to obtain intracellular antibodies starting from genes is greatly simplified and accelerated, since the genes of interest are directly inserted into the vector for the IACT selection, avoiding the need to express and purify the corresponding proteins for the selection. This technology was called SPLINT (Visintin *et al.*, JIM, 2004).

The possible applications of the intracellular antibodies spans from the *in vitro* investigations of the protein-protein interactions to the protein knock-out, to applications in the neurological and other disorders, as also recently reviewed by Miller and Messer (Mol Therapy, 2005).

SUMMARY

In this part of the Thesis the results obtained in the selection and characterization of a specific anti-NGF antibody in the form a scFv will be presented.

Antibodies are an important tool for the study of the interaction between proteins *in vitro*. In the case of m-proNGF, however, no antibody was commercially available until recently, and even at present, the only antibodies against proNGF that can be purchased, are uniquely polyclonal ones. Moreover, as it was demonstrated in the previous part, these polyclonal antibodies are not reaching the required sensitivity for certain experiments, like ELISA assay.

For this reason, in the frame of the research on proNGF described in this thesis work, it was decided to work on the selection of a specific monoclonal antibody against m-proNGF, that would allow the availability of an important tool both as structural probe for m-proNGF protein-protein interactions, and for structural studies.

This antibody was selected in the scFv format exploiting the IACT and SPLINT technologies (Visintin et al, PNAS 1999) and its binding properties were first tested upon expression in the periplasm of *E.coli*.

Once the antibody was proven to be valid, a new approach was established for a scaling up in its expression. In particular, the scFv was expressed in the cytoplasm of *E.coli* and the optimization of the *in vitro* refolding of the protein from inclusion bodies was possible, and the protein could be refolded with satisfactory yields from *E.coli*.

A complete analysis of the protein was carried out, both from the biochemical and from the binding properties point of view.

The scFv was therefore proven to be a very important tool in the further analysis of the proNGF biological function: the antibody is very stable and can be purified in the monomeric form; moreover, it is characterized by a very good affinity and selectivity for its antigen.

Finally, a structural characterization of the scFv by means of SAXS was carried out.

1. Selection and characterization of a novel anti-proNGF antibody in the scFv format

Given the available techniques in the working group, it was decided to look for a specific anti-proNGF antibody in the format of a single chain Fab fragment (scFv), exploiting the yeast-two hybrid as a technique for the selection.

In particular, the IACT technology (Intracellular Antibody Capture Technology) (Visintin, M. *et al.*, 2002) was employed, that was developed in the group of prof. Cattaneo. The selection of the scFv anti-proNGF antibody was performed in collaboration with the working group of Lay Line Genomics in Trieste.

The IACT, described in the introduction allows the selection of the antibodies that are able to function in the intracellular environment of the cell. This technology has been further ameliorated by the SPLINT technology (Visintin, M. *et al.*, JIM, 2004), that allows the selection of the antibodies directly from the genes. In this way the selection of the antibodies becomes much faster, since there's no requirement any more to purify the target proteins for the selection.

This technology has been employed in this PhD thesis work to select a valid antibody, in the scFv format, against the pro-peptide of m-proNGF.

1.1 Cloning of the constructs for the SPLINT selection

The SPLINT library used for this selection is a naïve library of scFv fragments expressed directly in the yeast cytoplasm in a format such that antigen-specific intrabodies can be isolated directly from gene sequences, with no manipulation of the corresponding proteins (Visintin *et al.*, JIM, 2004). The library was constructed from the natural V regions cloned from total RNA extracted from lymphocytes pooled from three mouse spleens (Visintin *et al.*, JIM, 2004).

To select the best domain in the m-proNGF protein that could be used for the selection in vivo from the SPLINT library, a set of deletion mutants of the m-proNGF were cloned. The sequences and the complete features of the clones are fully described in the Experimental Section. Briefly, the baits used for the SPLINT selection were:

- the entire pro-peptide of m-proNGF with the first 14 amino acids of mature NGF (*proNGF*);
- the entire pro-peptide of m-proNGF with the first 14 amino acids of mature NGF, with a mutation in the cleavage site for furin (*proNGFmut*);
- the entire pro-peptide of m-proNGF with furin mutation, without mature NGF amino acids (*pro*);
- the entire pro-peptide of m-proNGF with furin mutation, with a deletion of 10 amino acids at the C-terminus (*pro-10*);
- the entire pro-peptide of m-proNGF with furin mutation, with a deletion of 20 amino acids at the C-terminus (*pro-20*);
- the entire pro-peptide of m-proNGF with furin mutation, with a deletion of 30 amino acids at the C-terminus (*pro-30*);
- the entire pro-peptide of m-proNGF with furin mutation, with a deletion of 41 amino acids at the C-terminus (*pro-41*);
- the entire pro-peptide of m-proNGF with furin mutation, with a deletion of 10 amino acids at the N-terminus (*pro-N-10*)

A schematic representation of the used baits is given in fig. 1.1.1.

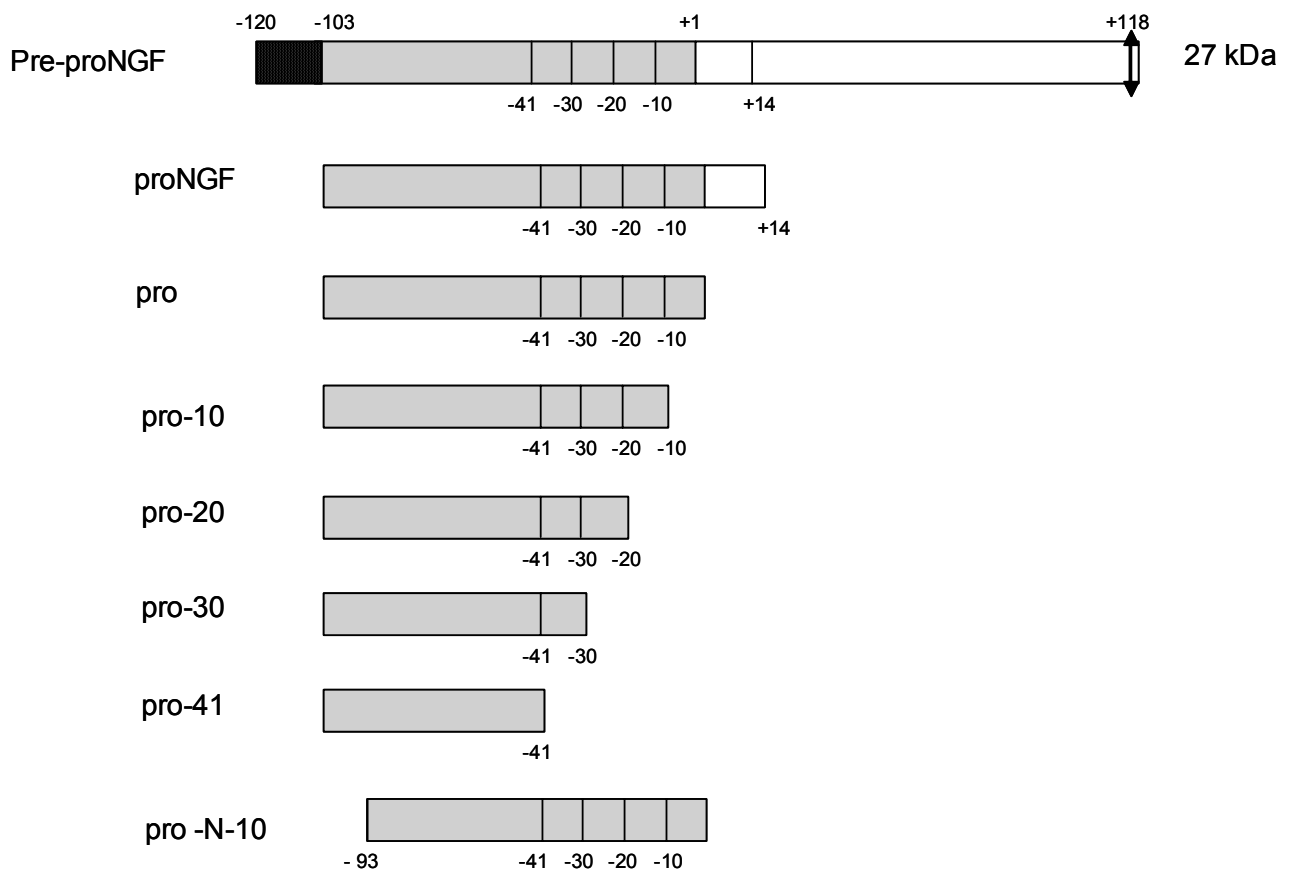


Figure 1.1.1 – Schematic representation of the baits used for the SPLINT selection. The signal peptide of pre-proNGF is black, the pro-peptide is grey and the mature NGF is white. The numbers represent the location of the deletions.

All the clones were expressed in yeast, where the preliminary tests for the expression levels of the proteins and the verifications of the lock of trans-activation properties of the baits were carried out.

The baits were proven to be expressed in high quantity in yeast, but the most part of them resulted to be highly transactivating for the reporter genes used in the selection technology, as it can be verified in Table 1.1.1 and 1.1.2 and in Fig.1.1.2, that depicts the result of the β -galactosidase test for the trans-activation.

bait	-UKW	-UKWH	X-gal
proNGF	+	+	+
proNGFmut	+	+	+
pro	+	+	+
Pro-10	+	+	+
Pro-20	+	+	+/-
Pro-30	+	+	-
Pro-41	+	+	+/-
proN-10	+	+	+

Table 1.1.1. m-proNGF and its deletion mutants have been expressed in the yeast strain L40 and the transactivation property of genes His and LacZ for every bait have been tested. As it can be observed, only bait pro-30 presents absence of transactivation of lacZ gene, however presenting transactivation for the histidine gene.

Bait + VP16	-UKWL	-WHULK	X-gal
ProNGF+ VP16	+	+	+
ProNGFmut + VP16	+	+	+
Pro + VP16	+	+	+
Pro-10 + VP16	+	+	+
Pro-20 + VP16	+	+	+/-
Pro-30 + VP16	+	+	-
Pro-41 + VP16	+	+	+
proN-10 + VP16	+	+	+

Table 1.1.2. m-proNGF and its deletion mutants have been expressed in the yeast strain L40 together with the transcription activation domain VP16 and the transactivation property of genes His and LacZ for every bait have been investigated. As it can be observed, only bait pro-30 presents absence of transactivation of lacZ gene, however presenting transactivation for the histidine gene.

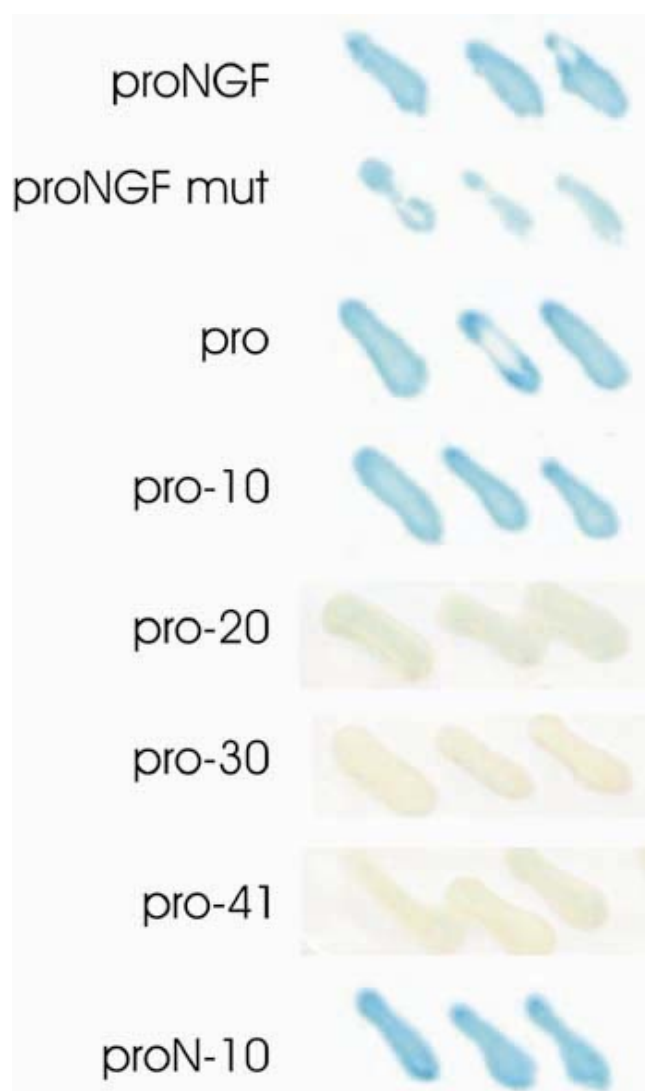


Figure 1.1.2. Xgal analysis for the verification of the transactivation property of the baits. The result clearly shows the auto-transactivation property of proNGF *in vivo*.

To decrease the transactivation property of the various prepared baits, some tests were conducted using various concentrations of Histidine Inhibitor 3AT. In Table 1.1.3 the obtained results are described.

bait	-UKWH +25mM 3AT	-UKWH +50mM 3AT	-UKWH +75mM 3AT	-UKWH +100mM 3AT	-UKWH +125mM 3AT	-UKWH +150mM 3AT
proNGF	-	-	-	-	-	-
proNGFmut	-	-	-	-	-	-
pro	+	+	+	+/-	-	-
Pro-10	+	+	-	-	-	-
Pro-20	+/-	-	-	-	-	-
Pro-30	-	-	-	-	-	-
Pro-41	-	-	-	-	-	-
proN-10	+/-	+/-	-	-	-	-

Table 1.1.3. Transactivation test of proNGF mutants in a growing medium containing the Histine inhibitor 3AT. As it can be observed, 3AT resulted to be quite an efficient method to abolish the transactivation in Histidine reporter gene.

In light of these results, the bait pro-10 has been chosen for the selection of the SPLINT library, using a growing medium enriched with 75 mM of 3AT.

1.2 Selection of scFvs via SPLINT using the pro-10 bait

The SPLINT library has been tested against the lexA-proNGF-10, as previously described (Visintin *et al.*, PNAS, 1999; Visintin *et al.*, JMB, 2002). Only 9 clones grow in a medium without Histidine plus 75mM 3AT and became blue after the β -gal assay. All nine clones have been isolated from yeast with the established method (Visintin and Cattaneo, 2001), the isolated DNA was analyzed by fingerprinting and sequenced. The single clones were subsequently tested, in a secondary screening, against pro-10 and an irrelevant antigen (lamin) using IACT. After these tests, only one clone resulted to be a true positive one.

1.3 In vivo epitope mapping of the selected scFv anti-proNGF

The deletion mutants of proNGF pro-10, pro-20, pro-30 and pro-41 were subsequently used for an *in vivo* epitope mapping (IVEM – Visintin *et al.*, JMB, 2002) of the selected anti-proNGF antibody.

The results of the experiment are summarized in table 1.3.1 and fig.1.3.1. In particular, through the IVEM it has been possible to identify the region responsible for the recognition between the scFv and proNGF: it is the stretch between aminoacids -20 and -30 in the pro-peptide of proNGF. In fact, the pro-30 bait was not recognized by the anti-proNGF as strong as the longer deletion mutants baits pro-10 and pro-20.

It is interesting to notice that this same aminoacid stretch on the m-proNGF was used for the selection of the commercially available polyclonal antibodies.

Baits + anti-proNGF-10	-UKWL + 40mM 3AT	-WHULK +40mM3AT	X-gal
Pro-10	+	++	+
Pro-20	+	+	+
Pro-30	+	+/-	+
Pro-41	+	+/-	+

Table 1.3.1: The obtained results demonstrate that IVEM allowed the identification of the epitope (L1-L106) on the m-proNGF protein, recognized by the antibody selected via IACT.

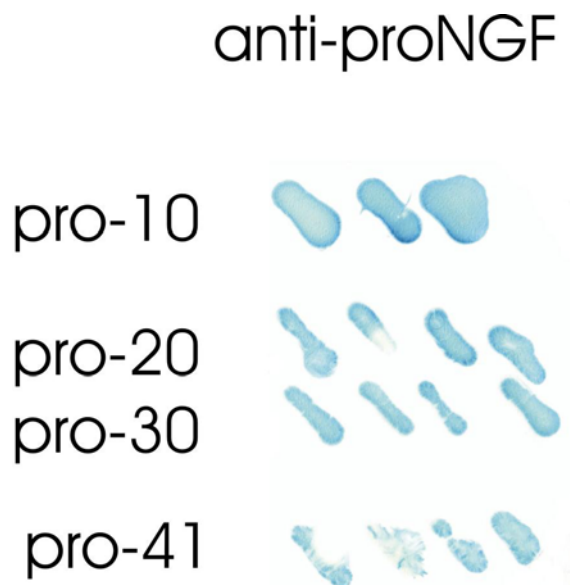


Fig.1.3.1 IVEM anti-proNGF: it illustrates the specificity of fragment scFv-anti-proNGF-10 when compared to the various deletion mutants *in vivo*. The binding epitope-scFv is highlighted through the IACT technology by measuring the transactivation of genes HIS3 and lacZ and the consequent capacity of the cells to grow on a medium without Histidine and to synthesize β -galactosidase.

1.4 Sequencing of the selected scFv

The DNA of the selected scFv anti-proNGF was sequenced, and the sequence is reported below. The sequences of the light chain (VL) and of the heavy chain (VH) domains are also highlighted, in yellow and green respectively; the linker is highlighted in cyan. The corresponding aminoacid sequence, obtained using the "Translate DNA-protein" tool on Expasy web server, is reported below the nucleotide sequence. From the primary sequence of the scFv it was also possible to identify the Complementary Determining Regions of the scFv, as shown below, using the Kabat numbering system for the antibodies (Kabat *et al.*, 1991); the CDRs are indicated on the protein sequence using the following color code: bold, black: CDR1; bold, red: CDR2; bold, blue: CDR3.

DNA: GCAAAAAAAAAAAAAAAAAAGTGGCCAAGCGGAGCGCGCATGCCGACATTGTTATGACCTGC
+1: A K K K K K V A K R S A H A D I V M T C

DNA: AGTGCCAGCTCAAGTGTAAGTTACATGCACTGGTACCAGCAGAAGTCAAGCACCTCCCC
+1: S A S S S V S Y M H W Y Q Q K S S T S P

DNA: AAACCTCTGGATTTATGACACATCCAAACTGGCTTCTGGAGTCCCAGGTCGCTTCAGTGGC
+1: K L W I Y D T S K L A S G V P G R F S G

DNA: AGTGGGTCTGGAAACTCTTACTCTCTCACGATCAGCAGCATGGAGGCTGAAGATGTTGCC
+1: S G S G N S Y S L T I S S M E A E D V A

DNA: ACTTATTACTGTTTTTCAGGGGAGTGGGTACCCGTACACGTTCCGAGGGGGGACAAAGTTG
+1: T Y Y C F Q G S G Y P Y T F G G G T K L

DNA: GAAATAAAACGTTCCGGAGGGTCGACCAGCGGTTCTGGGAAACCAGGTTCCGGTGAAGGC
+1: E I K R S G G S T S G S G K P G S G E G

DNA: TCGAGCGGTACCGAAGTGATGCTGGTGGAGTCTGGGGGAGGCTTAGTGAAGCCTGGAGGG
+1: S S G T E V M L V E S G G G L V K P G G

DNA: TCCCTGAAACTCTCCTGTACAGCCTCTGGATTCACTTTCAGCAACTATGCCATGTCTTGG
+1: S L K L S C T A S G F T F S N Y A M S W

DNA: ATTCGCCAGTCTCCAGAGAAGAGGCTGGAGTGGGTCGGAGAAATTAGTAACGGCGGTAGT
+1: I R Q S P E K R L E W V G E I S N G G S

DNA: AACACCTACTATCCAGGCAGTGTGACGGGCCGATTCACCATCTCCAGAGACAATGCCGAA
+1: N T Y Y P G S V T G R F T I S R D N A E

DNA: GACACCCTGTACCTGGAATGAGCAGGCTGAGGTCAGAGGACACGGCCATATATTACTGT
+1: D T L Y L E M S R L R S E D T A I Y Y C

DNA: GTAAGGGACGGTTTCTATGCTATGGACTACTGGAGTCAAGGAACCTCAGTCACCGTCTCC
+1: V R D G F Y A M D Y W S Q G T S V T V S

DNA: TCAGCTAGCGTC
+1: S A S V

1.5 Expression and purification of the scFv anti-proNGF in the periplasm of *E.coli*

To characterize the isolated scFv from the biochemical point of view and evaluate its solubility, aggregation propensity and stability (Worn and Pluckthun, Biochem., 1999), the DNA of the antibody was subcloned into the vector pDAN3 for the expression in *E.coli* periplasm (Sblattero and Bradbury, Nat. Biotech., 2000), using the methodology described in the experimental section. The protein was

expressed in the *E.coli* strain HB2151 and purified from the periplasm as described in the experimental section.

The purification of the periplasmic preparation is conducted by two subsequent chromatographic steps: a first one consisting on an affinity chromatography using the His-tag at the C-terminus of the protein, and a second one consisting of a size exclusion chromatography, to isolate the monomeric fraction of the protein preparation.

The affinity chromatography was conducted on a manually packed column using the NiNTA resin purchased by QIAgen. The elution of the product was performed using imidazole and the selection of the best product-containing fractions was done by loading a sample of the fractions on an SDS-PAGE, stained with Coomassie Blue.

After the purification step, the protein resulted to be very clean, as demonstrated by the gel shown in fig.1.5.1, where two different preparations of scFv anti-proNGF were analyzed.

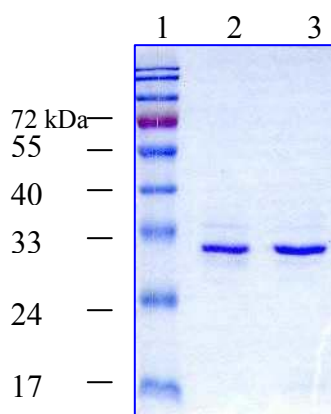


Figure 1.5.1 - SDS-PAGE stained with Coomassie blue with anti-proNGF samples. Lane 1: molecular weight marker; lane 2, 3: two preparations of purified anti-pro-10

To determine the aggregation state of the protein, the sample was loaded on a size exclusion chromatography column, namely a Superdex 75 (Amersham Pharmacia). As shown in fig.1.5.2, the protein resulted to mainly elute as a monomeric product of around 30 kDa, as it should be expected from the theoretically calculated molecular weight of 29 kDa. This is in agreement with the fact that the scFv selected from the SPLINT library with the IACT selection method have a lower tendency of aggregation than scFv selected with traditional techniques, that, on the contrary, form multimeric scFv complexes through intermolecular interactions (Visintin *et al.*, JIM, 2004).

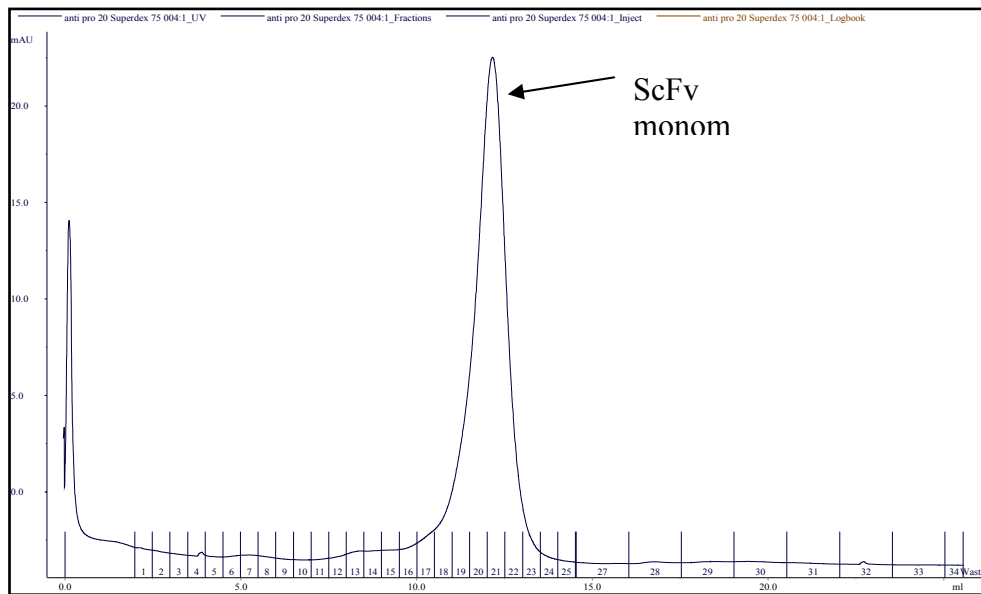


Figure 1.5.2. Purification of the scFv on a size exclusion chromatography column, Superdex 75 (Amersham).

1.6 Binding properties of the scFv – ELISA assay

A first analysis on the binding properties of the selected scFv antibody was performed by ELISA assay (Enzyme-Linked ImmunoSorbent Assay).

The test has been performed in two different formats, both with the antigen (rm-proNGF) coated on the plate and the scFv used as a primary antibody in solution (format 1), and in the reversed format, with the scFv coated on the plate and the antigen loaded in solution (format 2). A schematic representation of the formats is given in fig. 1.6.1.



Figure 1.6.1 – Schematic representation of the two formats used in the ELISA assay. Format 1 is depicted on the left; format 2 is depicted on the right.

All the proteins used in the experiments were produced in the laboratory, and the scheme of the experiments is described in the experimental section.

From both kind of ELISA experiments, it was possible to verify that the scFv has a good recognition capacity for the rm-proNGF, and is not able to detect neither m-NGF nor an unrelated protein like GST. The result is valid for both configurations of the experiment: with the antigen in coating and with the scFv in coating. As a control, an irrelevant scFv has been used, that was not giving any positive signal on any protein.

The results of the first ELISA assay (Format 1) are shown in fig.1.6.2, with two distinct representations of the same result. The experiment was done with two preparations of scFv, named *a* and *b*.

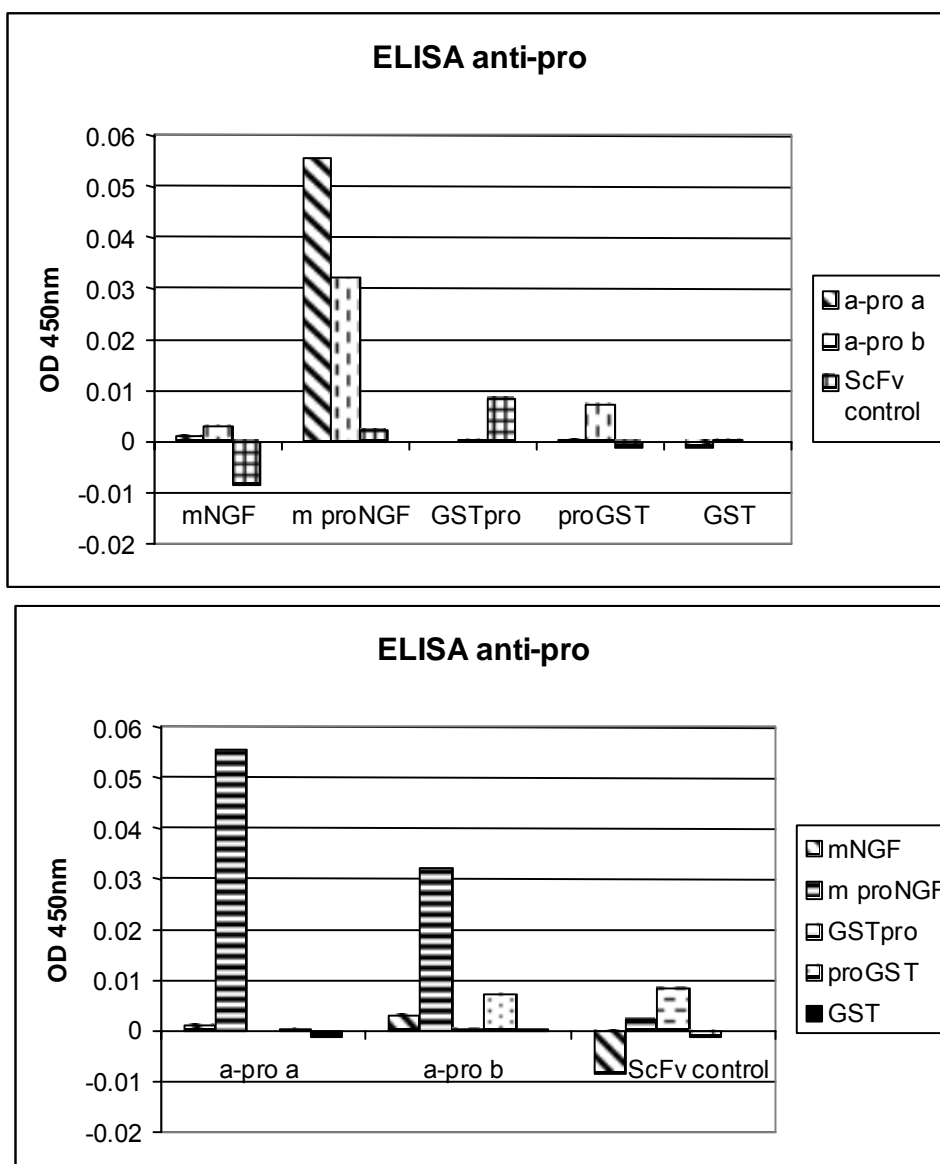


Figure 1.6.2 – ELISA assay for the binding properties of the scFv anti-proNGF.

Format 1 The coating with the various proteins indicated was performed at 5 µg/mL. The incubation of the scFv was performed at a concentration of 2 µg/mL, and the as primary antibodies, the surnatants anti-SV5 (for the scFv anti-proNGF) and 9E10 (for the control) scFv were used at a 1:10 dilution.

The second ELISA assay (Format 2) was also confirming the same results, as it's clear from the representation of the experimental data in fig.1.6.3. Also in the case where the scFv is bound on the plastic surface of the plate, it is able to specifically recognize its antigen rm-proNGF; it is interesting to see that this is true both for the mouse and the human species. It is also noteworthy that the relative intensity of the signal changes significantly from m- to h-proNGF when different primary antibodies anti-NGF are used (namely the polyclonal anti-NGF and the monoclonal αD11).

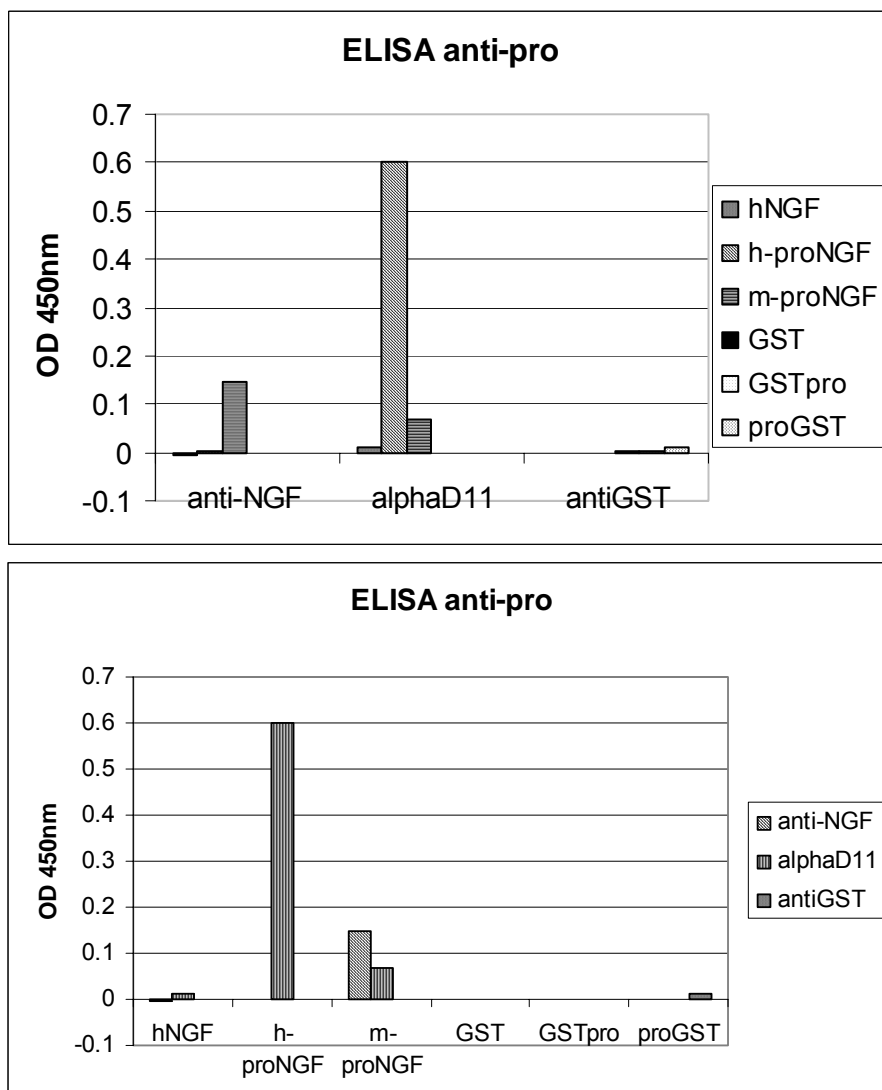


Figure 1.6.3 – ELISA assay for the binding properties of the scFv anti-proNGF.

Experiment 2 The coating with the scFv was performed at 5 µg/mL. The incubation with the various proteins indicated, was performed at a concentration of 10 µg/mL. The primary antibodies were: the supernatants α D11 (for NGF and proNGF) at a 1:2 dilution, the polyclonal anti-NGF antibody at a 1:8000 dilution, the anti-GST polyclonal antibody at a 1:8000 dilution.

1.7 Behaviour of the scFv anti-proNGF in vivo

The behaviour of the scFv anti-proNGF in living cells was tested. In particular, the cDNA of the scFv was cloned into a suitable vector for cells transfection, with the protein expressed as fusion construct with the GFP protein. The experiment was then performed on HEK293 cells.

A typical picture is displayed in fig. 1.7.1: it appears clearly that the scFv is quite soluble, lacking the presence of diffused aggregates.

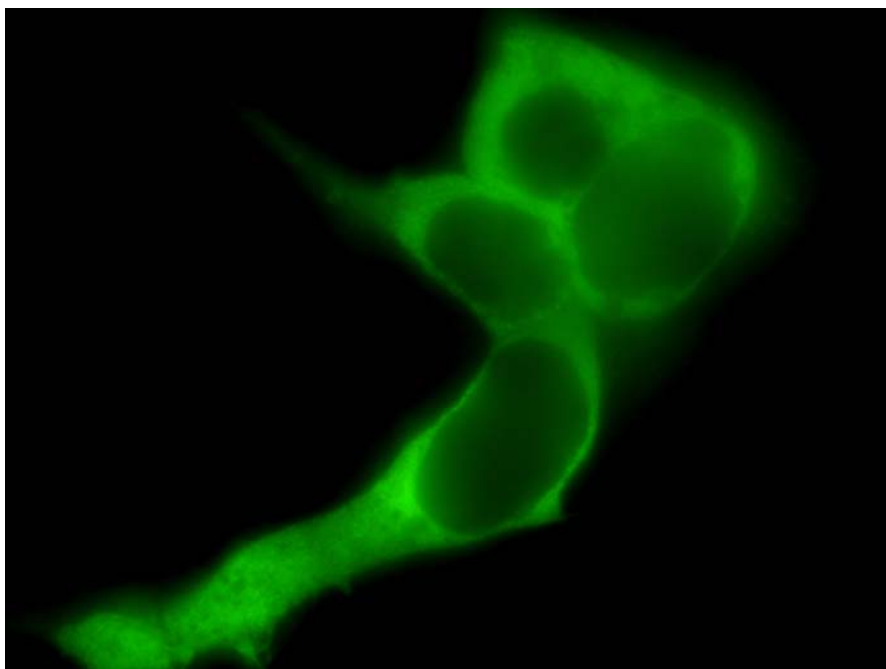


Figure 1.7.1 – Immunofluorescence of the transfected scFv anti-proNGF on HEK293 cells.

2. Cloning, expression, refolding and physico-chemical characterization of the selected scFv anti-proNGF in the cytoplasm of *E.coli*

Due to the low yields obtained by expressing the scFv in the periplasm of *E.coli* (around 300 µg per litre of culture), it was decided to look a new strategy for an increased yield. In particular, the strategy of looking for the expression in the cytoplasm of *E.coli* has been investigated.

The scFvs, in fact, are characterized by the presence of two disulfide bridges, one in the light and one in the heavy chain of the protein. However, in the IACT selection method, the scFv are selected intracellularly, and therefore the most stable scFv are chosen, that are stable in the reductive cellular environment, when no disulfide bridge can form. Therefore, it should be possible, in principle, to express the scFv directly in the cytoplasm of *E.coli*, although this is a reductive environment.

For this purpose, the DNA of the scFv has been subcloned into an expression vector suitable for the expression in *E.coli*, namely the vector pETM-13.

During the cloning procedure, an unwanted mutation in the protein has occurred, in particular the first Histidine was changed into an Aspartate residue. However, it has been decided to proceed to the expression trials anyway.

2.1 Expression of the scFv in *E.coli* cytoplasm

The scFv cloned into the pETM-13 vector was used to transform the *E.coli* strain BL21, optimized for protein expression.

At first, the protein has been expressed in standard conditions for cytoplasmic protein expression, as described in the experimental section.

Then, a sample of both the cytoplasmic preparation and the pellet was loaded on an SDS-PAGE, together with a sample of the protein expression, before and after induction with IPTG. The protein was nicely expressed, as it appears from the picture of the gel in fig.2.1.1 (the protein is indicated by an arrow), but unfortunately the most part of the protein was retained in the pellet. This fact probably means that although the scFv is stable also in absence of disulfide bridges, as it is in the intracellular

environment of the IACT, it is probably not stable in the reductive environment of the cytoplasm of *E.coli* and it is sent to the inclusion bodies.

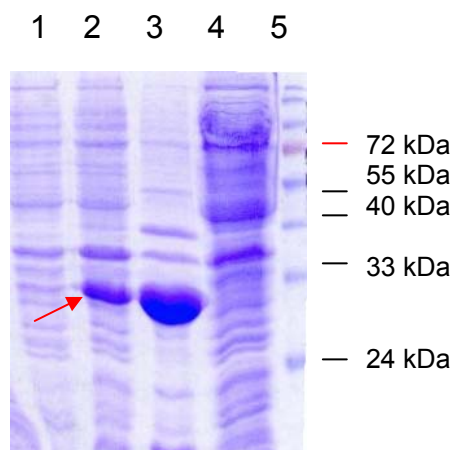


Figure 2.1.1 – SDS-PAGE with the control of the expression of the scFv in the cytoplasm of *E.coli*.

Lane 1: pre-induction control; lane 2: post-induction control; lane 3: pellet of insoluble protein; lane 4: cytoplasmic fraction; lane 5: molecular weight marker

2.2 Establishing a refolding procedure of the scFv from the IB of *E.coli*

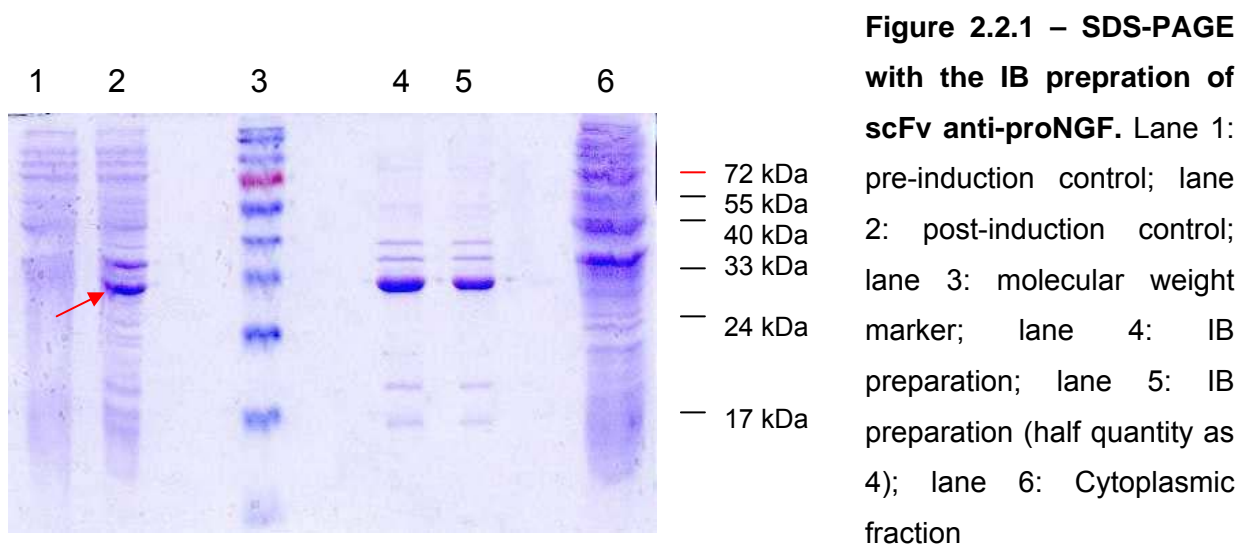
Due to the impossibility of purifying the scFv directly from the cytoplasm of *E.coli*, it has been decided to investigate the possibility of obtaining the scFv from inclusion bodies (IB) after a refolding procedure.

It was already shown (Umetsu *et al.*, JBC, 2003) that it is possible to obtain scFv from refolding of protein solubilized from the IB. In the published experiment, however, the technique used for the refolding has been the one by dialysis. In the present case, on the contrary, the technique of the refolding by dilution was investigated, as the method already described for the preparation of the rm-proNGF protein.

For this reason, a first trial for the refolding conditions was performed. The protein was expressed with the same conditions already used for the expression of rm-proNGF previously described. Then, the IB preparation was carried out, according to the established protocols (see Experimental Section). In the case of the scFv, the resuspension buffer for the IB preparation has been the same one described in Umetsu *et al.*, JBC, 2003.

The SDS-PAGE in fig.8.9.1 represents a control for the expression of the protein (samples of the pre- and post-induction controls) and the composition of both the cytoplasmic and the IB fractions. It appears quite clearly that the protein is

expressed in the insoluble form in the inclusion bodies, that are very clean after the preparation procedure, containing almost uniquely the desired protein scFv anti-proNGF (indicated by the arrow).



Subsequently, the IB were solubilized as described in the experimental section and the denatured protein solution was employed for the refolding trial.

Having no reference for the refolding by dilution conditions for a scFv, it was decided to start from the conditions already employed for the refolding of the rm-proNGF, and to make a small condition-scouting to select the best conditions for the refolding of the new protein.

For this reason, four different refolding buffer compositions were selected, by changing the pH of the solution and the concentration of the protein to be used for each pulse of the refolding by dilution procedure. The refolding was carried out at 4°C and at the end of the pulses, the refolding solution was left for 48 hours in resting conditions. The buffers for the refolding were:

- 1 100mM Tris pH 8, Arg 0.4M, 375uM GSSG, 5mMEDTA, 25 µg/mL
- 2 100mM Tris pH 8, Arg 0.4M, 375uM GSSG, 5mMEDTA, 50 µg/mL
- 3 100mM Tris pH 9, Arg 0.4M, 375uM GSSG, 5mMEDTA, 25 µg/mL
- 4 100mM Tris pH 9, Arg 0.4M, 375uM GSSG, 5mMEDTA, 50 µg/mL

After the refolding, the protein needed to be purified. Taking in account the theoretical value of the pI of the protein, equal to 5.97 (according to the ExPASy web server calculations with ProtParam program), it was decided to try a purification by ion exchange at basic pH using an anion exchange chromatography. For this reason, the refolding solution was dialyzed to remove the Arginine and to equilibrate the protein solution in the same buffer used for the anion exchange chromatography, namely Tris pH 8.

The four refolding solutions were loaded on a HiTrap Q column (Amersham Pharmacia), and the protein was eluted with a linear gradient of NaCl in the buffer.

As it possible to see from the representation of the obtained chromatograms in fig.1.9.2, a certain part of the protein is refolded, since it binds the column, although from the simple chromatogram it was not possible to really establish the nature of the eluted protein.

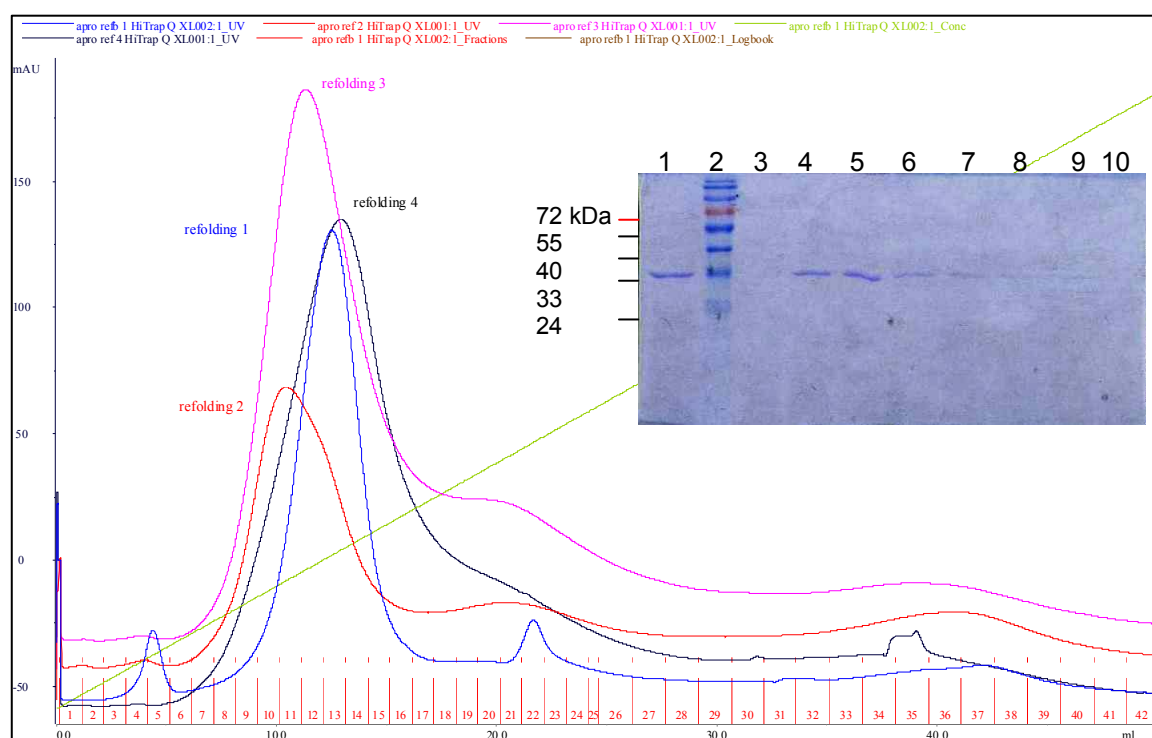


Figure 2.2.2 – Elution profile of the four refolding conditions for the scFv that were tested. On the right side: SDS-PAGE with the fractions from the IEX on the scFv anti-proNGF. Elution profile of the refolding mixture: in all the cases the used buffers were 20 mM Tris, pH 8 as A buffer and 20 mM Tris, pH 8 + 1 M NaCl as B buffer. The chromatograms of the four different refolding conditions are represented with different

colours: condition 1, blue; condition 2, red; condition 3, magenta; condition 4, black. The central fractions of the elution of the condition 1 were loaded on the SDS-PAGE represented on the right side of the picture: lanes 1, 3-10: fractions 12, 11, 13, 15, 17, 19, 21, 23, 25 respectively; lane 2: molecular weight marker.

To confirm the identity of the protein eluted from the IEX, a western blot was performed, by loading on an SDS-PAGE a sample of the central fraction of each one of the eluted peaks. The western blot membrane was challenged with both an anti-SV5 and an anti-His tag antibody, to verify the presence of both tags on the protein. The western blot was developed with the alkaline phosphatase method.

As it appears from the picture of the western blot in fig.2.2.3, the molecular weight of the protein is correct, since it is same of the scFv sample expressed in the periplasm (lane 1). Moreover, all the four peaks contain the scFv, although it is difficult to say in which amount, since all the signals are saturated; anyway, in all the cases, the protein contains both the SV5 (left side of the western blot; lanes 1-5) and the His tags (right side of the western blot; lanes 7-10). Moreover, it has to be noted that besides the main product of the scFv, there's also a lower molecular weight component, around 20 kDa: this is probably a cleavage product; in fact, if the scFv for any reason is cleaved at the linker, the two VH and VL regions are released. In this particular case, the cleavage product is most probably the VH, that has retained the SV5 tag, but has lost the His-tag; or it might also still contain the His-tag but be not detected due to the lower sensitivity of the anti-His antibody in comparison to the anti-SV5 one.

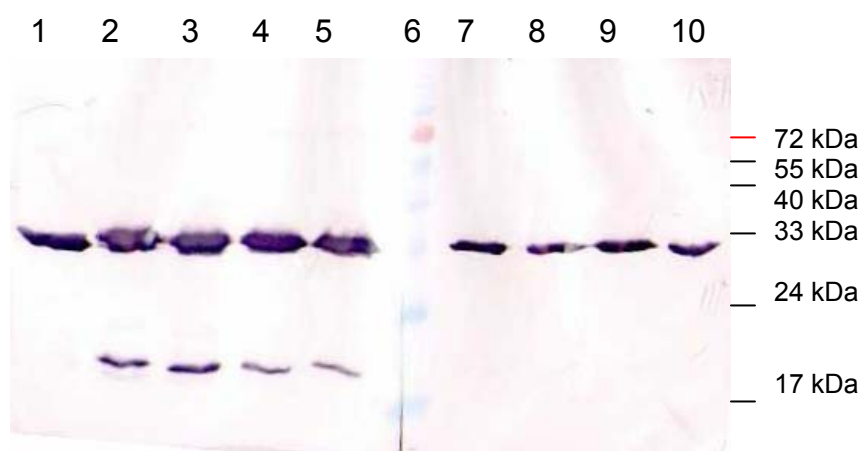


Figure 2.2.3 – Western blot for the correct assignment of the scFv fractions in the elution of the IEX (fig. 8.9.2). Lanes 1-5: anti-SV5 antibody as primary antibody; lanes 7-10: anti-His tag antibody as primary antibody. Lane 1: scFv from periplasmic preparation; lanes 2,7: fraction 12 of refolding 1; lanes 3,8: fraction 11 of refolding 2; lanes 4,9: fraction 12 of refolding 3; lanes 5, 10: fraction 13 of refolding 4; lane 6: molecular weight marker

From the small scouting for the best conditions for the refolding, it was possible to select an intermediate situation, to optimize both the protein quantity (maximum for pulses with more protein) and the degree of purity of the peak in the ion-exchange purification (maximum for a higher pH). For this reason, the best conditions for the refolding of the scFv were chosen to be a refolding in Tris pH 8.5, with pulses of 35 µg/mL of protein.

The protein scFv was therefore expressed and refolded in the newly established conditions and the overall strategy resulted to be quite a good one, since it was possible to obtain a reasonable protein quantity at the end of the purification procedure (10 mg of protein per litre of culture), almost ten times higher than in the periplasmic expression. Moreover, the scFv has a good degree of purity, already after the ion-exchange purification step using the HiTrap Q column (see chromatogram in fig.2.2.4).

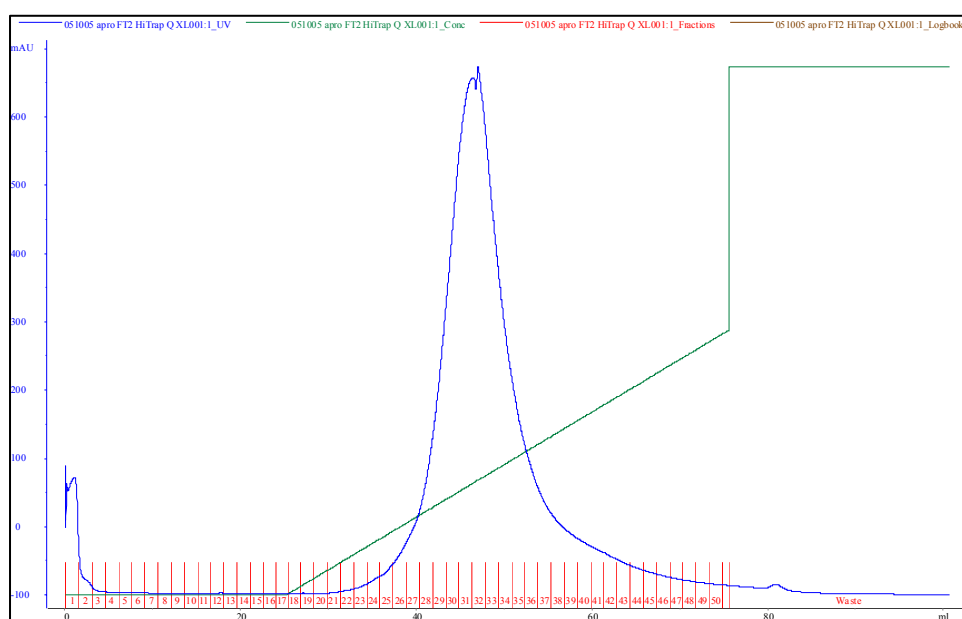


Figure 2.2.4 – Anion-exchange chromatography profile of a typical purification of the scFv anti-proNGF. The trend of the elution gradient is represented (cross line). The

buffers used for the purification were the same described in the previous IEX elution (see caption of fig. 2.2.2)

To establish the aggregation state of the protein, the sample collected from the ion-exchange was concentrated and loaded on a size exclusion chromatography. As it is clear from fig.2.2.5, the protein elutes almost uniquely as a monomeric sample of 30 kDa: this is quite a good indication of stability, considering that scFvs usually have a quite high tendency to aggregate (Worn and Plücktun, Biochemistry, 1999).

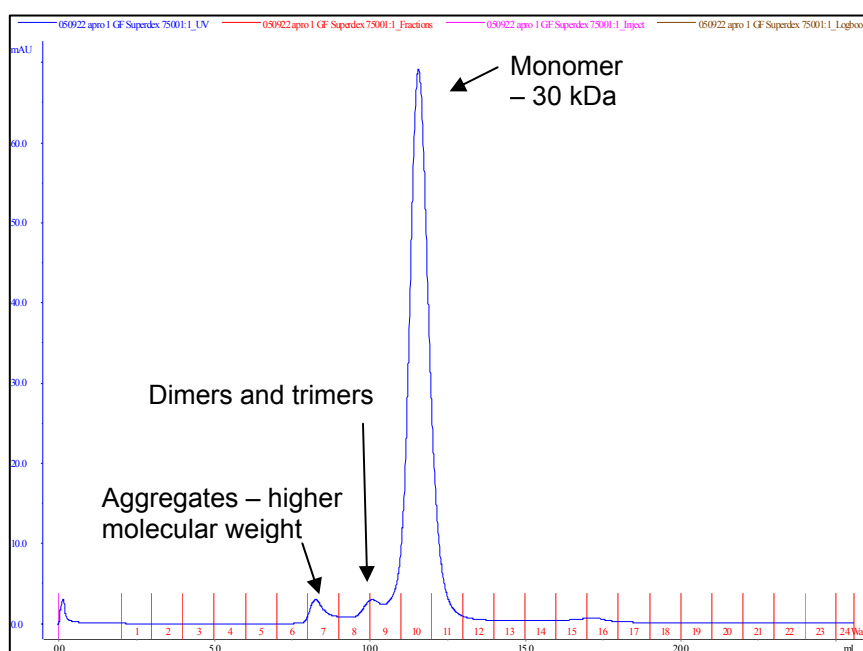


Figure 2.2.5 – Size exclusion chromatography of a typical preparation of the scFv anti-proNGF. The main aggregation states are indicated on the chromatogram by the arrows labels.

To establish the degree of purity of the protein at the end of the purification process, the samples of the central peak of the gel filtration (GF) were loaded on an SDS-PAGE. It is interesting to see in fig.2.2.6 how the distribution of the intact scFv and of the cleaved VH is different in the fractions: the scFv is mainly monomeric (fraction 10 – lane 4), with a small presence of monomeric VH, while the VH has a bigger tendency to aggregation if compared to the scFv (see fraction 9 – lane 3, the relative distribution of the components).

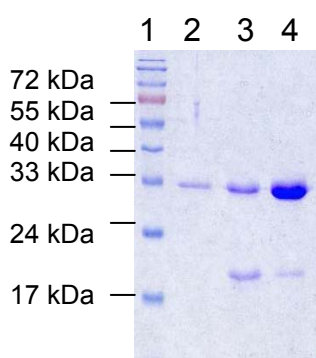


Figure 2.2.6 – SDS-PAGE with the purified scFv anti-proNGF. Lane 1: molecular weight marker; lane 2: fraction 7 from GF; lane 3: fraction 9 from GF; lane 4: fraction 10 from GF

2.3 Physico-chemical characterization of the expressed scFv

The expressed and refolded scFv was characterized from a physico-chemical point of view, to verify the identity and the integrity of the protein.

First, an isoelectric focusing experiment was carried out on the scFv sample, to verify the correct isoelectric point of the protein. The scFv was therefore loaded on an isoelectric focusing gel using the Phast system (Amersham Pharmacia). As it appears from the picture of the gel in fig.2.3.1, the protein is not perfectly homogeneous, since there are two faint bands besides the main one (red arrow), that are characterized by a more acidic pI. However, the experimental pI value of around 6.3 for the scFv results to be in very good agreement with the theoretical value of 6.

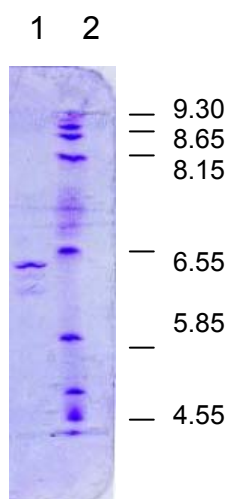


Figure 2.3.1 – Isoelectric focusing for the experimental measurement of the pI of the scFv anti-proNGF. Lane 1: scFv from refolding; lane 2: marker of pI

The secondary structure composition of the protein was established using the far-UV CD spectroscopy, with a JASCO system.

The resulting spectrum (fig. 2.3.2) presents the typical trace of a whole- β protein, as expected from an immunoglobulin-like protein like a scFv. This experiment makes it clear that the scFv that was expressed in *E.coli* and refolded is actually correct from the point of view of its global folding, and is therefore a further proof for the validity of the refolding method.

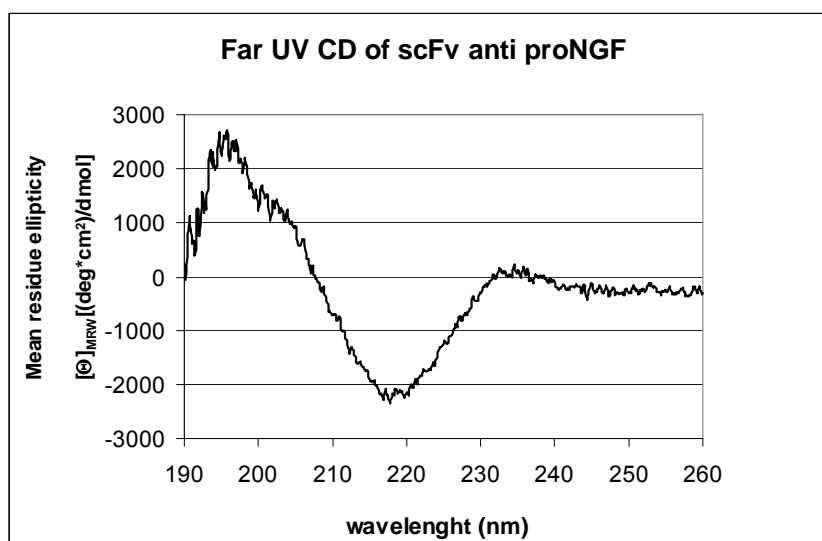


Figure 2.3.2 – Far-UV CD spectrum for scFv anti-proNGF. The mean residue ellipticity value is plot against the wavelength.

To verify the stability of the refolded scFv and compare it to the average one for scFv, a Guanidinium - denaturation curve has been performed, using fluorescence as a technique to follow the changes.

The experiment has been conducted using the protocols already established to be valid for the scFv (Jäger and Plückthun, FEBS, 1999): briefly, the scFv was incubated for 24 hours at 16°C in increasing Guanidinium concentrations, and the fluorescence spectrum of all the samples was subsequently measured. The used excitation wavelength has been 295 nm, the traditional one for scFvs, that is more reliable although the fluorescence intensity is lower than the one obtained at an excitation of 280 nm, due to the fact that only Tryptophanes are excited, and Tyrosine are not.

To evaluate the stability of the protein, the value of the emission maximum against the Guanidinium concentration was plot, to measure the shift of the maximum by the change in denaturant concentration. All the values were blank corrected.

The plot is shown in fig.2.3.3 (red curve), and it appeared clearly that the denaturation curve is completely overlapping to the one previously reported for others scFvs (Jäger and Plückthun, FEBS, 1999), presenting a sigmoidal shape, with a changing point around 1.8 M Guanidinium. Therefore, one can conclude that the refolded scFv presents the same stability properties of an average scFv expressed with other techniques. The shape of the curve and the denaturation point did not

change significantly after a longer incubation time, of 48 hours instead of 24 hours, as it appears clearly from the plot of the data in fig.2.3.3 (blue curve).

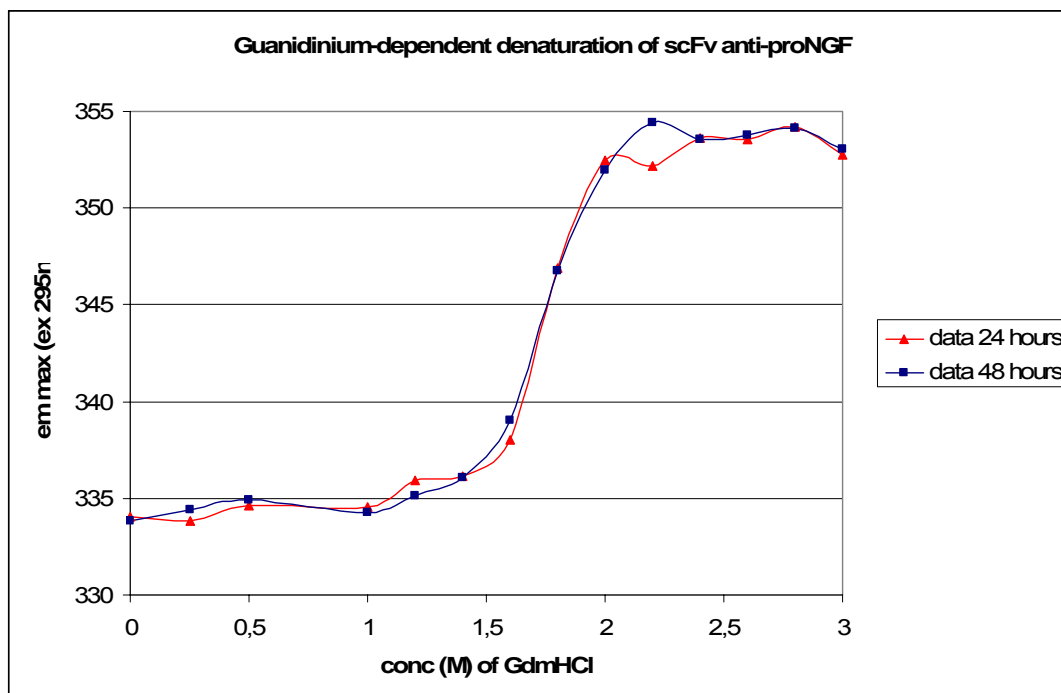


Figure 2.3.3 – Guanidinium-dependent denaturation of scFv anti-proNGF. The shift in the value of the emission maximum (with an excitation value of 295nm) is plot against the increasing Guanidinium concentration. Red line with triangles: values after 24 hours incubation. Blue line with squares: values after 48 hours incubation.

The fluorescence emission spectra of the scFv anti-proNGF in native and denatured conditions are displayed in fig. 2.3.4, in order to compare the spectrum in the extremes of the conditions used for the guanidinium-dependent denaturation. The selected excitation wavelength was 295 nm.

The fluorescence maximum of native scFv anti-proNGF is 334 nm, while in denaturing conditions the maximum is shifted towards higher wavelengths and results to be at 353 nm; the fluorescence intensity, on the contrary, is decreased if compared to the native spectrum. Overall, the fluorescence spectra allowed to confirm that the protein was in its native conformation.

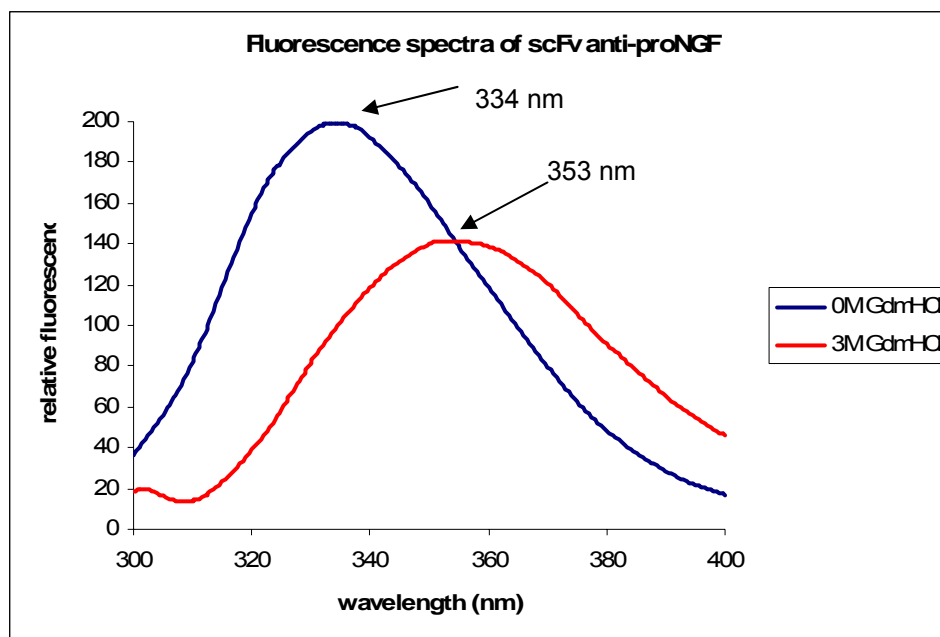


Figure 2.3.4 – Fluorescence emission spectra of the scFv anti-proNGF. The blue curve indicates the spectrum in native conditions, while the red one represents the one in denaturing conditions.

The stability of the scFv was also tested through the monitoring of the changes in the aggregation state in function of different treatment of the sample. In particular, the most common conditions of the treatments reserved to a protein during experiments were tested: saving for several hours (*i.e.* overnight, 16 hours) at 4°C; repeated freezing and thawing cycles; concentration of the sample with a concentration device; dialysis of the protein overnight at 4°C.

The property of the protein chosen for this test was the change in the elution profile from a size exclusion chromatography column, *i.e.* the change in the aggregation state.

Overall, the result was very encouraging: as shown by the fig. 2.3.5, the scFv anti-proNGF remained mainly monomeric even after the described operations on the protein. This last finding push towards a high stability of the protein in solution.

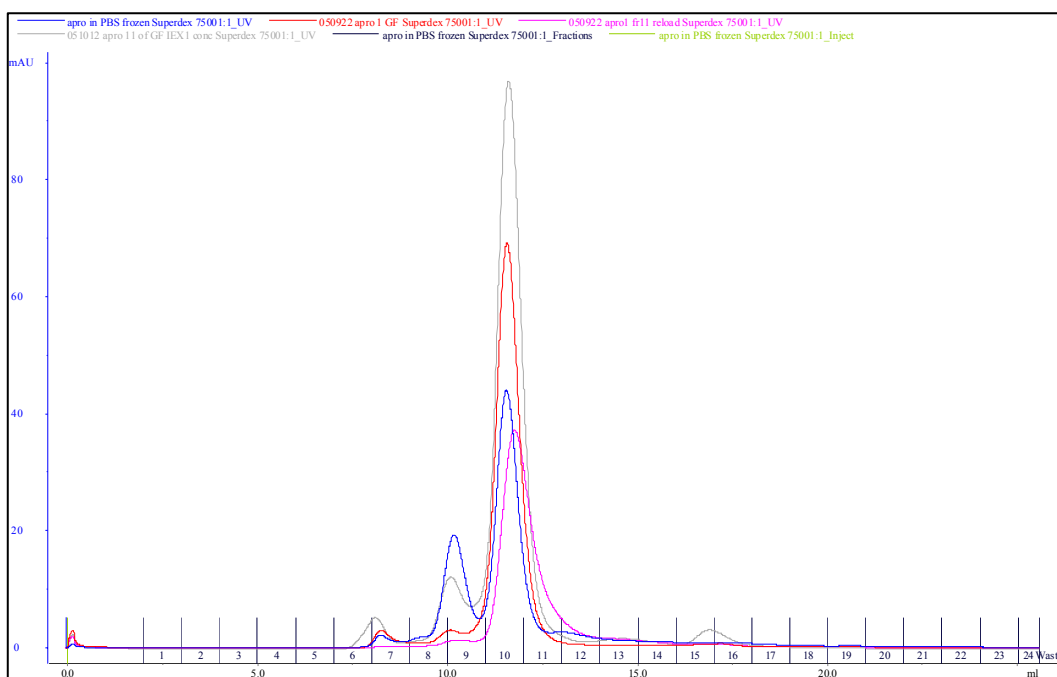


Figure 2.3.5 – Size exclusion chromatography with the scFv anti-proNGF after several kinds of treatments. The arrow marks the monomeric peak of the 30 kDa protein. Colours legend: blue curve, sample dialyzed and concentrated; pink curve, sample frozen and thawed; red curve: sample saved for several hours at 4°C; grey curve: sample concentrated at 6 mg/mL.

3. Binding properties of the selected scFv anti-proNGF

The binding properties of the scFv anti-proNGF were tested by means of two *in vitro* techniques, namely ELISA assay and BIAcore.

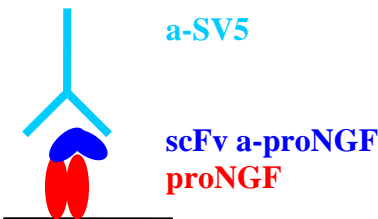
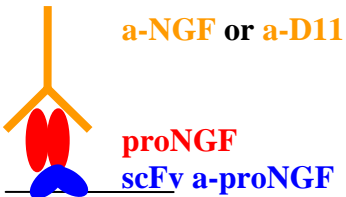
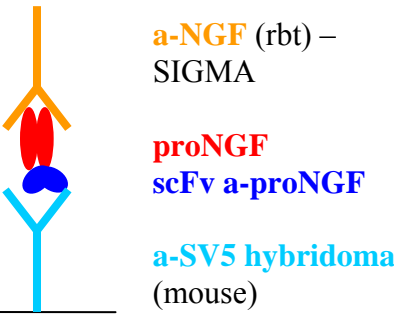
Among the variety of possible applications of an antibody, one of the most interesting is the use of the antibody to selectively detect the protein of interest in a sample coming from leaving material, like a cell lysate of a homogenization of a certain tissues. In particular, in the case of the scFv anti-proNGF, one of the possible applications would be the use of the protein to detect the levels of m-proNGF in brain, and to compare it to the one of NGF. Therefore, besides the determination of the affinity of this scFv for its antigen, the optimization of an ELISA assay for the detection of proNGF in solution using the scFv anti-proNGF is an important step towards the developing of a suitable method for the measurement of proNGF amounts in biological fluids.





The further properties of the scFv anti-proNGF as a primary antibody in western blotting assay were tested and its ability to recognize the specific antigen in solution was proven by mean of immunoprecipitation assay followed by western blotting analysis.

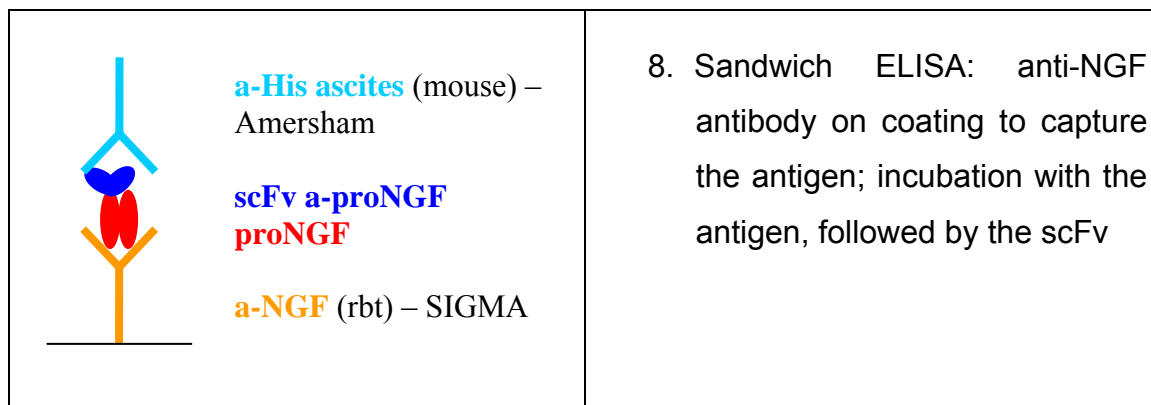
The results will be presented in separated sections.

3.1 ELISA assay for the binding properties of the scFv anti-proNGF

Different format were used to test the binding properties of the refolded scFv, to verify its ability to selectively recognize the specific antigen rm-proNGF. They are summarized in the following table:

Schematic representation of the used format	Description of the format
	1. Antigen coated on the plastic surface and scFv used in the incubation step
	2. scFv coated on the plastic surface and antigen used in the incubation step
	3. Sandwich ELISA: anti-SV5 antibody on coating to capture the scFv; incubation with the scFv, followed by the antigen

 <p>a-SV5 monoclonal (mouse) –SIGMA</p> <p>scFv a-proNGF proNGF</p> <p>a-NGF (rbt) – SIGMA or aD11(rat) hybridoma</p>	<p>4. Sandwich ELISA: anti-NGF antibody on coating to capture the antigen; incubation with the antigen, followed by the scFv</p>
 <p>a-SV5 polyclonal (rbt) – SIGMA</p> <p>scFv a-proNGF proNGF</p> <p>aD11(rat) hybridoma</p>	<p>5. Sandwich ELISA: αD11 antibody on coating to capture the antigen; incubation with the antigen, followed by the scFv</p>
 <p>a-SV5 HRP</p> <p>scFv a-proNGF proNGF</p> <p>aD11(rat) hybridoma or a-NGF(rbt) - SIGMA</p>	<p>6. Sandwich ELISA: αD11 or anti-NGF antibody on coating to capture the antigen; incubation with the antigen, followed by the scFv</p>
 <p>a-SV5 hybridoma (mouse) or a-SV5 monoclonal (mouse) –Invitrogen</p> <p>scFv a-proNGF proNGF</p> <p>a-NGF (rbt) – SIGMA</p>	<p>7. Sandwich ELISA: anti-NGF antibody on coating to capture the antigen; incubation with the antigen, followed by the scFv</p>



Among these formats, not all were giving convincing results.

The first two described formats were giving convincing positive results, demonstrating a high specificity of the scFv anti-proNGF for its antigen and a low a-specific binding with other antigens. They will be presented in the following paragraph.

Format 1 - Antigen coated on the plastic surface and scFv used in the incubation step.

Although this experiment has been performed several times, the recorded signal was always very low and it was difficult to really establish if the result was positive. A typical experiment profile is shown in fig.3.1.1. The controls were given by BSA as coating agent instead of rm-proNGF and by an unrelated scFv (anti-thymosine) instead of the anti-proNGF in the incubation step.

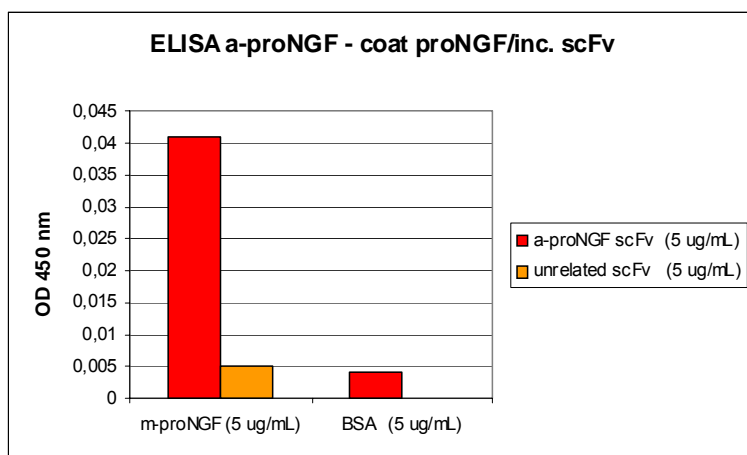


Figure 3.1.1 – ELISA assay for the binding properties of the scFv anti-proNGF. Red bars: response of the scFv anti-proNGF; orange bars: negative control with an irrelevant scFv. The coating agent is indicated on the x-axis. The anti-SV5 (purified) was used as 1°Ab at 1:2000 dilution.

Format 2 - scFv coated on the plastic surface and antigen used in the incubation step

This experiment was performed several times, and it was always giving a convincing result, despite the scFv or rm-proNGF preparation and with all the anti-NGF used as primary antibodies, both the polyclonal one and the monoclonal α D11.

Typical results are shown in fig.3.1.2: it is very clear that the signal is specific, because only the rm-proNGF is detected and no other antigens, and there is no signal given by an unrelated scFv or an unrelated antibody.

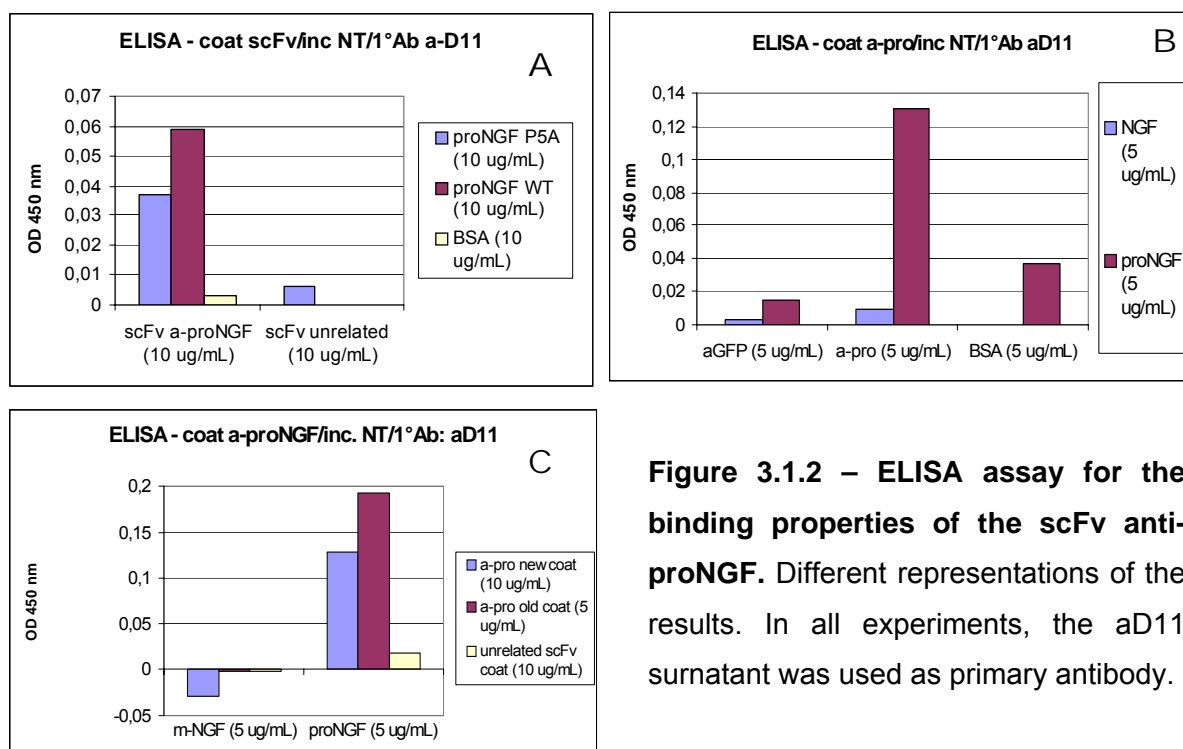


Figure 3.1.2 – ELISA assay for the binding properties of the scFv anti-proNGF. Different representations of the results. In all experiments, the aD11 surnatant was used as primary antibody.

Panels legends. Panel A: blue bars: binding response towards the P5A mutant rm-proNGF; magenta bars: binding response towards the rm-proNGF; yellow bars: binding towards BSA. The scFv used in coating are displayed on the x-axis. Panel B: blue bars: binding response towards NGF; magenta bars: binding response towards the rm-proNGF. The coating agents are displayed on the x-axis. Panel C: blue and magenta bars: coating with two different preparations of scFv anti-proNGF; yellow bars: coating with an irrelevant scFv. The neurotrophin used in incubation is indicated on the x-axis.

Format 6 - Sandwich ELISA: α D11 or anti-NGF antibody on coating to capture the antigen; incubation with the antigen, followed by the scFv

If the two previously described “simple” formats were giving convincing results, it was very difficult, on the contrary, to get a completely convincing data using the sandwich formats, the ones described from 3 to 8. The main problem was represented by the high background of the used polyclonal antibodies and by the cross-reactivity of the secondary HRP antibodies with primary antibodies of different species. The best results were achieved with the use of an HRP-conjugated anti-SV5 antibody (described in the table as format 6), that allowed to decrease the a-specific background. In this case the result was partially positive, although not completely convincing, as it appears for the summary of the experiment in fig.3.1.3: besides the positive signal for rm-proNGF, in fact, there is also quite a significant a-specific signal arising both for the use of a different scFv and for the use of BSA instead of rm-proNGF.

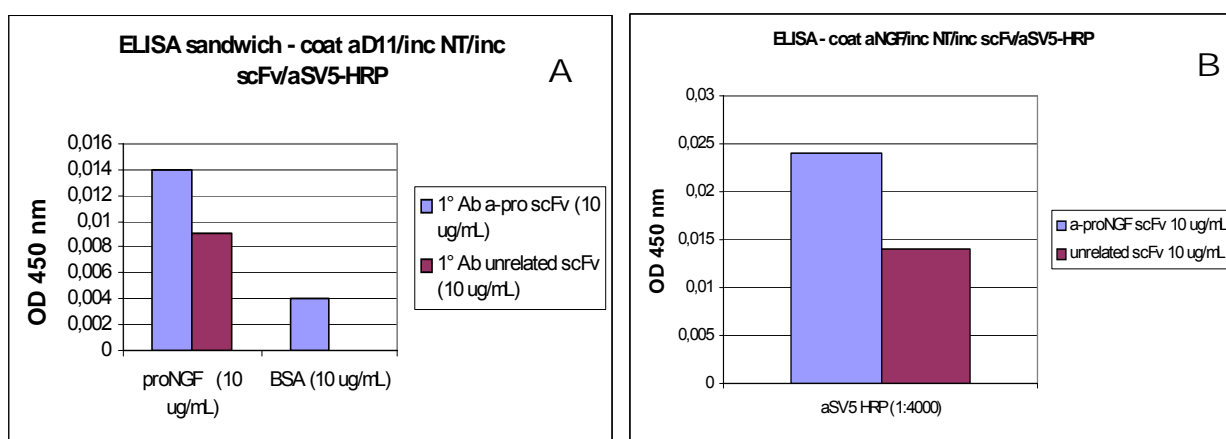


Figure 3.1.3 – ELISA assay for the binding properties of the scFv anti-proNGF.

Different representations of the results. Panel A: coating with the α D11 (purified) at 10 μ g/mL. Legend - blue bars: incubation with scFv anti-proNGF; magenta bars: incubation with irrelevant antibody; the incubation samples are shown on x-axis. Panel B: coating with the polyclonal anti-NGF at 10 μ g/mL; incubation of rm-proNGF at 10 μ g/mL. Legend - blue bar: incubation with scFv anti-proNGF; magenta bar: incubation with irrelevant scFv.

The possibility of improving the result in this format of the sandwich ELISA allows to make the hypothesis that it would be possible to obtain positive results by

using an HRP-conjugated primary antibody, instead of the conjugated secondary ones, to decrease the background due to cross-reactivity. Investigations in this direction are currently ongoing.

In conclusion, many ELISA formats were investigated, to find the best one for the use of the scFv as a probe for the presence of proNGF in solution. The best one in terms of sensitivity and specificity is the one described as number 2 in this section. However, improvements can be made to optimize also the other formats, especially the sandwich ones, and investigations are currently ongoing in this direction.

3.2 ELISA assay – concentration dependency of the scFv/proNGF binding

Once it was established that the ELISA format number 2 was the best one for an ELISA assay using the scFv anti-proNGF to recognize its antigen in solution, it was necessary to verify the concentration dependency of the binding, to evaluate its strength.

The format that has been chosen to perform the experiment was the number 2 described in the previous session, that was the one more reliable in terms of reproducibility and specificity of the signal.

The experiment has been performed according to the described protocols for the ELISA format number 2, following the same scheme:

- coating: anti-proNGF scFv at various concentrations (2.5, 5 and 10 $\mu\text{g/mL}$); as a control use anti-thymosine scFv at the maximum concentration (10 $\mu\text{g/mL}$)
- incubation: rm-proNGF at various concentrations (0.3, 0.62, 1.25, 2.5, 5, 10 $\mu\text{g/mL}$); as a control, use m-NGF at same molar concentrations (0.15, 0.3, 0.62, 1.25, 2.5, 5 $\mu\text{g/mL}$)
- 1°Ab: monoclonal αD11 antibody (supernatant)
- 2°Ab: horse radish peroxidase conjugated anti-rat antibody

The overall results are exposed in fig.3.2.1: it clearly emerged that the binding mode of the scFv is concentration-dependent, both from the concentration of the antigen (higher rm-proNGF concentrations give higher signal intensity) and from the scFv concentration. It is curious to notice how a lower coating concentration of the scFv gave rise to a higher signal intensity, on the opposite than it would have been

expected. Maybe the reason resides into a saturation of the surface, that renders the binding to the antigen less specific above the threshold.

The signal, however, results to be very specific, since the use of m-NGF as an antigen instead of the rm-proNGF gave rise to a complete abolishment of the signal (blue trace in the graph in fig.3.2.1). The same is true when an irrelevant scFv is used against rm-proNGF instead of the specific anti-proNGF scFv (purple line in fig.10.2.1).

Concluding, the selected scFv against rm-proNGF, expressed in *E.coli* and refolded from IB, resulted to be very specific for its antigen and to have a good concentration-dependent tendency.

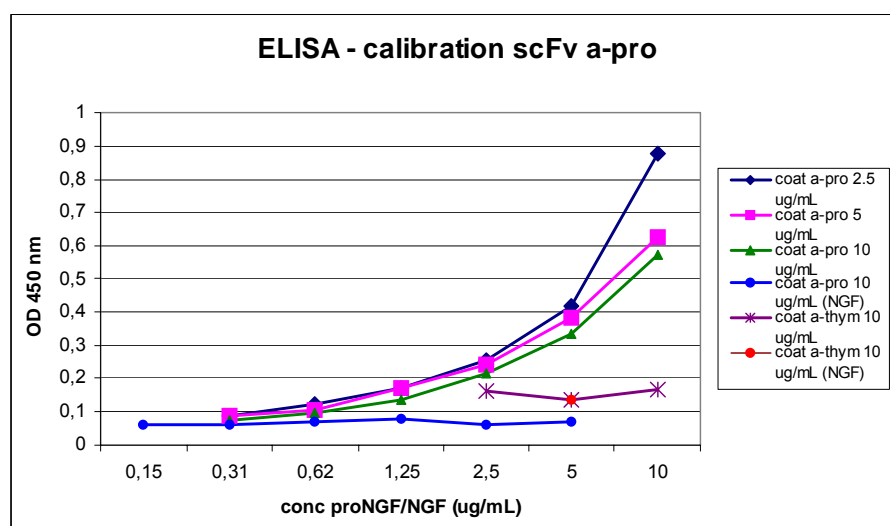


Figure 3.2.1 – ELISA assay for the concentration dependency of the binding properties of the scFv anti-proNGF. The plate was coated with the proteins indicated in the legend on the right side of the figure and protein concentrations used in the incubation step are indicated on the x-axis.

3.3 Binding properties – dependency from the aggregation state

The binding properties of the scFv, tested by ELISA assay, were also tested for the dependency from the aggregation state of the anti-proNGF.

In particular, an ELISA assay was performed using as scFv on coating on the plate the different fractions of a run of the scFv over a size-exclusion chromatography column. As already shown in fig.2.2.5, the scFv anti-proNGF is mainly in the

monomeric state in solution, although a certain fraction of the protein is forming aggregates of higher molecular weight, mainly dimers.

Therefore, the fractions corresponding to the different species were collected and used to coat an ELISA plate. Then, rm-proNGF was used as antigen in solution and the ELISA was developed as described in the previous sections.

The overall result is shown in fig 3.3.1: the tested fractions were the monomeric (fraction 10), dimeric (fraction 9) and aggregated (fraction 7) ones of two different gel filtration runs. It is interesting to see that the monomeric fractions are responding better than the aggregated ones in the recognition of the rm-proNGF antigen. As a control, BSA was used as an antigen and an unrelated scFv was employed as a coating agent; both controls resulted to be completely negative, as expected.

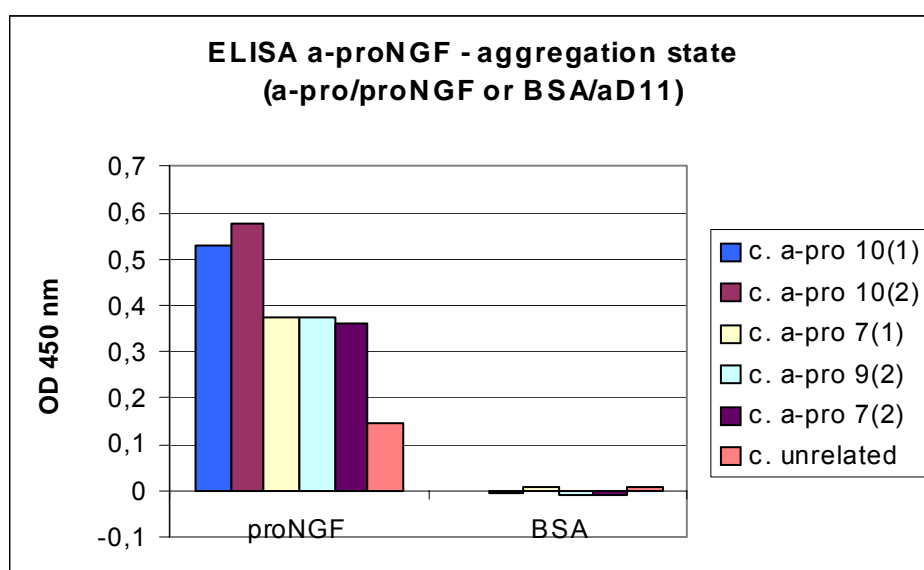


Figure 3.3.1 – ELISA assay with different aggregation states of the scFv anti-proNGF. The legend of the bars colours is indicated on the right side of the figure, for the different coating agents. On the x-axis, the incubation samples are indicated. Both the coating with the scFv (anti-proNGF and unrelated) and the incubation with rm-proNGF or BSA was carried out at the concentration of 10 µg/mL.

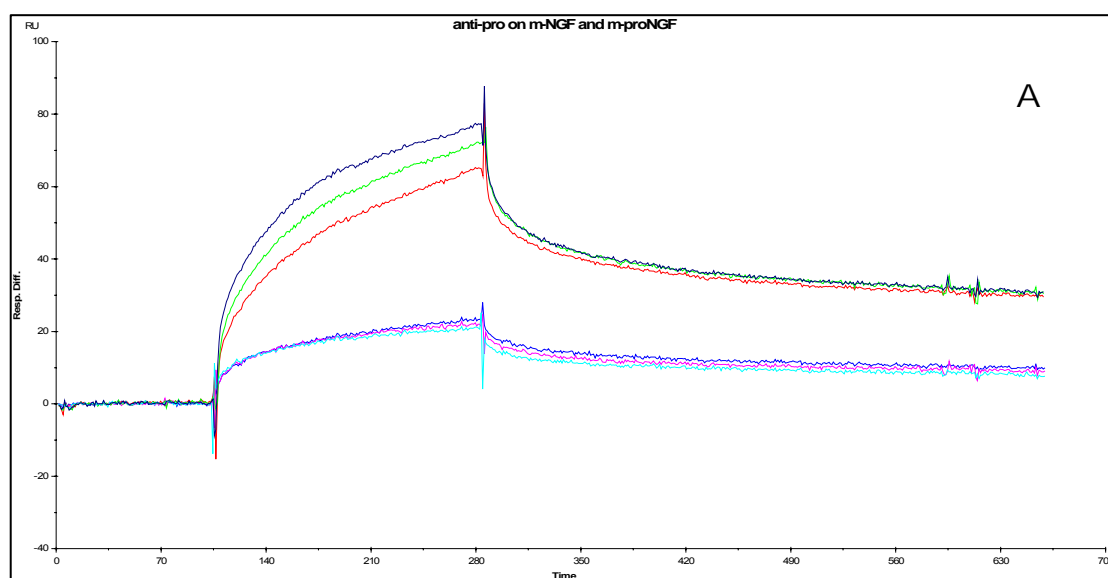
3.4 Kinetic analysis of binding using BIAcore

After establishing the binding properties of the scFv anti-proNGF, it was performed a complete kinetic analysis on the binding using Surface Plasmon Resonance through BIAcore.

Due to the stickiness characteristics of rm-proNGF, the format used for the analysis was the binding of rm-proNGF as a ligand on a CM5 chip and the use of scFv as an analyte in solution.

As controls, m-NGF was used as a ligand and an irrelevant scFv was employed as an analyte.

The results are summarized in fig.3.4.1: the three upper curves represent the binding to rm-proNGF, and the three lower ones, the binding to m-NGF. Although the response of the scFv on m-NGF is not completely null, one should consider that there is no concentration-dependence of this response, while, on the contrary, there is such dependence in the rm-proNGF response, as it appears even more clearly in fig.3.4.1-B (lower panel), where only the curves of the response on rm-proNGF are represented, for a concentration range between 62 nM and 250 nM. This fact allowed to establish that the scFv has a specific binding response to rm-proNGF.



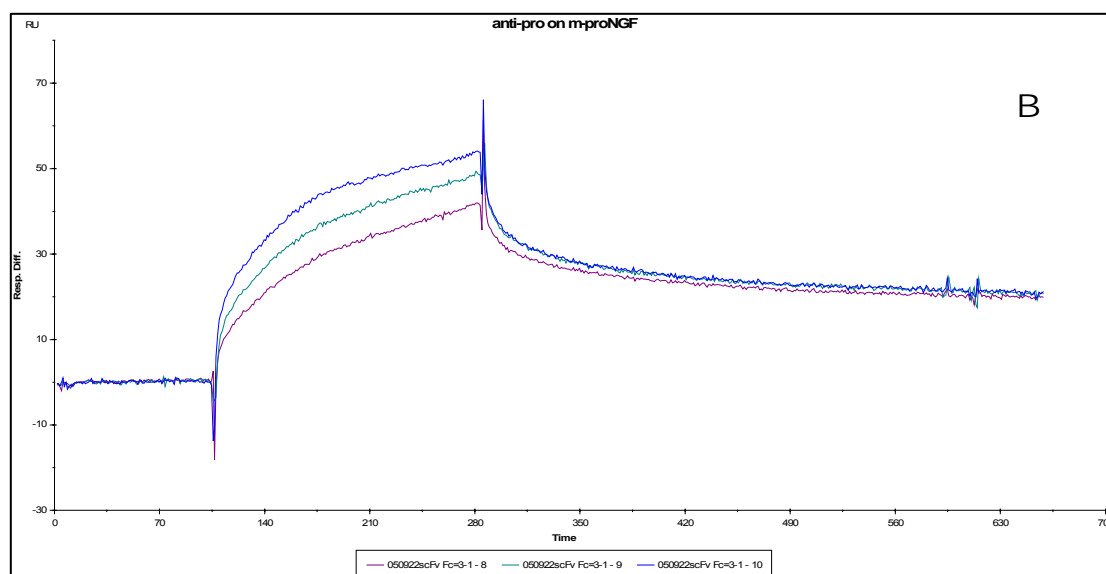


Figure 3.4.1 – Summary of BIAcore results for the binding of scFv anti-proNGF towards both rm-proNGF and m-NGF as a control. Panel A: summary of kinetic analysis of both m-NGF and rm-proNGF. Panel B: plot of only the binding towards rm-proNGF.

A complete kinetic analysis could be performed on the curves of the binding of the anti-proNGF to rm-proNGF. Regardless from the kind of method used for the analysis (if a simultaneous or sequentially parameters determination), the values of the parameters were almost the same. In particular, the calculated parameters were:

$$K_A = 7.4 \cdot 10^7 \text{ M}^{-1}$$

$$K_D = 1.6 \cdot 10^{-8} \text{ M}$$

With a χ^2 value of 0.4.

These parameters, therefore describe a very good binding of the scFv to the rm-proNGF.

3.5 Formation of the complex scFv antiproNGF/proNGF

For a further experimental evidence on the formation of the complex between the rm-proNGF and its specific scFv two types of analysis were carried out: native PAGE and size-exclusion chromatography. According to the theoretical stoichiometry, the expected complex should be 1:1 in moles, consisting of one scFv molecule for each rm-proNGF molecule, as depicted in the scheme in fig. 3.5.1, giving rise to a complex of around 110 kDa.

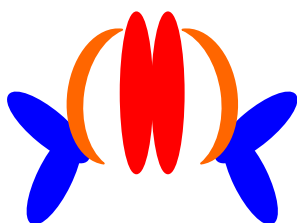


Figure 3.5.1 – Schematic representation of the theoretical complex formed by scFv anti-proNGF and m-proNGF. The red/orange shape represents the m-proNGF dimer (pro-peptides in orange and mature NGF dimer in red); the blue shapes represent two scFv molecules.

In the first experiment, the samples were loaded on a PAGE in native conditions, *i.e.* in an acrylamide gel without detergent (SDS) and reducing agent (DTT). Next to the single components, rm-proNGF and scFv anti-proNGF, two different mixtures of the components were analyzed, prepared with different stoichiometric ratios. In particular, a 1:1 and a 4:1 scFv:rm-proNGF mixtures were prepared and loaded on the gel.

As indicated in fig. 3.5.2, the complex forms in the case of the excess of scFv, as indicated by the red arrow (lanes 3 and 5), both in the case of the rm-proNGF and of its mutant P5A. Unfortunately is not possible to check the position of the rm-proNGF on the gel, because the protein, due to its high charge, is not running in the acrylamide matrix in the employed conditions (see the empty lanes 1 and 7), but is stacked in the stacking component of the gel. Another consideration should be driven for the scFv sample: as already demonstrated by the denaturing SDS-PAGE and by the isoelectric focusing gel in the previous chapters, the scFv is not a completely single component: a second band appears in the native gel (black arrow on lane 4), probably arising from the VH component present as a “contaminant”. The relative amount of this band, however is not significant in comparison to the predominant intact scFv component.

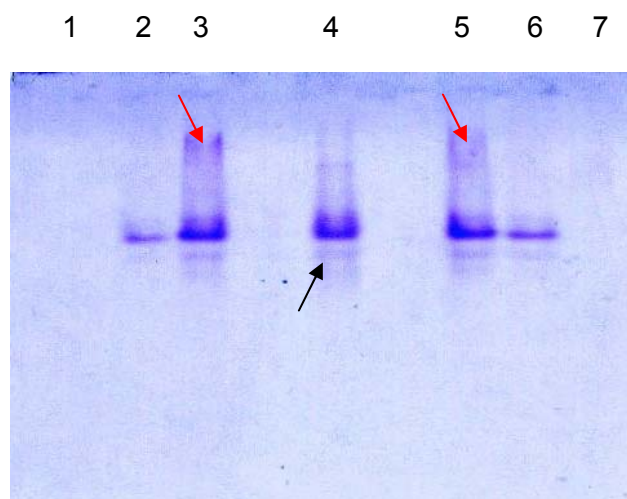


Figure 3.5.2 – Native PAGE with the samples for the formation of the complex scFv/m-proNGF. Lane 1: m-proNGF; lane 2: complex scFv/m-proNGF in 1:1 ratio; lane 3: complex scFv/m-proNGF in 4:1 ratio; lane 4: scFv anti-proNGF; lane 5: complex scFv/P5A m-proNGF in 4:1 ratio; lane 6: complex scFv/P5A m-proNGF in 1:1 ratio; lane 7: P5A m-proNGF.

The second approach used to check the actual formation of the complex was the size exclusion chromatography. In this case, however, only an indirect check could be done, due to the aspecific stickiness of rm-proNGF for the resin of the column, as already shown in the case of the formation of the complex between rm-proNGF and the α D11 monoclonal antibody. The experiment was anyway carried out, but as already shown in the case of the complex with α D11, there was no appearance of a new high molecular weight peak, but only a decrease in the intensity of the peak of the scFv (data not shown). Although indirect, this was again a confirm that the complex between scFv and rm-proNGF is indeed forming in solution, even if no precise determination of the stoichiometry and the molecular weight of the complex was possible.

3.6 The use of the scFv anti-proNGF as a primary antibody

Once the binding properties of the scFv anti-proNGF was proven by ELISA and BIAcore, the efficacy of the scFv as a primary antibody in biochemical assays was tested.

In particular, the antibody was tested in western blot analysis, using different experimental assays.

In a first assay, a western blot was carried out, loading on an SDS-PAGE different amounts of rm-proNGF and m-NGF as a control and using the scFv as a primary antibody to detect the proteins. It appeared clearly that the scFv is very efficient in detecting specifically the rm-proNGF blotted on a nitrocellulose membrane, although at higher concentrations than an average monoclonal antibody. The experiment was repeated using different concentrations of scFv and the pictures of the corresponding western blots are shown in fig.3.6.1. It should be underlined, however, that the scFv was not very stable in the buffer used for the incubation (a milk-PBS solution) and it was necessary to incubate the scFv in presence of protease inhibitors to increase its half-life.

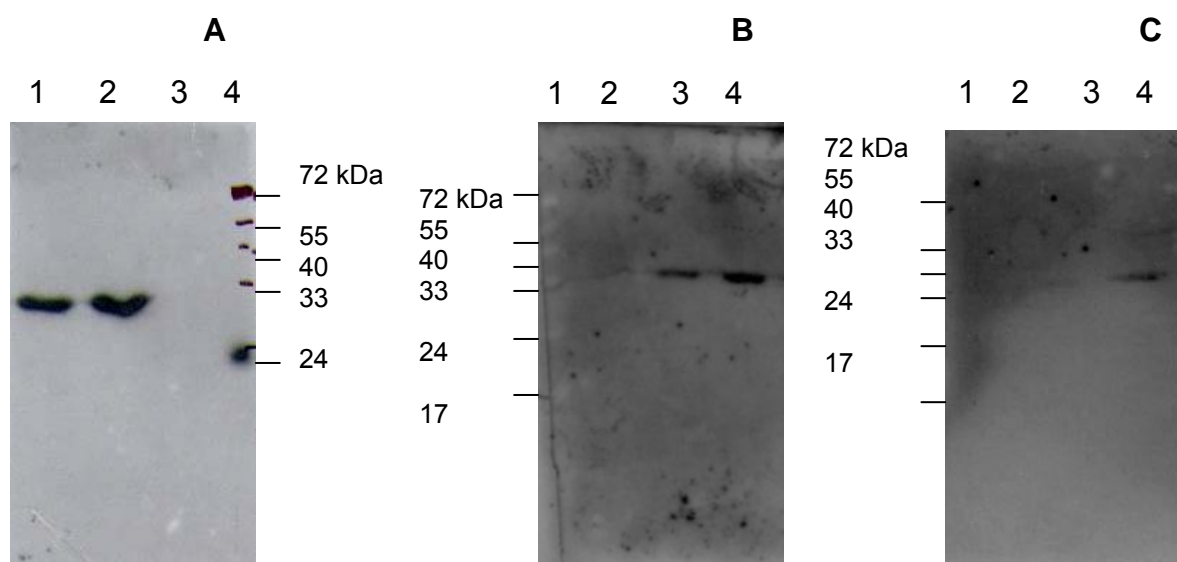


Figure 3.6.1 – Western blot using the scFv anti-proNGF as a primary antibody. Panel A: scFv used at a concentration of 80 μ g/mL. Lanes 1 and 2: 1 μ g and 2 μ g of rm-proNGF respectively; lane 3: 1 μ g of m-NGF; lane 4: molecular weight marker. Panel B: scFv used at a concentration of 40 μ g/mL. Lane 1: 500ng of m-NGF; lanes 2 and 3: 500ng and

1 µg of rm-proNGF respectively. Panel C: scFv used at a concentration of 20 µg/mL. Lane 1: 500ng of m-NGF; lanes 2 and 3: 500ng and 1 µg of rm-proNGF respectively.

Subsequently, the ability of the scFv to recognize and selectively bind the rm-proNGF in solution was evaluated. The technique of choice was the immunoprecipitation using Protein-G, followed by a western blot analysis. As negative controls, both NGF and an irrelevant scFv were chosen.

The result was encouraging: although rm-proNGF does stick to the resin ProteinG also in absence of the scFv, the intensity of the selective band in presence of scFv is much higher, therefore indicating a selective binding. The results are summarized in fig.3.6.2. The reference protein rm-proNGF in lane 3 runs with an apparent molecular weight different from the test one because the sample was loaded in presence of DTT, while the immunoprecipitated samples were loaded in absence of DTT, to avoid interference by the light chains of the used monoclonal antibodies.

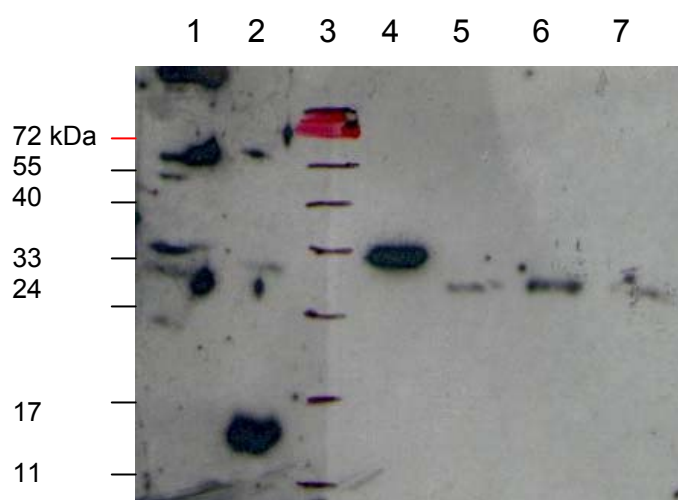


Figure 3.6.2 – Western blot of the immunoprecipitation of rm-proNGF with the scFv anti-proNGF. Lanes 1 and 2 were probed with a primary anti-NGF polyclonal antibody. Lanes 4-7 were probed with a primary anti-proNGF polyclonal antibody. Lane 1: immunoprecipitation of m-NGF with the scFv anti-proNGF; lanes 2 and 4: reference m-NGF and rm-proNGF respectively; lane 3: molecular weight marker; lane 5: immunoprecipitation of rm-proNGF without the scFv anti-proNGF; lane 6: immunoprecipitation of rm-proNGF with the scFv anti-proNGF; lane 7: immunoprecipitation of rm-proNGF with an irrelevant scFv

In conclusion, the scFv anti-proNGF was tested to be a good antibody in both native (ELISA and BIAcore) and denaturing conditions (western blot), and these properties may be used in a wide range of possible applications.

One further application of the scFv anti-proNGF would be in the study of the binding interaction with its antigen in the presence of the immunoadhesins for the receptors TrkA and p75^{NTR}: the result of this experiment would be a further indication of the amino acid regions on the proNGF that are involved in the binding to the receptors. Moreover, this set of experiments would allow to check the possible blocking properties of the scFv versus the binding of proNGF to one or the other of its receptors.

4. Structural characterization of the scFv and of its complex with rm-proNGF

The overall fold of scFvs is known: it is characterized by an overall immunoglobulin-like fold. However, it is not an easy task to achieve the crystallization of scFvs, mainly due to their tendency to aggregate.

The scFv anti-proNGF described in this Thesis in the previous chapters is a new one and no structure information is known about it. Therefore, after the biochemical/biophysical analysis performed for its characterization and described in the previous chapters, a more detailed structural analysis of the scFv was performed. In particular, the first approach that was selected was the one of taking advantage of SAXS as a technique to achieve a first insight into the structure of the scFv anti-proNGF.

The results achieved through this experimental approach will be presented in the next two paragraphs. In particular, the first one will deal with the SAXS experiment performed on the scFv alone, while the second one will present the data regarding the analysis of the complex between the scFv and the rm-proNGF.

4.1 Structural analysis of scFv anti-proNGF by SAXS data

The SAXS data were recorded at the SAXS beamline of EMBL at DESY. Hamburg, using the same experimental conditions described in Part 1 for the rm-proNGF.

In particular, the protein solution containing the scFv was analyzed at different concentrations, in order to achieve the best conditions for a reasonable monodisperse solution. The scFv has shown a relatively low tendency to aggregate and it was possible to obtain a reasonable clean experimental scattering curves, as shown by fig. 4.1.1.

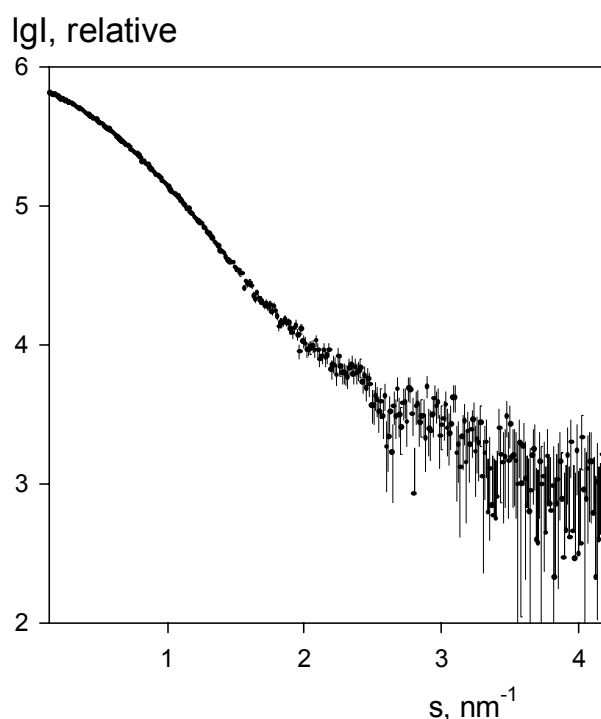


Figure 4.1.1 - X-ray scattering pattern of scFv anti-proNGF. The plot displays the logarithm of the scattering intensity as a function of momentum transfer $s=4\pi\sin(\theta/2)/\lambda$ where θ is the scattering angle and $\lambda=1.5 \text{ \AA}$ is the X-ray wavelength.

The analysis of the scattering curve, gave at first a good prediction of the molecular mass of the scFv, and the calculated Porod volume (40 nm^3) was consistent with the predicted molecular weight of 29 kDa for the monomeric protein. Indeed, the calculated molecular mass for the scFv from the scattering curve was of 31 kDa. The other calculated parameters were $R_g=2.44 \text{ nm}$ and $D_{\text{max}}=8.0 \text{ nm}$.

The modelling of the scattering data to achieve a low resolution structure determination of the scFv was not an easy task, given that no structural information is available for the protein, and a complete analysis is still ongoing.

To obtain a suitable model for the scFv, homology modelling using the Swiss Model web server (on Expasy web server) was performed on the two VL and the VH domains separately. The most similar structures by homology for the single domains were identified (PDB: 1EO8 for VL and 1H0D for VH), and based on these structures, it was possible to reconstruct an homology model for the whole scFv. In particular, two reconstructions were done: one taking the structural scaffold of the most similar VL PDB entry and the other with the scaffold of the most similar VH one. They are presented in fig. 4.1.2.

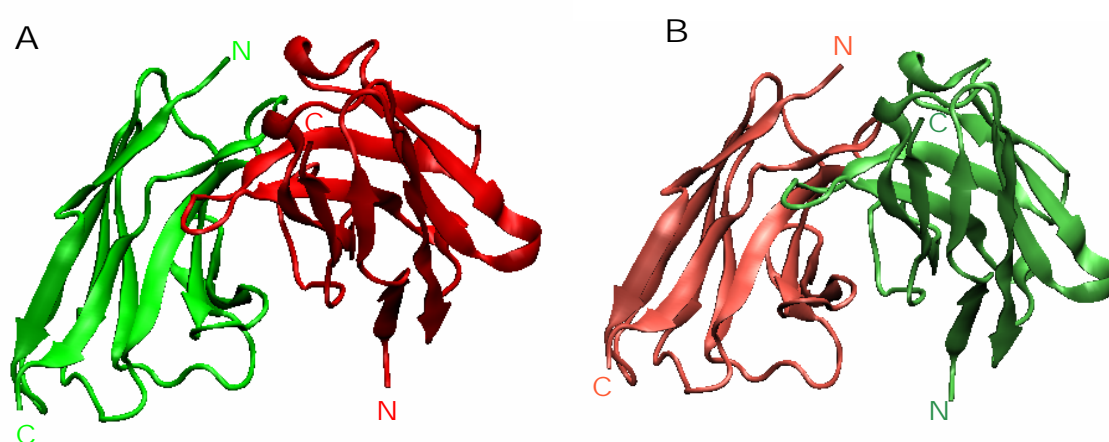


Figure 4.1.2 – Homology modelling of the scFv. The models were reconstructed with the SwissModel from PDB. In particular, the homology search was done with the VL and VH separately. These domains were then used to reconstruct the model for the scFv (with program O - Jones, T. A., et al., (1991) Acta Crystallogr. Sect. A), on the structural scaffolds of the antibodies entries for the best VL and the best VH respectively; the linker was not modelled. In panel A the reconstructed model on the scaffold of the best VL is displayed (VL in green, VH in red); in panel B the reconstructed model on the scaffold of the best VH is displayed (VL in pink, VH in mauve). In both cases, the N- and C-termini of the two domains are indicated.

Although these two models are only homology models, they might be useful in the reconstruction of the overall orientation of the domains in solution, according to the experimental SAXS data.

A further help in the reconstruction of the model came from the identification of the contact regions between the domains, according to the standard Kabat numbering of antibodies. In particular, for the scFv anti-proNGF the following contact regions were identified:

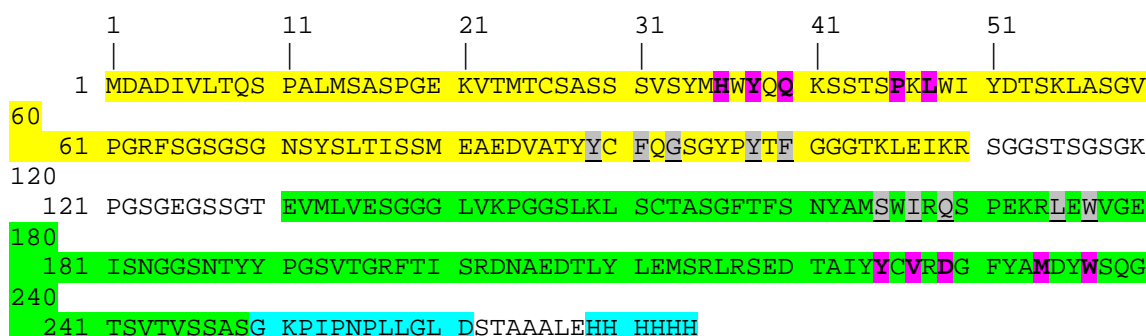


Figure 4.1.3 – Identification of the contact regions between the VL and the VH regions of the scFv anti-proNGF according to the Kabat numbering of the primary sequence of the antibody. The yellow colour indicates the VL domain; the green colour indicates the VH domain; the cyan colour indicate the SV5 and the His tags. The uncoloured region between the domain represents the linker. The bold purple residues and the underlined grey ones are those giving rise to the first and the to the second contact regions respectively between the two domains – the same colour code is used in the two domains.

A further step in the reconstruction of the structure of the scFv according to the SAXS data was performed using the program BUNCH for the reconstruction of the missing chains of a structure, modelling the missing chain of the linker between the VL and VH regions on the models of the two domains obtained by the Swiss Model program. Moreover, the program CRY SOL was used for a rigid-body modelling of the VH and VL domains, adding the restrains of the contact regions according to Kabat numbering. The data analysis is not completed yet, since the presence of a certain dimer component in solution (around 20%) makes it difficult to obtain a good fitting to the experimental data taking in account the single monomeric component, mainly due to a discrepancy between the experimental excluded volume and the most likely models. Therefore, the next steps will include the generation of a possible dimer for the scFv by homology modelling and the reconstruction of the most likely monomer in solution by fitting the experimental data taking in account the homology models.

4.2 Structural analysis of the complex between the scFv anti-proNGF and the rm-proNGF by SAXS data

The scFv anti-proNGF was shown to have good binding properties for its antigen, rm-proNGF. It was also possible, through the IVEM in yeast described in previous chapters to map the region involved in the epitope. Besides those information, however, it would be interesting to get more detailed indications on the interaction between the two proteins in solution.

For this reason, a SAXS analysis on the complex between the two interacting partners has been carried out.

Once the actual formation of the complex scFv/rm-proNGF was verified, it was possible to proceed to its SAXS analysis.

Having no clear information on the best stoichiometric ratio, it was necessary to prepare solutions with varying stoichiometry, in order to identify the best ratio protein:ligand for the complex to be the predominant moiety in solution.

By analysing the different samples, it was possible to indeed isolate the best sample in terms of complex presence. In Fig.4.2.1 the x-ray scattering pattern for the complex proNGF/scFv and for the individual components are shown.

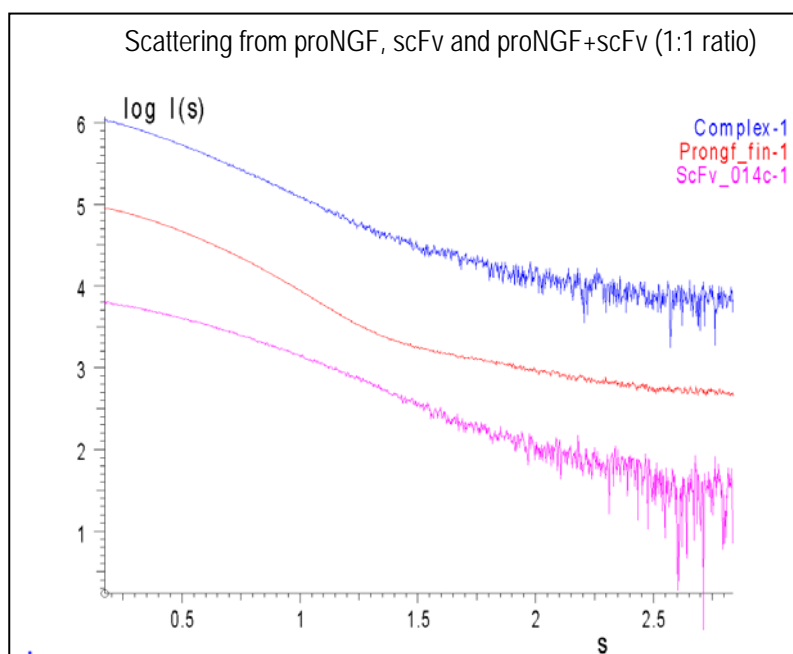


Figure 4.2.1 - X-ray scattering pattern of proNGF+scFv complex (pink curve on bottom), proNGF protein (blue curve on top), scFv (red curve in the middle). The plot displays the logarithm of the scattering intensity as a function of momentum transfer $s=4\pi\sin(\theta/2)/\lambda$ where θ is the scattering angle and $\lambda = 1.5 \text{ \AA}$ is the X-ray wavelength.

From the experimental scattering curves it was possible to evaluate the radius of gyration, R_g , for the complex proNGF/scFv 3.5 nm, and the D_{\max} was equal to 13 nm. The calculated molecular weight for the complex in solution was around 70 kDa, therefore too small, if compared to the theoretical value of 110 kDa for a 1:1 complex. Indeed, the excluded volume value (150 nm^3) as well as the other computed parameters, allow to affirm that the properties of the complex sample are not very different from the ones of the two single components. Therefore, there is the confirm that the complex is forming in solution, although it is not the main component.

A complete analysis of the scattering curves to reconstruct a model of the structural arrangement of the complex was therefore not possible. A fitting of the experimental data with the program OLIGOMER as a linear combination from ScFv and proNGF curves to identify the composition of a solution mixture was run. The data were very well fitted by these two curves, meaning that the mixture contains both the two single components (scFv and proNGF) and the complex.

An attempt to obtain an *ab initio* model for the complex in solution was anyway performed with the program DAMMIN, but as depicted in fig. 4.2.2 (panels A and B) the overall shape resulted to be very similar to the elongated model already found to describe the solely rm-proNGF in solution (see chapter 7).

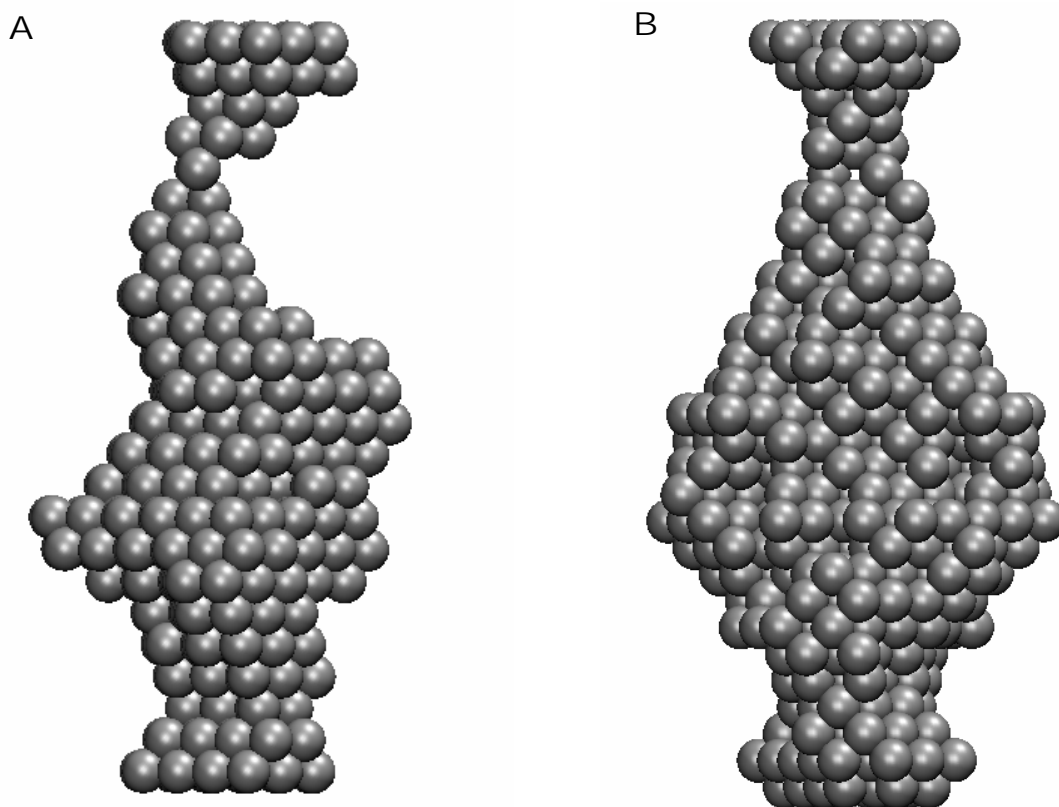


Figure 4.2.2 - *Ab initio* models for the shape determination of the complex scFv/rm-proNGF. Panel A: DAMMIN model P1. Panel B: DAMMIN model P2. The figures were generated using the program VMD

A more complex experimental approach will be therefore necessary to achieve a structural analysis of the complex between the scFv anti-proNGF and the rm-proNGF protein, probably using different stoichiometric ratios allowing to obtain a more significant presence of complex in solution.

DISCUSSION AND PERSPECTIVES

In the recent years, the precursor of NGF, proNGF, resulted to be an emerging actor in the field of neurotrophins, thanks to a series of interesting findings arising from different publications as illustrated in the Introduction.

The work described in this Thesis aimed to proceed on the road of the investigations of the 3D-structure of proNGF and of its functional role, especially in the field of neurodegeneration. In this work, the attention was on the mouse proNGF, given the availability of a mouse model for Alzheimer Disease (AD), and therefore the possibility to prove *in vivo* the results discovered *in vitro*, by means of various techniques, both in field of both biochemistry and structural biology.

The results achieved by this Thesis work will be briefly discussed in the present Section, in an overall “panoramic view”.

A first general result was on the conservation of the biochemical properties of the NGF pro-peptide, by comparison of the present data on the mouse proNGF with the ones previously reported for the human one (Rattenholl et al, 2001). In fact, despite the difference in sequence between the human and the mouse protein (homology higher than 80%), the physico-chemical properties of the two proteins were substantially the same. The mouse protein could be expressed and refolded *in vitro* from *E. coli* using the same procedure optimized from the human one, and the subsequent characterization of the protein from the spectroscopic point of view allowed to confirm that the properties of the two proteins were comparable, but for some minor differences due to the diversity in the amount of aromatic amino acids. This is a further confirmation of the importance of the pro-sequence of proNGF: the high degree of structural and functional homology and the analogue properties of proteins of different origin allows to assert that, besides the folding-aid properties, this protein could cover other important biological roles.

An approach in the understanding of the functional role of the pro-peptide was also presented in this work, through the cloning of two fusion constructs of the pro-peptide alone with the GST protein, at the N-terminus and C- terminus respectively. These constructs were selected for the possibility of performing an *in vitro* study of the pro-peptide out of its usual environment and check if it possesses (despite the fusion partner) certain biochemical properties that are intrinsic in the sequence. The

efficient cloning and expression of the two proteins has been shown to be feasible; on the contrary, the achievement of high amounts of these fusion constructs was not possible, due to purification problems. One of the future goals will be therefore to optimize the purification procedure for these fusion constructs, in order to obtain enough protein amounts to perform biochemical experiments such as BIAcore studies or structural analysis.

Regarding the analysis of proNGF, an important result was achieved through this Thesis' work: for the first time an insight into the structural arrangement of the protein has been obtained. In fact, it was possible in fact, to bypass the problems arising from the high degree of flexibility of the protein that impedes the crystallization of proNGF. Small Angle X-ray Scattering (SAXS) was chosen as the technique for a complete analysis of the structure and dynamics of the protein in solution.

SAXS experiments demonstrated that proNGF is dimeric in solution and allowed a low resolution reconstruction of its shape. From the outcome of the *ab initio* data analysis, the structure of proNGF appears to be very anisometric if compared with the compact NGF dimer, suggesting that the pro-peptide domains have a rather extended conformation. Both the *ab initio* shape reconstruction based on dummy residues, and the modelling through addition of the missing portions to the NGF dimer, gave as an output two configurations of the N-termini, both equally nicely fitting to the scattering data.

In one configuration, rm-proNGF can be depicted as a “crab-like” shape, composed by the compact core of the NGF dimer and by the two “arms” that represent the pro-regions of the protein.

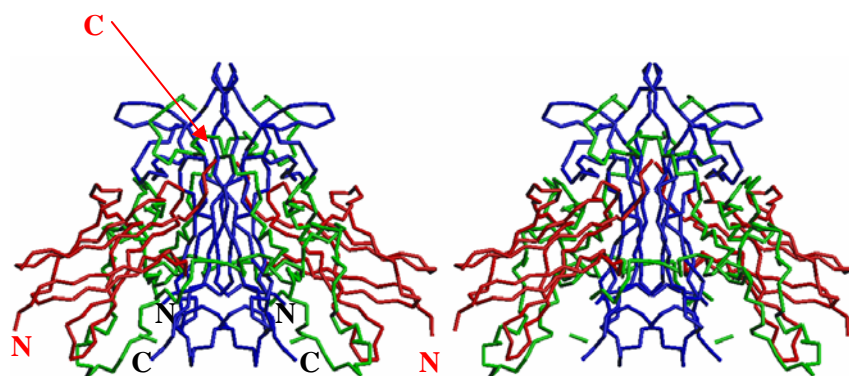
The flexible arms of proNGF partially hinder the binding region of NGF that has been shown to be involved in the interaction with Ig-like domain d5 of TrkA (Wiesman *et al*, 1999) (see panel A in figure). This clearly supports the lower level of TrkA activation in comparison to NGF, as previously observed (Fahnestock *et al*. 2004) and confirmed by the bioassays presented in this Thesis, both in the differentiation experiments of PC12 cells and in the TrkA phosphorylation assays. Both experiments, indeed, have shown that proNGF is able to trigger signaling through the TrkA receptor and cell differentiation, although to a lower extent than mature NGF. It is noteworthy that our assays have been carried out with the short

proNGF form, while all the previously reported studies were performed using the long proNGF form (Lee *et al.*, 2001, Fahnstock *et al.*, 2004) (see Introduction).

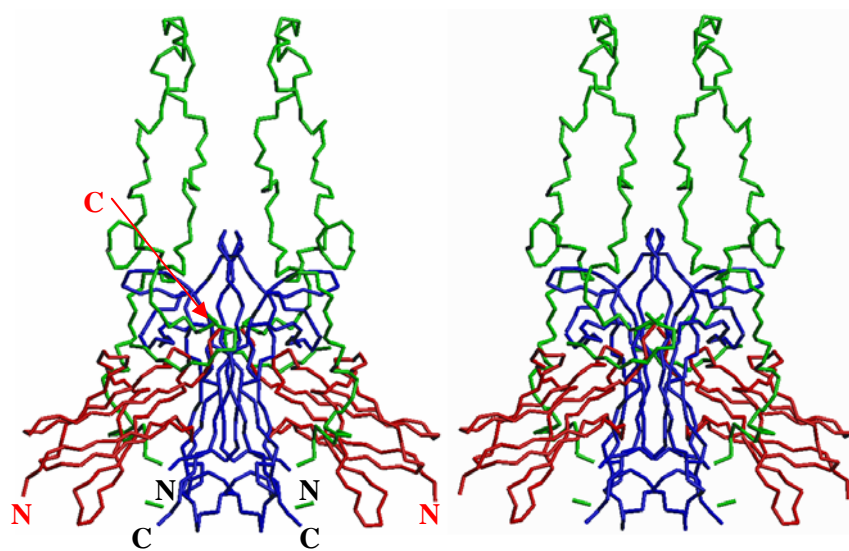
The SAXS-based model of the short form of proNGF is also in agreement with the reported interaction between NGF and the p75^{NTR} receptor, as observed in the crystal structure and in the solution X-ray scattering studies of the NGF-p75^{NTR} complex (He and Garcia, Science, 2004; Aurikko *et al.*, JBC, 2005). The regions of NGF interacting with p75^{NTR} are orthogonal to the pro-peptide regions with respect to the NGF dimer. Therefore it is tempting to speculate that the interaction between p75^{NTR} and the NGF region of proNGF is not affected by the pro-peptide, which in turn could even provide a further “hot site” for binding, supporting the reported increased affinity of p75^{NTR} to proNGF with respect to NGF (Lee *et al.*, 2001). This is true for both the models with one and two molecules of p75^{NTR} bound to one NGF monomer, as reported respectively in the crystal structure (He and Garcia, Science, 2004) and in the SAXS models (Aurikko *et al.*, JBC, 2005). The SAXS model of proNGF presented in this thesis where superimposed with both the possible stoichiometries for the binding to p75^{NTR} (see panels C and C' in figure). The SAXS model for proNGF, however, does not allow to distinguish between one or the other stoichiometry due to the fact that no high resolution structure is obtained. From the superimposition, indeed, both models could be possible.

An alternative model yielding an equally good fit of the experimental data is characterized by an elongated rod-like shape with the pro-regions protruding outwards on the opposite side of the N- and C-termini of NGF. This model is also compatible with the above biological data in as much as the NGF moiety is free to interact with the Ig-like domain d5 of TrkA (see panel B in figure), still exposing an elongated and even more extended surface available for p75^{NTR} receptor binding (see panel D and D' in figure, for the monomeric and dimeric p75^{NTR}-NGF complex respectively).

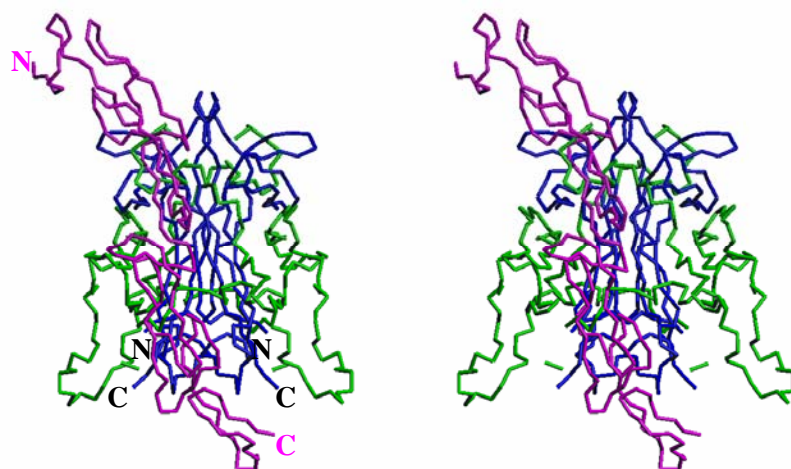
A

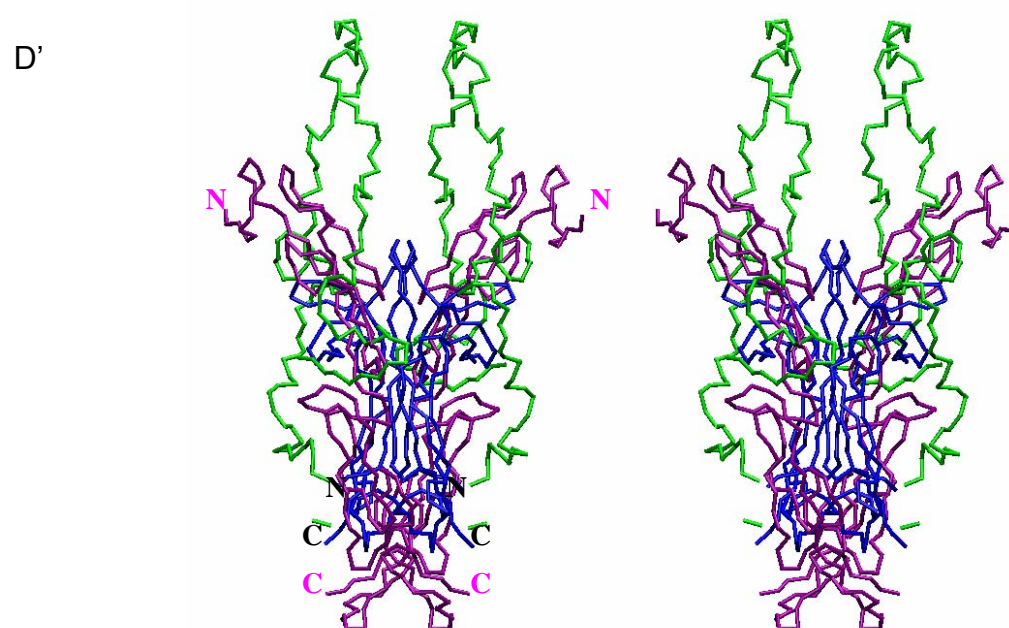
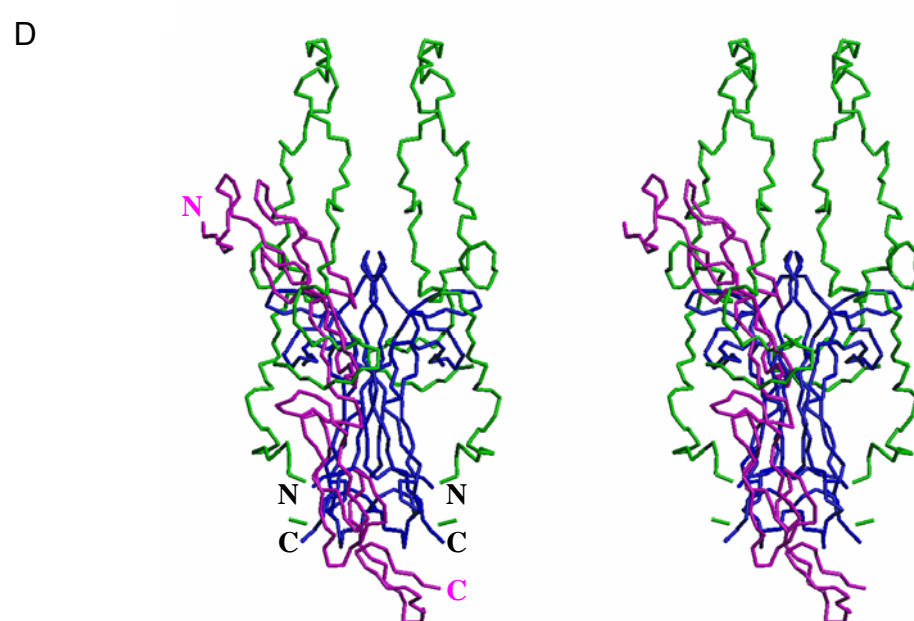
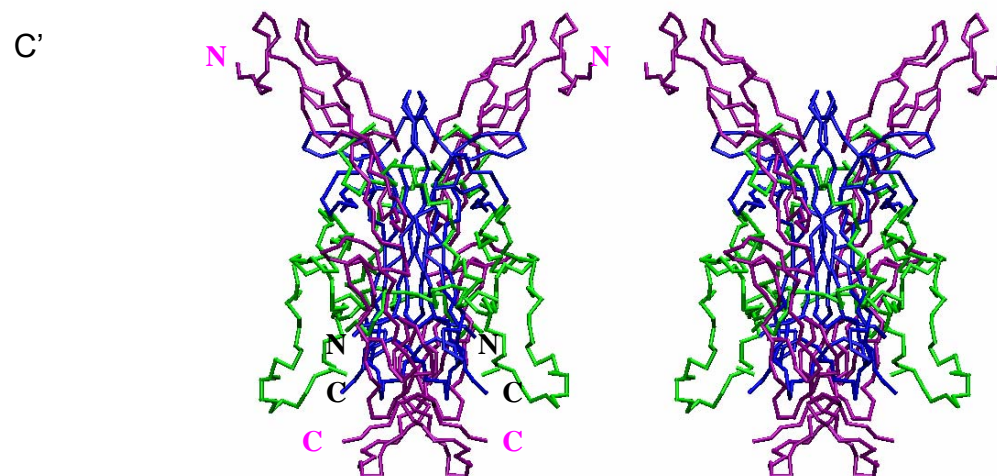


B



C





Stereo-views of the SAXS-derived models of proNGF superimposed on the 3D-crystal structures of the complexes of NGF with its receptors (see details in Material and Methods section). ProNGF models “crab-like” and “elongated” in complex with the Ig-like domain d5 of TrkA colored in red (Panel **A** and **B**) and in complex with p75^{NTR} receptor colored in magenta, both as monomer like in the crystal structure of the complex NGF/p75NTR (Panel **C** and **D**) and as dimer, like in the SAXS complex (Panel **C'** and **D'**). In the models, NGF and the pro-regions are colored in blue and in green respectively. The N- and C-termini of NGF, Ig-like domain d5 of TrkA and p75^{NTR} receptor are indicated.

Altogether the SAXS data therefore prompt to an extended conformation of the pro-sequence of proNGF suggesting a significant level of flexibility and the existence in solution of an equilibrium between a range of conformations. This was also anticipated by the analysis on the aminoacid sequence by FoldIndex© web server (Prilusky *et al*, 2005). The discussed models may represent the extremes of a range of conformations characterizing an intrinsic disorder of the pro-peptide region.

A set of BIAcore data on the binding of rm-proNGF towards the two receptors (TrkA and p75^{NTR}) equally point to an active role of proNGF in receptor binding. As also previously reported for similar experiments performed with the human short proNGF protein (Nykjaer *et al.*, , Nature, 2004), no important difference was found in the kinetic properties of the binding of proNGF towards these receptors, although the experiments performed *in vivo* reported an increased affinity of proNGF for the p75^{NTR} receptor. An explanation for the change in binding properties in the different experiments was already stated in the paper by Nykjaer and colleagues: the p75^{NTR} could become a high affinity receptor for proNGF only upon interaction with the specific sortilin receptor, and this might explain the different behavior observed *in vivo* and *in vitro* for binding experiments. It should be noted that the BIAcore experiments presented in this Thesis and the one previously reported (Nykjaer *et al.*, Nature, 2004) were performed with different receptors forms. The proteins used in the present experiments are in the immunoadhesin format (Cattaneo *et al*, 1999, Chamow 1996), therefore they are substantially different from the solely extracellular domains used in the previously reported experiments; moreover, the source of the protein is different, and this might introduce a further level of complication, represented for example by the different glycosylation patterns.

The discovery of Sortilin as a specific receptor for proNGF introduces a further actor on the scene, and it would be interesting to perform a complete structural/functional set of studies involving proNGF and all its binding partners.

As far as the stoichiometry of the complex NGF/p75^{NTR} concerns, from our experiments with BIAcore no further insight into the discrepancy of the stoichiometry of the p75^{NTR}/NGF complex, due to the design chosen for the presented experiments. In fact, by immobilizing the immunoadhesin receptor on the chip surface and using the neurotrophin as analyte in solution, only a direct binding can be observed and a 1:1 interaction is analyzed.

Indeed, to clarify this point, a further set of BIAcore experiments was already designed and planned, by selecting a sandwich approach in the experiment. In particular, the p75^{NTR} will be first bound on the chip surface, then NGF/proNGF will be injected on the surface and subsequently p75^{NTR} will be injected. With this approach, if a binding of the second p75^{NTR} will be observed, this will mean that two p75^{NTR} molecules can bind one NGF dimer (1:1 complex – like proposed by Aurikko and colleagues (JBC, 2005). On the other side, if the second p75^{NTR} molecule will not bind, the asymmetric 1:2 complex would be more likely, as suggested by He and Garcia (Science, 2004). To complete the experiment, the same kind of approach will be used also for the TrkA and for the investigation of the possible formation of the hetero-complex NGF-p75^{NTR}-TrkA, always keeping in mind the discrepancy of the upside-down orientation of the two receptors versus NGF according to the available crystal structures of the complex of NGF with the two receptors. Finally, it would be interesting to check if any difference can be observed in the sandwich format by comparing the binding of NGF and proNGF.

Besides the binding properties of rm-proNGF towards the receptors, a detailed analysis was also performed for the binding *versus* a panel of well characterized anti-NGF monoclonal antibodies, that were tested for binding both by ELISA assay and BIAcore experiments. The availability of these antibodies for a binding study allowed to use them as structural probes, to add pieces of information on the different way of binding between NGF and proNGF and of the possible functional role of the pro-peptide.

The binding experiments were particularly deepened in the case of the α D11 anti-NGF monoclonal antibody, since it is at the basis of the AD11 mouse model for AD (Ruberti *et al*, 2000, Capsoni *et al*, 2000). In particular, it was interesting to verify

that there was both a qualitative and a quantitative difference between NGF and proNGF towards the binding to the antibody. The binding of the antibody to NGF was found to be characterized by a smaller dissociation constant than in the case of proNGF ($KD = 10^{-12}$ and 10^{-9} for NGF and proNGF respectively). Overall, the antibody is then characterized by higher affinity for NGF than for proNGF, with a different kinetics of binding towards the two neurotrophins forms. From the analysis of these data a fascinating hypothesis for the role of proNGF in the neurodegeneration of AD11 mice can arise. Since the binding of the α D11 antibody is stronger for NGF than for proNGF, it could be possible that in the brain of these mice NGF is less abundant, because almost irreversibly “sequestered” by the antibody; on the contrary, given the equilibrium present in binding α D11/proNGF, the latter would result to be more abundant and therefore free to interact with its partners. In particular, proNGF could activate the apoptosis pathway through interaction with the sortilin and $p75^{NTR}$ receptors. To prove this hypothesis, it will be crucial to perform the experiments aimed to reveal the relative quantities of NGF and proNGF in the brains of the AD11 mice and to compare them to control ones. The preliminary results obtained in this Thesis to optimize the detection of NGF and proNGF in tissues was till now performed in submandibular glands and the data are encouraging, opening the way for the next step on brain homogenates, to verify the validity of the hypothesis.

In the frame of the interpretation of the binding of the neurotrophins to α D11 antibody, SAXS analysis additionally confirmed the different binding mode of the antibody to NGF and proNGF. The SAXS measurements performed on the complex Fab α D11/rm-proNGF, although not yet completely analyzed, allowed to state, that the complex formation of the Fab of α D11 with rm-proNGF was in fact different from the one with NGF. The latter complex was recently analyzed and its structural organization is becoming available (Covaceuszach *et al.*, manuscript in preparation); it was therefore possible to compare these data to those of proNGF. It emerged that the regions involved in the contact between the Fab and NGF are partially hindered from the pro-peptide of proNGF, both in the globular “crab-like” and in the extended “rod-like” forms. A preliminary analysis suggests that it is quite likely that binding to the antibody will be looser in the case of proNGF, due to steric hindrance. A more accurate analysis of the SAXS data and hopefully the possibility of achieving the

crystallization of the discussed complexes should allow to shed new light on the problem and give a sound answer to the question.

In the context of a wider comprehension of the biological role of proNGF, one point that remains still obscure deals with the different physiological function, if any, of the two main proNGF forms: the short and the long ones (Edwards *et al*, 1986).

Aiming at unraveling the different functions of the proNGF forms, it would be also interesting to check if the *in vitro* results presented in the Thesis for the short form of rm-proNGF would be reproducible also with the long form, and to what extent. For this purpose, the effort was made to establish a similar refolding protocol for the expression of the long rm-proNGF form in inclusion bodies of *E. coli* as it was established for the short one. The expression and refolding of the long construct was achieved, although the procedure for the purification of this protein still needs some optimization steps. This fact, however, might already represents a difference in the behavior of the short and the long proNGF, and a more accurate investigation of the biochemical properties of the two proteins could probably help in unraveling those differences.

Besides the biochemical – biophysical analysis of rm-proNGF, a new tool was developed for a more accurate analysis of the protein-protein interactions of this protein: an anti-proNGF antibody. This novel antibody was selected in the scFv format using to the IACT technology for the selection of intrabodies (Visintin *et al*, 1999 and 2004), and its complete biochemical-biophysical characterization was carried out. The antibody properties turned out to be very interesting, being characterized by quite a high affinity constant, a high specificity towards the antigen and very low cross reactivity, as revealed both by ELISA assay and BIAcore analysis. Moreover, the scFv was proven to be quite soluble, both *in vitro* and *in vivo*, and to have a low tendency to aggregate, according to gel filtration experiments.

To widen the application of this scFv, its expression in *E. coli* was optimized. The usual technique for the *in vitro* expression of these proteins is in fact usually achieved in the periplasm of *E. coli*, that allows the formation of the disulfide bridges formation in the recombinant protein. However, the reduced space represented by the periplasm of *E. coli* and the fact that the disulfide-bond isomerases helping the oxidation of the Cystein residues are not optimized for the recombinant protein expression, produce the disadvantage of a low amount of purified protein. In this Thesis, a new procedure for the refolding of the scFv from inclusion bodies in *E. coli*

was optimized, based on the previously reported data for refolding of scFv (Umetsu et al., 1999). However, instead of the described refolding by dialysis, the refolding by dilution was employed, which allowed the expression and purification of reasonably high amount of protein. The optimization of the purification procedure was carried out and the protein was finally characterized from a biochemical – biophysical point of view. It showed the correct folding and the same binding properties of the one obtained by traditional expression means. The optimized refolding technique was therefore proven to be a valid tool for the expression and purification of the scFv and increases the chances both to have high amounts of protein for structural and biochemical studies and to apply the same technique to other scFv selected via the same technique.

Due to its interesting properties, the study of the scFv anti-proNGF will be further developed. For example, the possibility will be checked that this scFv has blocking properties, that would allow a wider applications spectrum.

A further investigation was performed to characterize the scFv anti-proNGF also from the structural point of view. As a first approach, the structural analysis was performed using the SAXS technique: it was quite interesting to notice that the scFv sample resulted to be reasonably monodisperse, containing mainly the monomeric form, although a minor fraction of dimeric protein was also detected. Despite the reasonably good quality of the data and the availability of a homology modeling to the most similar scFv by sequencing alignment with proteins of known crystallographic structure, it was not yet possible to reconstruct a model for the protein in solution. It is most likely that the dimeric form of scFv, although as minor component, contributes to the build-up of strong interpolymeric interactions strongly affecting the interpretation of the data of the sample in solution. The analysis is currently ongoing to reconstruct the model according to the available homology modelling for both a monomer and a dimer of scFv, taking into account the relative amounts of each component present in solution. By considering all these parameters, it should be possible to reconstruct the best model for the monomeric scFv fitting with the experimental SAXS data.

A step forward aimed at a preliminary structural analysis of the complex between anti-proNGF scFv and rm-proNGF. However, the solution was quite polydisperse, indicating that both the complex and the single components were present. Moreover, the complex was not the major component in the solution, making

it not possible to reconstruct a model for it. Further analysis in this sense will be necessary to isolate better stoichiometric and biochemical conditions for the formation of the complex in solution.

Due to the difficulties encountered with the SAXS analysis, but taking in account the reasonably good biochemical behavior of the anti-proNGF scFv in solution, one of the future goals will include the designing of a crystallographic screening for the structural analysis of the complex. Indeed, it has been demonstrated that antibodies, also in the scFv form, can be a valid aid in helping the crystallization of flexible protein (Kovari *et al*, Structure, 1995; Shea *et al*, J Str Func Genomics, 2005). In the present case, although the flexibility of the pro-peptide of proNGF makes the crystal formation impossible, it could be stabilized by the presence of the scFv, which could help “fixing” the region corresponding to its epitope. These experiments are currently under design, looking for the best operating conditions, and might represent an important tool towards the determination of the 3D-structure of m-proNGF at high resolution.

Albeit not conclusive, the outcomes of these studies open up interesting possibilities for further scientific developments and applications. In particular, the former will include a more extensive biochemical analysis through the optimization of the *in vitro* expression of the alternative form of proNGF and of some of its fusion proteins. Likewise, a wider structural analysis will be performed, which should allow the reconstruction of the binding of proNGF towards both its receptors and its antibodies, and contribute to the understanding of some of the biological results still not completely understood. At the same time, a complete analysis of the different forms of proNGF would shed light on the biological role of these protein forms *in vivo*, including the comparison of behavior in normal and in pathological conditions. For this reason, a further line of development of this project would include more application-targeted aspects.

The possibility was verified to obtain large amounts of mature mouse NGF by cleavage of rm-proNGF, as already reported for the recombinant-human proNGF (Rattenholl *et al.*, 2001). The procedure of the proteolysis with trypsin was optimized according to the previously available data and it was verified that also in the case of the mouse proNGF it was possible to achieve a high efficiency of cleavage to obtain intact and pure NGF. It was interesting to verify, by mass spectrometric analysis, that the cleaved m-NGF was intact, and that no further cleavage due to trypsin had taken

place, neither at N-terminus nor at C-terminus, at variance with what was previously reported for the human proNGF. The efficiency of the protein cut from proNGF as a growth factor was tested in differentiation experiments of PC12 cells, which demonstrated that the cleaved m-NGF could be as efficient as a commercial one in inducing cell differentiation, from a qualitative point of view. This result represented the extension of previously reported data in the recombinant production of NGF (Rattenholl *et al.*, 2001), and might represent a valid alternative to the traditional way of producing of m-NGF by extraction from submandibular glands. Moreover, a further improvement of the approach could come from the use of furin as a protease instead of trypsin. As it was demonstrated in a series of experiments of this Thesis, in fact, recombinant furin was found to be very efficient in the cleavage of proNGF to release mature NGF. The optimization of this procedure needs however still to be finalized, to find out the best conditions for a purification of the cleavage product.

Among other possible applications of the results of this Thesis, one should mention the availability of the scFv anti-proNGF. Indeed, this scFv represents, as far as we know, the first monoclonal anti-proNGF antibody, and this is already a relevant outcome, that opens many possible applications. Moreover, the scFv was selected as a recombinant protein, and this fact represents by itself the possibility of a versatile tool in the use of the antibody.

One of most interesting applications of the newly selected anti-proNGF antibody, will be its use as a tool to study the cell biology of proNGF, and in particular by looking at the distribution of the protein inside the cell and for a better understanding of the interaction with sortilin.

From the available literature on sortilin and proNGF, the main point raised is that sortilin is involved in the apoptosis induced by proNGF, together with p75, and that sortilin is indeed necessary to induce apoptosis. Of course, it is not yet clear, in which way does sortilin contributes to the apoptotic effect of proNGF. As also stated in the Introduction, by referring on the recent review by Bronfman and Fainzilber (EMBO reports, 2004), it has been proposed that pro-neurotrophin/Sortilin interactions could commence intracellularly within the secretory pathway. Sortilin binding to the pro-domain of the neurotrophin in the Golgi apparatus protects it from proteolytic cleavage, and the molecules could then travel to the cell surface in a preformed pro-apoptotic p75-activating complex. Therefore, Sortilin regulation might be a way for the cell to possess a mechanism of active suicide. Alternatively, cell-

surface cleavage of Sortilin could release a soluble Sortilin/pro-neurotrophin complex into the extracellular space. This kind of complex could represent a circulating reservoir of pro-neurotrophin protected from cleavage to the mature form and available for interaction with receptors on adjacent or distant cells. The representation of this proposed scenario is represented in fig. 3.2.5 of the Introduction (p.30).

In particular, to the aim of unravelling the function of sortilin in the proNGF intracellular pathway, the anti-proNGF antibody could be used as an intrabody (Biocca and Cattaneo, Trends in Cell Biology, 1995; Cattaneo and Biocca, 1997). Among other applications in this respect, one possible use could be to target the antibody to different stages of the secretory pathway, in order to be able to identify (by immunoprecipitation followed by western blotting) at which stage inside the cell it happens the actual processing of proNGF.

Moreover, the selection of this scFv anti-proNGF is an important result not only for the availability of a tool for the biochemical analysis of m-proNGF through the analysis of its interactions with different partners, but also as a tool to detect and quantify the presence of proNGF in pathological tissues. In principle, the anti-proNGF scFv could be used as a diagnostic and imaging tool, for the detection of proNGF as a disease marker.

Taken together, the outcomes of this Thesis allow to validate the hypothesis that proNGF may be considered as a moonlighting protein that exposes different interacting/binding regions to its partners depending on the physiological cellular conditions. In conclusion, proNGF is confirmed to be an emerging actor in the complex scenario of neurotrophins, and in particular in the subtle equilibrium that involves them in the fate of a cell to live or die.

CONCLUDING REMARKS

The work presented in this Thesis will be subject of publications. In particular:

- the first part of the results will be presented in the following manuscript in preparation:

Title: STRUCTURAL DISORDER THROWS NEW LIGHT ON proNGF MOONLIGHTING

Authors: Francesca Paoletti, Sonia Covaceuszach, Peter V. Konarev, Elisabeth Schwarz, Dmitri I. Svergun, Antonino Cattaneo and Dorian Lamba

- the second part of the thesis was the subject of a patent query:

Patent title: Compositions able to prevent neurodegenerative processes and methods of assaying the same

Patent number: WO2005044293

Patent inventors: Capsoni Simona, Cattaneo Antonino, Covaceuszach Sonia, Paoletti Francesca, Visintin Michela

Application number: WO2004IT00612 20041108

Publication date: 2005-05-19

REFERENCES

- Angeletti P.U., Levi-Montalcini R., Caramia F., Ultrastructural changes in sympathetic neurons of newborn and adult mice treated with Nerve Growth Factor, *Journal of Ultrastructure Research* (1971) **36**, 24-26
- Aurikko J.P., Ruotolo B.T., Grossmann G.J., Moncrieffe M.C., Stephens E., Leppänen V-M., Robinson C.V., Saarma M., Bradshaw R.A., Blundell T.L., Characterization of symmetric complexes of nerve growth factor and the ectodomain of the pan-neurotrophin receptor, p75^{NTR}, *The Journal of Biological Chemistry* (2005) **280**, 33453-33460
- Barde Y.A., Death of injured neurons caused by the precursor of nerve growth factor, *Proceedings National Academy of Science* (2004) **101**, 5703-5704
- Barker P.A., p75NTR is positively promiscuous: novel partners and new insights, *Neuron* (2004) **42**, 529-533
- Bax B., Blundell T.L., Murray-Rust J., McDonald N.Q., Structure of mouse 7S NGF: a complex of nerve growth factor with four binding proteins, *Structure* (1997) **15**, 1275-1285
- Beattie M.S., Harrington A.W., Lee R., Kim J.Y., Boyce S.L., Longo F.M., Bresnahan J.C., Hempstead B.L., Yoon S.O., ProNGF induces p75-mediated death of oligodendrocytes following spinal cord injury, *Neuron* (2002) **36**, 375-386
- Berger E.A., Shooter E.M., Evidence for pro-b-nerve growth factor, a biosynthetic precursor to b-nerve growth factor, *Proceedings National Academy of Science* (1977) **74**, 3674-3651
- BIACore Application Note 38, BIACORE AB, Uppsala, Sweden
- Bierl M.A., Isaacson L.G., Increased NGF proforms in aged sympathetic neurons and their targets, *Neurobiology of aging* (2005) [Epub ahead of print]
- Bierl M.A., Jones E.E., Crutcher K.A., Isaacson L.G., "Mature" nerve growth factor is a minor species in most peripheral tissues, *Neuroscience Letters* (2005) **380**, 133-137
- Biocca S., Cattaneo A., Intracellular immunization: antibody targeting to subcellular compartments, *Trends in Cell Biology* (1995) **5**, 248-252

Bocchini V., Angeletti P.U., The Nerve Growth Factor: purification as a 30,000-molecular-weight protein, *Proceedings National Academy of Science* (1969) **64**, 787-794

Boulin, C. J., Kempf, R., Gabriel, A. & Koch, M. H. J.. *Nucl. Instrum. Meth. A* (1988) **269**, 312-320

Bradshaw R.A., Blundell T.L., Lapatto R., McDonald N.Q., Murray-Rust J., Nerve Growth Factor revisited, *Trends in Biochemical Sciences* (1993) **18**, 48-52

Bronfman F.C., Fainzilber M., Multi-tasking by the p75 neurotrophin receptor: sortilin things out?, *EMBO reports* (2004) **5**, 867-871

Calissano P., Cattaneo A., Biocca S., Aloe L., Mercanti D., Levi-Montalcini R., The Nerve Growth Factor. Established findings and controversial aspects, *Experimental Cell Research* (1984) **154**, 1-9, Academic Press

Capsoni S., Ugolini G., Comparini A., Ruberti F., Berardi N., Cattaneo A., Alzheimer-like neurodegeneration in aged antinerve growth factor transgenic mice, *Proceedings National Academy of Science* (2000) **97**, 6826-6831

Capsoni S., Giannotta S., Cattaneo A., β -Amyloid Plaques in a model for sporadic Alzheimer's Disease based on transgenic anti-Nerve Growth Factor antibodies, *Molecular and Cellular Neuroscience* (2002) **21**, 15–28

Cattaneo A., Biocca S., Intracellular antibodies: development and applications (Cattaneo, A., & Biocca S. eds), Springer-Verlag, New York USA (1997)

Cattaneo A., Biocca S., The selection of intracellular antibodies, *Trends in Biotechnology* (1999) **17**, 115-121

Cattaneo A., Capsoni S., Margotti E., Righi M., Kontsekkova E., Pavlik P., Filipcik P., Novak M., Functional blockade of Tyrosine Kinase A in the rat basal forebrain by a novel antagonistic anti-receptor monoclonal antibody, *The Journal of Neuroscience* (1999) **19**, 9687-9697

Cattaneo A., Rapposelli, B. and Calissano, P., Three distinct types of monoclonal antibodies after long-term immunization of rats with mouse nerve growth factor, *Journal of Neurochemistry* (1988) **50**, 1003-10

Chamow S.M., Ashkenazi A., Immunoadhesins: principles and applications, *Trends in Biotechnology* (1996) **14**, 52-60

Chao M.V., Neurotrophins and their receptors: a convergence point for many signalling pathways, *Nature Reviews Neuroscience* (2003) **4**, 299-309

Chao M.V., Bothwell M.A., Neurotrophins. To cleave or not to cleave, *Neuron* (2002) **33**, 9-12

Chao M.V., Bothwell M.A., Ross A.H., Koprowski H., Lanahan A.A., Buck R.C., Sehgal A., Gene Transfer and molecular cloning of the human NGF receptor, *Science* (1986) **232**, 518-521

Chao M.V., Hempstead B.L., p75 and Trk: a two-receptor system, *Trends in Neuroscience* (1995) **18**, 321-326

Chapman B.S., Kuntz I.D., Modeled structure of the 75-kDa neurotrophin receptor, *Protein Science* (1995) **4**, 1696-1707

Clos J., Dicou E., Two peptides derived from the nerve growth factor precursor enhance cholinergic enzyme activities in vivo, *Developmental Brain Research* (1997) **99**, 267-270

Cohen S., Levi-Montalcini R., A nerve growth-stimulating factor isolated from snake venom, *Proceedings National Academy of Science* (1956) **42**, 571-574

Cohen S., Purification and metabolic effects of a nerve growth-promoting protein from snake venom, *Journal of Biological Chemistry* (1959) **234**, 1129-1137

Cohen S., Purification of a nerve-growth promoting protein from the mouse salivary gland and its neuro-cytotoxic antiserum, *Proceedings National Academy of Science* (1960) **46**, 302-311

- Colangelo A.M., Finotti N., Ceriani M., Alberghina L., Martegani E., Aloe L., Lenzi L., Levi-Montalcini R., Recombinant human nerve growth factor with a marked activity *in vitro* and *in vivo*, *Proceedings National Academy of Science* (2005) **102**, 18658-18663
- Counts S.E., Mufson E.J., The role of Nerve Growth Factor receptors in cholinergic basal forebrain degeneration in prodromal Alzheimer Disease, *Journal of Neuropathological Experimental Neurology* (2005), **64**, 263-272
- Covaceuszach S., Cassetta A., Cattaneo A., Lamba D., Purification, crystallization, X-ray diffraction analysis and phasing of a Fab fragment of monoclonal neuroantibody α D11 against nerve growth factor, *Acta Crystallographica Section D – Biological Crystallography* (2004) **D60**, 1323-1327
- De Rosa R., Garcia A.A., Braschi C., Capsoni C., Maffei L., Berardi N., Cattaneo A., Intranasal administration of nerve growth factor (NGF) rescues recognition memory deficits in AD11 anti-NGF transgenic mice, *Proceedings National Academy of Science* (2005) **102**, 3811–3816
- Dicou E., Expression of recombinant human nerve growth factor in *Escherichia coli*, *Neurochemistry International* (1992) **20**, 129-134
- Dicou E., Nerrière V., Evidence that natural autoantibodies against the nerve growth factor (NGF) may be potential carriers of NGF, *Journal of Neuroimmunology* (1997) **75**, 200-203
- Dicou E., Pflug B., Magazin M., Lehy T., Djakiew D., Ferrara P., Nerrière V., Harvie D., Two peptides derived from the Nerve Growth Factor Precursor are biologically active, *The Journal of Cell Biology* (1997) **136**, 389–398
- Diederichs, K. (1995) *Proteins*, **23**, 187-195.
- Dirr H., Reinemer P., Huber R., X-ray crystal structures of cytosolic glutathion S-transferases, *European Journal of Biochemistry* (1994) **220**, 645-661
- Edwards R.H., Selby M.J, Garcia P.D., Rutter W.J., Processing of the native Nerve Growth Factor precursor to form biologically active nerve growth factor, *The Journal of Biological Chemistry* (1988) **263**, 6810-6815

Edwards R.H., Selby M.J, Rutter W.J., Differential RNA splicing predicts two distinct nerve growth factor precursors, *Nature* (1986) **319**, 784-787

Evan, G.I., Lewis, G.K., Ramsay, G. and Bishop, J.M., Isolation of monoclonal antibodies specific for human c-myc proto- oncogene product, *Molecular and Cellular Biology* (1985) **5**, 3610-3616

Fahnestock M., Michalski B., Xu B., Coughlin M.D., The precursor pro-Nerve Growth Factor is the predominant form of Nerve Growth Factor in brain and is increased in Alzheimer's Disease, *Molecular and Cellular Neuroscience* (2001) **18**, 210-220

Fahnestock M., Scott S.A., Jetté N., Weingartner J.A., Crutcher K.A., Nerve growth factor mRNA and protein levels measured in the same tissue from normal and Alzheimer's disease parietal cortex, *Molecular Brain Research* (1996) **42**, 175-178

Fahnestock M., Yu G., Coughlin M.D., ProNGF: a neurotrophic or an apoptotic molecule?, *Progress in Brain Research* (2004) **146**, 101-110

Fahnestock M., Yu G., Michalski B., Mathew S., Colquhoun A., Ross G.M., Coughlin M.D., The nerve growth factor precursor proNGF exhibits neurotrophic activity but is less active than mature nerve growth factor, *Journal of Neurochemistry* (2004) **89**, 581-592

Farhadi H., Pareek S., Day R., Dong W., Chrétien M., Bergeron J.J.M., Seidah N.G., Murphy R.A., Prohormone convertases in mouse submandibular gland: co-localization of Furin and Nerve Growth Factor, *The Journal of Histochemistry and Cytochemistry* (1997) **45**, 795-804

Gill, S. C. & von Hippel, P. H.,. Calculation of protein extinction coefficients from amino acid sequence data. *Analytical Biochemistry* (1989) **182**, 319-326.

Greene L.A., Tischler A.S., Establishment of a noradrenergic clonal line of rat adrenal pheochromocytoma cells which respon to nerve growth factor, *Proceedings National Academy of Science* (1976) **73**, 2424-2428

Guinier, A. *Ann. Phys. (Paris)* (1939).**12**, 161-237.

Hanke, T., Szawlowski, P. and Randall, R.E. Construction of solid matrix-antibody-antigen complexes containing simian immunodeficiency virus p27 using tag-specific monoclonal antibody and tag-linked antigen, *Journal of Genetic Virology* (1992) **73**, 653-60

Harrington A.W., Leiner B., Blechschmitt C., Arevalo J.C., Lee R., Mörl K., Meyer M., Hempstead B.L., Yoon S.O., Giehl K.M., Secreted proNGF is a pathophysiological death-inducing ligand after adult CNS injury, *Proceedings National Academy of Science* (2004) **101**, 6226-6230

He X., Garcia C.K., Structure of Nerve Growth Factor complexed with the shared neurotrophin receptor p75, *Science* (2004) **304**, 870-875

Hefti F., Nerve Growth Factor promotes survival of septal cholinergic neurons after fimbrial transections, *The Journal of Neuroscience* (1986) **6**, 2155-2162

Hempstead B.L., Martin-Zanza D., Kaplan D.R., Parada L.F., Chao M.V., High-affinity NGF binding requires coexpression of the trk proto-oncogene and the low-affinity NGF receptor, *Nature* (1991) **350**, 678-683

Hempstead B.L., The many faces of p75^{NTR}, *Current Opinion in Neurobiology* (2002) **12**, 260-267

Hogue Angeletti R., Bradshaw R.A., Nerve Growth Factor from mouse submaxillary gland: amino acid sequence, *Proceedings National Academy of Science* (1971) **68**, 2417-2420

Holliger P., Hudson P.J., Engineered antibody fragments and the rise of single domains, *Nature Biotechnology* (2005) **23**, 1126-1136

Ibáñez C.F., Emerging themes in structural biology of neurotrophic factor, *Trends in Neuroscience* (1998) **21**, 438-444

Ibáñez C.F., Jekyll-Hyde neurotrophins: the story of proNGF, *Trends in Neuroscience* (2002) **25**, 284-286

Jäger M., Plückthun A., Domain interactions in antibody Fv and scFv fragments: effects on unfolding kinetics and equilibria, *FEBS Letters* (1999) **462**, 307-312

Jones, T. A., Zou, J. Y., Cowan, S. W., Kjeldgaard M., *Acta Crystallographica. Section. A* (1991) **47**, 110-119.

Kabat E.A., Wu T.T., Perry H.M., Gottesman K.S., Foeller C., Sequences of proteins of immunological interest, 5th Ed., United States Department of Health and Human Services, Public Health Service, National Institutes of Health, NIH Publications No. 91, 3242, 1991

Kaplan D.R., Miller F.D., A move to sort life from death, *Nature* (2004) **427**, 798-799

Kilmartin, J. V., Wright, B., Milstein, C., Rat monoclonal antitubulin antibodies derived by using a new nonsecreting rat cell line. *The Journal of Cellular Biology* (1982) **93**, 576-582

Kliemann M., Rattenholl A., Golbik R., Balbach J., Lilie H., Rudolph R., Schwarz E., The mature part of proNGF induces the structure of its pro-peptide, *FEBS Letters* (2004) **566**, 207-212

Koch, M. H. J. & Bordas, J., *Nucl. Instrum. Methods* (1983) **208**, 461-469

Konarev, P. V., Volkov, V. V., Sokolova, A. V., Koch, M. H. J. & Svergun, D. I.. *J. Appl. Crystallogr.* (2003) **36**, 1277-1282.

Korsching S., Thoenen H., Two-site enzyme immunoassay for nerve growth factor. In: "*Methods in Enzymology*" (1987) **147**, 167-185, Academic Press

Kovari L.C., Momany C., Rossmann M.G., The use of antibody fragments for crystallization and structure determinations, *Structure* (1995) **3**, 1291-1293

Kurokawa Y., Yanagi H., Yuras T., Overproduction of bacterial protein Disulfide Isomerase (DsbC) and its modulator (DsbD) markedly enhances periplasmic production of human Nerve Growth Factor in *Escherichia coli*, *The Journal of Biological chemistry* (2001) **276**, 14393-14399

Lee R., Kermani P., Teng K.K., Hempstead B.L., Regulation of cell survival by secreted proneurotrophins, *Science* (2001) **294**, 1945-1948

Leighton M, Kadler KE., Paired basic/Furin-like proprotein convertase cleavage of Pro-BMP-1 in the trans-Golgi network. *J Biol Chem* (2003) **278**, 18478-84.

Levi-Montalcini R., Booker B., Destruction of the sympathetic ganglia in mammals by an antiserum to a nerve-growth protein, *Proceedings National Academy of Science* (1960) **46**, 384-391

Levi-Montalcini R., Angeletti P.U., The activation of Nerve Growth Factor on sensory and sympathetic cells, in: Dehaan R.L. and Ursprung H. eds., *Organogenesis*, New York, 187-198 (1965)

Levi-Montalcini R., The Nerve Growth Factor, *Scientific American* (1979) **240**, 68-77

Levi-Montalcini R., Developmental neurobiology and the natural history of Nerve Growth Factor, *Annual Reviews Neuroscience* (1982) **5**, 341-362

Levi-Montalcini R., The Nerve Growth Factor 35 Years Later, *Science* (1987) **237**, 1154-1162

Levi-Montalcini R., Aloe L., Alleva E., A role for Nerve Growth Factor in nervous, endocrine and immune systems, *Progress in NeuroEndocrinImmunology* (1990) **3**, 1-10

Levi-Montalcini R., Dal Toso R., della Valle F., Skaper S.D., Leon A., Update of the NGF saga, *Journal of the Neurological Sciences* (1995) **130**, 119-127

Levi-Montalcini R., The Saga of the Nerve Growth Factor. Preliminary Studies, Discovery, Further Development, World Scientific Series in 20th Century Biology – Vol. 3, World Scientific Publishing, 1997

Lobos E., Gebhardt C., Kluge A., Spaniel-Borowski K., Expression of nerve growth factor isoforms in the rat uterus during pregnancy: accumulation of precursor proNGF, *Endocrinology* (2005) **146**, 1922-9.

Longo F.M., Massa S.M., Neurotrophin-based strategies for neuroprotection, *Journal of Alzheimer's Disease* (2004) **6**, S13-S17

Lu B., Pang P.T., Woo N.H., The Yin and the Yang of neurotrophin action, *Nature Reviews Neuroscience* (2005) **6**, 603-614

Mazella J., Sortilin/neurotensin receptor-3: a novel tool to investigate neurotensin signaling and cellular trafficking?, *Cellular Signalling* (2001) **13**, 1-6

McDonald N.Q., Blundell T.L., Crystallization and characterization of the high molecular weight form of nerve growth factor (7S NGF), *The Journal of Molecular Biology* (1991) **219**, 595-601

McDonald N.Q., Chao M.V., Structural determinants of neurotrophin action, *The Journal of Biological Chemistry* (1995) **270**, 19669-19672

McDonald N.Q., Lapatto R., Murray-Rust J., Gunning J., Wlodawer A., Blundell T.L., New protein fold revealed by a 2.3-Å resolution crystal structure of nerve growth factor, *Nature* (1991) **354**, 411-414

Miller T.W., Messer A., Intrabody applications in neurological disorders: progress and future prospects, *Molecular Therapy* (2005) **12**, 394-401

Mowla S.J., Pareek S., Farhadi H.F., Petrecca K., Fawcett J.P., Seidah N.G., Morris S.J., Sossin W.S., Murphy R.A., Differential sorting of Nerve Growth Factor and Brain-Derived Neurotrophic Factor in Hippocampal neurons, *The Journal of Neuroscience* (1999) **19**, 2069-2080

Murray S.S., Perez P., Lee R., Hempstead B.L., Chao M.V., A novel p75 neurotrophin receptor-related protein, NRH2, regulates Nerve Growth Factor binding to the TrkA receptor, *The Journal of Neuroscience* (2004) **24**, 2742-2749.

Narhi, L. O., Rosenfeld, R., Talvenheimo, J., Prestrelski, S. J., Arakawa, T., Lary, J. W., Kolvenbach, C. G., Hecht, R., Boone, T. & Miller, J. A.. Comparison of the biophysical characteristics of human brain-derived neurotrophic factor, neurotrophin-3, and nerve growth factor, *The Journal of Biological Chemistry* (1993) **268**, 13309-13317

Neet K.E., Campenot R.B., Receptor binding, internalization, and retrograde transport of neurotrophic factors, *Cellular and Molecular Life Science* (2001) **58**, 1021-1035

Nykjaer A., Lee R., Teng K.K., Jansen P., Madsen P., Nielsen M.S., Jacobsen C., Kliemann M., Schwarz E., Willnow T.E., Hempstead B.L., Petersen C.M., Sortilin is essential for proNGF-induced neuronal cell death, *Nature* (2004) **427**, 843-848

Nykjaer A., Willnow T.E., Petersen C.M., p75^{NTR} – live or let die, *Current Opinion in Neurobiology* (2005) **15**, 49-57

Pedraza C.E., Podlesniy P., Vidal N., Arévalo J.C., Lee R., Hempstead B., Ferrer I., Iglesias M., Espinet C., Pro-NGF isolated from the human brain affected by Alzheimer's Disease induces neuronal apoptosis mediated by p75NTR, *The American Journal of Pathology* (2005) **166**, 533-543

Petoukhov, M. V., Eady, N. A., Brown, K. A. & Svergun, D. I., Addition of missing loops and domains to protein models by X-ray Solution Scattering, *Biophysical Journal* (2002) **83**, 3113-3125

Petoukhov, M. V. & Svergun, D. I., Global rigid body modeling of macromolecular complexes against small-angle scattering data., *Biophysical Journal* (2005) **89**, 1237-50

Poo M., Neurotrophins as synaptic modulators, *Nature Reviews Neuroscience* (2001), **2**, 24-32

Porod, G.. Small-angle X-ray scattering, edited by O. Glatter & O. Kratky, pp. 17-51. London: Academic Press (1982).

Price D.L., New perspectives on Alzheimer's disease, *Annual Reviews Neuroscience* (1986) **9**, 489-512

Prilusky J., Felder C.E., Zeev-Ben-Mordehai T., Rydberg E.H., Man O., Beckmann J.S., Silman I. and Sussman, J.L. *Bioinformatics* (2005) **21**, 3435-3438.

Rattenholl A., Untersuchungen zur Pro-Sequenz-vermittelten Faltung von rekombinantem, humanen Nervenwachstumsfaktor, Dissertation zur Erlangung des akademischen Grades doctor rerum naturalium (Dr. rer. nat.) vorgelegt der Mathematisch-Naturwissenschaftlich-Technischen Fakultät der Martin-Luther-Universität Halle-Wittenberg, 2001

Rattenholl A., Lilie H., Grossmann A., Stern A., Schwarz E., Rudolph R., The pro-sequence facilitates folding of human nerve growth factor from *Escherichia coli* inclusion bodies, *European Journal of Biochemistry* (2001) **268**, 3296-3303

Rattenholl A., Ruoppolo M., Flagiello A., Monti M., Vinci F., Marino G., Lilie H., Schwarz E., Rudolph R., Pro-sequence assisted folding and disulfide bond formation of human Nerve Growth Factor, *The Journal of Molecular Biology* (2001) **305**, 523-533

Reynolds A.J., Bartlett S.E., Hendry I.A., Molecular mechanisms regulating the retrograde axonal transport of neurotrophins, *Brain Research Reviews* (2000) **33**, 169-178

Reinshagen M., Geerling I., Eysselein V.E., Adler G., Huff K.R., Moore G.P., Lakshmanan J., Commercial recombinant human β -Nerve Growth Factor and adult rat Dorsal Root Ganglia contain an identical molecular species of Nerve Growth Factor Prohormone, *Journal of Neurochemistry* (2000) **74**, 2127-2133

Ruberti F., Capsoni S., Comparini A., Di Daniel E., Franzot J., Gonfloni S., Rossi G., Berardi N., Cattaneo A., Phenotypic Knockout of Nerve Growth Factor in adult transgenic mice reveals severe deficits in basal forebrain cholinergic neurons, cell death in the spleen, and skeletal muscle dystrophy, *The Journal of Neuroscience*, (2000), **20**, 2589–2601

Rudolph, R., Böhm, G., Lilie, H. & Jaenicke, R., Folding proteins. In: Protein Function: A Practical Approach (Creighton, T.E., ed.), pp 57-99, IRL-Press, Oxford University Press, Oxford, New York, Tokyo (1997)

Sblattero D., Bradbury A., Exploiting recombination in single bacteria to make large phage antibody libraries, *Nature Biotechnology* (2000) **18**, 75-80

Schmid, F. X., Optical spectroscopy to characterize protein conformation and conformational changes, In: Protein Structure: A Practical Approach (2nd edn., Creighton, T. E., ed.), pp 261-297, IRL-Press, Oxford University Press, Oxford, New York, Tokyo. (1997)

Scott J., Selby M., Urdea M., Quiroga M., Bell G.I., Rutter W.J., Isolation and nucleotide sequence of a cDNA encoding the precursor of mouse nerve growth factor, *Nature* (1983) **302**, 538-540

Seidah N.G., Benjannet S., Pareek S., Savaria D., Hamelin J., Goulet B., Laliberté J., Lazure C., Chrétien M., Murphy R.A., Cellular processing of the nerve growth factor precursor by the mammalian pro-protein convertases, *Biochemical Journal* (1996) **314**, 951-960

Selby M.J., Edwards R., Sharp F., Rutter W.J., Mouse Nerve Growth Factor Gene: Structure and Expression, *Molecular and Cellular Biology* (1987) **7**, 3057-3064

Shamovsky I.L., Ross G.M., Riopelle R.J., Weaver D.F., The interaction of neurotrophins with the p75NTR common neurotrophin receptor: a comprehensive molecular modeling study, *Protein Science* (1999) **8**, 2223-2233

Shea C., Bloedorn L., Sullivan M.A., Rapid Isolation of single-chain antibodies for structural genomics, *Journal of Structural and Functional Genomics* (2005) **6**, 171-175

Shooter E.M., Early days of the Nerve Growth Factor proteins, *Annu. Rev. Neurosci.* (2001) **24**, 601–29

Srinivasan B., Roque C.H., Hempstead B.L., Al-Ubaidi M.R., Roque R.S., Microglia-derived Proneurotrophin promotes photoreceptor cell death via p75 neurotrophin receptor, *The Journal of Biological Chemistry* (2004) **279**, 41839-41845

Suter U., Heymach J.V., Shooter E.M., Two conserved domains in the NGF propeptide are necessary and sufficient for the biosynthesis of correctly processed and biologically active NGF, *The EMBO Journal* (1991) **10**, 2395-2400

Svensson H.G., Hoogenboom H.R., Sjöbring U., Protein LA, a novel hybrid protein with unique single-chain Fv antibody- and Fab-binding properties, *European Journal Biochemistry* (1998) **258**, 890-896

Svensson H.G., Wedemeyer W.J., Ekstrom J.L., Callender D.R., Kortemme T., Kim D.E., Sjöbring U., Baker D., Contribution of amino acid side chains to the kinetics and thermodynamics of the bivalent binding of Protein L to Ig κ light chain, *Biochemistry* (2004) **43**, 2445-2457

Svergun, D. I., Determination of the regularization parameter in indirect-transform methods using perceptual criteria, *Journal of Applied Crystallography* (1992).**25**, 495 - 503.

Svergun, D. I.. *J. Appl. Crystallogr.* (1993) **26**, 258-267.

Svergun, D. I., Barberato, C., Koch, M. H. J., CRY SOL – a program to evaluate X-ray solution scattering of biological macromolecules from atomic coordinates, *Journal Applied Crystallography* (1995). **28**, 768-773.

Svergun DI, Restoring low resolution structure of biological macromolecules from solution scattering using simulated annealing, *Biophysical Journal* (1999) **76**, 2879-86.

Svergun D.I., Koch M.H.J., Advances in structure analysis using small-angle scattering in solution, *Current Opinion in Structural Biology* (2002), **12**, 654–660

Svergun, D. I., Koch, M. H. J., Small-angle scattering studies of biological macromolecules in solution. *Reports on Progress in Physics* (2003) **66**, 1735-1782

Teng K.K., Hempstead B.L., Neurotrophins and their receptors: signaling trios in complex biological systems, *Cellular and Molecular Life Sciences* (2004) **61**, 35-48

Teng H.K., Teng K.K., Lee R., Wright S., Tevar S., Almeida R.D., Kermani P., Torkin R., Chen Z., Lee F.S., Kraemer R.T., Nykjaer A., Hempstead B.L., ProBDNF induces neuronal apoptosis via activation of a receptor complex of p75^{NTR} and Sortilin, *The Journal of Neuroscience* (2005) **25**, 5455-5463

Thoenen H., Neurotrophins and neuronal plasticity, *Science* (1995) **270**, 593-598

Thomas G., Furin at the cutting edge: from protein traffic to embryogenesis and disease, *Nature Reviews Molecular Cell Biology* (2002) **3**, 753-766

Timm D.E., Neet K.E., Equilibrium denaturation studies of mouse β -nerve growth factor, *Protein Science* (1992) **1**, 236-244

Ullrich A., Gray A., Berman C., Dull T.J., Human β -nerve growth factor gene sequence highly homologous to that of mouse, *Nature* (1983) **303**, 821-825

Umetsu M., Tsumoto K., Hara M., Ashish K., Goda S., Adschiri T., Kumagai I., How additives influence the refolding of immunoglobulin-folded proteins in a stepwise dialysis system, *The Journal of Biological Chemistry* (2003) **278**, 8979-8987

Varon S., Nomura J., Shooter E. M., The isolation of the mouse Nerve Growth Factor protein in a high molecular weight form, *Biochemistry* (1967) **6**, 2202-2209

Varon S., Nomura J., Shooter E. M., Reversible dissociation of the mouse Nerve Growth Factor protein into different subunits, *Biochemistry* (1968) **7**, 1296-1303

Visintin M., Tse E., Axelson H., Rabbitts T.H., Cattaneo A., Selection of antibodies for intracellular function using a two-hybrid *in vivo* system, *Proceedings National Academy of Science* (1999) **96**, 11723-11728

Visintin, M. and Cattaneo, A. (2001) Selecting intracellular antibodies using the two-hybrid system. In: R. Kontermann, & Dubel, S., eds (Ed) *Antibody Engineering*, Vol. 1, Springer Lab Manual. Springer, Heidelberg, Germany, p. 790.

Visintin M., Settanni G., Maritan A., Graziosi S., Marks J.D., Cattaneo A., The Intracellular Antibody Capture Technology (IACT): Towards a consensus sequence for Intracellular Antibodies, *Journal of Molecular Biology* (2002) **317**, 73-83

Visintin M., Quondam M., Cattaneo A., The intracellular antibody capture technology: towards the high-throughput selection of functional intracellular antibodies for target validation, *Methods* (2004) **34**, 200–214

Visintin M., Meli G.A., Cannistraci I., Cattaneo A., Intracellular antibodies for proteomics, *Journal of Immunological Methods* (2004) **290**, 135– 153

Westergaard U.B., Kirkegaard K., Sørensen E.S., Jacobsen C., Nielsen M.S., Petersen C.M., Madsen P., SorC3 does not require propeptide cleavage to bind nerve growth factor, *FEBS Letters* (2005) **579**, 1172-1176

Wiesmann C., Ultsch M.H., Bass S.H., de Vos A.M., Crystal structure of nerve growth factor in complex with the ligand-binding domain of the TrkA receptor, *Nature* (1999) **401**, 184-188

Woo S.B., Whalen C., Neet K.E., Characterization of the recombinant extracellular domain of the neurotrophin receptor TrkA and its interaction with nerve growth factor (NGF), *Protein Science* (1998) **7**, 1006-1016

Worn, A. and Plückthun, A., Different equilibrium stability behaviour of ScFv fragments: identification, classification, and improvement by protein engineering, *Biochemistry* (1999) **38**, 8739-50

Zampieri N., Chao M.V., The p75 NGF receptor exposed, *Science* (2004) **304**, 833-834

APPENDIX 1

SEQUENCE ALIGNMENTS

CLUSTAL W (1.82) multiple sequence alignment of NGF precursors **of different species**

```
P01138      ----MSMLFYTLITAFLLIGIQAEPHSESN----VPAGHTIPQVHWTKLQHS�DTALRRAR 52 human
Q9N2F1      ----MSMLFYTLITAFLLIGTQAEPHSESN----VPAGHTIPQAHWTKLQHS�DTALRRAR 52 chimpanzee
P01139      ----MSMLFYTLITAFLLIGVQAEPYTDSN----VPEGDSVPEAHWTKLQHS�DTALRRAR 52 mouse
P25427      ----MSMLFYTLITAFLLIGVQAEPYTDSN----VPEGDSVPEAHWTKLQHS�DTALRRAR 52 Norway rat
P20675      ----MSMLFYTLITALLIGVQAEPYTDSN----LPEGDSVPEAHWTKLQHS�DTALRRAR 52 african rat
P19093      ----MSMLFYTLITVFLIGIQAEPYSDSN----VLSGDTIPQAHWTKLQHS�DTALRRAR 52 guinea pig
P13600      -----AFLIGIQAAPHTESN----VPAGHAIPQAHWIKLQHS�DTVLRRAH 42 cow
Q29074      -----LIGIQAEPHTESN----VPAGHAIPQAHWTKLQHS�DTALRRAR 40 pig
P05200      MHSVMSMLYYTLIIAFLIGTQAAPKSEDNGPLEYPAEHS�PSTQQSNGQHIAKAAQTTH 60 chicken
P34128      ----MSMLCYTLIIAFLIGIWAAPKSEDNVPLGSPAKSDFSDTNCAQTHEGLKTSRNTDQ 56 krait
P21617      ----MSMLYYTLIIAILISVQAAPKTKDH-----APARSSAKSRIPHHTHRTKSL 46 xenopus
P34129      -----MRSSMLVLFLI-----FSAQAVAPIIGVLCVSTTAQQ 32 fish
      :      :      **      :      :      :      :      :
```

```
P01138      SAPAAA-IAARVAGQTRNITVDPRLFKKRRRLRSRVLFFSTQPPREAAQTQDLDFEVGGAA 111 human
Q9N2F1      SAPAAA-IAARVAGQTRNITVDPRLFKKRRRLRSRVLFFSTQPPPEAAQTQDLDFXVGGAA 111 chimpanzee
P01139      SAPTAP-IAARVTGQTRNITVDPRLFKKRRRLHSRVLFFSTQPPPTSSDTLDLDFQAHGTI 111 mouse
P25427      SAPAEP-IAARVTGQTRNITVDPKLFKKRRRLRSRVLFFSTQPPPTSSDTLDLDFQAHGTI 111 Norway rat
P20675      SAPAAP-IAARVTGQTRNITVDPRLFKKRRRLRSRVLFFSTQPPPTSSDTLDLDFQAHGTI 111 african rat
P19093      SAPAAP-IAARVAGQTLNITVDPRLFKKRRRLHSRVLFFSTQPPPLSTDAQDLDFEVDGAA 111 guinea pig
P13600      SAPAGP-IAARVAGQTHNITVDPKLFKKRRRLRSRVLFFSTQPPPVAAQTQDLDFEAGGAS 101 cow
Q29074      SAPAGA-NSARVAGQTRNITVDPKLFKKRRRLRSRVLFFSTQPPPVAAQTQDPDLEASGAA 99 pig
P05200      GRFAWM-PDG---TEDLNIAMDQNFFKKRRFRSSRVLFSTQPPPVSRKGQSTGFLSS-AV 115 chicken
P34128      HHPTPKKSEDQELGSAANIIVDPKLFQKRRFQSPRVLFSTQPPPLSRDEQSVKFLDT-ED 115 krait
P21617      HSHGK-LEAKEPSYFRNVTVDPKLFRKRKFRSRVLFFSTQPPPLSEDFQHLEYLDD-EE 104 xenopus
P34129      DHPTSI-----PTVDPKLFNKRRHLSRVLFFSSQPP-----DAEPAGGQ 71 fish
      .      :      *      .      *      *      :      *      *      *      *      *      :
```

```
P01138      PFNRTHRSKRSSSHPIFHRGEFSVCDSVSVWVGDKTTATDIKGKEVMVLGEVNINNSVFK 171 human
Q9N2F1      PFNRTHRSKRSSSHPIFHRGEFSVCDSVSVWVGDKTTATDIKGKEVMVLGEVNINNSVFK 171 chimpanzee
P01139      PFNRTHRSKRSSSTHPVFHMGFEFSVCDSVSVWVGDKTTATDIKGKEVTVLAEVNINNSVFR 171 mouse
P25427      SFNRTHRSKRSSSTHPVFHMGFEFSVCDSVSVWVGDKTTATDIKGKEVTVLGEVNINNSVFK 171 Norway rat
P20675      SFNRTHRSKRSSSTHPVFQMGFEFSVCDSVSVWVGDKTTATDIKGNEVTVLGEVNINNSVFK 171 african rat
P19093      SVNTHRSKRSSSTHPVFHMGFEFSVCDSVSVWVGDKTTATDIKGKEVTVLAEVNVNNSVFR 171 guinea pig
P13600      SFNRTHRSKRSSSHPVLRHGEFSVCDSISVWVGDKTTATDIKGKEVMVLGEVNINNSVFR 161 cow
Q29074      SFNRTHRSKRSSSHPVFHRGEFSVCDSVSVWVGDKTTATDIKGKEVMVLGEVNINNSVFK 159 pig
P05200      SLNRTARTKR-TAHPVLHRGEFSVCDSVSMWVGDKTTATDIKGKEVTVLGEVNINNSVFK 174 chicken
P34128      TLNRNIWANN-ENHPVHNQGEFSVCDSISVWVTNKTKATDIKGNVTVMVDVNLNNEVYK 174 krait
P21617      SLNKTIRAKR-TVHPVLHKGEYSVCDSVSMWVGEEKTKATDIKGKEVTVLGEVNINNSVFK 163 xenopus
P34129      GVSRRTRRQP-----QHRGVYSCESVSVWVGDKTKATDISGKEVTVLPHYNNINNVKKK 125 fish
      .      :      :      .      :      *      .      *      *      *      *      *      *      *      *      :
```

(continue on following page)

P01138	QYFFETKCRDPNPVDSGCRGIDSKHWNSYCTTTHTFVKALTMDGKQAAWRFIRIDTACVC	231 human
Q9N2F1	QYFFETKCRDPNPVDSGCRGIDSKHWNSYCTTTHTFVKALTMDGKQAAWRFIRIDTACVC	231 chimpanze
P01139	QYFFETKCRASNPVESGCRGIDSKHWNSYCTTTHTFVKALTTDEKQAAWRFIRIDTACVC	231 mouse
P25427	QYFFETKCRAPNPVESGCRGIDSKHWNSYCTTTHTFVKALTTDDKQAAWRFIRIDTACVC	231 Norwayrat
P20675	QYFFETKCRARNPVESGCRGIDSKHWNSYCTTTHTFVKALTTDDRQAAWRFIRIDTACVC	231 africanrat
P19093	QYFFETKCRDPSPVDSGCRGIDSKHWNSYCTTTHTFVKALTTANKQAAWRFIRIDTACVC	231 guineapig
P13600	QYFFETKCRDPNPVDSGCRGIDAKHWNSYCTTTHTFVKALTMDGKQAAWRFIRIDTACVC	221 cow
Q29074	QYFFETKCRDPNPVDSGCRGIDSKHWNSYCTTTHTFVKALTMDGKQAAWRFIRIDTACVC	219 pig
P05200	QYFFETKCRDPRPVSSGCRGIDAKHWNSYCTTTHTFVKALTMEGKQAAWRFIRIDTACVC	234 chicken
P34128	QYFFETKCRNPVPVPSGCRGIDSRHWNSYCTTTDTFVKALTMENRASWRFIRIDTACVC	234 krait
P21617	QYFFETKCRDPKPVSSGCRGIDAKHWNSYCTTTHTFVKALTMEGKQAAWRFIRIDTACVC	223 xenopus
P34129	QYFFETTCHSPPSGSRCLGIDARHWNSHCTNSHTFVRALTSSENQVAWRLIRINVACVC	185 fish

*****.*: . * * ***:*****:*.:.***:*** .:.***:***:*****

P01138	VLSRKAVRRA	241 human
Q9N2F1	VLSRKAVRRA	241 chimpanzee
P01139	VLSRKATRRG	241 mouse
P25427	VLSRKAARRG	241 Norway rat
P20675	VLTRKAPRRG	241 african rat
P19093	VLNRKAARRG	241 guinea pig
P13600	VLSRKTGQAP	231 cow
Q29074	VLSRKAGRRA	229 pig
P05200	VLSRKSGRP-	243 chicken
P34128	VISRKTENF-	243 krait
P21617	VLSRK-GRT-	231 xenopus
P34129	VLSRKSWQH-	194 fish

*:.**: .

Multiple sequence alignment of the mouse short precursors of various species performed with the CLUSTAL W software. The signal sequence is indicated in red, the short precursor appears in black and the mature NGF in blue.

Besides the recent findings on the functional role of proNGF, interesting studies on the other neurotrophins are also shading new light of the entire field of pro-neurotrophins. All neurotrophins, in fact, are initially synthesized as large pro-peptides of comparable size and are subsequently processed to mature neurotrophins. A multiple sequence alignment of the mouse long precursors of the three neurotrophins pre-proNGF, pre-proBDNF and pre-proNT-3 is shown in fig. 4.2.1. It is interesting to note that the conservation of the precursor peptides of the different neurotrophins is much less marked than that of the mature neurotrophins.

[illegible]

256

APPENDIX 2

A NOVEL EXPERIMENTAL APPROACH TO THE REFOLDING OF PROTEINS ON A WESTERN BLOTTING NITROCELLULOSE MEMBRANE

Introduction

Certain antibodies do recognize their antigens in native, but not in denaturing conditions, and this represents an obstacle, when using them in techniques, like western blotting analysis.

To overcome this problem, one possibility is to refold the protein blotted on the nitrocellulose membrane, before performing the recognition with the antibody. One example of this approach is described in the Sambrook textbook. In the established protocols, the proteins on the membrane are first completely denatured by soaking of the membrane in a Guanidium-hydrochloride buffer; then, the refolding of the proteins is achieved by stepwise change of the buffer with a gradual reduction of the Guanidinium concentration.

An alternative approach is to help the refolding starting from the blotting conditions, by mean of a refolding adjuvant: cyclodextrin.

Cyclodextrins are natural occurring cyclic oligosaccharides, produced from starch by the action of the enzymes glycosyltransferases. The most well known cyclodextrins are the α -, β - and γ -cyclodextrin, depending on the type of link between residues. They form a the “cage-like” structural organization in solution, as indicated in fig. 1, describing a toroid with the opening presenting hydroxyl groups to the solvent and a hydrophobic interior due to the glycosidic oxygen atoms.

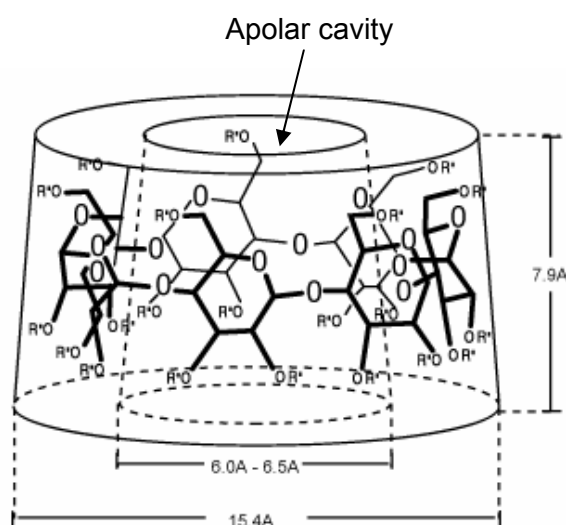


Figure 1 – Schematic representation of the “cage-like” toroidal configuration of cyclodextrins in solution.

The apolar cavity indicated by the arrow marks the space for the guest hydrophobic molecules. (Figure taken from Szejtli and Osa)

Thanks to this property, they are very efficient detergent scavenger and are used during the refolding step in the *in vitro* refolding technique for recombinant proteins production: they are employed as artificial chaperones for their ability to strip the detergent from the protein in solution, allowing proper refolding (Rozema and Gellman, JACS, 1995). Moreover, cyclodextrin also interacts with bulky hydrophobic amino acid chains, increasing the solubility of folding intermediates (Cooper, JACS, 1992), and thus decreasing aggregation during the renaturation procedure.

The generality of the properties of cyclodextrins was demonstrated by the positive results in the *in vitro* refolding of various kinds of proteins (Rudolph and Lilie, FASEB J., 1996; Lange and Rudolph, 2005). Recently, the cyclodextrins were also employed to develop a new refolding method, based on the use of nanogels as support for the protein to be refolded in presence of cyclodextrins, opening the possibility to a more efficient refolding method, both in chromatographic and in batch refolding conditions (Nomura *et al.*, FEBS, 2003).

Besides the natural cyclodextrins, various enzymatic modifications were carried out, to increase their solubility properties.

For these reason, cyclodextrins were chosen to prove the refolding of blotted proteins, since they should be able to remove the denaturing agent SDS bound on the blotted proteins, and allow them to refold. In the results presented in this thesis, methyl- β -cyclodextrin was chosen, for its solubility properties.

Aim

In the last part of the thesis, a completely new approach was investigated, for the refolding of proteins on nitrocellulose membrane will be described, based on the use of cyclodextrins as adjuvant in the membrane-refolding of the proteins. A new technique was developed, that allows the refolding of denatured proteins on a nitrocellulose membrane, to open the possibility to the use of conformation-dependent antibodies. As refolding-agent the cyclodextrin molecule was employed, and the efficacy of the methodology was optimized for the monoclonal anti-NGF antibody α D11: it was indeed possible to increase the detection properties of the antibody in western blotting in the recognition of NGF and proNGF proteins.

Results

The binding properties of the α D11 anti-NGF monoclonal antibody when applied as a primary antibody were tested using western blotting as a technique. However, it was not possible to detect NGF on the membrane with a high sensitivity. Given this result, the main hypothesis was that the antibody is an epitope-sensitive one, that is not able to recognize its antigen in denaturing conditions, like it is the case of an SDS-PAGE. A confirm of this hypothesis came from a set of experiments where the NGF was loaded on the SDS-PAGE in semi-denaturing conditions, *i.e.* without heating and/or the addition of reducing agent. Indeed, in these conditions, the mAb α D11 was improving the detection sensitivity (data not shown).

On the contrary, when α D11 antibody was used to detect m-proNGF in western blotting, the result was interesting, since the NGF was not detected, but the proNGF was, as indicated in fig. 1.1. This observation could be explained by the fact that proNGF could “shield” NGF in the SDS-PAGE step, thus preventing the epitope for α D11 on the NGF moiety from a complete denaturation.

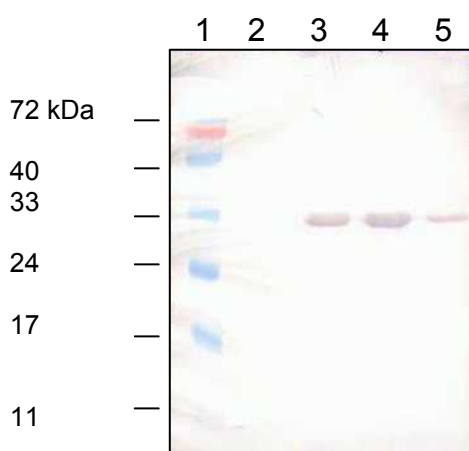


Figure 1.1 – Western blotting with α D11 antibody – m-proNGF samples.

Lane 1: molecular weight marker, lane 2: 1 μ g of m-NGF; lane 3: 2 μ g of rm-proNGF; lane 3: 2 μ g of rm-proNGF P5A; lane 3: 0.5 μ g of rm-proNGF.

By means of the described experiments, it was possible to establish that α D11 is for sure a conformation-dependent antibody, that is able to detect its antigen in native conditions: if it is poor in detecting the antigen in denaturing conditions in western blot analysis, in fact, it is on the contrary very efficient in the interaction with both NGF and proNGF in native conditions like it's the case of the ELISA and BIAcore experiments described in the previous parts of this thesis.

Refolding on the membrane by means of cyclodextrins

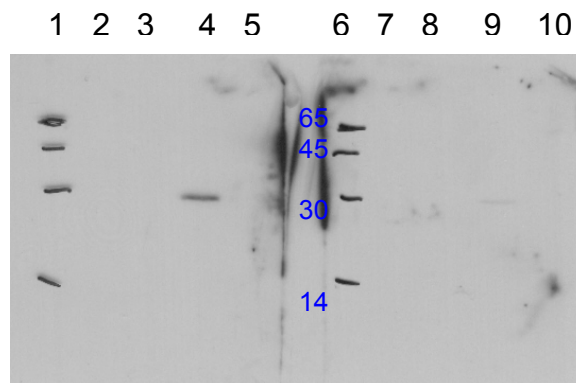
Trying to improve the binding properties of the α D11 antibody also in western blot analysis, a new approach was designed, to investigate the possibility of performing a refolding of the blotted proteins on the nitrocellulose membrane used for western blot analysis.

For the first time cyclodextrins were used to refold a protein blocked on a nitrocellulose membrane.

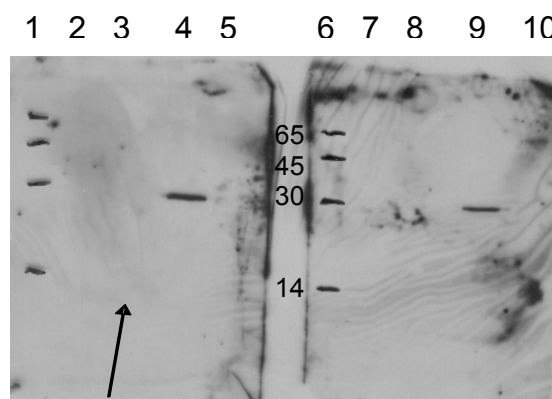
The design of the experiment has been quite simple: in the traditional protocol used in the western blot analysis, a new step was introduced, namely an overnight incubation step at 4°C immediately after the blotting of the gel, with a solution of PBS containing methyl- β -cyclodextrins 500mM. After a washing step, the normal protocol was followed.

The result was quite surprising, and can be explained by looking at fig. 2.1 (panel A and B): it appears clearly that in presence of cyclodextrins, the α D11 antibody is more efficient in the detection of NGF and proNGF.

A



B



C

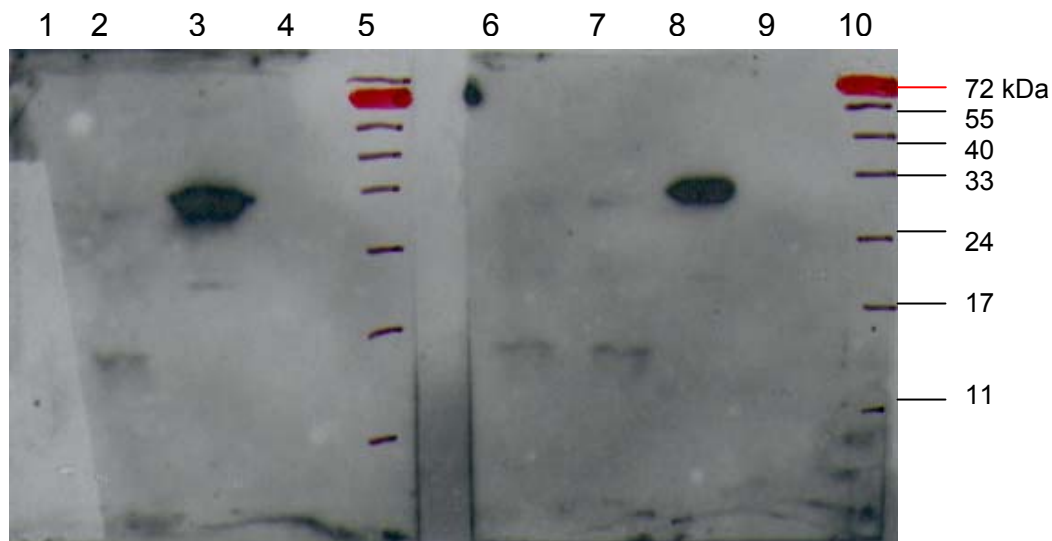


Figure 2.1 – Western blot analysis with refolding on membrane through methyl- β -cyclodextrins. Panel A and B: Two exposures (5' in A and overnight in B) of a western blot treated with cyclodextrins. Lanes 1-5: with cyclodextrins; lanes 6-10: without cyclodextrins. Lanes 1, 6: molecular weight marker; lanes 2, 7: 100ng m-NGF; lanes 3, 8: 200ng m-NGF; lanes 4, 9: 200ng m-proNGF; lanes 5,10: 200ng BSA; the arrow on lane 3 on the right side of the figure marks the presence of a faint band of m-NGF. Panel C: Another western blot treated with cyclodextrins. Lanes 1-5: with cyclodextrins; lanes 6-10: without cyclodextrins. Lanes 1, 6: 300ng m-NGF; lanes 2, 7: 600ng m-NGF; lanes 3, 8: 600ng m-proNGF; lanes 4,9: 500ng BSA; lanes 5, 10: molecular weight marker.

It is interesting to note that also the cyclodextrins effect is much higher on the proNGF when compared to the NGF samples, as if the help in refolding of the mature NGF normally carried out by the pro-peptide would be increased by the presence of the cyclodextrins. On the contrary, the *in vitro* refolding of the NGF part, known to be a very slow process (see Rattenholl, JMB, 2001), could remain still a slow process, and not benefit of the help of the cyclodextrins.

The experiment was also repeated using the normal β -cyclodextrin (non-methylated), But the lower solubility of this product in respect to the methylated one makes it impossible to achieve a high concentration of cyclodextrin in solution. The consequence was that in this case, no major difference could be detected when

comparing the western blot done in presence or absence of additive, as it clearly emerges from fig. 2.2.

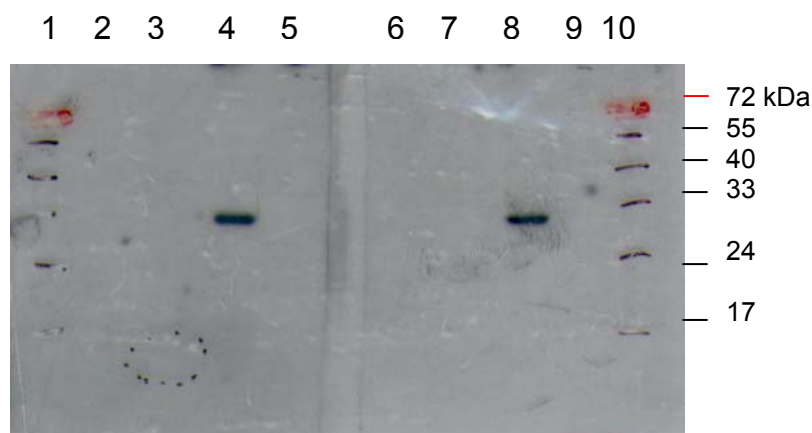


Figure 2.2 – Western blot analysis with refolding on membrane through β -cyclodextrins. Lanes 1-5: with cyclodextrins; lanes 6-10: without cyclodextrins. Lanes 1, 6: 300ng m-NGF; lanes 2, 7: 600ng m-NGF; lanes 3, 8: 600ng m-proNGF; lanes 4,9: 500ng BSA; lanes 5, 10: molecular weight marker. The dotted circle marks the position of a weak band indicating the presence of NGF.

Discussion

A new technique was developed in this thesis, to increase the performances of conformational antibodies to detect denatured proteins, like in western blotting analysis. In particular, a new methodology for the refolding on the nitrocellulose membrane was developed, by means of cyclodextrins.

The methodology was optimized for the anti-NGF α D11 antibody, characterized normally by a poor ability to function as a primary antibody in western blot analysis. After a refolding on-membrane of the blotted proteins by means of cyclodextrins, the detection properties of the antibody in western blot were sensibly higher.

The approach was proven to be very efficient and thanks to it another property of proNGF was verified: its ability of helping the refolding of a denatured NGF also on the membrane of a western blot. This finding is in agreement with the previous discoveries on proNGF activity.

Moreover, an unexpected but interesting result obtained by this experiment was to verify the function of proNGF as a folding promoter also when immobilized on a membrane. Indeed, that the detection properties of the α D11 antibody in western blotting were much higher for proNGF than for NGF, both in absence and in presence of cyclodextrins, giving a substantial further confirm of the important biochemical role of proNGF, that is able on one side to “protect” the NGF moiety from completely denaturation in an SDS-PAGE and on the other side to help it to correctly renature even in the apparently rigid environment of a nitrocellulose membrane, as previously reported in renaturation experiments in solution.

The result of the experiment could be also improved by the use of redox shuffling system, like the GSSG/GSH couple, applied together with the cyclodextrins, to introduce a further step in the reanaturation procedure.

In general, this new application of cyclodextrins opens a wide spectrum of possible applications, to enlarge the group of antibodies to be used in western blotting and to ameliorate the detection signals of an antibody-antigen interaction on a membrane also with conformation-dependent antibodies.

Bibliography

Cooper A., Effect of cyclodextrins on the thermal stability of globular proteins, *J. Am. Chem. Soc.* (1992) **114**, 9208-9209

Lange C., Rudolph R., Protein Folding Handbook – Chapter 38, Production of recombinant proteins for therapy, diagnostics and industrial research by *in vitro* folding., Wiley-VCH, Weinheim, 2005

Nomura Y., Ikeda M., Yamaguchi N., Aoyama Y., Protein refolding assisted by self-assembled nanogels as novel artificial molecular chaperones, *FEBS Letters* (2003) **553**, 271-276

Rozema D., Gellman S.H., Artificial Chaperones: protein refolding via sequential use of detergent and cyclodextrin, *J. Am. Chem. Soc.* (1995) **117**, 2373-2374

Rudolph R., Lilie H., In vitro folding of inclusion body proteins, *The FASEB Journal* (1996) **10**, 49-56

Sambrook, J.; Fritsch, E.F.; Maniatis, T.; Molecular Cloning - A Laboratory Manual, Volume 3, pag.18.53; Cold Spring Harbor Laboratory, Cold Spring Harbor, New York; 3rd edition

Szejtli J., Osa T., Cyclodextrins (Volume 3 – in “Comprehensive Supramolecular Chemistry”), Elsevier Science Inc., New York

APPENDIX 3

FLUORESCENCE CYCLOHEXIMIDE AS A TOOL FOR THE VISUALIZATION OF PROTEIN SYNTHESIS IN LIVING CELLS

During the first year of my PhD Thesis, I have been involved in a different project, than the one presented in the previous chapters.

In particular, the project I have worked on, was dealing with the investigation of obtaining a tool for the visualization of protein synthesis in living cells through chemical modification of the protein synthesis inhibitor cycloheximide.

The outcome of this work will be presented in two manuscripts, ready to be submitted.

The abstracts of these two works is included in this Appendix.

The first abstract presents the chemical strategy for the modification of cycloheximide, the second one, the cell biology applications.

1. Chemistry

A NEW APPLICATION OF AN OLD REACTION: THE SYNTHESIS OF FLUORESCENT CYCLOHEXIMIDE

Francesca Paoletti^{1,*}, Cristiana Campa^{2,3,*}, Ivan Donati², Kevin Ainger^{1,4}, Antonino Cattaneo^{1,5,6} and Amedeo Vetere²

¹ Neurobiology Sector, SISSA-ISAS, Building Q1, AREA Science Park - Basovizza, 34012 Trieste, Italy

² Department of Biochemistry, Biophysics and Macromolecular Chemistry, University of Trieste, Italy

³ *Present address:* Bracco Imaging SpA, CRM-TS, AREA Science Park, Building Q, I-34012 Basovizza, Trieste

⁴ *Present address:* Adriacell, Area Science Park - Basovizza, S.S 14 Km 163.5, 34012 Trieste, Italy

⁵ LayLine Genomics S.p.A., via di Castel Romano 100, 00128 Roma, Italy

⁶ European Brain Research Institute, Via del Fosso di Fiorano, 00178 Rome, Italy

* These two authors contributed equally to the present work

A novel approach to the chemical modification of cycloheximide, a protein synthesis inhibitor, is presented. The effect of different functional groups on the biological activity of cycloheximide was studied upon their modification through suitable strategies, i.e., acetylation of the hydroxyl group and reductive amination of the ketone group. The first route induced a complete loss of biological activity, while the second approach allowed a retained inhibition of protein synthesis, as demonstrated

by in vitro translation assays. Various fluorescent dyes for reductive amination were tested (i.e. ANTS, APTS, Rhodamine-123), and the success of the syntheses was demonstrated by various analytical techniques like CE-UV, HPLC-UV, fluorescence and ESI-MS. Cycloheximide labelling with fluorescent dyes is a promising approach for developing fluorescence reporters for various applications, both in vitro (fluorescence spectroscopy) and in vivo (live imaging with fluorescent microscopy).

2. Cell Biology

IMAGING SITES OF PROTEIN SYNTHESIS IN LIVING CELLS.

Kevin Ainger¹, Francesca Paoletti¹, Cristiana Campa², Amedeo Vetere², and Antonino Cattaneo¹

Biophysics Sector, International School for Advanced Studies¹, Department of Biochemistry, Biophysics and Macromolecular Chemistry^{2,°}, University of Trieste, Italy.

Since the fungal antibiotic cycloheximide binds specifically to actively elongating ribosomes, the intracellular distribution of cycloheximide binding sites should accurately reflect the sites of ongoing protein synthesis. Cycloheximides modified with different fluorescent moieties were synthesized, purified and demonstrated to retain antibiotic activity by in vitro translation and metabolic labeling assays. APTS-cycloheximide (APTS-CHX) specifically labeled perinuclear structures consistent with the structure and motility of the endoplasmic reticulum, as well as the leading edge of motile fibroblasts. Fluorescence loss induced by photobleaching (FLIP) after scrape-loading of APTS-CHX in the presence of puromycin revealed that all APTS-CHX binding is specifically competed by puromycin. Functional imaging of active synapses showed that some dendritic APTS-CHX labeling was localized near active synapses. Sites of protein synthesis have been visualized for the first time in living cells and the sites of local protein synthesis in neuronal dendrites have been shown to be near synapses with actively recycling synaptic vesicles.

ACKNOWLEDGEMENTS

At this point of the PhD course, it is quite difficult for me to write this acknowledgements, due to fear of forgetting somebody of the many persons I met during the four year of my graduate studies at SISSA. However, I will try to let my memory recall everybody. And if I forget somebody, I apologize from the beginning!

The first big thanks is of course for my supervisors: prof. Cattaneo and dr. Lamba. I am very much indebt to Antonino for offering me the opportunity to work in the “evergreen” and stimulating field of neurotrophins, and for keeping me trained in developing new questions to be answered and teaching me how to deal in approaching a new scientific problem. A special thanks goes to Doriano, who constantly followed my scientific progresses with enthusiasm and curiosity, and helped me to learn a new way of thinking on structure and dynamics of proteins, always stimulating the investigation of new approaches.

To Sonia I reserve a big “grazie”, for the friendship at first, grown up in these years of bench-sharing, and for having introduced me to the experimental approach on learning about structure/function properties of proteins.

From Italy to Germany, I cannot forget the enthusiasm and the warmth that prof. Rainer Rudolph and dr. Elisabeth Schwarz reserved me during my months in Halle (Saale). They really made me feel like home at the Institute für Biotechnologie with a continuous involvement in my old and new scientific problems and opened me the new field of protein folding!

Back to my home lab, I would really like to say a special thank to Giada, for the friendship and the nice scientific discussions, and to Federica, whose long-time lasting friendship was enriched with the sharing of the many challenges in dealing with BIAcore sensograms...

Many thanks also to Gabriella, for “taking care” of the cell cultures I used and for the joy she always spreads in the lab. And thanks to Jess, not only for the sequencing of my plasmids, but also for the happiness and the nice talks.

Thanks a lot to Michela, for the big amount of work in the selection of the scFv and for giving me always the good hints to the “antibody world”. And to Isabella too, I say thanks, not only for the help with the scFv, but also for her joyful presence!

From protein to protein, many thanks to Ivet, always ready to help me with new protein techniques and to share with me the drinking of fruit juice!

Back to Halle, a special thank is to Marco K., who introduced me in the refolding of proteins, and was always ready to answer my questions about every single experimental step. And in Halle, I must acknowledge the skillful help of Michael with the new approaches to BIAcore measurements, the help of Hauke with the learning of the biophysical techniques

for protein analysis, the aid of Grit with the fermentation and that of Mirko at various stages of protein analysis, the nice talks with Brigitte.

And going even more North, I want to thank the help of dr. Dmitri Svergun and Peter Konarev at EMBL-Hamburg, for the enthusiasm and the time spent to teach us the SAXS world and for being always ready to answer my many questions! And of course thanks also to dr. Mafred Roessle, for the help at the beamline.

More thanks go to Kevin, for the teaching of the cell biology “under the microscope”. And thanks to Miranda, Simona and Sabina for the help with the experiments on animal tissues, as well as to Massimo for the help with the cell cultures. And thanks to Sergio for answering my computer questions and to Tullio for the technical assistance with all the instruments.

And of course thanks to Teresa, Giovanni, Daniela, Luisa and everybody else in the SISSA Neurobiology lab for providing a stimulating working environment, to the whole BioLab at Elettra, to the people at the Institut für Biotechnologie in Halle as well as to everybody in the T17-T21 labs of BBCM, especially Ivan and Amedeo for the help in the “cycloheximide adventure”.

Coming to more “personal” thanks, I want to acknowledge the constant presence of Cristiana at any stage of the PhD, both as an enthusiastic scientist and as a reliable friend, and always ready to offer her skillful help on novel problems and to cheer me up in the “dark days”.

I cannot forget my family: my mother, who always supported me during these years and whose curiosity in my research always stimulated me to go on; my father, who participated with very much enthusiasm in my scientific progresses, always encouraging me to go deeper in finding answers to the questions; Lella, my “little” sister, for her artistic presence in the family and the nice and long talks about the future.

And finally, last but not least, Marco, who was always next to me, supporting me at any stage, with patience for the absence of timetables in my life and especially in these last months of increasing concentration on the end of the PhD work. Thanks because together with him music and science become the two sides of the same will of understanding the unknown, in the spirit as well as in the mind.